

**Comparison of the Heterogeneous Enantioselective Hydrogenation of 2,3-  
butanedione over Cinchona Modified Platinum Catalysts in Three  
Different Reactors**

Thesis submitted in accordance with the requirements of the University of  
Cardiff for the degree of Doctor of Philosophy by

Nicholas François Dummer

October 2004

UMI Number: U583969

All rights reserved

INFORMATION TO ALL USERS

The quality of this reproduction is dependent upon the quality of the copy submitted.

In the unlikely event that the author did not send a complete manuscript and there are missing pages, these will be noted. Also, if material had to be removed, a note will indicate the deletion.



UMI U583969

Published by ProQuest LLC 2013. Copyright in the Dissertation held by the Author.  
Microform Edition © ProQuest LLC.

All rights reserved. This work is protected against  
unauthorized copying under Title 17, United States Code.



ProQuest LLC  
789 East Eisenhower Parkway  
P.O. Box 1346  
Ann Arbor, MI 48106-1346

## **Abstract**

The enantioselective hydrogenation of 2,3-butanedione has been studied in the liquid and gas phase over cinchonidine modified Pt/silica catalysts. Reactions were conducted in three different reactors; a stirred autoclave, a fixed-bed trickle-bed reactor and a micro-flow gas phase reactor.

Screening of eight powder and four granular (0.5-1.0 mm) 2.5 % Pt/silica catalysts was conducted in the autoclave to identify ideal support characteristics. The rate of 2,3-butanedione enantioselective hydrogenation was used as the means to determine these characteristics. The support characteristics used for the manufacture of extruded silica gel supports were: PV > 0.40 ml/g, PD > 50 Å and a SA ≥ 300 m<sup>2</sup>/g (< 600 m<sup>2</sup>/g). Optimum values of rate and enantiomeric excess were identified with (i) pre-reduction at 200°C for 2 h of catalyst samples, (ii) modifier concentration of 1.89 mM, (iii) toluene with 0.1 M acetic acid additive, (iv) hydrogen pressure was 30 bar and (v) stirring speed of 1000 rpm. Under these conditions the rate achieved 1104 mmol/h/g<sub>cat</sub> in DCM was comparable to the reference catalyst EUROPT-1.

The granular catalysts were used in the trickle-bed reactor to identify optimum reaction conditions and support characteristics. Ultraviolet spectroscopy of cinchonidine modification protocols and cyclohexene hydrogenation were employed to facilitate optimisation. *In situ* and *ex situ* pre-modification of the bed with cinchonidine were investigated. Conversion of dione was ca. 10 % for catalysts which possessed an unrestrictive pore structure. The ee of (*R*)-hydroxybutanone achieved was ca. 12 %, however, was at its maximum initially after *in situ* pre-modification. Whereas, the enantiomeric excess tended to increase over an *ex situ* modified catalyst bed. Continual replacement of modifier

was necessary to ensure an ee was maintained. The reaction conditions used for the study of the catalyst with extruded silica gel support were, (i) *ex situ* pre-modification with 16.98 mM cinchonidine in DCM, (ii) 1 ml/min of feedstock with 0.1 M reactant and 8.49 mM CD in DCM, (iii) hydrogen pressure of 0.5 barg (4800 /h), (iv) catalyst bed consisting of 2g of catalyst and SiC fines. Hydrogenation of methyl pyruvate under these conditions yielded an initial conversion of 80 % and an ee of 52%.

Hydrogenation of 2,3-butanedione and methyl pyruvate over an extrudate catalyst bed under the optimised conditions achieved an ee of 12 % and 36 % respectively at low conversion. Bed pre-modification was determined to be essential to achieve an enantiomeric excess.

Hydrogenation of 2,3-butanedione was attempted at the gas/solid interface over pre-modified platinum catalysts. The strength of adsorption of the dione prevented a sustained reaction. An ee of 15 % at 35°C was achieved with a saturator temperature of 0°C. The addition of cinchonidine to the catalyst proved beneficial for greater reaction times.

The lower strength of adsorption pyruvate esters on platinum facilitated the identification of optimum reaction conditions. The highest values of enantiomeric excess of (*R*)-lactate ester were achieved when (i) catalyst samples were pre-modified *ex situ* with 3.4 mM CD in DCM, (ii) reaction temperature of 40°C, (v) helium then helium/hydrogen passed over bed prior to reaction, (iii) hydrogen concentration of 25 % in helium with a total flow rate of 80 ml/min, (iv) methyl pyruvate at 20°C (0.066 g/h). Under these reaction conditions an ee of ca. 36 % (*R*)-lactate ester was achieved over a 2.5 % Pt/SiO<sub>2</sub> catalyst (0.025 g) at 100 % pyruvate conversion for 5 h. This was enhanced to ca. 43 % by pre-treatment of the bed with the (*R*)-lactate for 100 minutes prior to the reaction. Methyl and ethyl pyruvate were used to investigate the enantioselective site on the Pt surface. The outcome indicated that the site is substrate specific after 100 minutes on-line.



## **Abstract (Microfiche)**

The enantioselective hydrogenation of 2,3-butanedione has been studied in the liquid and gas phase over cinchonidine modified Pt/silica catalysts. Reactions were conducted in three different reactors; a stirred autoclave, a fixed-bed trickle-bed reactor and a micro-flow gas phase reactor. The rate of 2,3-butanedione hydrogenation in the autoclave was used to compare a number of platinum catalysts. The outcome of this screening program resulted in an ideal set of support characteristics for the manufacture of an extruded silica gel support for use in the trickle-bed reactor. Further experiments were undertaken to optimise the rate and end enantiomeric excess in the autoclave. These included increased pressure and lower modifier concentration. Techniques of modifier pre-adsorption in the trickle-bed reactor were studied. Hydrogenation over the extruded catalysts indicated that the trickle-bed reactor was a suitable reactor for fine chemical synthesis with this class of reaction. Reactions were additionally carried out at the gas/solid interface in a flow reactor for comparison to the liquid phase studies. This extended to the use of pyruvate esters to probe the enantioselective site adsorbed on the platinum surface in the absence of solvent.

## Acknowledgements

I have many, many people to thank for helping me to complete this thesis and the work it contains. Firstly to Graham Hutchings, to who I am very grateful for all the help and support bestowed over the four years. Secondly to Stuart Taylor whose help with the most mundane of questions were always satisfied with grace and good humour. Additionally to Dave Willock who helped with trickier aspects of the work. Then there are all the post-docs who have advised me with matters scientific; Phil Landon, Paul McMorn, Jon Bartley, Dan Enache, Nianxue Song and Richard Wells. Additionally thanks must go to Peter Wells for fruitful debates and for fair and helpful criticism.

I would like to thank the IMI-2 team for their support and the beneficial discussions that took place at the meetings. Thanks to all involved for the 'opportunity to shine' and the generosity shown with the great meeting locations.

Thanks must go to the supporting staff, who without them nothing would get done. To Gary and Robin for putting up with my constant interruptions of their breaks. To Alun and Ricky who have helped with the creation of working apparatus from my sloppy doodles. To Pat for knowing where I'm supposed to be and helping without question. To Rob, who has more on his plate than most but always spared the time to help and discuss the intricacies of the subject.

Then, to all the friends from the many labs I have worked in. Thanks to John G, OJK, Nicola, Becky, Rajinder, Charlie, Ash, Silvio, Toni, Luisa, Chris J, Sarah G, Tom, Chen, Jenny, Leng Leng, Graham L, Hongmei, Jo, Pete, Javi, Pablo, Marco and lastly Darragh. I always had fun in the lab and on the (many) nights out.....thanks for the hang-overs.

My sincerest thanks and love go to Aleks, who I am positive can't imagine how much you have helped and inspired me, dziekuje bardzo. Kocham cie bardzo mocno, zawsze.

Lastly the biggest thank you to my parents, who have given everything for me to be here and complete this book. Your love and encouragement have helped tremendously and I am forever in your debt. Thank you.

## Table of Contents

<b>Chapter One: Introduction</b>	<b>1</b>
1.1 Introduction	1
1.1.1 History	1
1.2 Definitions and terms	2
1.2.1 Catalyst and catalysis	2
1.2.2 Selectivity	4
1.2.3 Chirality and enantiomers	4
1.3 Enantioselective catalysis	7
1.3.1 Homogeneous enantioselective catalysis	7
1.3.2 Heterogeneous enantioselective catalysis	11
1.4 The Orito reaction: enantioselective hydrogenation of $\alpha$ -ketoesters over cinchona-modified platinum	12
1.4.1 Cinchona alkaloids	13
1.4.2 Alkaloid structure	14
1.4.3 Alkaloid adsorption	15
1.4.4 Proposed enantioselective site	16
1.5 Further Work on the Orito reaction	19
1.5.1 Catalyst	20
1.5.2 Other metals investigated	24
1.5.3 Other pro-chiral substrates	25
1.5.3.1 $\alpha$ -Diketones	26
1.5.4 Alkaloid modifier concentration	31

1.5.5 Catalyst pre-modification vs. <i>in situ</i> modification	32
1.5.6 Reaction conditions	33
1.5.7 Solvent	34
1.6 Reactors used in catalysis	34
1.6.1 Background	35
1.6.2 Reactor types used in heterogeneous enantioselective hydrogenation reactions	39
1.7 IMI	43
1.8 Aims of the project	45
1.8.1 objectives	45
1.9 References	46
 <b>Chapter Two: Experimental</b>	 <b>54</b>
 2.1 Materials	 54
2.1.1 Catalysts used	54
2.1.1.1 IMI2 2.5 % Pt/SiO <sub>2</sub> Catalysts	54
2.1.1.2 EUROPT-1 Reference catalyst	57
2.1.1.3 Other platinum catalysts	57
2.1.1.4 Preparation of 1 % Pt/ $\alpha$ -Alumina catalyst	58
2.1.2 Cinchona alkaloids	59
2.1.3 Other materials	60
2.2 Reactors used in the current study	61
2.2.1 Stirred tank reactor	61
2.2.2 Trickle-bed reactor	63

---

2.2.3 Gas-phase reactor	64
2.3 Procedures	65
2.3.1 Catalyst characterisation	65
2.3.1.1 Surface area and pore analysis	66
2.3.1.2 Powder X-ray diffraction	67
2.3.2 Reduction of catalyst samples	68
2.3.3 Experimental procedure	69
2.3.2.1 Autoclave procedure I: <i>in situ</i> modification	69
2.3.2.2 Autoclave procedure II: pre- modification	70
2.3.2.3 Trickle-bed reactor procedure I: <i>in situ</i> modification	70
2.3.2.4 Trickle-bed reactor procedure II: <i>ex situ</i> modification	71
2.3.2.5 Loading of the Trickle-bed reactor	71
2.3.2.6 Gas-phase reactor procedure for the standard reaction	72
2.4 Product recovery	72
2.5 Product analysis	73
2.5.1 Gas chromatography	73
2.5.1.1 Liquid samples	74
2.5.1.2.1 Enantioselective hydrogenations	74
2.5.1.2.2 Cyclohexene hydrogenations	77
2.5.1.2 Gas phase analysis	77
2.5.2 UV/Vis Spectroscopy	78
2.5.2.1 Analysis of cinchonidine solutions	78
2.6 Determination of the rate of reactions	80
2.7 Measuring the vapour pressure of methyl pyruvate	81
2.8 References	81

---

<b>Chapter Three: Enantioselective Hydrogenations under Standard Conditions in the Autoclave Reactor</b>	<b>83</b>
3.1 Introduction	83
3.2 Results of 2,3-butanedione enantioselective hydrogenation	83
3.2.1 Standard reaction	83
3.2.2.1 Standard reaction in the absence of alkaloid	85
3.2.2.2 Standard reaction over EUROPT-1	87
3.2.2 Modification protocol	88
3.3 Optimisation of the standard reaction	90
3.3.1 Influence of the alkaloid concentration	90
3.3.2 Influence of solvent	91
3.3.3 Influence of pressure	93
3.3.4 Influence of stirrer speed	95
3.4 Cyclohexene hydrogenation	96
3.3.1 Results of cyclohexene hydrogenation	96
3.3.2 Addition of Cinchonidine	97
3.5 Discussion	98
3.5.1 Standard Reaction	98
3.5.2 Optimisation	102
3.5.3 Cyclohexene Hydrogenation	107
3.6 Conclusions	108
3.7 References	109

---

<b>Chapter Four: Trickle-bed Reactor</b>	<b>111</b>
4.1 Introduction	111
4.2 Results of modification protocol	111
4.3 Results of cyclohexene hydrogenation	115
4.4 Results of 2,3-butanedione hydrogenation over M0202X series catalysts	118
4.4.1 Hydrogenation of 2,3-butanedione in the absence of alkaloid	119
4.4.2 Influence of <i>in situ</i> modification of the catalyst bed on 2,3-butanedione hydrogenation	120
4.4.3 Influence of <i>ex situ</i> modification of the catalyst bed on 2,3-butanedione hydrogenation	121
4.5 Results of methyl pyruvate hydrogenation	122
4.5.1 Hydrogenation over <i>ex situ</i> modified M02023 in DCM	123
4.5.2 Hydrogenation over <i>ex situ</i> modified M02023 in ethanol	123
4.6 Results of enantioselective hydrogenation over extrudate catalysts	125
4.6.1 Hydrogenation of cyclohexene over extruded catalyst M03217	126
4.6.2 Hydrogenation of 2,3-butanedione over extrudate catalysts	127
4.6.3 Hydrogenation of methyl pyruvate over extruded catalysts	129
4.7 Discussion	132
4.7.1 Modification protocol	132
4.7.2 Cyclohexene hydrogenation	134
4.7.3 2,3-Butanedione hydrogenation	135
4.7.4 Methyl pyruvate hydrogenation	138
4.8 Conclusions	141
4.9 References	142

---

**Chapter Five: Enantioselective hydrogenation conducted in the Gas-phase Reactor 143**

5.1 Introduction	144
5.2 Results of the hydrogenation of substrates at gas/solid interface	144
5.2.1 Hydrogenation of 2,3-butanedione over pre-modified catalysts	144
5.2.2 Hydrogenation of 2,3-butanedione over un-modified catalyst	146
5.2.3 Standard reaction experiments carried out with pyruvate esters	146
5.2.3.1 Hydrogenation of methyl pyruvate over alkaloid pre-modified catalyst samples	147
5.2.3.2 Hydrogenation of methyl pyruvate over un-modified catalyst samples	149
5.2.3.3 Hydrogenation of ethyl pyruvate over catalyst M01271	150
5.3 Investigation of the enantioselective site with methyl and ethyl pyruvate	151
5.3.1 The effect of removing the reactant from the gas stream on the standard reaction	152
5.3.2 Sequential experiments	154
5.3.3 Introduction experiments	155
5.3.4 Reaction of both methyl and ethyl pyruvate over pre-modified catalyst	158
5.3.5 Influence of lactate pre-treatment on the standard reaction	159
5.4 Influence of the reaction conditions on the standard reaction	161
5.4.1 Influence of alkaloid on the standard reaction	161
5.4.2 Influence of furnace temperature on the standard reaction	161
5.4.3 Influence of saturator temperature	163
5.4.4 Addition of dichloromethane to methyl pyruvate	164
5.4.5 Effect of catalyst mass on the standard reaction	166



5.4.6 Influence of pre-modification solvent on the standard reaction	167
5.5 Discussion	168
5.5.1 Justification of hydrogenation at the gas/solid interface	168
5.5.2 2,3-Butanedione hydrogenation	170
5.5.3 Pyruvate ester Hydrogenation	171
5.5.4 Influence of the pre-modification conditions on the standard reaction	179
5.5.4.1 Pre-modification modifier concentration	179
5.5.4.2 Pre-modification solvent	180
5.5.4.3 Influence of alkaloid	182
5.5.4.4 Influence of reaction temperature and saturator temperature	183
5.5.4.5 Effect of catalyst mass	184
5.5.4.6 Influence of solvent addition to the saturator	184
5.6 Conclusions	185
5.7 References	186
<b>Chapter Six: Final comments and future work</b>	<b>188</b>
6.1 Final comments	188
6.2 Future work	189
<b>Chapter Seven: Appendix</b>	<b>192</b>

*Chapter*  
*One*

DECLARATION

This work has not previously been accepted in any substance for any degree and is not being concurrently submitted in candidature for any degree

Signed.....(candidate)

Date.....

STATEMENT 1

This thesis is the result of my own investigations, except where otherwise stated. Other sources are acknowledged by footnotes giving explicit references. A bibliography is appended.

Signed.....(candidate)

Date.....

STATEMENT 2

I hereby give consent for my thesis, if accepted, to be available for photocopying and for inter-library loan, and for the title and summary to be made available to outside organisations.

Signed.....(candidate)

Date.....

## **Abstract**

The enantioselective hydrogenation of 2,3-butanedione has been studied in the liquid and gas phase over cinchonidine modified Pt/silica catalysts. Reactions were conducted in three different reactors; a stirred autoclave, a fixed-bed trickle-bed reactor and a micro-flow gas phase reactor.

Screening of eight powder and four granular (0.5-1.0 mm) 2.5 % Pt/silica catalysts was conducted in the autoclave to identify ideal support characteristics. The rate of 2,3-butanedione enantioselective hydrogenation was used as the means to determine these characteristics. The support characteristics used for the manufacture of extruded silica gel supports were: PV > 0.40 ml/g, PD > 50 Å and a SA ≥ 300 m<sup>2</sup>/g (< 600 m<sup>2</sup>/g). Optimum values of rate and enantiomeric excess were identified with (i) pre-reduction at 200°C for 2 h of catalyst samples, (ii) modifier concentration of 1.89 mM, (iii) toluene with 0.1 M acetic acid additive, (iv) hydrogen pressure was 30 bar and (v) stirring speed of 1000 rpm. Under these conditions the rate achieved 1104 mmol/h/g<sub>cat</sub> in DCM was comparable to the reference catalyst EUROPT-1.

The granular catalysts were used in the trickle-bed reactor to identify optimum reaction conditions and support characteristics. Ultraviolet spectroscopy of cinchonidine modification protocols and cyclohexene hydrogenation were employed to facilitate optimisation. *In situ* and *ex situ* pre-modification of the bed with cinchonidine were investigated. Conversion of dione was ca. 10 % for catalysts which possessed an unrestrictive pore structure. The ee of (*R*)-hydroxybutanone achieved was ca. 12 %, however, was at its maximum initially after *in situ* pre-modification. Whereas, the enantiomeric excess tended to increase over an *ex situ* modified catalyst bed. Continual replacement of modifier

*Chapter*  
*One*

## Chapter 1: Introduction

### 1.1 Background

#### 1.1.1 History

The term catalyst was first used in 1836 by Berzelius [1], upon his assessment of previous work carried out by Davey and Döbereiner in 1817. Döbereiner combusted hydrogen and oxygen over porous platinum at room temperature. Faraday explained after similar investigations in 1825 that the activity of the platinum derived from a process of adsorption. This led Berzelius to investigate other gaseous combustions over platinum. Terming the process of ‘catalysis’ as “awaking affinities which are asleep”. Further work in the field of catalytic processes led to improved definitions. Ostwald in 1902 defined catalysts “as agents which accelerate chemical reactions without affecting the chemical equilibrium. Later Sabatier defined catalysis as “a mechanism whereby some substrates are involved in the process of accelerating chemical reactions without being products of the reaction” [2].

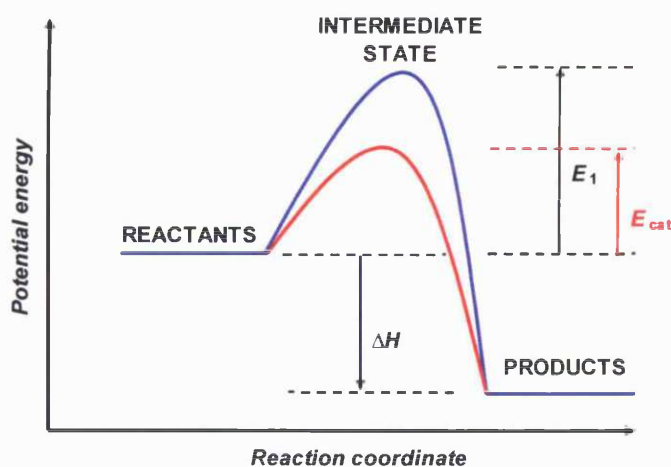


Fig. 1.1 The simplified energetics of a thermal (—) and catalysed (—) reaction

One hundred and fifty years later catalysis now accounts for nine-tenths of the chemical manufacturing processes. Synthetically made items such as plastics and fibres, drugs and fertilizers have all been made via a catalytic route. This has improved the quality of life for billions of people. However, many significant challenges remain to improve existing processes and to develop new ones.

## 1.2 Definitions and terms

### 1.2.1 Catalyst and catalysis

A substance defined by its ability to increase the rate at which a chemical reaction reaches equilibrium, however, does not become permanently involved in that reaction is known as a catalyst. Illustrated in Figure 1.1 is the potential energy of a thermal and catalytic reaction with the reaction coordinate. This is a much simplified representation of the energy requirements of a catalytic reaction. However, the reduced energy required to complete the reaction; from reactants to products is a primary characteristic of catalytic reactions and the reason for their widespread use.

Catalysis can be chiefly categorized into the following: homogeneous, heterogeneous and enzymatic. The distinction between the categories can be distinguished by the number of phases present when the catalyst is added.

For a homogeneous catalytic reaction the reactant and the catalyst are dissolved in the same phase. An example of this class of reaction is the well understood hydrogenation of an olefin with phosphine complexes of rhodium; Wilkinson's catalyst [3]. The catalytic hydrogenation of the olefin reactant is understood to occur after the rhodium centre is protonated. This process increases the oxidation state of the rhodium allowing the olefin to

bind via the C=C bond, where upon it can be hydrogenated. The reaction can be described as a catalytic cycle as the rhodium complex returns to the original oxidation state post olefin hydrogenation.

Heterogeneous catalysis is generally more complex and takes place at a phase boundary. This occurs when there is a distinct phase present that is liquid-solid or gas-solid, where the solid is the catalyst. An example of this is carbon monoxide oxidation on a metal surface, such as palladium (Fig. 1.2). This reaction occurs in the 'catalytic converter' of an automobile. The substrates, carbon monoxide and oxygen are gases and adsorb onto the metal surface to react, thus passing through the phase boundary. Oxygen undergoes a process of dissociative adsorption which facilitates the surface reaction with the adsorbed carbon monoxide. The product of this surface reaction is carbon dioxide, which desorbs into the gas phase. After the gases are removed the catalyst may be recycled for further reactions.

Enzymatic catalysis exists between both homogeneous and heterogeneous catalysis. All enzymes generally consist of proteins and have high molecular weights. Generally the active site is highly substrate specific and the overall polymer structure is very complex in character. Supported enzymes are principally used to mimic natural processes such as fermentation of beverages and many biological products. These processes are undertaken with organisms with a large number of enzymes with complex organic molecules. Production of biological products on a commercial scale can be conducted with individual enzymes. Typically the enzyme is bound to a solid such as porous glass or a solid polymer [4]. One such process is the conversion of glucose to fructose over glucose-isomerase ionically bonded to DEAE-cellulose. However, the complex structure is stable at only mild conditions, similar to those found in natural environment.



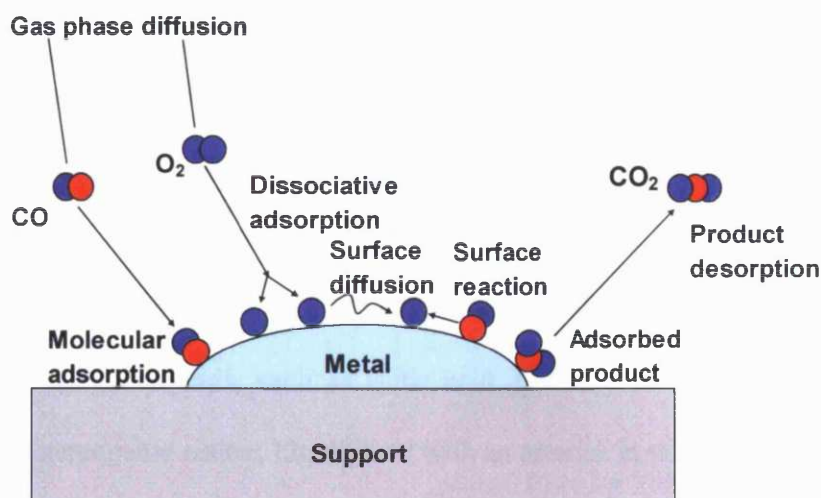


Fig. 1.2 Molecular and atomic events during a catalytic cycle [5]

#### 1.2.4 Selectivity

Reactions carried out over a catalyst typically proceed to a number of products. Particularly for industrial applications the ratio of these products must favour one at the expense of the others. This is termed selectivity, where a reaction must proceed to a large excess of a desired product. Thus, the same reaction over different catalysts can result in different products, due to the different low energy pathways afforded by a particular metal. This phenomenon is illustrated with the catalytic reaction of carbon monoxide and hydrogen over different metals (Table 1.1). The reactions described therein, are thermodynamically viable and have negative values of  $\Delta G_{\text{reaction}}$ .

#### 1.2.5 Chirality and enantiomers

The concept of chirality was borne from investigations carried out in the early 19<sup>th</sup> century. In 1809 the French physicist E. L. Malus discovered plane-polarised light [6]. Light

can be passed through a suitable medium; a polaroid, which only allows light to pass in one plane. The angle of the plane is determined by the line of the molecules in the polaroid. However, it was not until Jean Baptiste Biot placed a solution after the polaroid which rotated the plane of the light was the concept of chirality born [7]. The solution had been described as being optically active and the components of the solution are, therefore, said to be chiral. Organic compounds, such as lactic acid, typically contain a stereogenic centre (Fig. 1.3). The stereogenic centre, highlighted with an asterisk in this case is the carbon atom with the four different substituents attached.

Table 1.1 Selectivity of different products from catalytic reaction of carbon monoxide and hydrogen over different metals

Entry	Reactants	Metal	Products	Industrial Company
1	$\text{CO} + 3\text{H}_2$	Ni	$\text{CH}_4 + \text{H}_2\text{O}$	British Gas, UK
2	$\text{CO} + 2\text{H}_2$	Cu/ZnO/alumina	$\text{CH}_3\text{OH}$	ICI, UK
3	$12\text{CO} + 6\text{H}_2$	Ru, Fe	$\text{C}_6\text{H}_{12} + 6\text{CO}_2$	By-product of Fischer-Tropsch synthesis. Sasol, SA
4	$11\text{CO} + 7\text{H}_2$	Ru, Fe	$\text{C}_6\text{H}_{13}\text{OH} + 5\text{CO}_2$	Sasol, SA

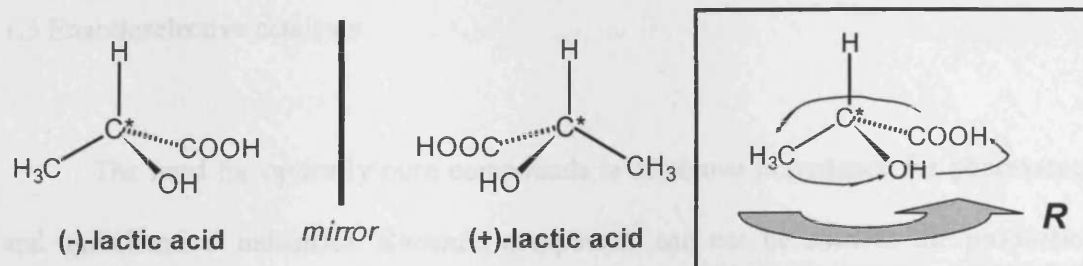


Fig. 1.3 Mirror images of lactic acid. *Insert*: determining enantiomers from substituents, i.e.

(-)-lactic acid is the (*R*)-enantiomer

An enantiomer is defined as the mirror image of a chiral molecule, which can not be superimposed upon the other. Enantiomers can be identified by the rotation of plane polarised light, as the angle of rotation for each is opposite. This phenomenon was identified by Pasteur after experimenting with solutions from a manually separated mixture of recrystallised sodium ammonium tartrate [8]. Later Le Bel and Van Hoff in 1874 expanded on this work, and proposed the theory of quadrivalent carbon [9,10]. Enantiomers are assigned with the identifier *R* or *S*, which derive from the order, according to priority, of the substituents about the stereogenic centre. The nomenclature was proposed by Cahn, Ingold and Prelog in 1966 [11]. This concept is illustrated in the insert of Figure 1.3, where (-)-lactic acid can be described as *R* and the mirror image *S*. Enantiomers have identical physical properties and as such are difficult to separate. However, in the natural world one enantiomer may be utilised in a very different way to the other. In the case of lactic acid, the naturally occurring substance found in muscle tissue is optically active. However, synthetic lactic acid is not, as it is a racemic mixture. This phenomenon is of particular concern for synthetically produced compounds in the pharmaceutical and agrochemical business.

### 1.3 Enantioselective catalysis

The need for optically pure compounds is of utmost importance for pharmaceutical and agrochemical industries. Racemic compounds can not be used in the production of clinical drugs for example, after the thalidomide tragedy. This highlighted the differing effects of certain enantiomers; in this case (*R*)-enantiomer is an effective sedative for prevention of morning sickness in pregnant women, the (*S*)-enantiomer caused foetal damage. Therefore, there is considerable effort to develop strategies to produce the desired enantiomer efficiently and cleanly, which affords great interest in the use of catalysis.

Two strategies will be discussed in the following sections; homogeneous and heterogeneous systems. Both offer advantages and disadvantages in the synthesis of desired enantiomers, which will be highlighted.

#### 1.3.1 Homogeneous enantioselective catalysis

Homogeneous catalysts have demonstrated high activity and selectivity which in some cases rivals the use of enzymes. Typically consisting of a transition metal centre as the active site, in a complex with organic ligands. The choice of ligand and its substituents afford a high degree of reaction tuneability, affording desired products where applicable. Additionally the use of kinetic measurements and spectroscopic studies are more applicable to determine the reaction mechanism than heterogeneous systems. Where the ligands are optically active the reaction proceeds enantioselectively, such as the hydrogenation of pro-chiral olefins using Wilkinson's catalyst  $\{\text{Rh}(\text{PPh}_3)_3\text{Cl}\}$  [3]. The active site is a rhodium atom to which is chemically bound optically active phosphine ligands, forming a chiral environment. Such an environment directs the pro-chiral substrate to the active site and a

chiral product can be formed. The ligands and their various substituents contribute to the sense of enantiomer generated.

However, there are drawbacks to such a system, which give a comparative heterogeneous system an advantage, specifically for industrial applications. The separation of catalyst from the reaction medium can be an involved and difficult process to achieve. Additionally the recovered homogeneous catalyst generally performs poorly upon re-use. From an industrial perspective the amount of usually expensive ligand generally required for high activity and excellent enantioselectivity can be comparable to the amount of substrate. Yet a greater proportion of intermediate fine chemical synthesis is via a homogeneous catalytic route. A commercial example of the use of a homogeneous catalyst used for enantioselective hydrogenation is Rh(DIPAMP) (Fig. 1.4a). This catalyst is used in the production of L-DOPA (Fig. 1.4b), an anti-Parkinson's drug and was the first large scale application of asymmetric hydrogenation [12].

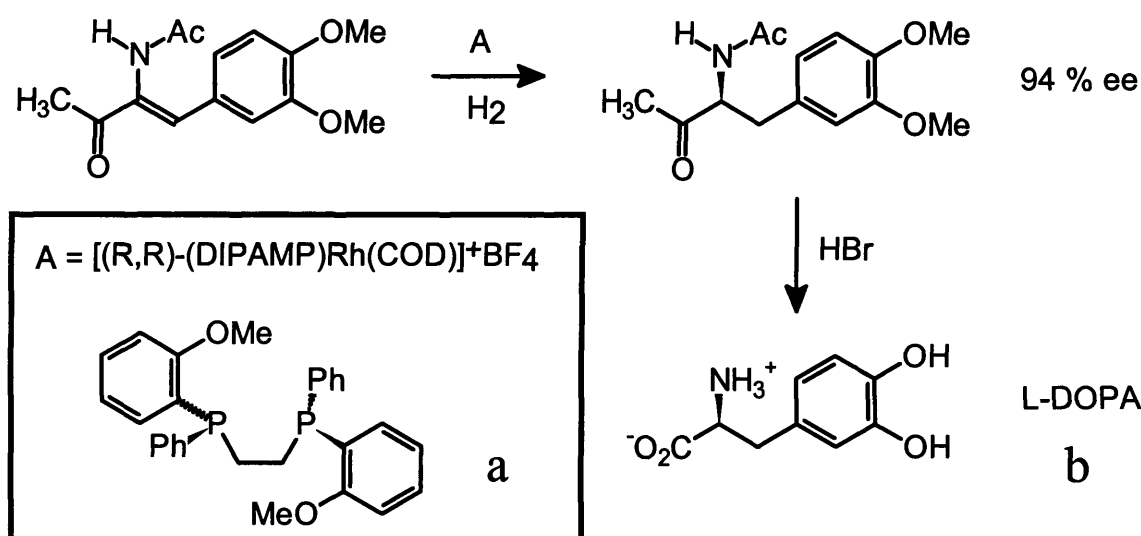


Fig. 1.4 The use of enantioselective homogeneous hydrogenation in the production of L-DOPA

Enantioselective hydrogenation of pro-chiral C=O containing species over homogeneous catalysts have been very successful (Table 1.2). High enantiomeric excesses have been achieved, typically with ruthenium or rhodium based complexes. However, the ligands bound to the metal centre are a vital component in the direction of the enantioselectivity. This is illustrated with the hydrogenation of ethyl pyruvate, where different chiral ligands afford an excess of either (*R*) or (*S*)-lactate (Table. 1.2 entry 1) [13]. Both catalysts contain a ruthenium centre, for an excess of (*S*)-ethyl lactate the ligand (2*S*, 3*S*)-NORPHOS is used. Whereas, to achieve an ee of (*R*)-lactate the ligand used is (2*S*, 4*S*)-BPPM.

Other C=O containing substrates have been successfully hydrogenated enantioselectively with high substrate conversion. Acetophenone can be hydrogenated in the presence of a ruthenium catalyst resulting in high ee > 98 % to (*R*)- or (*S*)-product (Table 1.2 entry 3). In both reactions the ligands bound to the metal centre are a chiral phosphine and a chiral diamine. The chirality of the phosphine in this reaction dictates the enantioselectivity, in agreement with Noyori [14]. For the reaction to the (*R*)-1-phenylethyl alcohol the substrate to catalyst molar ration was high at 20000 [15].

Recently there has been interest in coordinating or immobilising a homogeneous complex on an organic or mineral support. Work reported in [16] details attempts to immobilise novel dirhodium complexes on a silica support (Table 1.2 entry 6). This has many benefits including separation and potential continuous operation. However, with this technique leaching of the metal to the liquid phase remains a concern despite the high ee of (*R*)-pantolactone achieved. Anchoring of a chiral ligand to mesoporous silica which allowed coordination of Rh or Pd complexes has been reported by [17] for enantioselective hydrogenations. The ee was found to be higher than their homogeneous counterparts.

Table 1.2 Values of enantiomeric excess of hydrogenation reactions conducted with homogeneous catalysts

Entry	Reactant	Enantiomeric excess (%)	Catalyst	Ref.
1		89 ( <i>S</i> )	Rh( <i>nbd</i> )Cl <sub>2</sub> + (2 <i>S</i> ;3 <i>S</i> )-NORPHOS <sup>a</sup>	13
		71 ( <i>R</i> )	Rh( <i>nbd</i> )Cl <sub>2</sub> + (2 <i>S</i> ;4 <i>S</i> )-BPPM <sup>b</sup>	
2		1. 97 ( <i>S</i> )	Ru-( <i>S</i> )-BINAP <sup>c</sup>	18
		2. 99 ( <i>R</i> )	Ru-( <i>R</i> )-MeO-BIPHEP <sup>d</sup>	
3		99 ( <i>R</i> )	Ru-( <i>R</i> )-xylyl-PhanePhos <sup>e</sup> (+ ( <i>S,S</i> )-DPEN <sup>f</sup> )	15
		98 ( <i>S</i> )	Ru-( <i>S</i> )-xylyl-PhanePhos <sup>e</sup> (+ ( <i>R,R</i> )-DACH <sup>g</sup> )	
4		72 ( <i>R</i> )	Rh-( <i>R</i> )-BINAP <sup>c</sup>	19
		90 ( <i>R</i> )	Rh-( <i>R</i> )-MeO-BIPHEP <sup>d</sup>	
5		96 ( <i>R</i> )	( <i>R,R</i> )-Ru-BICP <sup>h</sup> (+ ethylthioethylamine)	20
		93 ( <i>S</i> )	( <i>S,S</i> )-Ru-BICP <sup>h</sup> (+ ethylthioethylamine)	
6		91 ( <i>R</i> )	Soluble di-Rh <sup>i</sup>	16
		91 ( <i>R</i> )	Silica supported di-Rh <sup>j</sup>	

*nbd* = norbornadiene; *a* = (2,3)-bis-(diphenylphosphino)-bicyclo-[2.2.1]-hept-5-ene;

*b* = (2,4)-bis-(*para*-phosphophenyl)methane;

*c* = 2,2'-bis(diphenylphosphino)-1,1'-binaphthyl; *d* = 6,6'-dimethoxy-2,2'-bis(diphenylphosphino)-1,1'-biphenyl; *e* = 4,12-bis(diphenylphosphino)-[2.2]paracyclophane; *f* = 1,2-diphenylethylenediamide;

*g* = *trans*-1,2-diaminocyclohexane; *h* = (2,2')-bis(diphenylphosphanyl)-(1,1')-dicyclopentane; *i* = di( $\mu$ -

carboxylato)bis(aminophosphinephosphinite)dirhodium; *j* = silica supported-*i*

### 1.3.2 Heterogeneous enantioselective catalysis

An advantage of a heterogeneous catalytic strategy over a homogeneous system is the separation of product and catalyst. This represents a cost advantage, as costly separation is replaced by simple filtration in the case of the heterogeneous system. There are also advantages with respect to 'green' chemistry and application of continuous operation. Hence why there is currently large interest in heterogeneous enantioselective catalysis.

However, the use of a supported metal to catalyse a reaction enantioselectively is difficult to achieve. The metal surface is non-specific; that is the reaction would produce either *R* or *S*, but in the same quantity i.e. racemic. To achieve enantioselectivity the reaction must take place in a chiral environment, which includes the metal atoms that constitute the active site. Examples of this are the dehydrogenation of the racemic butan-2-ol by Schwab *et al.* in 1932 [21]. The reaction took place over quartz supported Pt, Pd, Ni and Cu catalysts. The chiral environment was generated by the quartz, after cleaving the surface of the crystals to expose an available enantiomorph. An enantiomeric excess of ca. 10 % was obtained. Natural fibres were later used to support several metals for the hydrogenation of  $>C=N-$  and  $>C=C<$  functions. Akabori *et al.* [22] used silk fibroin in 1956, polysaccharides were used by Balandin *et al.* [23] in 1959 and cellulose was employed by Harada *et al.* in 1970 [24]. The Pd/Silk catalyst achieved 66 % ee, however, the results proved un-reproducible [22]. For the other fibres the enantiomeric excess achieved was found to be very low.

Another technique used to generate a chiral environment at a metal surface has been the addition of a chiral molecule. This was first shown in 1939 with the publication of results from modifying nickel with glucose and platinum with a hydrocinchonine salt by Lipkin and Stewart [25]. For the reaction involving the modification of platinum, the salt was from the compound  $\beta$ -methyl-cinnamic acid. The resulting optical yield of the hydrogenation to  $\beta$ -



phenylbutyric acid was shown to be ca. 8 %. The use of chiral acids to modify Pt and Ni catalysts was undertaken by Nakamura [26] in 1940 and later Isoda [27] and Izumi [28]. Forming the basis to what has become the well known enantioselective catalytic system; Raney Ni/tartrate/NaBr for the hydrogenation of  $\beta$ -ketoesters. Izumi achieved an ee of 92 % in 1960 with this system which demonstrated that heterogeneous enantioselective catalysis was viable and efficient [29]. However, there are only two reaction systems for hydrogenation of C=O containing compounds that have shown such high values of enantiomeric excess. The other system was discovered by Orito and co-workers in 1979 [30]. Their system comprised cinchona alkaloid modified supported platinum catalysts for the hydrogenation of  $\alpha$ -ketoesters. This system will now be discussed in detail.

#### 1.4 The Orito Reaction: Enantioselective Hydrogenation of $\alpha$ -Ketoesters over Cinchona-modified Platinum

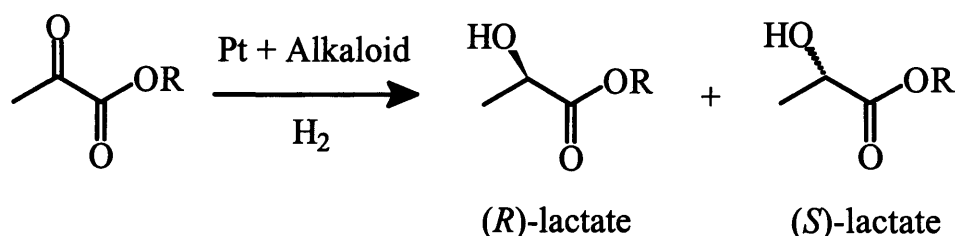


Fig. 1.5 The Orito reaction. Where R = CH<sub>3</sub>; methyl pyruvate, C<sub>2</sub>H<sub>5</sub>; ethyl pyruvate

In 1979 the Orito group in Japan reported the first enantioselective hydrogenation of  $\alpha$ -ketoesters over cinchona modified platinum catalysts [30,31,32] (Fig. 1.5). Pre-treatment of the catalyst (5 % Pt/C) was conducted by stirring in a 1 % solution of either cinchonidine (Fig. 1.6a) or quinine for 20 h. This modified catalyst was used to hydrogenate methyl pyruvate and preferentially gave (*R*)-methyl lactate in high excess. Where the pre-treatment involved the near enantiomer cinchonine (Fig. 1.6b) the opposite sense was preferentially

produced, that is (*S*)-methyl lactate. It was shown that in the absence of cinchona modifiers the rate of reaction was found to be substantially slower. Modification of the catalyst gave a rate enhancement for this reaction up to a factor of 100. However, the enhancement is commonly found to be a factor of 20 to 40. The reaction is nominally carried out in the liquid phase in a stirred tank reactor at ambient temperature and elevated pressure. Orito and co-workers investigated catalyst preparation and the choice of carbon support yielded variations in the ee. The differences in ee was attributed to the catalyst morphology; specifically the mean Pt particle size. Pre-heating the catalyst in an atmosphere of hydrogen prior to modification was studied. They found that heating to 573 K was optimal; resulting in an improved enantioselectivity.

#### 1.4.1. Cinchona alkaloids

The adsorption of a chiral molecule on to the metal surface of a heterogeneous catalyst has the potential to direct the formation of products enantioselectively. In practice, however, this supposition is applicable to currently only two systems;  $\beta$ -ketoesters/tartaric acid modified Ni and  $\alpha$ -ketoesters/alkaloid modified Pt; the Orito reaction.

The exact nature of the adsorption and subsequent enantioselective site during the Orito reaction remains debatable. Several theories have been suggested and work in this area is still very active. The following will be discussed; the structure of the cinchona alkaloids, their adsorption onto Pt, the proposed enantioselective site and diversification of the modifier.

## 1.4.2 Alkaloid structure

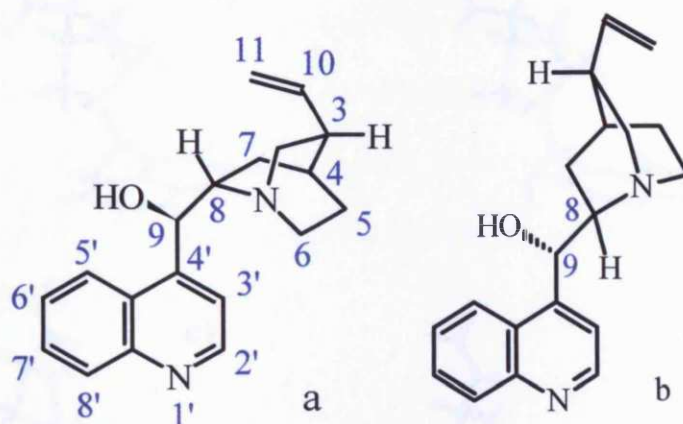


Fig. 1.6 The structure of cinchonidine (a) and cinchonine (b)

Cinchonidine (Fig. 1.6a [33]) and its near enantiomer cinchonine (Fig. 1.6b) consist of two relatively rigid entities connected by a functionalised carbon atom. The carbon atoms are numbered, such that the separating C atom is termed C<sub>9</sub>. The first entity is an aromatic quinoline ring, the second an aliphatic quinuclidine ring which has an additional vinyl group attached to C<sub>3</sub>. The molecule contains four chiral centres; C<sub>3</sub>, C<sub>4</sub>, C<sub>8</sub> and C<sub>9</sub>, for cinchonidine C<sub>8</sub> and C<sub>9</sub> are configured *S* and *R* respectively. This is reversed for cinchonine; that is C<sub>8</sub> are configured *R* and C<sub>9</sub> *S*. The conformation of cinchonidine is principally determined from the two torsional angles  $\tau_1$ : C<sub>3</sub>'-C<sub>4</sub>'-C<sub>9</sub>-C<sub>8</sub> and  $\tau_2$ : C<sub>4</sub>-C<sub>9</sub>-C<sub>8</sub>-N<sub>1</sub>. About these angles the molecule displays hindered rotation. From those six conformers, optimisation results in four conformers of minimum energy. These have been labelled *closed 1*, *closed 2*, *open 4* and *open 3* (Fig. 1.7a/b/c/d). A 'closed' conformation indicates that the lone pair of the N in the quinuclidine ring points to the quinoline moiety. Whereas, an 'open' conformation denotes that the lone pair points away from the quinoline ring.

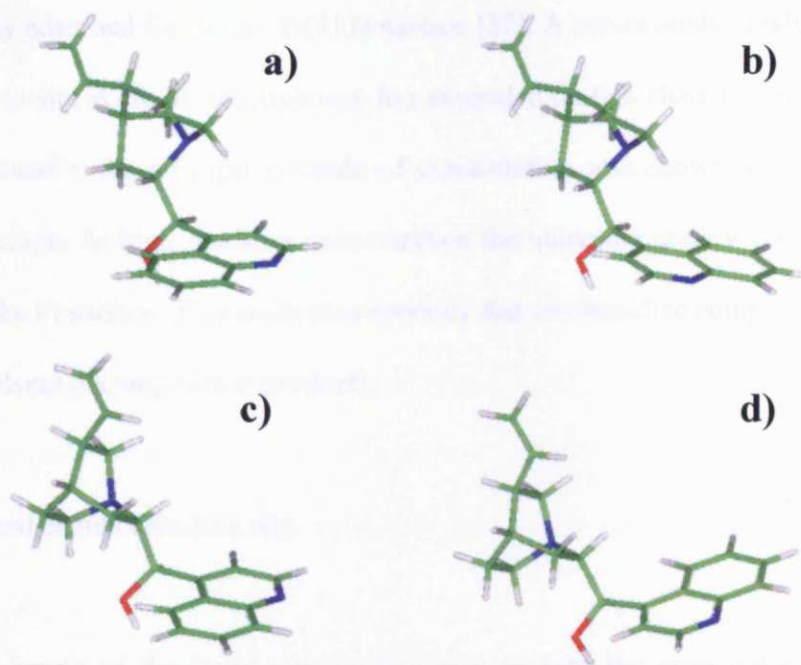


Fig.1.7 Low energy conformers of cinchonidine:

a) closed 1, b) closed 2, c) open 4, d) open 3

### 1.4.3 Alkaloid adsorption

The use of Cinchona alkaloids with supported Pt catalysts were shown to be enantioselective for pyruvate ester hydrogenation. The enantioselectivity was suggested to arise from adsorption of the alkaloid on the Pt surface, forming a chiral active site. Blaser and co-workers proposed that the cinchona molecule adsorbs via the quinoline ring moiety [34]. This was supported by deuterium exchange experiments carried out by Wells *et al.* which demonstrated the protons on the quinoline ring were exchanged [35]. Additionally the hydroxy H on C<sub>9</sub> was rapidly exchanged for D, however, no exchange took place on the quinuclidine ring. The vinyl group of C<sub>10</sub> and C<sub>11</sub> has been shown experimentally to be relatively easy to hydrogenate under reaction conditions [36]. This has been supported by ultrahigh-vacuum NEXFAS investigations which revealed that 10,11-dihydrocinchonidine is

preferentially adsorbed flat to the Pt(111) surface [37]. A recent study conducted by Baiker *et al.* using in situ ATR-IR spectroscopy has expanded on this close to reaction conditions [38]. Additionally, the adsorption mode of cinchonidine was shown to be dependent on surface coverage. At high modifier concentration the quinoline moiety was found to angle away from the Pt surface. This study also revealed that cinchonidine competes for adsorption sites with solvent decomposition products.

#### 1.4.4 Proposed enantioselective site

This aspect of the Orito reaction has been perhaps the most debated amongst the various groups. Wells first proposed the *Template Model* to interpret the enantioselectivity of (*R*)-lactate obtained through adsorption of cinchonidine on a supported Pt surface [39]. The model describes ordered arrays of alkaloid adsorption on the platinum surface. Such that the substrate can only adsorb on free Pt in a certain way or enantiofacially. This model could explain the sense of enantioselectivity when cinchonidine or cinchonine is adsorbed. However, the model was let down by the experimental data available [40]. Chiefly, that at low modifier concentration an enantiomeric excess was still obtained and that it was relatively high compared to higher concentrations. This prompted Augustine to postulate that the chiral active site was at the edge and corner sites of the platinum particle [41]. A further study of the alkaloid 10,11-dihydrocinchonidine on Pt(111) with XPS, LEED and NEXFAS disproved this theory [42]. The alkaloid adsorbed via the quinoline ring, however, the adsorption was not ordered. From these investigations it was additionally theorised that an interaction between the quinuclidine N of the adsorbed alkaloid and the substrate was via a half hydrogenated state (Fig. 1.8a) [43].

The strong interaction of cinchonidine and pyruvate in solution prompted Margitfalvi to theorise that the reaction took place principally in the liquid phase [44]. The surface of the platinum activates the hydrogen and presents it to the incoming 1:1 complex of alkaloid and reactant. From NMR, kinetic measurements and molecular modelling the quinoline ring of the alkaloid was shown to *chemically shield* one side of the C=O bond. This model then ascribes that the enantioselectivity is achieved in the liquid phase interaction of modifier and substrate. However, activation of hydrogen can occur on all of the group 8 to 10 metals and as such the reaction should proceed with those metals as catalysts, this is not the case.

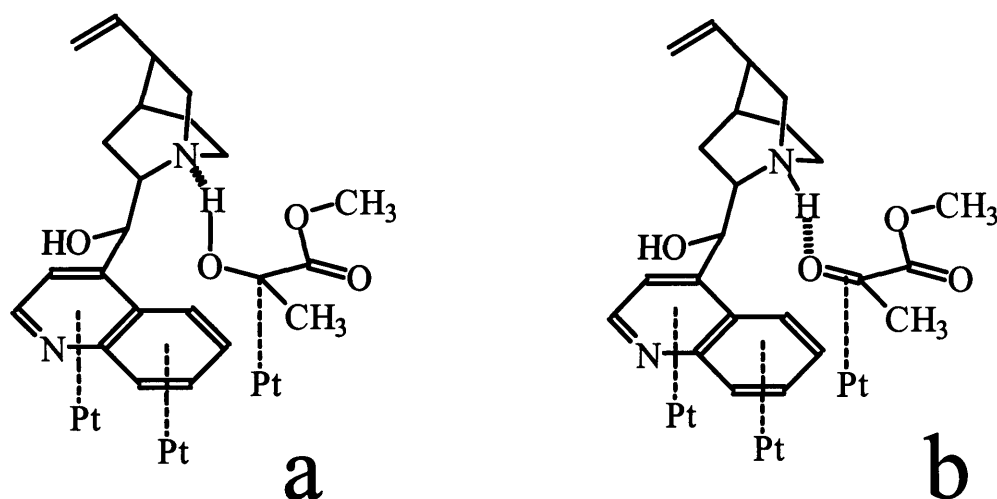


Fig. 1.8 Representation of the proposed intermediate states of the enantioselective hydrogenation of methyl pyruvate.

Another model was proposed by Baiker and co workers with the aim to address the experimental shortcomings of the *Template Model*. Specifically that at very low modifier concentration high enantioselectivity was still achievable [34]. The proposed model describes a 1:1 interaction between adsorbed alkaloid and the pyruvate [43]. The quinuclidine N is able to interact with the substrate as either a nucleophile or after protonation in an acidic medium as an electrophile. This interaction is assumed to arise from

the *open 3* conformation of the adsorbed alkaloid and the pyruvate adsorbed flat via the  $\pi$ -system (Fig. 1.8a/b).

This conformation is prevalent in apolar or acidic media, in which the highest enantioselectivities have been achieved. Furthermore, methylation of the quinuclidine N of cinchonidine results in complete loss of enantioselectivity [45]. Therefore, the substrate adsorbs enantiofacially adjacent to the modifier, termed *pro-(R)* or *pro-(S)*-pyruvate (Fig. 1.9), which dictates the hydrogenated chiral product. Molecular calculations were undertaken which revealed that the *pro-(R)* exists at a lower energy in a complex with cinchonidine, whereas, the reverse is true of *pro-(S)* with cinchonine [46].

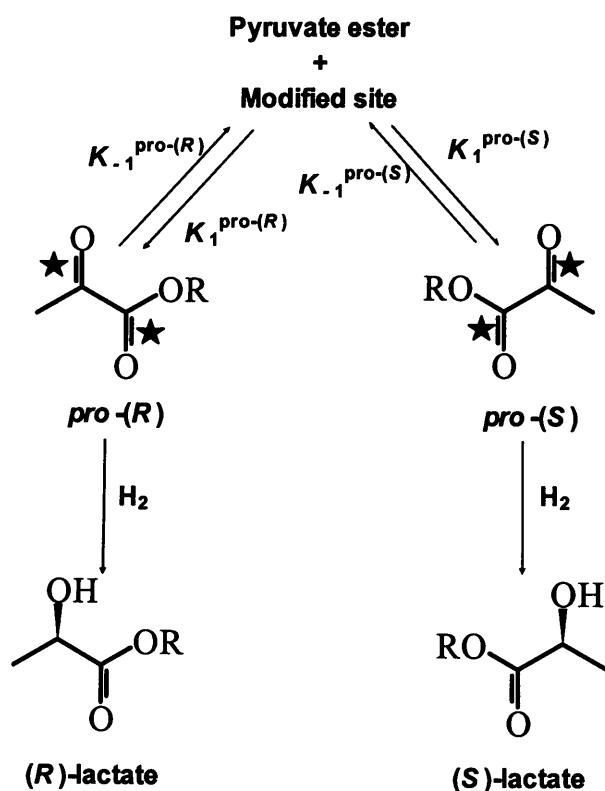


Fig. 1.9 Pyruvate ester adsorbed enantiofacially {*pro-(R)* and *pro-(S)*} and the subsequent hydrogenation products

Adsorption of the pyruvate has been investigated both computationally and experimentally. There are four possible adsorption modes in a complex with cinchonidine; *pro-(R)* and *pro-(S)* in *cis* or *trans* conformations. It was determined that for the *trans pro-(R)* isomer of methyl pyruvate an ee of 92 % was calculated, compared to 17 % for the *cis* [47]. This is due to the lower energy of the *trans* pyruvate-alkaloid complex [48]. However, this model assumes that the pyruvate is adsorbed flat to the Pt surface via both the unsaturated carbonyl groups [49]. Recent XANES studies have shown that the angular plane with respect to the surface was determined to be 72° [50]. This decreased to 58° under an atmosphere of hydrogen. Recent DFT work by Willock *et al.* has shown that for simple C=O containing compounds such as acetone, offer a different adsorption mode [51]. The calculations indicated that C=O preferentially adsorbed 'end-on' to the Pt surface. Yet for hydrogenation to occur the pyruvate must be nearly flat or flat to the surface, therefore, more work is required.

Currently the proposed enantioselective site for hydrogenation of pro-chiral C=O containing compounds is a 1:1 interaction with alkaloid in an *open 3* conformation at the platinum surface.

### 1.5 Further Work on the Orito Reaction

A great number of preparative and reaction variables have been investigated since the Orito reaction was first reported. Two groups; Wells (University of Hull) and Blaser (Ciba-Geigy, Basle) revived interest in the reaction *ca.* 1986. A third group, that of Baiker (ETH, Zurich) began collaborating with Blaser shortly there after. Since then many groups around



the world have investigated this reaction, of note are Margitfalvi (Hungarian Academy of Sciences, Budapest) and Blackmond (Max-Planck, Mülheim an-der-Ruhr).

### 1.5.1 Catalyst

Catalyst preparation and subsequent reduction have been shown to have a large influence on the enantiomeric excess of  $\alpha$ -ketoester hydrogenation. The platinum may be supported on alumina, silica, titania, carbon or zeolites [52]. Studies carried out by Wells *et al.* used a silica supported catalyst; the reference catalyst 6.3 % Pt/SiO<sub>2</sub> EUROPT-1 [53] which obtained an ee of 77 % [39]. More commonly used is an alumina supported catalyst (5 % Pt/Al<sub>2</sub>O<sub>3</sub>), used by Blaser, Baiker and Blackmond. The alumina supported catalyst was found to be the most effective with >80 % ee achievable with little optimisation [54]. Of particular importance to the outcome of such hydrogenation reactions are metal particle size and the dispersion [55]. The EUROPT-1 catalyst has a reported mean particle size of 2 nm and a dispersion of 60 %. This compares to the alumina supported catalyst which has a platinum particle size of 3 to 4 nm, with a much lower dispersion of 10 to 20 %. The larger platinum clusters on the alumina were reported to be more effective for enantioselectivity and activity [56]. However, work by Zuo *et al.* with polyvinylpyrrolidone stabilised Pt clusters gave the highest reported ee of 97 % [57]. The mean size of the platinum clusters was 1.4 nm. The particular importance of metal particle size for this reaction may be due to the distribution of exposed face, edge or corner atoms and therefore the variation on organic adsorption potentials [58].

The morphology of the supported platinum is a vital component in enantioselective hydrogenation of pro-chiral compounds. The relationship between metal particle size and ee is well known, however, less is known about the effect of the metal crystal morphology.

EUROPT-1 is described to have metal particles arranged as a 'raft' consisting of about 55 Pt atoms configured as 7x7 in (111), with a further 8 atoms lying on top [59]. This gives the platinum a dispersion of about 60%. The effect of heating in hydrogen on this catalyst is pronounced. Increasing the reduction temperature increases the ee but the rate is reduced indicating either change in particle size and/or metal morphology. Heat pre-treatment generally leads to low index planes, which have been postulated to improve enantioselectivity with the Orito reaction. This is supported by the reduced selectivity for catalysts with mean metal particle sizes below 2 nm with supported catalysts. However, pre-heating Pt/Al<sub>2</sub>O<sub>3</sub> in air or a vacuum leads to no improvements in enantioselectivity [60]. The morphology of the platinum was found to be cube like with facets under hydrogen after heating to 450-625°C, compared to spherical particles under air or N<sub>2</sub> [61,62].

The morphology of the metal is determined by the platinum pre-cursor and the support. It has been noted in [63] where preparative methods of Pt/Al<sub>2</sub>O<sub>3</sub> catalysts were found to be crucial for ethyl pyruvate hydrogenation. Directly reducing the catalyst chemically with formaldehyde, without drying or calcining gave 94 % conversion and 80 % ee after 17 h. Compared to a more traditional approach with drying and calcining in an atmosphere of hydrogen, which obtained a conversion of ca. 100 % and an ee of 95 % in 0.2 h. The mean particle size of platinum for the former method was 3.9 nm and for the later; 3.1 nm. However, it was determined that the interaction of Pt with the support were crucial to the activity. From XRD measurements the former method presented more diversity concerning platinum index planes compared to the later preparative method.

The influence of the support on directing the morphology of the Pt particle has been reported [64]. Mallet and co-workers determined with HRTEM investigations that after hydrogen pre-treatment faceted particles were observed only on crystalline  $\gamma$ -alumina.

Whereas, on less crystalline regions of the  $\gamma$ -alumina the Pt particles were found to be more spherical in shape.

The choice of support can play an important role in the enantioselective hydrogenation of pyruvate esters (Table 1.3). The influence of the support characteristics affect the metal and hence the activity in a number of ways. These include the method of metal addition, through techniques such as incipient wetness, reduction-deposition and ion-exchange along with the solvent used in each case. This can be seen when comparing the residual chloride present after reduction of Pt/SiO<sub>2</sub> and Pt/Al<sub>2</sub>O<sub>3</sub> catalysts prepared with aqueous chloroplatinic acid [59]. The alumina supported catalyst retained a considerable amount of chloride, compared to very little for Pt/SiO<sub>2</sub>. Where chloroplatinic acid has been dissolved in water the strength of adsorption is stronger on alumina than carbon. When dissolved in acetone the opposite is true, this affects the distribution of metal through the support [59, 60]. Stronger adsorption generally results in an egg shell distribution, whereas, weaker adsorption leads to a more uniform distribution. This can be advantageous in certain reactions and reactor types, 'egg shell' catalysts being particularly useful for continuous operation where mass transfer can be limited. The use of different metal salts can similarly affect the dispersion and morphology. Chloroplatinic acid is adsorbed much more strongly on alumina and carbon compared to Pt(NH<sub>3</sub>)<sub>4</sub>Cl<sub>2</sub> [60]. This strength of adsorption can be affected by the amount of surface oxygen present.

Sonification of the catalyst and of the catalyst in the presence of cinchonidine and hydrogen has improved the enantioselectivity in pyruvate hydrogenation. The former technique resulted in the highest observed ee of up to 98 % for (*R*)-lactate [61]. Investigations of the effect of using sonification have determined that at an optimal ultrasound frequency decreases the metal particle size and leads to a more homogeneous

metal particle-size distribution. Further sonification at higher than the optimal frequency or for longer time periods was found to be detrimental.

Table 1.3 Enantiomeric excess of (*R*)-ethyl lactate achieved over different supported Pt catalysts

Entry	Support	Catalyst	ee (%)	Ref
1	Alumina	5 % Pt/Al <sub>2</sub> O <sub>3</sub>	95	39
2	Silica	6.3 % Pt/SiO <sub>2</sub> (EUROPT-1)	77	33
3	Carbon	5 % Pt/C <sub>g</sub>	75	30
4	MCM-41	1.6 % Pt-MCM-41	64	68
5	PVP*	Pt-PVP	97	57

\* = polyvinylpyrrolidone

Recently it has been shown by Hess *et al.* that catalyst pre-treatment involving stirring in toluene for 1 h in the presence of cinchonidine had a dramatic effect on the particle size and distribution [69]. Prior to stirring in toluene the catalyst underwent heat treatment in H<sub>2</sub> at 400°C, this had a broadening effect on the particle-size distribution and enlargement of mean particle size. After stirring in toluene with dissolved CD the particle size and distribution reverted back to a smaller range. The subsequent effect on the enantioselective hydrogenation of 3,5-di-(trifluoromethyl)-acetophenone increased substantially. Yet TEM images reveal little difference between untreated catalyst and heat and solvent/CD pre-treatment. Thus it was postulated that the CD ‘re-shapes’ the platinum surface yielding improved active sites. Yet the chirality of the modifier was unimportant, using quinoline during pre-treatment only modestly decreases the ee.

### 1.5.2 Other Metals Investigated

The Orito reaction has been investigated with other group 10 and noble metals. These include iridium, rhodium, ruthenium and palladium. Where the Orito reaction has been carried out over supported iridium catalysts, little or no enantioselectivity was achieved [70]. However, up to 40 % ee can be achieved when the catalysts were prepared within a narrow range of calcinations and reduction temperatures; 250-300°C [70]. With face-centred cubic structure, iridium resembles platinum. Yet no rate enhancement was observed with the use of an alkaloid modifier.

Rhodium metal has been used successfully in homogeneous enantioselective catalysis [13] and as a nanocluster stabilised with polyvinylpyrrolidone [71] in enantioselective  $\alpha$ -ketoester hydrogenation. Only one report of cinchonidine-modified Rh/Al<sub>2</sub>O<sub>3</sub> exists, where 20-30 % ee was achieved with ethyl pyruvate hydrogenation [55]. However, this has not been repeated in other laboratories.

The use of ruthenium for racemic [55] and enantioselective hydrogenations has been investigated with heterogeneous catalysts. When employed in homogeneous enantioselective catalysts, ruthenium has proved very successful for simple ketone hydrogenation [72]. Methyl pyruvate was hydrogenated over a cinchonidine modified 20 % Ru/SiO<sub>2</sub> catalyst, however, only achieving enantioselectivity in 5 % of reactions [55]. This was thought to arise from hydrogen being unable to remove surface oxygen, thus preventing absorption of reactant at chiral sites. Rate enhancement was shown with alkaloid modification and an ee of 10-12 % (*R*)-lactate was achieved in ethanol at 10 bar and 25°C under propyne (2 bar) [73].

When using supported palladium catalysts for the Orito reaction modified with cinchonidine the optical yield was in favour of (*S*)-lactate. Blaser *et al.* first reported the phenomenon of a low ee, favouring (*S*)-lactate over cinchonidine modified Pd/C [55].

Further investigations by Wells and co-workers revealed that the mechanism of pyruvate ester hydrogenation over Pd is different to that over Pt [74]. There were five main observations; (i) rate enhancement was absent upon alkaloid addition. (ii) The rate was determined to be half order with respect to hydrogen, compared to first order over Pt. (iii) Solvent choice was found to be more crucial in this reaction with palladium. (iv) Reduction temperature of Pd was beneficial for an increase in ee only at low temperatures, unlike for Pt. (v) When reacted in presence of deuterium the products formed over Pd were  $CX_3CX(OX)COOCH_3$  (where X=H or D). This compares the products formed over Pt which are limited to  $CH_3CX(OX)COOCH_3$ . This observation is the most important as it shows that the mechanism of hydrogenation for pyruvate over Pd occurs via the enol isomer at the  $\alpha$ -keto. However, this phenomenon only occurs when the catalyst has been modified under aerobic conditions [75]. Formation of the enol form of pyruvate has been deemed the rate determining step. As the hydrogenation of C=C is rapid over Pd, as a result it has found applications in enantioselective hydrogenation of C=C containing compounds [33].

Work by Collier *et al.* has shown that Pd can be used to hydrogenate pyruvate ester enantioselectively to the same enantiomer as the cinchona-Pt system [76]. Using colloidal stabilised Pd modified with cinchonidine it was found that solvent choice or substrate (methyl/ethyl pyruvate) could reverse the sense of enantioselectivity.

### 1.5.3 Other pro-chiral substrates

The Orito reaction has been applied to many other C=O containing pro-chiral compounds (Table 1.4) which were compiled by Baiker for a review [43]. These include  $\alpha$ -diketones (2,3-butanedione and 1-phenyl-1,2-propanedione) {entry 1,5}, pyruvate esters {2},  $\alpha$ -keto acetals {3},  $\alpha,\beta$ -diketones {4}, ketoacids {6}, trifluoroacetophenone {7} and

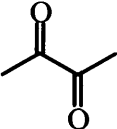
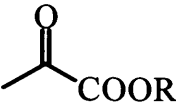
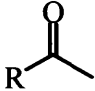
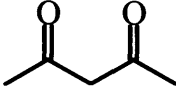
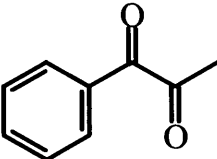
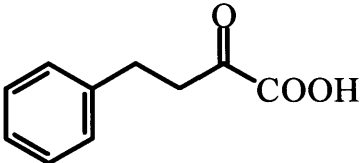
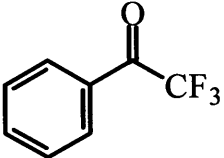
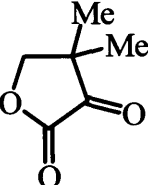
ketopantolactone {8}. Illustrated in Table 1.4 are the structure of the compound and the highest enantiomeric excess achieved. The following section will focus in detail on the  $\alpha$ -diketones; specifically 2,3-butanedione.

### 1.5.3.1 $\alpha$ -Diketones

The application of the  $\alpha$ -diketone, 2,3-butanedione to the Orito reaction has been less well studied and as such was chosen for study in this project. Enantiomerically pure hydroxyketones have found use as intermediates in the production of antifungals and chiral amino alcohols. These are used in the pharmaceutical industry and in particular the azole antifungals are of great interest for drugs to combat AIDS [77]. As such a heterogeneous enantioselective catalytic route would be attractive.

Vermeer and co-workers first reported the enantioselective hydrogenation of 2,3-butanedione in toluene over EUROPT-1 modified with cinchonidine [78]. The reaction proceeds to a hydroxyketone and then to a diol, this occurs in separate stages (Fig. 1.10). The initial hydrogenation which is termed *first stage* occurs exclusively until very little starting material remains. Where upon the reaction enters the *second stage* and the product from the first stage (hydroxyketone) undergoes further hydrogenation to the corresponding diol. Further work by Wells *et al.* identified several aspects of the modified reaction [79]. A third stage was shown to be present in which dimer molecules formed during the first stage are slowly hydrogenated to diol. The formation of dimers was found to only form in the presence of alkaloid. A modest enantiomeric excess of (*R*)-hydroxyketone is achieved in the first stage, typically between 20-40 %. During the second stage this value increases substantially to ca. 62-89 % through kinetic resolution of the minor enantiomer; (*S*)-hydroxyketone.

Table 1.4 Values of enantiomeric excess achieved with different substrates over  
cinchonidine modified platinum

Entry	Reactant	Enantiomeric excess (%)	Ref.
1		38	78
2	 R = Me, Et	95	48
3	 R = Alkyl, Aryl	12	40
4		20	40
5		65	80
6		82	81
7		61	82
8		92	83



Yet the chemical yield of the (*R*)-hydroxybutanone was very low ca. < 10 % by this stage. Additionally reported was the severe discrepancy between the rates of the first and second stages, found to be ca. 1275 mmol/h/g<sub>cat</sub> compared to ca. 30 mmol/h/g<sub>cat</sub> respectively. The effect of alkaloid addition to the reaction yields only a modest enhancement in rate of ca. 10-20 %.

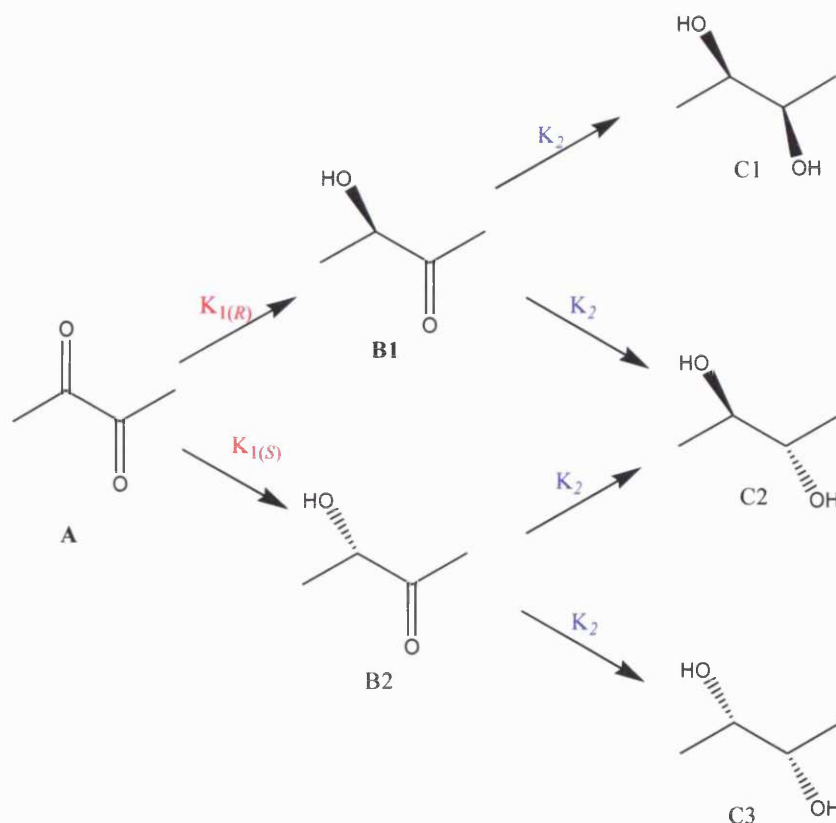


Fig. 1.10 Reaction pathways for the hydrogenation of 2,3-butanedione (A) to the first stage product, hydroxybutanone (B) and the second stage product; butandiol (C)

The effect of oxygen in this reaction was investigated and showed analogous results to the pyruvate ester system. Careful removal of oxygen from the solvent and substrate dramatically suppressed the rate of reaction and the enantiomeric excess to ca. 220 mmol/h/g<sub>cat</sub> and ca 5-8 % ee respectively. The effect of solvent and the addition of water to the reaction of butanedione have been reported over cinchonidine modified 5 % Pt/Al<sub>2</sub>O<sub>3</sub>

[84]. The solvents used were dichloromethane, ethanol, toluene and a toluene/1 M acetic acid mixture. A linear relationship exists of decreasing ee of (*R*)-hydroxyketone and increasing the dielectric constant of the solvent. In toluene an ee of 47 % was achieved compared to 44 % and 28 % for DCM and ethanol respectively. The use of an acid additive in toluene had a detrimental effect on the ee, the opposite is true for pyruvate ester hydrogenation. Doping of DCM with water was reported to be beneficial for methyl pyruvate due to the increased presence of pyruvic acid, from hydrolysis of the ester linkage. The increased acid content of the reaction mixture increases the distributional concentration of *open 3* cinchonidine and hence increases the ee. This obviously can not occur with the dione, resulting in no ee increase.

It was concluded that the sense of enantioselectivity of hydroxybutanone was achieved in an analogous way to that of pyruvate to lactate. That is a 1:1 interaction is formed between substrate and the adsorbed modifier on the surface of the platinum. The sense of enantioselectivity arises from the enantiofacial adsorption of the substrate, that is, *pro-(R)* or *pro-(S)*.

Studer *et al.* obtained similar results with modified 5 % Pt/Al<sub>2</sub>O<sub>3</sub> and achieved an ee of 50 % with 10,11-dihydrocinchonidine in toluene [85]. They described that the ee increased due to kinetic resolution.

Polymer-stabilised platinum nano-clusters have been used to hydrogenate butanedione in acetic acid and ethanol. The addition of cinchonidine gave modest ee to the (*R*)-hydroxybutanone of ca. 25 %. The optimal modifier concentration was investigated and reported as ca.  $2.2 \times 10^{-3}$  mol/L. This corresponds to a modifier:reactant ratio of 1:650, much higher when compared to the hydrogenation of methyl pyruvate at 1:13000 [86]. This was understood to be due to the stronger adsorption of the diketone on the Pt surface compared to pyruvate, similar to the findings of Wells [79]. Dimer formation was reported

with immobilized PVP-Pt clusters on alumina and additionally were used to ascertain solvent effects on the hydrogenation of 2,3-butanedione. When the reaction was carried out in acetic acid the conversion was 80 % and the ee 31 % at 60 min. this compared to 25 % conversion and 24 % ee for the same reaction time in dichloromethane. Dimer formation was reported, however, this was thought to arise from the reaction between ethanol, as the solvent, the dione or hydroxyketone and the residual HCl from Pt cluster preparation. The basic effect of the modifier was also found to be beneficial in neutralising acid catalysed hemiketal formation. This phenomenon was the opposite of that reported by Wells over supported platinum catalyst [79].

The addition of an electron withdrawing group has been shown by [80] to increase the ee of hydroxyketone by weakening the adjacent C=O. Hydrogenation of 1-phenyl-1,2-propanedione (Table 1.4 entry 5) over cinchonidine modified 5 % Pt/Al<sub>2</sub>O<sub>3</sub> gave the main products; (*R/S*)-1-hydroxy-1-phenyl-2-propanone of ca. 65 % ee (*R*) at 50 % conversion. Significantly the main hydroxyketone product formed acts as a key intermediate in the synthesis of many pharmaceuticals, for example L-ephedrine [87]. Above 50 % conversion the ee increased, through kinetic resolution similar to that of 2,3-butanedione hydrogenation and approached 100 %. It was noted that dimer formation was absent which was attributed to the increased reactivity compared to 2,3-butanedione. However, in the absence of modifier the phenyl ring system of the reactant could be hydrogenated albeit to low yields of < 5 %. This observation indicated that the adsorption of the substrate was tilted, as hydrogenation of the ring system could only occur when planar to the surface. Further work yielded that the optimum concentration of modifier went through a maxima and was close to a 1:1 molar ratio of modifier to surface Pt, corresponding to a substrate to modifier ratio of 370:1 [88]. Compared to 2,3-butanedione, the bulky phenyl substituent clearly effects the amount of modifier allowable at the surface. Furthermore the presence of alkaloid gave only a modest

rate acceleration of up to 30 %. The effect of solvent was studied experimentally and with computational methods. Toukonitty *et al.* determined that no correlation was observed between solvent dielectric constant and rate. Moreover, increasing the solvent dielectric constant caused a decrease in ee in a non-linear manner, being ca. 0 % in methanol. This compares to the linear decrease of ee for 2,3-butanedione [80]. However, for both substrates the highest enantiomeric excess was reported to be with toluene.

#### 1.5.4 Alkaloid modifier concentration

The concentration of the modifier in heterogeneous enantioselective hydrogenation is a vital component to the success of achieving a high ee. This aspect of such reactions are well known, having been extensively investigated [89]. Generally the enantiomeric excess and maximum rate pass through a maximum value with increasing alkaloid concentration. An explanation of this phenomenon concerns the surface coverage of alkaloid on the metal. At low concentrations the numbers of enantioselective sites available to the reactant are limited and thus the ee and rate are decreased. This is due to the much lower rate of reaction on unmodified racemic metal sites. The effect of increasing the concentration above the maxima was found to be similar. This was explained by overcrowding of the metal surface with alkaloid, through competitive adsorption with the substrate. The modifier effectively becomes a poison and hence the drop in enantiomeric excess and maximum rate. Blaser suggested that at higher surface coverage the chiral-active site is occupied by an alkaloid molecule [90]. A further explanation has been put forward by Stohr *et al.* involving investigations with NEXAFS spectroscopy [91]. This technique indicated that where there is surface crowding, the modifier adsorbs via the N atom on the quinoline ring system. This was analogous to the effect of temperature, where the quinoline ring is inclined at ca. 60° at

a temperature above 50°C [40]. At this angle the enantioselective environment is disrupted and the ee and rate decrease.

Interestingly the optimal alkaloid concentration can be affected by the solvent used as shown by Blaser [84]. With toluene as the solvent the maximum ee and rate achievable occur when there is one molecule of alkaloid per surface Pt atom. However, in acetic acid the ee and rate do not pass through a maximum of optimal concentration, rather increased to a plateau. This phenomenon has been ascribed to the prevention of alkaloid overcrowding due to the acid nature of the solvent weakening the modifier/Pt interaction [85].

#### 1.5.5 Catalyst pre-modification vs. *in situ* modification

The modification of catalyst as carried out by Orito *et al* involved stirring a slurry of catalyst and modifier in solvent for 24 h [30]. This has been repeated by other groups, however, they found that 24 h was unnecessary and that a pre-modification step was wasn't required. Wells showed that a pre-modification time of 10 min was suitable [94]. Blaser dispensed with pre-modification step and added the alkaloid with the reactant, solvent and catalyst, thus modifying the platinum *in situ* [95]. *In situ* catalyst modification was found to significantly enhance the rate and the ee achieved. Competitive adsorption between reactant and modifier leads to an optimum surface coverage and hence improved ee and rate. However, Hutchings has shown that pre-modification of the catalyst can prove beneficial as it can be stored for up to 7 days with little degradation in ee or rate [96].

### 1.5.6 Reaction conditions

The effect of temperature and pressure on the kinetics of enantioselective hydrogenation of  $\alpha$ -ketoesters has been investigated by a number of groups. The effect of temperature has been shown to have a profound influence on the ee for cinchona modified catalysts. For the unmodified catalyst the effect of increasing the reaction temperature from 25 to 70°C shows good linear Arrhenius behaviour [94]. For the modified catalysts a critical reaction temperature of above 50°C was reported by Wells *et al.* where above this temperature the rate and ee decreases. Interestingly, in the gas phase the critical temperature was found to be higher at 60°C [96].

The rate of enantioselective pyruvate ester hydrogenation was shown to be first order with respect to hydrogen pressure [97]. The enantiomeric excess has been reported by Blackmond to depend on the hydrogen concentration in the liquid phase [98]. Saturation of the solvent with dissolved hydrogen overcomes the mass transfer from the gas-phase to the metal surface. The consumption of hydrogen, therefore, by the reacting pyruvate ester has been shown to be lower than the dissolved hydrogen available [98]. The quinoline moiety of cinchonidine has been shown to be susceptible to hydrogenation at low surface coverage leading to loss of ee [45]. However, at higher alkaloid loading the quinoline system is resistant to hydrogenation at 10 bar hydrogen pressure. At hydrogen pressures up to 110 bar cinchona alkaloids remain efficient modifiers [94]. The vinyl group of cinchonidine is easily saturated during enantioselective hydrogenation. There is no discernable effect of this hydrogenation, however, it has been postulated that this can initiate a rearrangement of the ad-layer of modifier molecules.

### 1.5.7 Solvent

The choice of solvent has been of great interest in the enantioselective hydrogenation of  $\alpha$ -ketoesters. Discovery of a linear relationship between decreasing enantiomeric excess and increasing dielectric constants prompted further investigations in the nature of the chiral active site. Most favourable results were obtained with apolar solvents with a dielectric constant of between 2 and 10. The rate of reaction showed less variation with a change of solvent polarity. Reactions carried out in acetic acid, however, go against this trend where both reaction rate and enantiomeric excess have been the highest reported [54]. The influence of the solvent on the conformation of the adsorbed alkaloid modifier and, therefore, the chiral active site was shown to be vital. Cinchonidine is found to exist exclusively in the *open 3* conformation in acetic acid, due to protonation of the quinuclidine nitrogen. The conformation of adsorbed cinchonidine and the subsequent effect on the ee of pyruvate ester hydrogenation is discussed in 1.4.3. Interestingly ethyl pyruvate has been enantioselectively hydrogenated in the absence of solvent [94]. The reaction was successful and an ee of 80 % and a rate of 275 mmol/h/g<sub>cat</sub> was achieved over EUROPT-1 modified with dihydrocinchonidine.

### 1.6 Reactors used in catalysis

For this study three different multi-phase reactors were used in the enantioselective hydrogenation of pro-chiral carbonyl containing compounds. A stirred tank reactor termed an autoclave, a fixed-bed reactor termed the trickle-bed reactor and a gas-phase reactor which also has a fixed catalyst bed.

## 1.6.1 Background

At present fine chemical manufacture is dominated by the stirred tank reactor and batch-wise production and have been for over a hundred years. Patents filed in the 1880s for such batch production bare remarkable similarity to both those used today and being installed [99]. Indeed the design has changed little over five hundred years for small to intermediate scale manufacturing. The basics of this design comprise of a pressure vessel, the autoclave, a shaft driven impeller and a means of gas introduction (Fig. 1.11). Such an instrument can accommodate reactions for both homogeneous and heterogenous catalysis. This introduces plant flexibility for using one reactor for multiple applications.

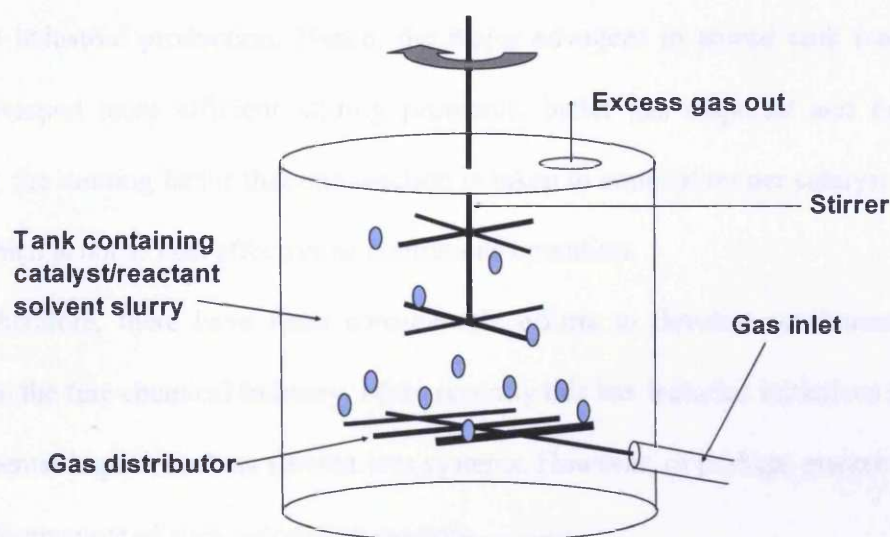


Fig. 1.11 Schematic representation of a stirred tank reactor

However, there are drawbacks to such a simple system, most prominent is transport limitations. Both heat and mass transfer limitations can greatly affect the efficiency of stirred tank reactors. Mass transfer whether between gas/liquid, liquid/solid or within the homogeneous liquid phase is hard to completely eradicate. Improved and specific stirrer design can reduce the transfer limitations. However, “dead” spots of slow moving or static



regions in the autoclave can disrupt the distribution of catalyst and hence result in unpredictable kinetics. This effect could translate to a reduction of product per reaction run and on an industrial scale, large losses in expected earnings. Heat transfer, due to the design of a large tank is also hard to overcome. Hotspots may develop in the centre of the reactor and may take an undesirable length of time to dissipate.

Of particular importance to industrial applications is reaction scale-up from laboratory investigations. Principally if one increases the size of the reactor and, therefore, the production, the process becomes more cost effective. However, the many variables involved, such as mixing, kinetics, geometry and gas bubbles do not scale-up accordingly. This results in unpredictable changes in the reaction dynamics from the laboratory bench to full scale industrial production. Hence, the major advances in stirred tank reactor design have developed more efficient stirring protocols, better gas dispersal and heat control. However, the limiting factor that one reaction is taken to completion per catalyst charge still exists, which is not as cost effective as continuous operation.

Therefore, there have been considerable efforts to develop continuous operation reactors in the fine chemical industry. More recently this has included initiatives focusing on environmental impact, such as solvent-less systems. However, of perhaps greater importance is cost effectiveness of such automated reactors.

The trickle bed reactor (Fig. 1.12) is one solution to continuous operation, however, with its own drawbacks of transfer limitations and scale-up. Nevertheless, for applications of fine chemical synthesis with heterogeneous catalysts the trickle bed reactor offers many advantages. Yet, until recently fixed-bed reactors like the trickle-bed reactors have generally been used in the production of bulk chemicals e.g. olefin plants.

The design is inherently focused on continuous operation, where the catalyst bed is in a fixed position or area where the reactants flow through the bed. The flow of the liquid

reactants are controlled in such a way that they trickle through the catalyst bed (Fig. 1.13). Increasing the flow rate can alter the flow regime of the reactants, typically spraying or foaming is the result. This changes the kinetics of the reaction and may lead to undesirable levels of conversion or thermal control issues. However, the understanding of the trickle-bed reactor is largely empirical, with little understanding of the physical transport properties.

The benefits of such a reactor are; elimination of separation/filtration of solid catalyst and the liquid reaction mixture after the reaction. Additionally batch processes require stirring, which can cause mechanical attrition of catalyst particles. In the fixed-bed reactor this is not required, as a result larger support particles can be used, which are easier and safer to handle.

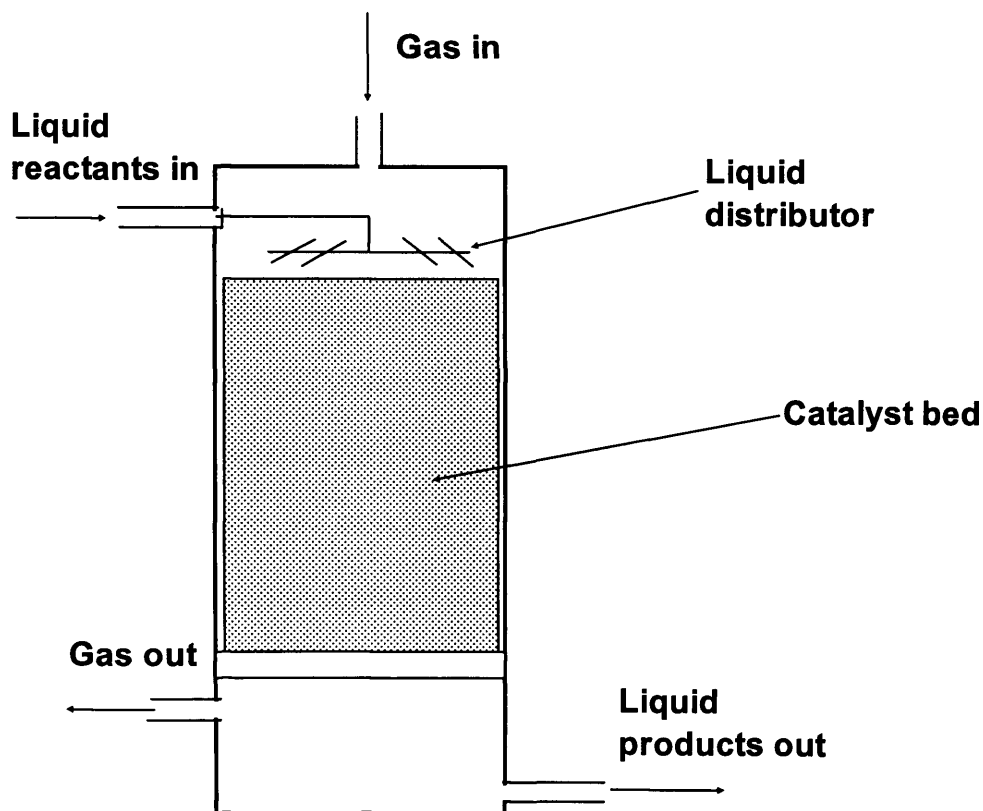


Fig. 1.12 Representation of a trickle-bed reactor

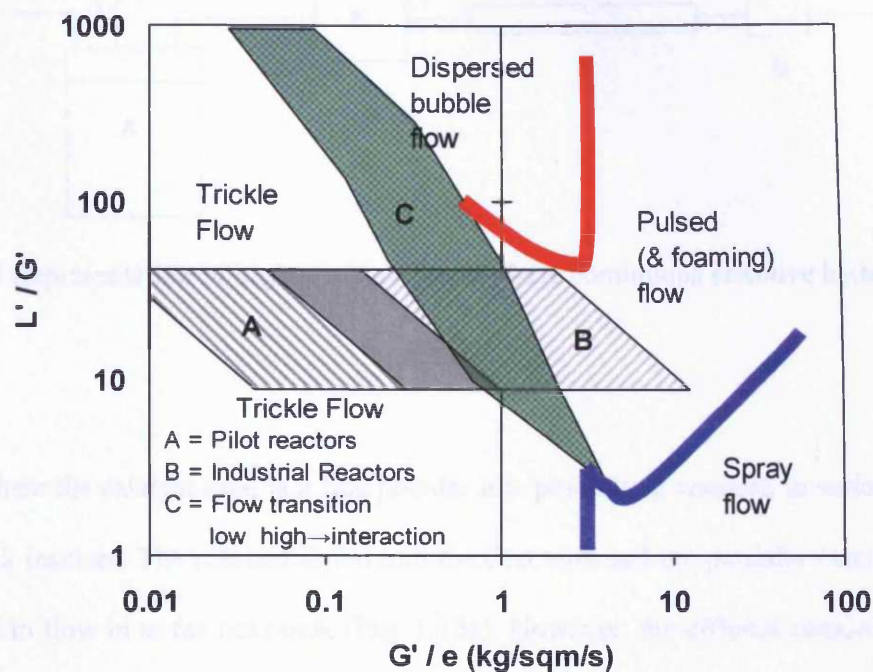


Fig. 1.13 Flow regimes of trickle-bed reactors (after Baker 1954) [100]

For small scale applications it is possible to replace the analytical column of an HPLC system with one containing catalyst (Fig. 1.14). The use of such a reactor necessitates hydrogen to be dissolved in the solvent. The gas is mixed with the solvent in an autoclave (A), up-stream of the catalyst bed. Typically another column is used to pre-mix the reagents prior to introduction into the reactor (B). For this purpose the column can be filled with inert glass beads. Very high pressures are attainable in the reaction column (C) if the catalyst is a fine powder or undiluted with glass spheres for example. Back pressure regulation is placed after the reaction column (D). This technique was used recently [101] for enantioselective hydrogenation of C=O containing substrates. However, the reaction is subjected to an increased bulk-liquid to surface mass transfer control in such a reactor.

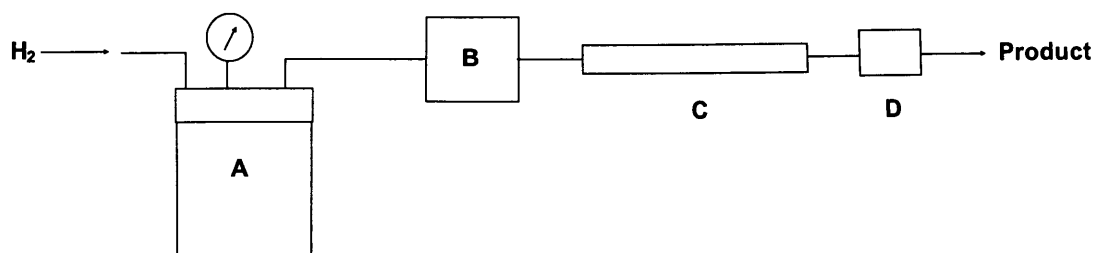


Fig. 1.14 Representation of high pressure liquid phase continuous selective hydrogenation reactor

Where the catalyst used is a fine powder it is possible to connect, in series a group of stirred-tank reactors. The reactant is fed into the first tank and the partially reacted substrate is allowed to flow in to the next tank (Fig. 1.15a). However, the effluent consists of product and a quantity of catalyst which is then filtered. Generally product yields are lower when compared to the batch reaction. A further extension of the stirred-tank reactor is the use of a spinning basket containing the catalyst (Fig. 1.15b). Reactant is fed into the tank and the gas is supplied below the basket which then passes upwards through it. The reactant is converted over the catalyst as it spins around and exits near the base of the reactor. A similar system utilises a circular fixed basket containing the catalyst with the impeller located in the centre of it (Fig. 1.15c). The reactant is drawn through the basket, however, this reactor is only used for vapour phase reactions.

### 1.3.2 Reactors types used in heterogeneous enantioselective hydrogenation

The use of stirred tank reactors is dominant for enantioselective hydrogenations over heterogeneous catalysts. This in part is due to its flexibility in laboratories for small scale applications and ease of use. However, the increasing need for continuous operation in

industrial sectors has recently led many groups to attempt such reactions in fixed-bed reactors.

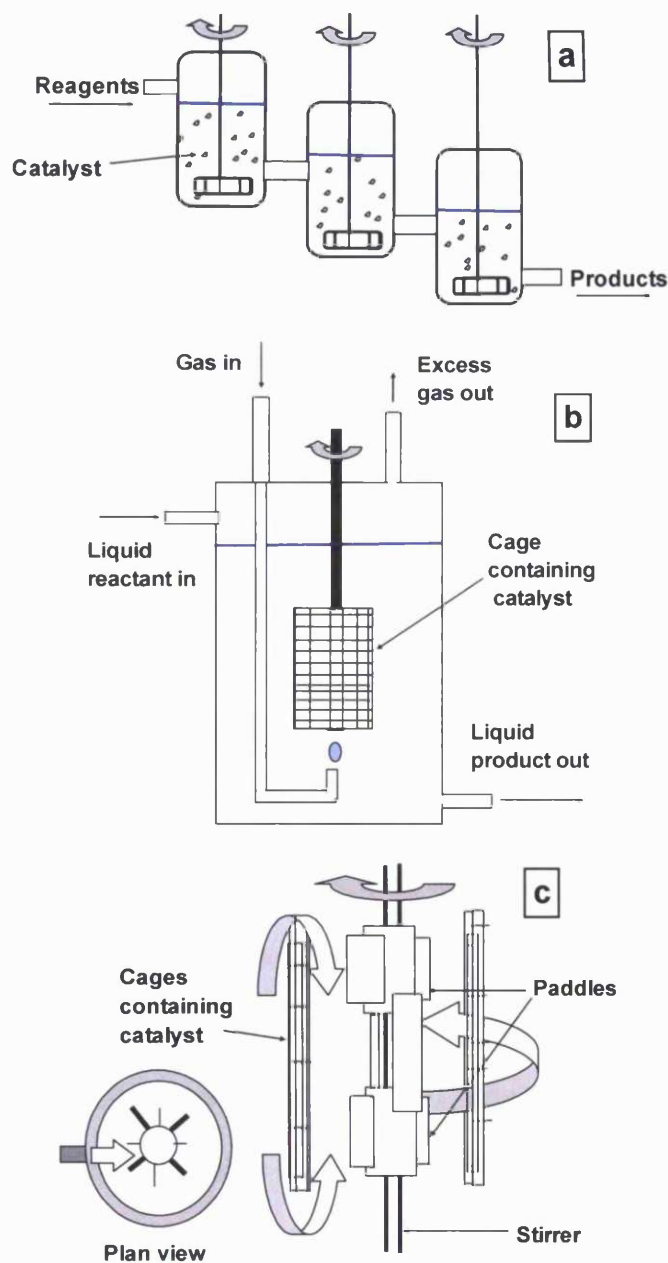


Fig. 1.15 Representations of different liquid phase reactor design: *a*; continuous stirred tank reactors in series, *b*; spinning basket reactor and *c*; fixed basket reactor

Wells *et al.* hydrogenated methyl pyruvate over cinchonidine modified EUROPT-1 in a static flow reactor at 10 bar, obtaining 7 % conversion with ca. 74 to 80 % ee [102]. These initial experiments were conducted to ascertain whether the cinchonidine would remain adsorbed and the catalyst active under flow conditions. During the 1 h reaction period the conversion remained stable and the ee decreased modestly. Shortly after this other groups began developing fixed-bed reactors for enantioselective hydrogenations. Baiker reported that high enantiomeric excess and conversion were possible with a high pressure trickle-bed reactor [103]. Ketopantolactone was hydrogenated (Table 1.4 entry 8) and ethyl pyruvate over 5 % Pt/Al<sub>2</sub>O<sub>3</sub> at 40 bar and 20°C. The catalyst was modified continuously with cinchonidine in the feed at ppm level. Conversion for both substrates were 100 % and the ee obtained for (*R*)-pantolactone and (*R*)-ethyl lactate was 83.4 % and 89.9 % respectively. However, when the modifier was not present in the feed the enantioselectivity was lost. Li *et al.* reported the enantioselective hydrogenation of ethyl-2-oxo-4-phenylbutyrate (Table 1.4 entry 6) in a fixed-bed reactor [104]. Conversion was stable ca. 100 %, however, the ee of (*R*)-(+)-ethyl-2-hydroxy-4-phenylbutyrate decreased over the reaction period from 68 %. Further diversification of reactant was shown by Toukoniitty *et al.* in fixed-bed reactors [105]. Using knitted silica fibres impregnated with 5 wt.% platinum for the enantioselective hydrogenation of 1-phenyl-1,2-propanedione (Table 1.4 entry 5) at 25°C and 5 bar. The bed was modified *in situ* with cinchonidine in the feed and resulted in an ee of 60 % of (*R*)-1-hydroxy-phenylpropanone. However, this product could then hydrogenate further to diols. They confirmed that constant feeding of modifier was required to maintain enantioselectivity. The use of ‘supercritical’ ethane and CO<sub>2</sub> has been investigated by Baiker *et al.* for the continuous enantioselective hydrogenation of ethyl pyruvate in a fixed-bed reactor [106]. The bed consisted of a 1:9 mix of 5 % Pt/Al<sub>2</sub>O<sub>3</sub> diluted with alumina and was continuously modified with cinchonidine. High rates and good enantioselectivities were

achieved, however, the intent was only to demonstrate the ability to perform such reactions in aggressive conditions. Another reactant used in the production of an intermediate for the manufacture of desirable fine chemicals isopropyl-4,4,4-trifluoroacetoacetate reported by Baiker *et al.* [107]. They described the use of trifluoroacetic acid as an additive to THF as the solvent, in which was dissolved reactant and the modifier; *O*-methyl cinchonidine. The highest ee obtained was 91 % at a low conversion of 7.4 %, with a reactor temperature of less than  $-10^{\circ}\text{C}$ . Recently enantioselective hydrogenations have been carried out in a packed HPLC column [101]. Ethyl pyruvate or ethyl benzoylformate were hydrogenated over alkaloid modified Pt/Al<sub>2</sub>O<sub>3</sub> at 0 to 20°C and at 60-200 bar. The reactor setup as shown in Figure 1.14 requires hydrogen to be dissolved in ethanol. They performed experiments where the modifier was present in the feed, then absent, the catalyst 'cleaned' at 50°C and the alkaloid reintroduced to the feed. A modest ee of 51 % was achieved during both enantioselective hydrogenation periods with ethyl pyruvate at high conversion. They were able to successfully modify the bed with CD first then introduce CN after the 'cleaning' period. This resulted in an inversion of ee with the corresponding modifier from ca. 58 % (*R*)-lactate with CD to ca. 41 % (*S*)-lactate with CN. It was also shown that the catalyst was active for the enantioselective hydrogenation of ethyl pyruvate and following a 'cleaning' period then active for ethyl benzoylformate.

The performance of the fixed-bed reactor with these preliminary enantioselective hydrogenations has led to an increased awareness of continuous operation on a larger scale. However, the need for the continuous feeding of modifier to the bed is of concern for final product purity. The use of aggressive solvents such as acetic acid and toluene and ethyl acetate is also a concern for applications towards 'green' chemistry.

Gas phase enantioselective hydrogenation with heterogeneous catalysts has rarely been reported, mainly due to the focus on the Orito and the Ni/tartaric acid systems. Both of

which have been confined to the liquid phase and primarily reacted in a stirred tank. From the literature only a hand full of heterogeneous enantioselective hydrogenation in the gas phase were revealed. The hydrogenation of 2-butanone over supported nickel catalysts was attempted by López-Martínez and Keane [108]. They reported that an *ex situ* treatment of an 11.9 wt. % nickel catalyst with L-tartaric acid and achieved an ee of 31 % to (*R*)-2-butanol. Initial work by Von Arx on alkaloid and amine modified Pt, Pd and Au catalysts on the gas phase hydrogenation of 1,3-butadiene and crotonaldehyde [109] was followed up with enantioselective hydrogenation of methyl pyruvate [96]. They showed that using stable pre-modified platinum supported on  $\alpha$ -Al<sub>2</sub>O<sub>3</sub>,  $\gamma$ -Al<sub>2</sub>O<sub>3</sub> and SiO<sub>2</sub> it was possible to achieve enantioselectivity of (*R*)-methyl lactate at high conversion in the absence of solvent. They reported an ee of 51 % over a 5 % Pt/Al<sub>2</sub>O<sub>3</sub> catalyst where an acid additive had been used in the pre-modification stage. Enantioselective hydrogenation was achieved over a prepared 1 % Pt/ $\alpha$ -Al<sub>2</sub>O<sub>3</sub> catalyst, which confirmed that the reaction occurs at the gas-solid interface.

## 1.7 IMI

The Innovative Manufacturing Initiative was set up with the aim of bringing together a number of industrial and academic centres to work in unison to address a number of scientific challenges. Previously the IMI-1 consortium had developed a small lab-scale trickle-bed reactor and an alumina supported catalyst. This led to advances in microkinetic characterisation and analysis of supported metal catalysts. The IMI-2 project offers an integrated approach to the quantitative design of trickle-bed catalytic reactors for the fine chemical and petroleum industries. The benefit of such a consortium allowed the scope of the project to be much larger than any one single member could embark upon. This involved Johnson Matthey, BP, Syntex (Now part of Johnson Matthey), Davison Catalysis, Robinson



Brothers and MSi as the industrial partners. The academic institutions involved were Cardiff, Glasgow, Birmingham and Cambridge. The following is a brief description of the overall objectives for each group:

1. Birmingham: Materials Centre; Develop a continuous manufacture process for extruded supported catalysts for use in trickle-bed reactors. Support material will be supplied by Grace Davison.
2. Birmingham: Reactor Studies; Conduct hydro-desulphurisation experiments over catalysts from 1. in a pilot-plant scale trickle-bed supplied by BP Amoco.
3. Cambridge: Magnetic Resonance Research Centre; Provide flow visualisation of two- and three-phase trickle-bed reactors for determination of catalyst activity at a point in the bed [110]. Additionally catalyst characterisation will be conducted with solid state  $^{29}\text{Si}$  NMR.
4. Cardiff: Molecular Modelling; Provide molecular simulation data for the reactions carried out by Cardiff and Glasgow experimental groups.
5. Cardiff: Experimental; Test catalysts supplied by Johnson Matthey and Birmingham Materials Centre in stirred tank and trickle-bed reactors with the enantioselective hydrogenation of 2,3-butanedione over  $\text{Pt}/\text{SiO}_2$ . Study to provide intrinsic reaction kinetics for comparison with molecular modelling and magnetic imaging.
6. Glasgow: Experimental; Test catalysts supplied by Johnson Matthey and Birmingham Materials Centre in stirred tank and trickle-bed reactors with the hydrogenation of *p*-toluidine to methylcyclohexylamine over  $\text{Rh}/\text{SiO}_2$ . Study to provide intrinsic reaction kinetics for comparison with molecular modelling and magnetic imaging.

## 1.8 Aims of the project

As part of the IMI-2 consortium the objectives of the investigation are related to the advancement of trickle-bed reactor design and processes. Only recently has the part of the focus of enantioselective hydrogenation reactions over supported catalysts shifted to look towards continuous operation [93, 94]. Therefore, the use of the low pressure, lab scale trickle-bed reactor developed in IMI-1 with the study reaction is opportune at this time.

### 1.8.1 Objectives

1. Use of the autoclave as a tool in the screening of the 2.5 % Pt/SiO<sub>2</sub> catalysts, to determine support characteristics suitable for the studied reaction. This will be achieved through kinetic rate measurements.
2. Continued use of the autoclave for particular aspects of reaction optimisation, such as solvent effects, modifier concentration and the use of cyclohexene as a probe molecule.
3. Develop a reaction protocol for the study reaction in the trickle-bed reactor. This will include the use of cyclohexene hydrogenation, catalyst modification techniques.
4. Utilise the reaction protocol developed in 3. with the extruded catalysts supplied by Birmingham.
5. Exploit the recent developments in gas-phase enantioselective hydrogenation of pyruvate esters [100] with the well characterised IMI-2 catalysts to gain new insights into aspects of the reaction. These will include investigation of the active site through reaction of pyruvate esters and reaction optimisation.

Objectives 1 and 2 are attended to in Chapter three, 3 and 4 are addressed in Chapter four and 5 is dealt with in Chapter five.

### 1.9 References

1. J.J. Berzelius, *Edinburgh New Philosophical Journal.*, **XXI** (1836) 223.
2. P. Sabatier, *La Catalyse in Chemie Organique.*, Librairie Poytechnique, Paris (1913).
3. J.A. Osborn, F.H. Jardine, J.F. Young and G. Wilkinson, *J. Chem. Soc.*, (A) (1966) 1711.
4. I. Chibata, T. Tosa and T. Sato, *J. Mol. Catal.*, **37** (1986) 1.
5. M. Bowker, *The Basis and Applications of Heterogeneous Catalysis, Oxford Chemistry Primers*, **53** (1998)
6. E.L. Malus, *Mem. Soc. d' Arcueil.*, **2** (1809) 143.
7. J.B. Biot, *Bull. Soc. Philomath.*, Paris (1815) p.190.
8. L. Pasteur, *C. R. Acad. Sci.*, **26** (1848) 535.
9. J.A. Le Bel, *Bull. Soc. Chim. Fr.*, **22** (1874) 337.
10. J.H. van't Hoff, *Arch. Neerl. Sci. Exact. Nat.*, **9** (1874) 445
11. R.S. Cahn, C.K. Ingold and V. Prelog, *Angew. Chem. Int. Ed. Engl.*, **5** (1966) 385.
12. W.S. Knowles, *J. Chem. Ed.*, **63** (1986) 222.
13. H.-U. Blaser, H.-P. Jalett and F. Spindler, *J. Mol. Catal. A: Chemical.*, **107** (1996) 85.
14. (a) T. Ohkuma, H. Ooka, S. Hashiguchi, T. Ikariya and R. Noyori, *J. Am. Chem. Soc.*, **117** (1995) 2675.; (b) T. Ohkuma, H. Ooka, T. Ikariya and R. Noyori, *J. Am. Chem. Soc.*, **117** (1995) 10417.; (c) T. Ohkuma, H. Ooka, M. Yamakawa, T. Ikariya and R. Noyori, *J. Org. Chem.*, **61** (1996) 4872.
15. M.J. Burk, W. Hems, D. Herzberg, C. Malan and A. Zanotti-Gerosa, *Org. Lett.*, **26** (2000) 4173.

16. J.-F. Carpentier, F. Agbossou and A. Montreux, *Tetrahedron: Asymmetry*, **6** (1995) 39
17. M.D. Jones, R. Raja, J.M. Thomas, B.F.G. Johnson, D.W. Lewis, J. Rouzaud and K. D.M. Harris, *Angew. Chem. Int. Ed.*, **42** (2003) 4326.
18. V. Ratovelomanana-Vidal and J.-P. Genêt, *J. Organometal. Chem.*, **567** (1998) 163.
19. S. Jeulin, S. Duprat de Paule, V. Ratovelomanana-Vidal, J.-P. Genêt, N. Champion and P. Dellis, *Pro. Natl. Acad. Sci. USA.*, **101** (2004) 5799.
20. D.G. Genov and D.J. Ager, *Angew. Chem. Int. Ed.*, **43** (2004) 2816.
21. G.M. Schwab and L. Rudolph, *Naturwiss.*, **20** (1932) 362.
22. S. Akabori, S. Sakurai, Y. Izumi and Y. Fuji, *Nature.*, **178** (1956) 323.
23. A.A. Balandin, E.I. Klabunovskii and Y.I. Petrov, *Dokl. Akad. Nauk. SSSR.*, **127** (1959) 557.
24. (a) K. Harada and T. Yoshika, *Naturwiss.*, **57** (1970) 306.; (b) K. Harada and T. Yoshika, *Naturwiss.*, **59** (1970) 131.
25. D. Lipkin and T.D. Stewart, *J. Am. Chem. Soc.*, **61** (1939) 3295.
26. Y. Nakamura, *Bull. Chem. Soc. Jpn.*, **16** (1941) 367.
27. T. Isoda, A. Ichikawa and T. Shimamoto, *Rikagaku Kenkyusko Hokoku.*, **34** (1958) 134.
28. Y. Izumi, *Adv. Catal.*, **32** (1983) 215.
29. Y. Izumi, M. Imaida, H. Fukawa, S. Akabori, *Bull. Chem. Soc. Jpn.*, **36** (1963) 155.
30. Y. Orito, S. Imai, S. Niwa, *J. Chem. Soc. Jpn.*, (1979) 1257.
31. Y. Orito, S. Imai, S. Niwa, *J. Chem. Soc. Jpn.*, (1980) 670.
32. Y. Orito, S. Imai, S. Niwa, *J. Chem. Soc. Jpn.*, (1982) 137.
33. P.B.Wells and R.P.K. Wells, in 'Chiral Catalyst Immobilisation and Recycling', (DeVos IFJ eds. Van Kelcom, P.A. Jacobs) WileyVCH (2000), p.123-154.
34. H.U. Blaser, M. Garland and H.P. Jalett, *J. Catal.*, **144** (1993) 569.
35. G.C. Bond and P.B. Wells, *J. Catal.*, **150** (1994) 329.

- 
36. H.U. Blaser, H.P. Jalett, D.M. Monti, A. Baiker and J.T. Wehrli, in '*Symposium on Structure-Activity Relationships in Heterogeneous Catalysis*', American Chemical Society, Boston (1990) p.79.
37. T. Evans, A.P. Woodhead, A. Gutierrez-Sosa, G. Thornton, T.J. Hall, A.A. Davis, N.A. Young, P.B. Wells, R.J. Oldman, O. Plashkevych, O. Vahtras, H. Agren, V. Carravetta, *Surf. Sci.*, 436 (1999) 691.
38. D. Ferri, T. Bürgi and A. Baiker, *J. Chem. Soc. Chem. Commun.*, (2001) 1172.
39. I.M. Sutherland, A. Ibbotson, R.B. Moyes and P.B. Wells, *J. Catal.*, 125 (1990) 77.
40. K.E. Simmons, P.A. Meheux, S.P. Griffiths, I.M. Sutherland, P. Johnston, P.B. Wells, A.F. Carley, M.K. Rajumon, M.W. Roberts and A. Ibbotson, *Recl. Trav. Chim. Pays-Bas.*, 113 (1994) 465.
41. R.L. Augustine, S.K. Tanielyan and L.K. Doyle, *Tetrahedron: Asymmetry.*, 4 (1993) 1803.
42. A.F. Carley, M.K. Rajumon, M.W. Roberts and P.B. Wells, *J. Chem. Soc. Faraday Trans.*, 91 (1995) 2167.
43. A. Baiker, *J. Mol. Catal. A: Chemical.*, 115 (1997) 473.
44. J.L. Margitfalvi, M. Hegedűs and E. Tfirst, *Tetrahedron: Asymmetry.*, 7 (1994) 571.
45. H.U. Blaser, H.P. Jalett, D.M. Monti, A. Baiker and J.T. Wehrli, *Stud. Surf. Sci. Catal.*, 67 (1991) 147.
46. A. Baiker, *J. Mol. Catal. A: Gen.*, 163 (2000) 205.
47. T. Bürgi and A. Baiker, *J. Catal.*, 194 (2000) 445.
48. O. Schwalm, J. Weber, B. Minder and A. Baiker, *J. Mol. Struc. (Theochem).*, 330 (1995) 353
49. G. Bond, K.E. Simmons, A. Ibbotson, P.B. Wells and D.A. Whan, *Catal. Today*, 12 (1992) 421.

50. T. Bürgi, F. Atamny, A. Knop-Gericke, M. Hävecker, T. Schedel-Niedrig, R. Schlögl and A. Baiker, *Catal Lett.*, **66** (2000) 109.
51. K.A. Avery, R. Mann, M. Norton and D.J. Willock, *Topics in Catalysis.*, **25** (2003) 89.
52. (a) U. Bohmer, K. Morgenschweiss and W. Reschetilowski, *Catal. Today.*, **24** (1995) 153.; (b) U. Bohmer, K. Morgenschweiss and J. Wiehl, in 'Chiral Reactions in Heterogeneous Catalysis' (ed. G. Jannes and V. Dubois), Plenum Press, New York, 1995, p. 111.
53. (a) G.C. Bond and P.B. Wells, *Appl. Catal.*, **18** (1985) 221.; (b) G.C. Bond and P.B. Wells, *Appl. Catal.*, **18** (1985) 225.; (c) J.W. Geus and P.B. Wells, *Appl. Catal.*, **18** (1985) 231.; (d) A. Frennet and P.B. Wells, *Appl. Catal.*, **18** (1985) 243.; (e) P.B. Wells, *Appl. Catal.*, **18** (1985) 259.
54. H.U. Blaser, H.P. Jalett and J. Wiehl, *J. Mol. Catal.*, **68** (1991) 215.
55. H.U. Blaser, H.P. Jalett, D.M. Monti, J.F. Reber and J.T. Wehrli, *Stud. Surf. Sci. Catal.*, **41** (1988) 153.
56. J.T. Wehrli, A. Baiker, D.M. Monti and H.U. Blaser, *J. Mol. Catal.*, **61** (1990) 207.
57. X. Zuo, H. Liu and M. Liu, *Tetra. Lett.*, **39** (1998) 1941.
58. R. Van Hardeveld and F. Hartog, *Surf. Sci.*, **15** (1969) 189.
59. S.D Jackson, M.B.T. Keegan, G.D. McLellan, P.A. Meheux, R.B. Moyes, G. Webb, P.B. Wells, R. Whyman and J. Willis, Preparation of Catalysts V (G. Ponchelot, P.A. Jacobs, P. Grange and B. Delmon, Eds. Elsevier, Amsterdam, 1991), p.211.
60. J.T. Wehrli, A. Baiker, D.M. Monti and H.U. Blaser, *J. Mol. Catal.*, **49** (1989) 195.
61. T. Wang, C. Lee and L.D. Schmidt, *Surf. Sci.*, **163** (1985) 181.
62. A.C. Shi and R. Masel, *J. Catal.*, **120** (1989) 421.
63. X. Li, X. You, P. Ying, J. Xiao and C. Li, *Topics in Catalysis.*, **25** Nos 1-4 (2003) 63.

64. T. Mallet, S. Frauchiger, P.J. Kooymen, M. Schürch and A. Baiker, *Catal. Lett.*, **63** (1999) 121.
65. V. Machek, V. Ruzika, M. Sourková, J. Kunz and L. Janacek, *Collect. Czech. Chem. Commun.*, **48** (1983) 517.
66. V. Machek, J. Hainka, K. Sporica, V. Ruzika, J. Kunz and L. Janacek, *Stud. Surf. Sci. Catal.*, **16** (1983) 69.
67. B. Török, K. Balázsik, M. Török, Gy. Szöllösi and M. Bartók, *Ultrasonics Sonochem.*, **7** (2000) 151.
68. T.J. Hall, J.E. Halder, G.J. Hutchings, R.L. Jenkins, P. Johnston, P. McMorn, P.B. Wells and R.P.K. Wells, *Topics in Catalysis*, 11-12 (2000) 351.
69. R. Hess, F. Krumeich, T. Mallat and A. Baiker, *Catal. Lett.*, **92** (2004) 141.
70. K.E. Simons, A. Ibbotson, P. Johnston, H. Plum and P.B. Wells, *J. Catal.*, **150** (1994) 321.
71. Y. Huang, J. Chen, H. Chen, R. Li, Y. Li, L. Min and X. Li, *J. Mol. Catal. A: Chem.*, **170** (2001) 143.
72. (a) R. Noyori and T. Ohkuma, *Angew. Chem.*, **113** (2001) 41.; *Angew. Chem. Int. Ed.*, **40** (2001) 40; (b) R. Noyori, *Angew. Chem.*, **114** (2002) 2108.; *Angew. Chem. Int. Ed.*, **41** (2002) 2008.
73. S.P. Griffiths, Ph.D. thesis (University of Hull, 1997).
74. T.J. Hall, P. Johnston, W.A.H. Vermeer, S.R. Watson and P.B. Wells, *Stud. Surf. Sci. Catal.*, **101** (1996) 221.
75. P.B. Wells and A.G. Wilkinson, *Topics in Catal.*, **5** (1998) 39.
76. P.J. Collier, T.J. Hall, J.A. Iggo, P. Johnston, J.A. Slipszenko, P.B. Wells and R. Whyman, *J. Chem. Soc. Chem. Commun.*, (1998) 1451.

77. D. Gala, D.J. DiBenedetto, J.E. Clark, B.L. Murphy and D.P. Schumacher, *Tetrahedron Lett.*, **37** (1996) 611.
78. W.A.H Vermeer, A. Fulford, P. Johnston and P.B. Wells, *J. Chem. Soc. Chem. Commun.*, (1993) 1053.
79. J. Slipszenko, S. Griffiths, P. Johnston, K. Simmons, W.A.H Vermeer and P.B. Wells, *J. Catal.*, **179** (1998) 267.
80. E. Toukoniitty, P. Mäki-Arvela, A.N. Vilella, A.K. Neyestanaki, T. Salmi, R. Leino, R. Sjöholm, E. Laine, J. Väyrynen, T. Ollonqvist and P.J. Kooyman, *Catal. Today*, **60** (2000) 175.
81. H.U. Blaser and H.P. Jalett, *Stud. Surf. Sci. Catal.*, **78** (1993) 139.
82. M. Schürch, O. Schwalm, T. Mallet, J. Weber and A. Baiker, *J. Catal.*, **169** (1997) 275.
83. M. Schürch, N. Künzle, T. Mallet and A. Baiker, *J. Catal.*, **176** (1998) 569.
84. R.P.K. Wells, N.R McGuire, X. Li, R.L. Jenkins, P.J. Collier, R. Whyman and G. Hutchings, *Phys. Chem. Chem. Phys.*, **4** (2002) 2839.
85. M. Studer, V. Okafor and H.U. Blaser, *J. Chem. Soc. Chem. Commun.*, (1998) 1053.
86. X. Zuo, H. Liu, J. Tian, *J. Mol. Catal. A: Chem.*, **157** (2000) 217.
87. V.B. Shukala, P.R. Kulkarni, *World J. Biotechnol.*, **16** (2000) 499.
88. E. Toukoniitty, B. Ševčíková, P. Mäki-Arvela, J. Warna, T. Salmi and D.Yu. Murzin, *J. Catal.*, **213** (2003) 7.
89. X. Li, N.F. Dummer, R.L. Jenkins, R.P.K. Wells, P.B. Wells, D.J. Willock, S.H. Taylor, P. Johnston and G.J. Hutchings, *Catal. Lett.*, **96** (2004) 147.
90. H.-U. Blaser, H.-P. Jallet, M. Garland, M. Studer, H. Thies and A. Wirth-Jijani, *J. Catal.*, **173** (1998) 282
91. J. Stohr, *NEXFAS Spectroscopy, Springer Series in Surface Science*, (eds. G. Ertl, R. Gommer and D.L. Mills), Springer, Berlin, 1992.



92. H.U. Blaser, M. Garland and H.P. Jallet, *J. Catal.*, **144** (1993) 569.
93. H.U. Blaser, D. Imhof and M. Studer, *Heterogeneous Catalysis and Fine Chemicals, Vol. IV*, (eds. H.U. Blaser, A. Baiker and P. Prins), Elsevier, Amsterdam, 1997, p. 175.
94. P. Meheux, A. Ibboston and P.B. Wells, *J. Catal.*, **128** (1991) 441.
95. H.U. Blaser, M. Garland, M. Muller and M. Studer, *J. Catal.*, **144** (1993) 569.
96. M. von Arx, N.F. Dummer, D.J. Willock, S.H. Taylor, R.P.K. Wells, P.B. Wells and G.J. Hutchings, *J. Chem. Soc. Chem. Commun.*, (2003) 1926.
97. G.D.H. Dijkstra, R.M. Kellogg and H. Wynberg, *J. Org. Chem.*, **55** (1990) 6121.
98. (a) Y. Sun, J. Wang, C. LeBlond, R.N. Landau and D.G. Blackmond, *J. Catal.*, **161** (1996) 759.; (b) Y. Sun, J. Wang, C. LeBlond, R.N. Landau and D.G. Blackmond, *J. Am. Chem. Soc.*, **118** (1996) 1348.; (c) Y. Sun, J. Wang, C. LeBlond, R.N. Landau and D.G. Blackmond, *J. Catal.*, **161** (1996) 752.
99. E.H Stitt, *Chem Eng. J.*, **90** (2002) 47.
100. E.H Stitt, personal communication.
101. Y. Zhao, F. Goa, L. Chen and M. Garland, *J. Catal.*, **221** (2004) 274.
102. P.A. Meheux, A. Ibbotson and P.B. Wells, *J. Catal.*, **128** (1991) 387.
103. N. Künzle, R. Hess, T. Mallat and A. Baiker, *J. Catal.*, **186** (1999) 239.
104. X. Li and C. Li, *Catal. Lett.*, **77** (2001) 251.
105. E. Toukoniitty, P. Mäki-Arvela, A.K. Neyestanaki, T. Salmi, R. Sjöholm, R. Leino, E. Laine, P.J. Kooyman, T. Ollonqvist and J. Väyrynen, *App. Catal. A: Gen.*, **216** (2001) 73.
106. B. Minder, T. Mallat, K.H. Pickel, K. Steiner and A. Baiker, *Catal. Lett.*, **35** (1995) 1.
107. N. Künzle, T. Mallat and A. Baiker, *App. Catal. A: Gen.*, **6187** (2002) 1
108. A. López-Martínez and M.A. Keane, *J. Mol. Catal. A: Chem.*, **153** (2000) 257.
109. M. von Arx and G.J. Hutchings, *New J. Chem.*, **27** (2003) 1367.

110. A.J. Sederman and L.F. Gladden, *Chem. Eng. Sci.*, **56** (2001) 2615.

*Chapter*  
*Two*

## **Chapter Two: Experimental**

### **2.1 Materials**

#### **2.1.1 Catalysts used**

In the present study only supported platinum catalysts were used, these were either provided externally by the industrial and academic partners or prepared. Primarily silica gel was used as the support substance; however, alumina was also employed for literature comparison. Reported here, where applicable, is the method of preparation and detailed characteristics.

##### **2.1.1.1 IMI2 2.5 % Pt/SiO<sub>2</sub> Catalysts**

For the IMI2 project a quantity of silica gel supported platinum and rhodium catalysts were developed. The rhodium catalysts were employed by the Glasgow group whilst the platinum catalysts were utilised by the Cardiff group. Sets of silica gel supports were developed and manufactured by Davison Catalysis. The metal was impregnated by Johnson Matthey using the incipient wetness technique using aqueous chloroplatinic acid. Characterisation of the un-doped support and the reduced catalyst was carried out by the two industrial groups and by the respective recipients. Details of the information obtained for the platinum catalysts and support used are displayed in Table 2.1, 2.2, 2.3 and 2.4. There are two sets of powdered catalysts which can be defined by either the particle size of the silica gel or the structure. The first set (Table 2.1) have the same support structure, however, each has a different particle size. The second set is the opposite of the first, that is, they have the

same particle size, yet different silica gel structure. The third set; have a granular appearance with a particle size of 0.5 - 1 mm and different surface areas and pore dimensions (Table 2.3). This set of catalysts was intended for use in the trickle-bed reactor; however some studies were carried out in the autoclave.

Table 2.1 Information on supplied support with the same pore character and particle size prior to and after metal impregnation

Support Code <sup>1</sup>	SA (m <sup>2</sup> /g)	PV (ml/g)	PD (Å)	PSD (µm)	MSA (m <sup>2</sup> /g)	NBA <sup>2</sup>	Catalyst Code <sup>3</sup>
SP2-9539.01	321	1.06	132	24.0	1.3	35	M01060
SP2-9539.02	321	1.06	132	49.9	0.6	31	M01037
SP2-9539.03	321	1.06	132	96.3	0.6	22	M01034
SP2-9539.04	321	1.06	132	241.0	1.2	22	M01061

SA = surface area; PV = pore volume; PD = pore diameter; PSD = particle size diameter (support); MSA = metal surface area

<sup>1</sup> support code supplied by Davison Catalysis

<sup>2</sup> Nitrobenzene activity; standard reaction carried out by Johnson Matthey (Fig. 2.1)

<sup>3</sup> Catalyst code supplied by Johnson Matthey

A fourth set of silica gel supports were developed by the Birmingham Materials group and the metal impregnated by Johnson Matthey. The support was created by mixing specific weight amounts of the silica gel powders from Table 2.1 and adding a cellulose binding agent, for example K15M or SMAS and for the preparation of one paste ammonia was added.

Support CFMNH17 comprised 9 g SP2-9538 (4.8 wt%), 21 g SP2-9537 (11.3 wt%), 30 g SP2-9536 (16.1 wt%), 6 g K15M (3.2 wt%), 115 g Water (61.9 wt%), 5g NH<sub>3</sub> (2.7 wt%). This system was mixed for 55 minutes in a kneader and extruded immediately following mixing.

Table 2.2 Information on supplied supports with different pore character but same support particle size prior to and after metal impregnation

Support Code <sup>1</sup>	SA (m <sup>2</sup> /g)	PV (ml/g)	PD (Å)	PSD (μm)	MSA (m <sup>2</sup> /g)	NBA <sup>2</sup>	Catalyst Code <sup>3</sup>
SP18-9528.01	398	1.78	179	8.9	0.2	30	M01069
SP2-9536	779	0.45	23	10.7	1.7	27	M01270
SP2-9537	388	1.02	106	9.5	1.1	33	M01071
SP2-9538	565	0.86	61	10.2	1.9	35	M01271

<sup>1</sup> support code supplied by Davison Catalysis

<sup>2</sup> Nitrobenzene activity; standard reaction carried out by Johnson Matthey (Fig. 2.1)

<sup>3</sup> Catalyst code supplied by Johnson Matthey

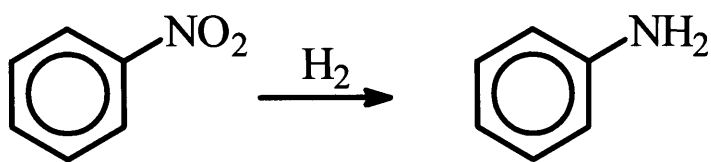


Fig. 2.1 Reaction scheme of nitrobenzene hydrogenation to aniline, Johnson Matthey standard catalyst test

Support CFM5MAS comprised 9 g SP2-9538 (4.3 wt%), 21 g SP2-9537 (10.0 wt%), 30 g SP2-9536 (14.3 wt%), 70 g water (33.3 wt%) and 50 g SMAS (38.1 wt%). The powder was wetted with water and then the SMAS added. This system was mixed for 45 minutes in a kneader and extruded immediately following mixing.

Both pastes were extruded at room temperature from a barrel of 25 mm diameter through a die of 3 mm diameter, L/D 8. CFMNH17 was cut after a short period of drying (1 h) while CFMSMAS was broken to length when dry. The un-doped supports were sintered at 700°C in air. Platinum was added by Johnson Matthey via the wetness impregnation technique as with the powder and granule catalysts.

#### 2.1.1.2 EUROPT-1 Reference catalyst

This standard reference catalyst was used in a number of experiments to rationalise some of the results obtained with the received IMI2 2.5 % Pt/SiO<sub>2</sub> catalysts. EUROPT-1 is a 6.3 % Pt/SiO<sub>2</sub> catalyst developed by the Research Group on Catalysis of the Council of Europe (EUROCAT) and manufactured by Johnson Matthey in 1976 [1a]. This catalyst has received extensive characterisation, the results of which are available in [1b-e], which is summarised in Table 2.5. The catalyst was prepared by impregnation of Pt(NH<sub>3</sub>)<sub>4</sub>Cl<sub>2</sub> on to silica by ion exchange, followed by reduction at 400°C. EXAFS spectroscopy suggested that the average metal particle is raft like typically consisting of 55 Pt atoms arranged in a 7x7 array in a (111) configuration, with a further 8 atoms on top.

## 2.1.1.3 Other Platinum Catalysts

Further experiments were conducted with 5 % Pt/Al<sub>2</sub>O<sub>3</sub> (Johnson Matthey 5R94B) for comparison to examples in the literature and experiments conducted in Cardiff [2].

2.1.1.4 Preparation of 1 % Pt/ $\alpha$ -Alumina catalyst

A 1% Pt/ $\alpha$ -alumina was prepared as follows.  $\gamma$ -alumina (Sasol Puralox SBA 200) of surface area 202 m<sup>2</sup>/g was heated in air at 1200°C for 5 h. XRD confirmed that the product was  $\alpha$ -alumina and the surface area was 5 m<sup>2</sup>/g. A sample of this  $\alpha$ -alumina was immersed for 5 h in an aqueous solution of hydrogen hexachloro-platinate(IV) hydrate (the precursor having been dissolved in the minimum amount of distilled water). The impregnated material was filtered off, dried by heating in air at 60°C for 3 h, and reduced in flowing 5% H<sub>2</sub>/Ar at 200°C for 2 h.

Table 2.3 Information on the supplied granular supports prior to and after metal impregnation

Support Code <sup>1</sup>	SA (m <sup>2</sup> /g)	PV (ml/g)	PD (Å)	PSD (mm)	MSA (m <sup>2</sup> /g)	Catalyst Code <sup>2</sup>
SP18-9725	320	1.2	150	0.5-1	1.7	M02023
SP18-8522.06	390	1.1	113	0.5-1	1.6	M02025
SP18-8749.05	540	0.9	67	0.5-1	0.6	M02027
SP18-8972.01	750	0.3	16	0.5-1	0.9	M02029

<sup>1</sup> support code supplied by Davison Catalysis, <sup>2</sup> Catalyst code supplied by Johnson Matthey



Table 2.4 Information on the extruded silica gel pellets prior to metal impregnation

Support Code <sup>1</sup>	SA (m <sup>2</sup> /g)	PV (ml/g)	PD (Å)	diameter (mm)	Length (mm)	Sinter temperature (°C)	Crush strength (MPa)	Catalyst Code <sup>2</sup>
CFMSMAS	292	0.94	129	5	2	700	3.3	M03216
CFMNH17	297	0.65	87	5	2	700	2.6	M03217

<sup>1</sup> support code supplied by Birmingham Materials Centre

<sup>2</sup> Catalyst code supplied by Johnson Matthey

Table 2.5 Information on the reference catalyst EUROPT-1

Catalyst code	SA (m <sup>2</sup> /g)	PV (ml/g)	PD (Å)	PSD (µm)	Pt loading (%)	Dispersion (%)	mPSD <sup>2</sup> (nm)
EUROPT-1 <sup>1</sup>	185	0.77	140	250-420	6.3	60	2.0

<sup>1</sup> = Preparation by Johnson Matthey

<sup>2</sup> = mPSD = metal particle size

### 2.1.2 Cinchona Alkaloids

Cinchona alkaloids are naturally occurring white crystalline solids. For this investigation cinchonidine (Fig. 2.2a) is primarily used to induce enantioselective hydrogenations by adsorption on the metal of the catalyst. Cinchonine (Fig. 2.2b) is the near enantiomer of cinchonidine and has been used in limited experiments to investigate its effect and to rationalise results compared to studies in the literature. Cinchonidine (Fluka, 98%) and cinchonine (Fluka, 98%) were used as received.

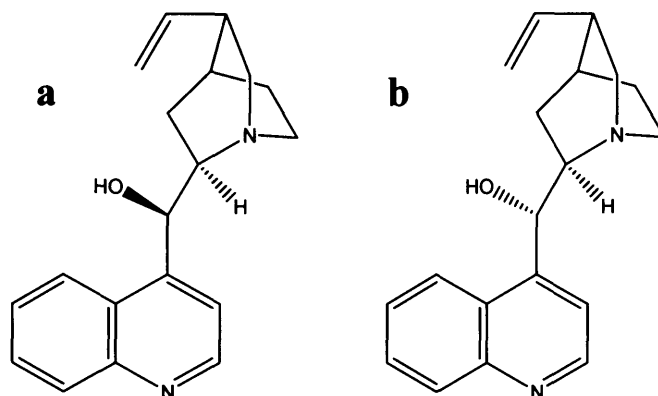


Fig 2.2 Representations of cinchonidine (a) and cinchonine (b)

### 2.1.3 Other materials

Other materials used are listed in Table 2.6. All were used as received unless otherwise stated.

Table 2.6 Other materials used in the current study

Entry	Material	Supplier	Specification
1	dichloromethane	Fisher	HPLC 99.9 %
2	ethanol	Fisher	HPLC 99.9 %
3	toluene	Fisher	99 %
4	Acetic acid	Fisher	Glacial
5	hydrogen	BOC	99.9995 %
6	helium	BOC	99.9995 %
7	5 % H <sub>2</sub> /Ar	BOC	Specshield
8	Silicon carbide	Washington Mills, UK	25 mm
8	$\gamma$ -alumina	Sasol	200 m <sup>2</sup> /g

## 2.2 Reactors used in the current study

### 2.2.1 Stirred tank reactor

Stirred tank hydrogenations were carried out in a high pressure stainless steel Baskerville autoclave (100 ml) (Fig. 2.3). Reactions took place within a glass liner (volume 80 ml) which was placed within the stainless steel jacket. The jacket was screwed into the body of the unit. To ensure the unit would maintain pressure a Teflon ring placed between the jacket and the mount compressed to form a seal. A Teflon gas entrainment impeller was connected to a sealed magnetic drive unit, which was rotated by a Parvalux DC shunt motor, located above the reactor. Agitation of the reactor contents was controlled by a variable resistance dial with the capability of up to 1400 rpm. The reaction mixture was typically stirred at 1000 rpm.

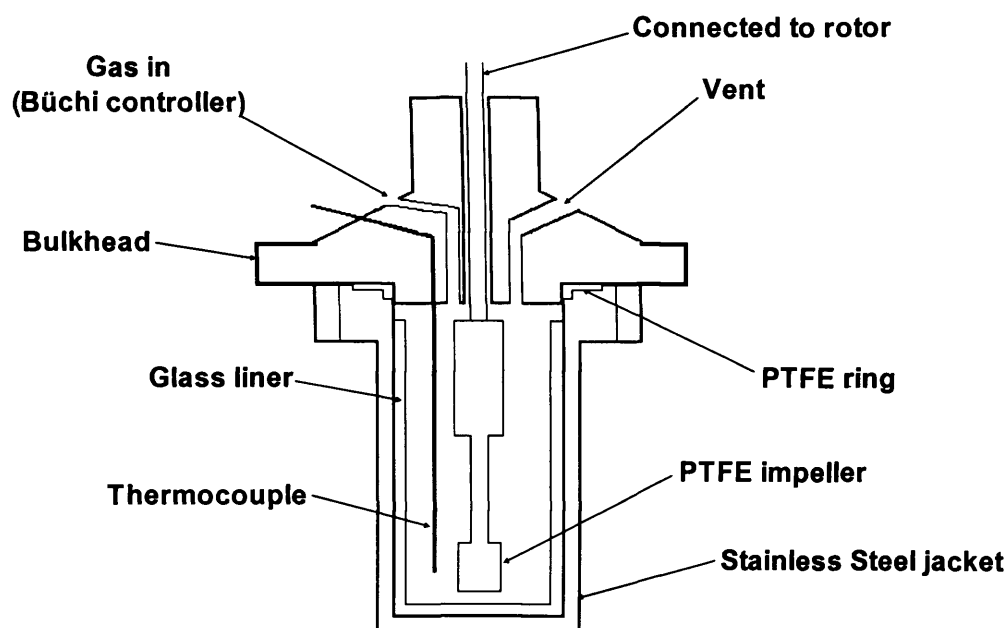


Fig. 2.3 Schematic representation of the Baskerville high pressure autoclave

Reaction temperature was monitored with a thermocouple connected to a digital temperature indicator. This indicator controlled an electric heating unit, which fitted around the reactor jacket when required. Reactions were normally carried out at  $25\pm 1^\circ\text{C}$ , an ice-water bath was used to regulate the temperature.

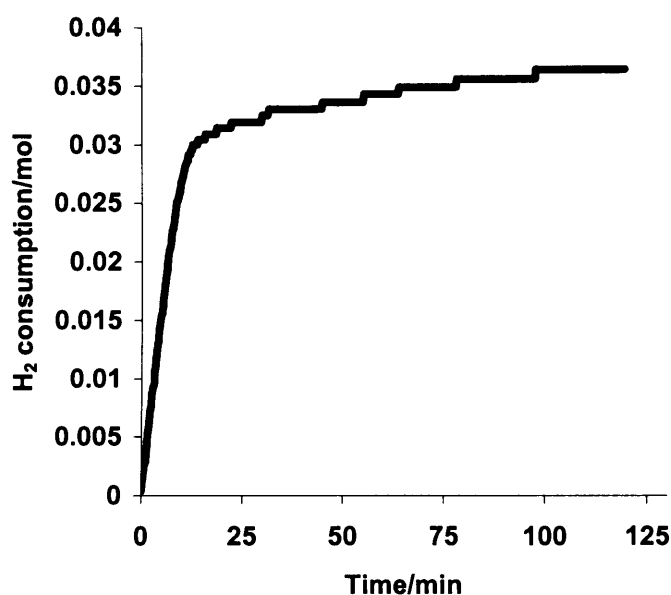


Fig. 2.4 Example of the hydrogen uptake data obtained with time of 2,3-butanedione hydrogenation over EUROPT-1 modified with cinchonidine

The progress of the catalytic reaction was monitored by a Büchi Pressflow computer controlled gas controller 9901, used in accordance with its instruction manual. The desired constant reaction pressure was input by the operator before reaction commenced. Reaction pressure was monitored by the unit as the reaction proceeded. This allowed the pressure in the unit to be maintained at the required pressure to within  $\pm 0.01$  bar. The uptake of gas consumed in the reaction, expressed in fractions of moles of gas at room temperature and 1 bar was recorded by a computer linked via a serial link cable. Specific software logged uptake data which could then be analysed using a program such as Microsoft *Excel*. A

typical hydrogen uptake curve is shown in Figure 2.4 and was obtained from the enantioselective hydrogenation of 2,3-butanedione over EUROPT-1.

### 2.2.2 Trickle-Bed Reactor

Hydrogenations over a fixed catalytic bed were carried out in the trickle-bed reactor (Fig. 2.5). The reactor is composed of four parts: the head, the glass reactor vessel, a Teflon ring and an aluminium clamp. The head contains the gas and liquid distributor along with a pressure gauge and vent valve. The catalytic bed rests on a glass frit (# 3 gauge) in the glass reactor vessel, which is 25 cm long with an outer diameter of 2.5 cm. Reactor integrity was ensured with the use of a Teflon ring and a clamp.

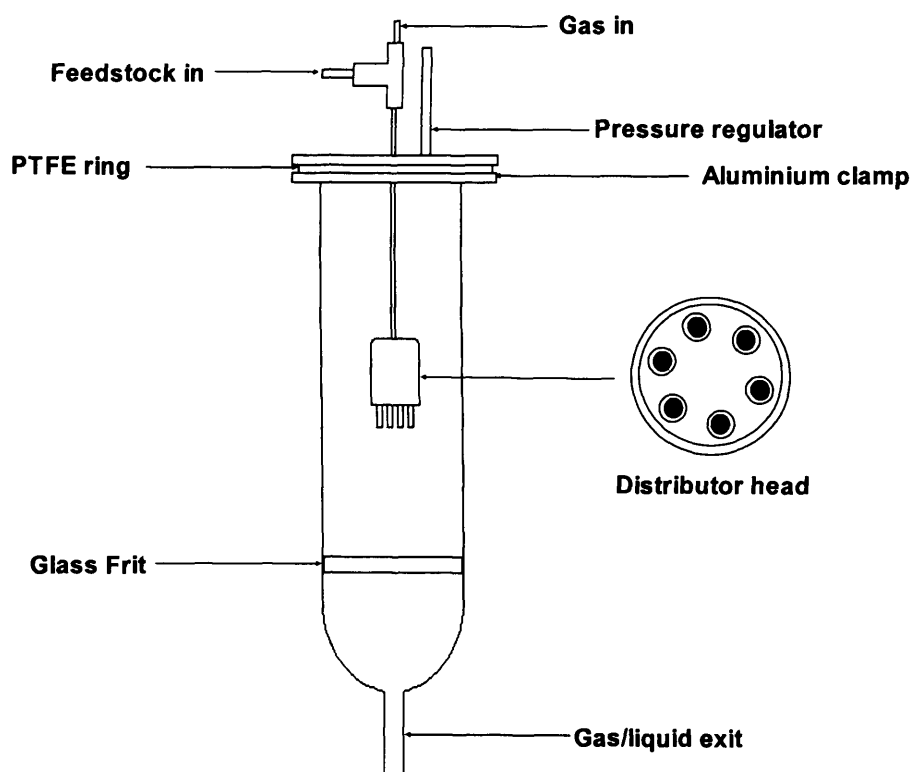


Fig. 2.5 Schematic representation of the trickle-bed reactor developed in IMI-1

This is placed between the head and the reactor vessel and vacuum grease (Dow Corning) is applied to both sides. A clamp is then used to seal the unit ready for experimentation. Liquid and gas were introduced in to the reactor through a T-union connected to a stainless steel distributor (see insert Fig. 2.5) located on the head. This consisted of a chamber with six exit tubes (1/8 inch OD) arranged around the edge of the distributor. The pressure inside the reactor was controlled with needle valves located on the incoming gas line and at the reactor vessel exit tube. To deliver the liquid feedstock typically at 1 ml/min to the reactor a HPLC pump was employed. The liquid exiting the bed could be collected for analysis or separated from the gas further upstream for liquid disposal.

### 2.2.3 Gas-Phase Reactor.

Hydrogenations in the gas-phase were carried out in a low pressure flow microreactor (i.d. 3.2 mm Cambridge Reactor Design, CRD 5000) constructed in glass and located in a tube furnace (Fig. 2.6). The catalyst bed was supported by silica wool. The furnace temperature was controlled with a Eurotherm digital controller. Thermocouples were located inside the reactor tube, above the catalyst bed and inside the furnace. Helium and hydrogen were controlled by Brooks 5850 mass flow controllers connected to a digital display. Hydrogen could be diluted in excess helium for the reaction. This He:H<sub>2</sub> mixture was diverted through the saturator to deliver reactant vapour to the catalyst. An additional saturator could be used for experiments involving a second reactant or pre-treatment with product. The desired gas flow could be diverted through both saturators if required. An isothermal water bath (Grant C2G) was used to maintain the temperature of the saturator. The water contained in the bath was cooled with a Grant cooling unit. The stainless steel tubes which delivered the reaction vapour and gases were lagged with Tyco

Isopad ITC heating tape. These were controlled with a variable resistance dial and typically held at  $75^{\circ}\text{C}\pm 2^{\circ}\text{C}$ . The exit gas was analysed on-line by chiral gas chromatography with a Varian 3400 fitted with a 25 m  $\beta$ -Chirasil-dex column.

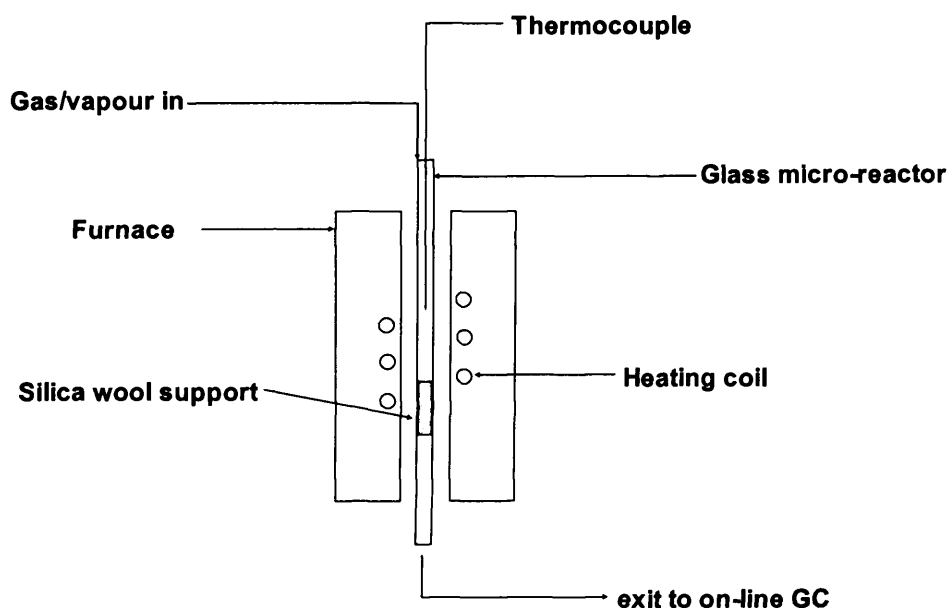


Fig. 2.6 Schematic representation of the gas-phase reactor

## 2.3 Procedures.

### 2.3.1 Catalyst Characterisation

The supplied catalysts were characterised prior to platinum impregnation. Surface areas and pore characteristics obtained by Davison Catalysis and the Birmingham materials centre is displayed in Tables 2.1-4. Additional experiments were carried out in Cardiff for comparison purposes.

## 2.3.1.1 Surface Area and Pore Analysis

The surface area and pore character of the catalysts and their corresponding supports was carried out in a Micrometrics BET instrument. The sample to be analysed was placed in a glass tube and secured in to the instrument. The sample was degassed by placing a heating jacket around the tube and heated to 150°C for ten minutes in helium. The jacket was removed and the sample was immersed in liquid nitrogen. The sample is held under vacuum and aliquots of nitrogen gas are allowed in to the tube of fixed volume. Physisorption of N<sub>2</sub> at low temperatures can be used to determine the surface area of porous materials. Nitrogen tends to form monolayers of closely packed molecules on the surface area of the material at cryogenic temperatures. The surface area of that material is then deduced from the BET equation derived by Brunauer, Emmett and Teller presented in the linearised form as follows

$$\frac{P}{V(P_0-P)} = \frac{1}{V_m \cdot C} + \frac{(C-1)}{V_m \cdot C} \cdot \frac{P}{P_0} \quad (2.1)$$

where  $V$  is the volume at STP of gas adsorbed at pressure  $P$ ,  $V_m$  is the volume required to cover the surface with one monolayer and  $C$  is a constant.  $P_0$  is the saturation pressure of the liquefied gas at the temperature of adsorption. The surface area of the sample is determined from the monolayer volume  $V_m$  at STP as follows

$$SA = V_m \cdot \frac{N_A}{V_A} \cdot A \quad (2.2)$$

where  $A$  is the area of the nitrogen molecule and  $N_A / V_A$  is Avogadro's number per unit volume gas. Typically the surface area of the sample is quoted as a function of mass, that is  $\text{m}^2\text{g}^{-1}$ , which is the surface area divided by the mass of sample used in the measurement.



Information was also obtained on the pore characteristics of the samples. Specifically the pore volume and the pore diameter, which can be displayed as a volcano plot showing, where applicable a size distribution range. Nitrogen is able to condense in the pores of the sample beyond the monolayer point and is related to the diameter of the pores and gas pressure. This is described by the Kelvin equation

$$\ln \left( \frac{P}{P_0} \right) = \frac{2\sigma V_0}{r_K RT} \quad (2.3)$$

where  $V_0$  represents the molar volume,  $\sigma$  is the liquid surface tension and  $r_K$  is the 'Kelvin pore radius'. Distribution of the pore sizes can then be calculated from

$$\Delta S = \frac{2\Delta V_P}{r_K} \quad (2.4)$$

where  $\Delta S$  is the differential surface area associated with a particular average pore radius and  $\Delta V_P$  is the pore volume determined from the  $P$ - $V$  isotherm.

### 2.3.1.2 Powder X-ray Diffraction

The  $\alpha$ -alumina sample recovered after heating  $\gamma$ -alumina to 1200°C was investigated with X-ray diffraction to confirm the structural change (Fig 2.7). Using an Enraf NONIUS FR590 powder x-ray diffractometer with a Cu- $K_\alpha$  source, samples were prepared and placed in X-ray path for investigation. The peaks shown in Figure 2.7 correspond to the diffraction from particular planes in the lattice and are dictated by the Bragg equation

$$n\lambda = 2d \sin\theta \quad (2.5)$$

where  $n$  is an integer,  $\lambda$  is the X-ray wavelength (0.154 nm),  $d$  is the particular lattice plane spacing and  $\theta$  is the Bragg diffraction angle. The sample analysed was compared to a standard pattern and was deemed to be  $\alpha$ -alumina.

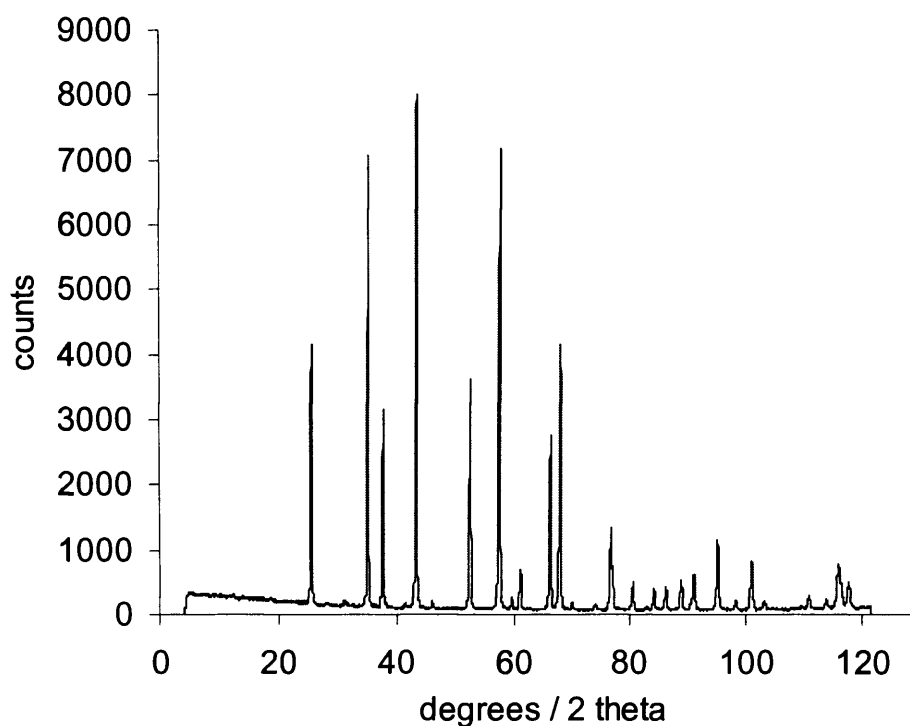


Fig. 2.7 Power XRD pattern of  $\alpha$ -alumina

### 2.3.2 Reduction of Catalyst Samples.

Catalyst samples as-received had been reduced by the manufacturer. Prior to reaction the catalyst sample (2.0 g) was re-reduced. Samples were placed in a Pyrex calcination boat and inserted into a horizontal tube furnace (Fig. 2.8). A continuous flow of 5 %  $\text{H}_2/\text{Ar}$  was

passed over the catalyst and the tube furnace was heated to the desired temperature. Typically the catalyst was reduced at 200°C for 1 h, and then cooled to ambient temperature under the flow of 5 % H<sub>2</sub>/Ar. Prepared samples were stored in a sealed vial and used within 1 week.

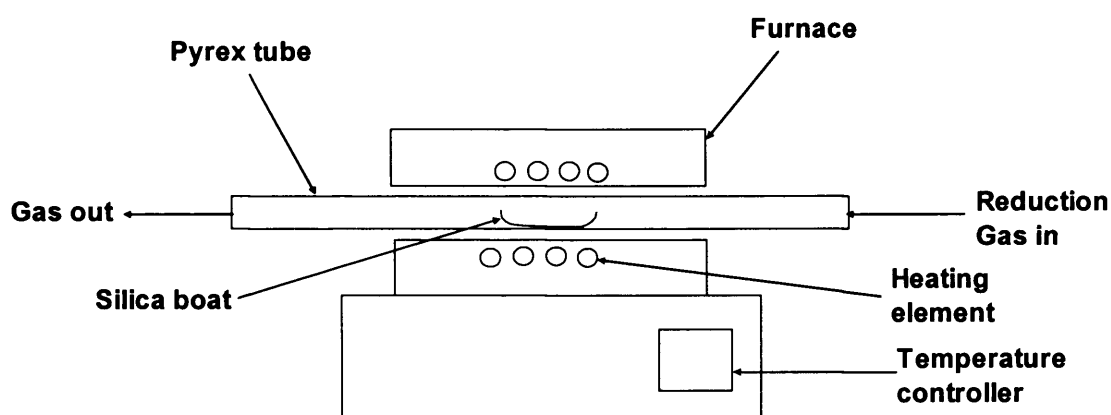


Fig. 2.8 Representation of the furnace used to reduce catalyst samples

### 2.3.3 Experimental Procedure

#### 2.3.3.1 Autoclave Procedure I: *in situ* modification

Modification of the catalyst with alkaloid was achieved as the reaction proceeded. Typically the reactant (34.5 mmol), modifier (0.02 g), catalyst (0.2 g) and solvent were placed in the glass liner and the autoclave sealed. Hydrogen was used to purge the system in three charges of 3-4 bar, then the final charge to the desired reaction pressure. Stirring commenced to the required speed and the recording software activated to begin the reaction.

### 2.3.3.2 Autoclave Procedure II: pre-modification

Pre-modification of the catalyst involved stirring a slurry of catalyst (0.2 g) and alkaloid (0.02 g) dissolved in solvent (25 ml) in the glass liner of the autoclave. This was carried out in aerobic conditions under atmospheric pressure. The glass liner was transferred to the autoclave where reactant (34.5 mmol) and additional solvent (5 ml) were added. The autoclave was sealed and the residual air was purged with hydrogen. The reaction commenced after the pressure was increased to the desired level, agitation and the recording software started.

### 2.3.3.3 Trickle-bed reactor procedure I: *in situ* modification

The bed was packed according to the Al-Dahahan and Duduovic method [3] as described in section 2.3.3.5 with catalyst granules or extrudates (2 g) and silicon carbide fines (25 gauge). Under helium (0.5 barg, 7 ml/s, 4800 /h GHSV) a solution of dissolved modifier in solvent was passed through the catalytic bed. Samples of the effluent were taken for UV analysis at intervals during the process. The reaction began when helium was switched for hydrogen and a feedstock of dissolved reactant (0.1 M) was allowed to flow through the bed at 1 ml/min. For continual modification of the bed the feedstock contained additional alkaloid ( $1.7 \times 10^{-4}$  M). Samples of reaction mixture were taken intermittently over the course of the reaction period for analysis.

#### 2.3.3.4 Trickle-bed reactor procedure II: *ex situ* modification

The amount of catalyst (2 g) required to make up the bed was stirred in a solution of cinchonidine in DCM for ten minutes in air. The catalyst was filtered and dried under vacuum then placed in the reactor with the silicon carbide fines according to the Al - Dahahan and Duduovic method [3]. Dichloromethane was then passed through the bed for 60 minutes at 1ml/min under Helium (0.5 barg, 4800 /h GHSV) and samples were taken for cinchonidine analysis with UV spectroscopy. The helium was switched for hydrogen (0.5 barg, 4800 /h GHSV) and a feedstock solution was permitted to pass through the bed. The feedstock solution contained reactant (0.1 M) with alkaloid (0.849 mM) dissolved in solvent. Samples were taken for GC analysis during the duration of the experiment.

#### 2.3.3.5 Loading of the trickle-bed reactor

Loading of the trickle-bed reactor was carried out according to the Al-Dahahan and Duduovic method with catalyst and fines [1]. The required mass of catalyst was placed into the reactor and the bed height was measured. The catalyst was removed and divided in to eight samples. Due to the granular nature of the catalyst a certain volume of void space remained. This void space was filled with an inert material, silicon carbide, to ensure even liquid distribution through the catalyst bed. The amount of fines required to fill the void space was determined as the amount of fines that increased the bed volume by 2 % of the original catalyst volume. This amount is then divided in to eight samples as with the catalyst. Loading of the bed for a reaction is reported as follows: A thin layer of fines is placed on to the glass frit of the reactor cell, a sample of the catalyst is then placed on top of this layer. The void spaces between the catalyst layer is filled with a sample of fines. The next catalyst

sample is added followed by a sample of fines. This is repeated until the samples of catalyst and fines have been placed in to the reactor. Finally a layer of silicon carbide is added exposing only the uppermost catalyst granules.

#### 2.3.3.6 Gas phase reactor procedure for the standard reaction

Hydrogenation was performed with the 2.5 % Pt/Silica catalyst M01271. Enantioselective hydrogenation was achieved with alkaloid pre-modified catalysts. These were prepared on a small batch scale for several experiments. Samples of catalyst (200 mg) were stirred in a slurry of alkaloid (20 mg), dissolved in dichloromethane (25 ml) under atmospheric air for 10 minutes. The catalyst was filtered and dried under vacuum before transfer to the glass reactor tube at 40°C. Catalyst samples (25 mg) were pre-conditioned in a He flow (80 ml/min) for 10 min followed by a 3:1 He:H<sub>2</sub> flow (80 ml/min) for a further 10 min. This mixture was then diverted through a saturator (20°C) containing the reactant. The exiting reaction gas was analysed by on-line GC at regular intervals during the reaction period.

#### 2.4 Product recovery

Reaction mixtures taken from the autoclave required separation from the catalyst. Normally this was achieved by filtration using a funnel with standard filter paper. However, for GC analysis an aliquot, typically 3 ml was passed through a pipette plugged with cotton wool in to a sample vial.

## 2.5 Product analysis.

### 2.5.1 Gas chromatography.

Analysis by gas chromatography, specifically gas-liquid chromatography is a commonly used tool for industry and academic institutions. Illustrated in Figure 2.9 is a schematic of a typical GC setup. The sample to be analysed is vaporised in the injector (typically 200°C) and enters the head of the chromatographic column. The sample is transported through the column by the flow of inert, gaseous mobile phase. The column itself contains a liquid stationary phase which is adsorbed onto the surface of an inert solid. For the present study the column used was coated with seven glucose units as a toroidal  $\beta$ -cyclodextrin polymer (Fig. 2.10). The hydroxyl groups are on the outside of the cavity, which is apolar and has an internal diameter of 0.75 nm. This phase was able to separate the enantiomers of methyl and ethyl lactate along with hydroxybutanone. This is achieved by size exclusion and by chiral recognition [4]. Column temperature is controlled to within tenths of a degree to ensure accurate results. The optimum column temperature is dependent upon the boiling point of the sample. Typically, a temperature slightly above the average boiling point of the sample results in an elution time of 2 - 30 minutes. Minimal temperatures give good resolution, but increase elution times.

The effluent from the column is mixed with hydrogen and air, and ignited. Organic compounds burning in the flame produce ions and electrons which can conduct electricity through the flame. A large electrical potential is applied at the burner tip, and a collector electrode is located above the flame. The current resulting from the pyrolysis of any organic compounds is measured. Flame ionisation detectors (FID) are mass sensitive rather than

concentration sensitive; this gives the advantage that changes in mobile phase flow rate do not affect the detector's response. The FID is a useful general detector for the analysis of organic compounds; it has high sensitivity, a large linear response range, and low noise. It is also robust and easy to use, but unfortunately, it destroys the sample. The measured current changes can be represented visually with a computer and the relevant software package. The chromatographs can be stored and recalled for future occasions.

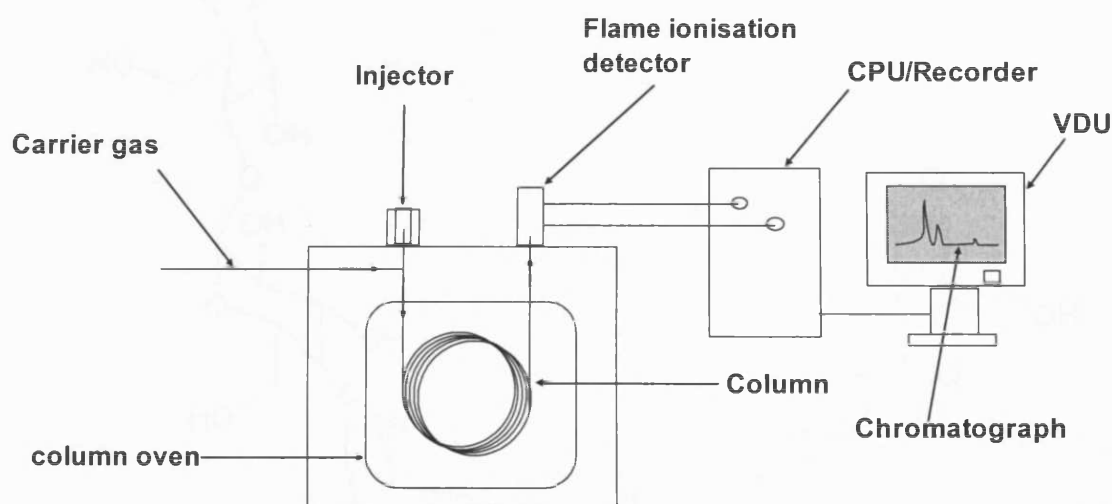


Fig. 2.9 Representation of a manual injection gas chromatography instrument

### 2.5.1.1 Liquid Samples

#### 2.5.1.2.1 Enantioselective hydrogenations

Reaction samples collected from the catalytic enantioselective hydrogenations carried out in the autoclave or the trickle-bed reactors were analysed by gas chromatography (GC). The GC (Varian 3800) was fitted with a  $\beta$ -TA Chrialdex™ chrial capillary column (30



m Chromopak) (Fig. 2.10) and FID with helium as the carrier gas. Data was recorded and could be analysed by the software package *Star Chromatography Workstation for Windows* (Varian).

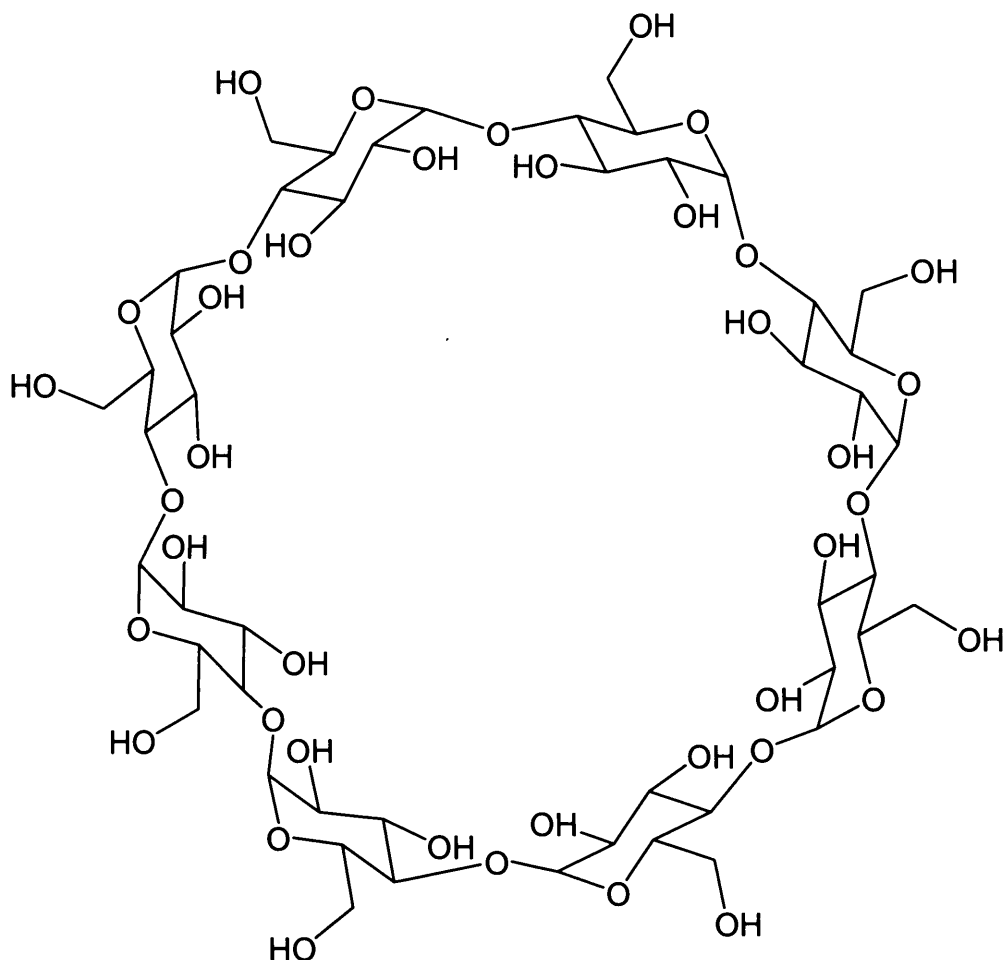


Fig. 2.10 Structural representation of  $\beta$ -cyclodextrin

Aliquots (0.1  $\mu$ l) of 2,3-butanedione hydrogenation products were analysed using a column temperature of 70°C (isothermal) and a column pressure of 10 psi. The FID was held at a temperature of 250°C and the split/splitless injector was at 200°C. A typical chromatograph is illustrated in Fig. 2.11. The peaks were eluted with increasing retention time as follows: solvent (DCM), 2,3-butanedione, (*R*)-hydroxybutanone, (*S*)-hydroxybutanone, *RR*-butandiol, *SS*-butandiol and *meso*-butandiol. Separation of all

products was achieved. The use of reference material confirmed the order of the diol forms: *RR*, *SS* and *meso*.

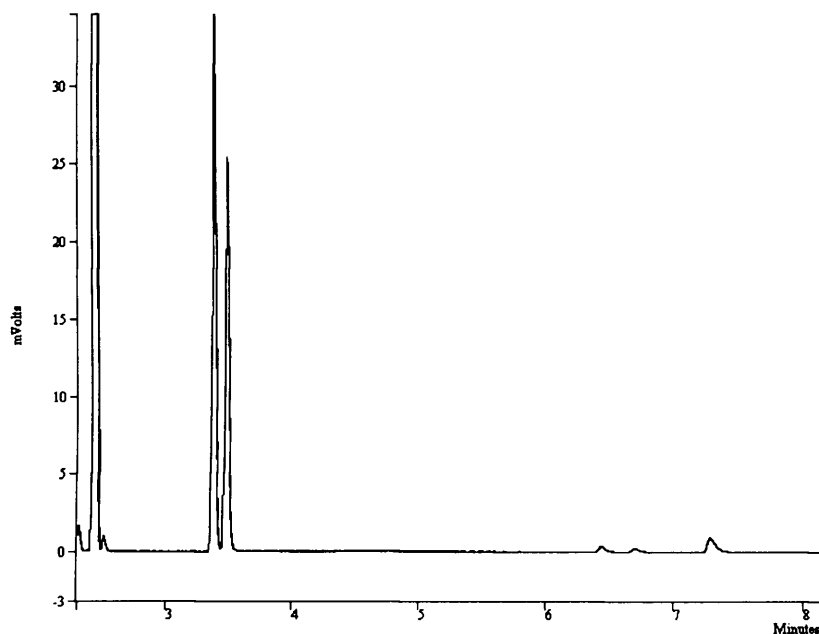


Fig. 2.11 Typical chromatograph for analysis of 2,3-butanedione hydrogenation products eluted as follows; DCM, 2,3-butanedione, (*R*)-hydroxybutanone, (*S*)-hydroxybutanone, *RR*-butandiol, *SS*-butandiol and *meso*-butandiol

Analysis of the hydrogenation products of methyl pyruvate was conducted with a column temperature of 80°C (isothermal) and a column pressure of 10 psi. Aliquots (0.1  $\mu$ l) of the reaction sample were injected into the chiral column. The injection temperature was 200°C and the FID was at 250°C. The peaks were eluted with increasing retention time as follows: solvent (DCM), methyl pyruvate, (*R*)-methyl lactate and (*S*)-methyl lactate. Complete separation of enantiomers was achieved (Fig. 2.11).

Conversion is defined by the equation:

$$\text{Conversion (\%)} = \frac{(\alpha_1 A_{[R]} + \alpha_2 A_{[S]})}{(\alpha_1 A_{[R]} + \alpha_2 A_{[S]} + A_{[SM]})} \times 100 \quad (2.6)$$

The enantiomeric excess (e.e.%) is defined by the equation:

$$\text{e.e. (\%)} = \frac{([R] - [S])}{([R] + [S])} \times 100 \quad (2.7)$$

#### 2.5.1.2.2 Cyclohexene hydrogenations

Reaction samples from the catalytic hydrogenation of cyclohexene, carried out in the autoclave and trickle-bed reactors were analysed by gas-liquid chromatography. A GC fitted with a HP1 crosslinked methylsiloxane gum coated capillary column (25 m, Chromopak) and an FID was used for analysis. The column temperature was 80°C and helium was used as the carrier gas at a pressure of 20 psi. The injection temperature was 200°C, with the FID at 250°C. Separation of reactant and product was achieved.

#### 2.5.2 Gas phase analysis

The exit gas from the fixed bed microreactor was analysed by chiral gas chromatography. Samples of fixed volume (1  $\mu$ L) were injected in to the column using a standard six port injector at a temperature of 200°C. The temperature of the chiral column ( $\beta$ -TA Chiraldex™) was at 68°C (isothermal). Helium was used as the carrier gas with a pressure of 24 psi. The signals from the FID (250°C) were measured by the software package *Star Chromatography Workstation for Windows* (Varian).

### 2.5.3 Ultraviolet spectroscopy

Ultraviolet Spectroscopy was employed to analyse samples from the pre-modification of the catalyst bed from the trickle-bed reactor. The technique involves passing a single beam of light through a cell containing a sample. The light source is monochromatic and can cover wavelengths from ultraviolet, visible to near infra-red. In this region of the electromagnetic spectrum molecules can undergo electronic transitions. The method is used in a quantitative way to determine concentrations of an absorbing species in solution, using the Beer-Lambert law (equ. 2.8)

$$A = \ln(I/I_0) = \epsilon.c.L \quad (2.8)$$

Where  $A$  is the absorbance of the solution which has no units,  $I$  is the transmitted intensity and  $I_0$  is the intensity of the incident light at a given wavelength. The constant  $\epsilon$  is referred to as the extinction coefficient,  $c$  is the concentration of the absorbing species and  $L$  is the cell length.

#### 2.5.3.1 Analysis of cinchonidine solutions

Analysis was conducted with a Perkin Elmer UV/Vis spectrometer (*Lambda 20*) for samples contained in a quartz cell of 1 cm path length. The concentration of cinchonidine exiting the bed was determined from the absorbance wavelength at 315 nm (Fig. 2.12). A calibration plot of absorbance against cinchonidine concentration was plotted. The concentration of cinchonidine ranged from 0 to 0.17 mM (Fig. 2.13).

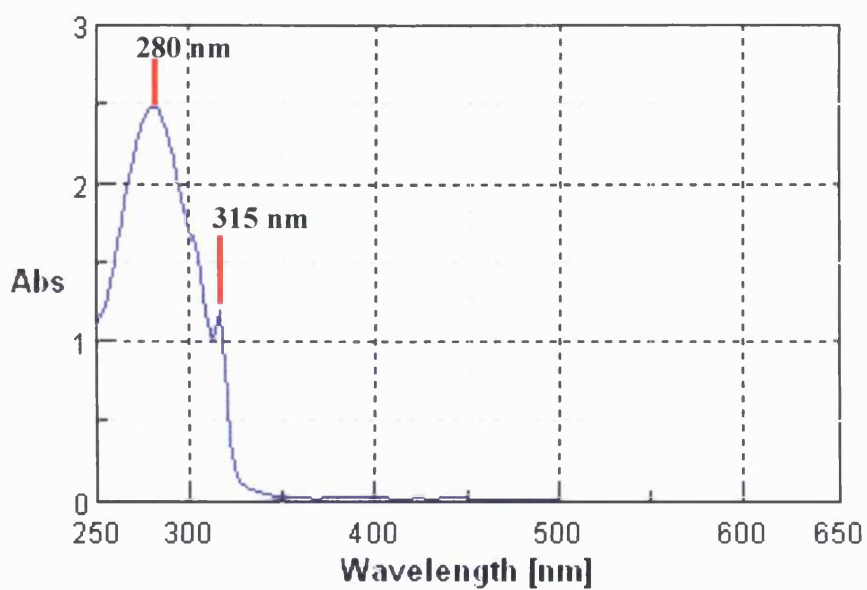


Fig. 2.12 UV spectrum of cinchonidine in DCM solution

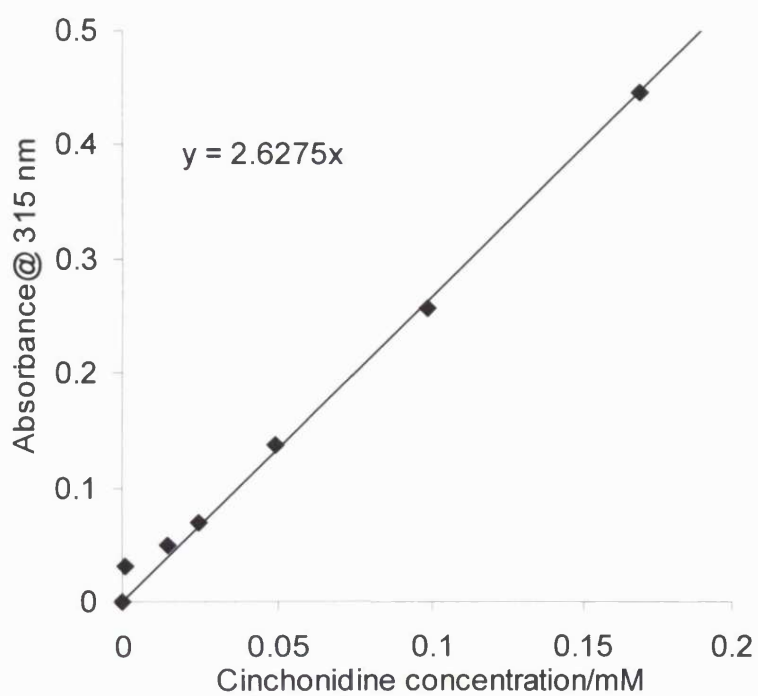


Fig. 2.13 Corresponding absorbance of cinchonidine in DCM at 315 nm with different concentrations

## 2.6 Determination of the Rate of Reactions

Using the software package Mathematica 4.2 (*Wolfram Research*) the rate of a reaction could be determined. The hydrogen uptake data obtained from a reaction could be input into a prepared script. The function of the script was to fit a line of best fit to the overall uptake profile (Fig. 2.14). Then through imbedded equations this best fit line could be expressed as the rate of the reaction in  $\text{mmol/h/g}_{\text{cat}}$ . For reactions involving 2,3-butanedione both the first and second stages rate were determined.

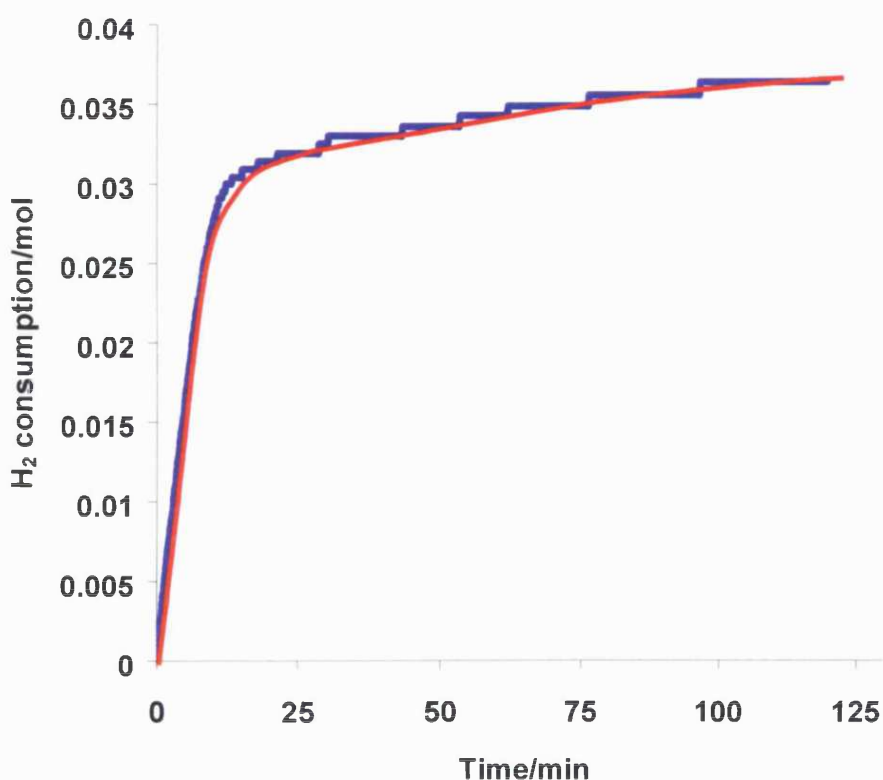


Fig. 2.14 Example of the best fit line (—) generated with hydrogen uptake data from the enantioselective hydrogenation 2,3-butanedione over EUROPT-1 (—)

### 2.7 Measuring the vapour pressure of methyl pyruvate

To measure the vapour pressure of methyl pyruvate a vacuum pump was used to reduce the pressure over liquid pyruvate at 0°C (Fig. 2.15). After pumping for 10 minutes the vessel was sealed and allowed to stand for a further 10 minutes to establish liquid/vapour equilibrium. The pressure was then measured using a standard gauge and the temperature increased in stages to 40°C.

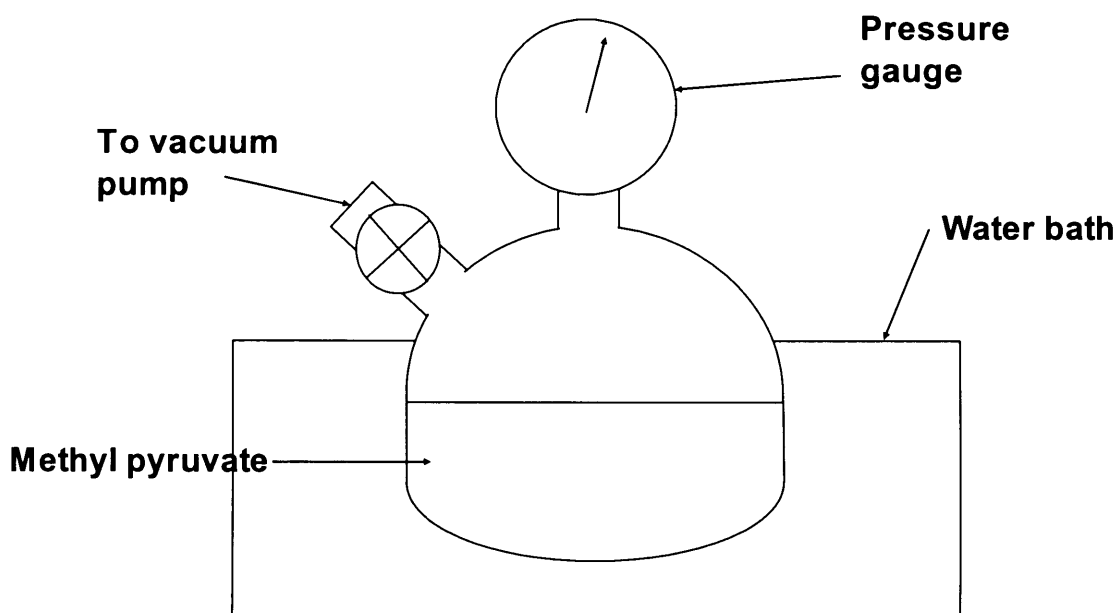


Fig. 2.15 Schematic representation of the apparatus used to measure the vapour pressure of methyl pyruvate

### 2.8 References

1. (a) G.C. Bond and P.B. Wells, *Appl. Catal.*, **18** (1985) 221.; (b) G.C. Bond and P.B.

- Wells, *Appl. Catal.*, **18** (1985) 225.; (c) J.W. Geus and P.B. Wells, *Appl. Catal.*, **18** (1985) 231.; (d) A. Frennet and P.B. Wells, *Appl. Catal.*, **18** (1985) 243.; (e) P.B. Wells, *Appl. Catal.*, **18** (1985) 259.
2. X. Li, N.F. Dummer, R.L. Jenkins, R.P.K. Wells, P.B. Wells, D.J. Willock, S.H. Taylor, P. Johnston and G.J. Hutchings, *Catal. Lett.*, **96** (2004) 147.
3. M.H. Al-Dahhan and M.P. Dudukovic, *AIChE J.*, **42** (1996) 2594.
4. Cyclobond™ Handbook, A Guide to using Cyclodextrin Bonded Phases, Astec, 1990.



*Chapter  
Three*

---

## Chapter 3: Enantioselective Hydrogenations under Standard Conditions in the Autoclave Reactor

### 3.1 Introduction

The use of batch reactors is widespread in the literature for heterogeneous enantioselective hydrogenation. Therefore, it will be possible to compare and contrast the results obtained in the present investigation. Use of the stirred autoclave in this investigation primarily concerns a catalyst screening program to determine the support characteristics best suited to enantioselective hydrogenation of 2,3-butanedione. These characteristics could then be implemented in the manufacture of an extruded catalyst support. Secondary to this, optimisation of the reaction in the autoclave was employed in the experimental protocol for the trickle-bed reactor.

### 3.2 Results of 2,3-butanedione enantioselective hydrogenation

#### 3.2.1 Standard Reaction

The 2.5 % Pt/SiO<sub>2</sub> powder and granular catalysts were investigated in the autoclave with the standard enantioselective hydrogenation reaction of 2,3-butanedione to compare the rate from the measured uptake data. Reactions were carried out over *in situ* modified 2.5 % Pt/SiO<sub>2</sub> at 25°C and 10 bar H<sub>2</sub> for 2 h in dichloromethane as the solvent. The hydrogen uptake profiles for catalysts with support particle of the same size of are illustrated in Appendix 7.1. Corresponding rate and conversion of the dione hydrogenation is reported in Table 3.1. Catalyst M01060 (entry 1) gave the best rate of 186 mmol/h/g<sub>cat</sub> with a conversion

of 89 % at 2 h. The enantiomeric excess of (*R*)-hydroxybutanone at 90 % conversion was 11.1 %.

For catalysts with the same particle size, yet with differing pore characteristics the hydrogen uptake profiles are displayed in Appendix 7.2. Table 3.1 contains the corresponding rate and conversion data. Catalyst M01271 (entry 8) performed the best with a rate of 204 mmol/h/g<sub>cat</sub> and conversion at 2 h of 92 %. An ee of 12.4 % at 90 % conversion was obtained with another reaction.

Table 3.1 Values of maximum rate and conversion at 2 h of the standard reaction of 2,3-butanedione hydrogenation over the received 2.5 % Pt/SiO<sub>2</sub> catalysts modified with cinchoinidine

Entry	Catalyst	Maximum Rate (mmol/h/g <sub>cat</sub> )	Conversion at 2 h (%)
1	M01060	186	89
2	M01037	48	18
3	M01034	54	13
4	M01061	144	73
5	M01069	24	5
6	M01270	78	23
7	M01071	84	51
8	M01271	204	92
9	M02023	114	81
10	M02025	90	53
11	M02027	54	43
12	M02029	27	15

[0.2 g catalyst; 27 ml dichloromethane; 34.5 mmol 2,3-butanedione; 5.66 mM cinchonidine;

10 bar H<sub>2</sub> pressure; 25°C; T = 25 ± 1°C; 1000 rpm]

The granular catalysts of the M0202X series were reacted according to the protocol in 2.3.2.3. Due to the nature of the catalysts the results presented in Table 3.4 are for undamaged catalysts. Several reactions were carried out in which the catalyst structure was compromised. The resulting increase in rate can be ascribed to reduction in the mass transfer of substrate to the inner metal sites (Fig. 3.4). Hydrogen uptake profiles over 2 h are given in Appendix 7.3 for the undamaged catalysts. The fastest rate was achieved by M02023 of 114 mmol/h/g<sub>cat</sub> and a conversion of 81 % at 2 h (Table 3.1 entry 9).

#### 3.2.1.1 Standard reaction in absence of alkaloid

The standard reaction was applied where cinchonidine was omitted from the protocol. Butanedione was hydrogenated over M01271 in dichloromethane at 10 bar of hydrogen pressure at room temperature (Fig. 3.1). The rate was measured for comparison to the modified reaction, from which the degree of rate enhancement afforded by the addition of alkaloid could be compared to the literature. Typically the rate enhancement afforded by alkaloid addition for 2,3-butanedione hydrogenation is ca. 10-20 %. The rate of hydrogenation to hydroxybutanone was found to be 480 mmol/h/g<sub>cat</sub> compared to 204 mmol/h/g<sub>cat</sub> for the modified reaction. Therefore, the addition of alkaloid at this concentration has inhibited the reaction. The second stage of the reaction; dione to hydroxybutanone proceeds at 18 mmol/h/g<sub>cat</sub>.

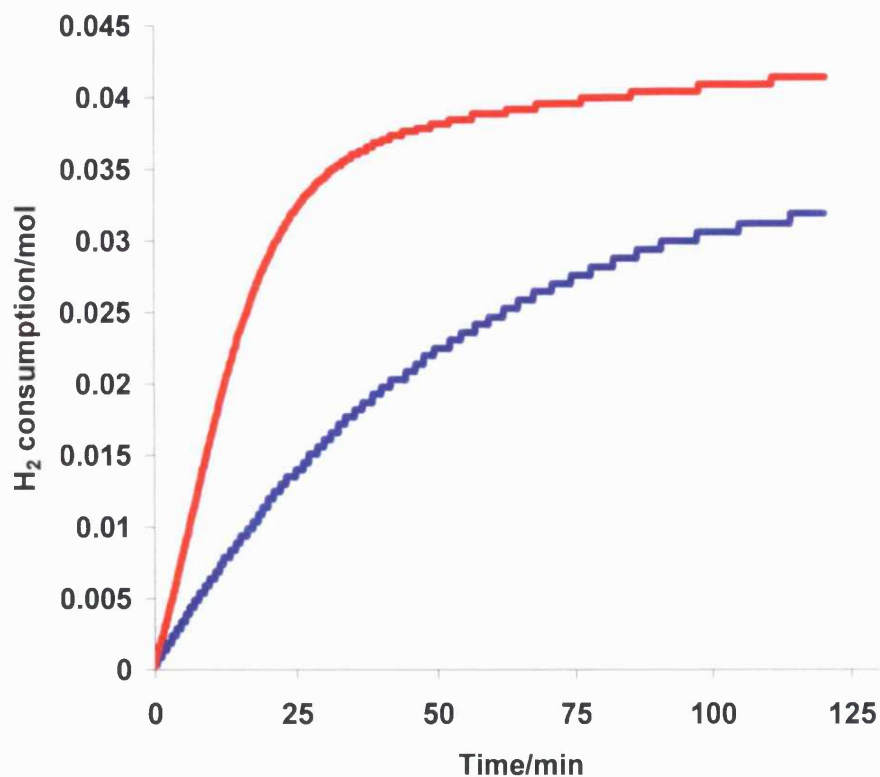


Fig 3.1. Hydrogen uptake curves for the standard 2,3-butanedione hydrogenation over modified M01271 (—) and unmodified M01271 (—)

[0.2 g catalyst; 27 ml dichloromethane; 34.5 mmol 2,3-butanedione; 5.66 mM cinchonidine; 10 bar H<sub>2</sub> pressure; 25°C; T = 25 ± 1°C; 1000 rpm]

The uptake profile for the unmodified reaction shows an indistinct transition to the second stage of the reaction. This is in contrast to uptake of the modified reaction over EUROPT-1, where the end of the first stage occurs when ca. 5-10 % of the dione persists.

## 3.2.1.2 Standard reaction over EUROPT-1

Enantioselective hydrogenations over the 6.3 % Pt/SiO<sub>2</sub> reference catalyst EUROPT-1 were used in this investigation to compare results obtained with the received catalysts and the literature. The standard reaction was the hydrogenation of 34.5 mmol of 2,3-butanedione in dichloromethane at 25 °C under 10 bar H<sub>2</sub> [1]. Catalyst, cinchonidine modifier and reactant were placed in the reaction vessel as detailed in Section 2.3.2.1. The resulting hydrogen uptake profile is shown in Figure 3.2. The profile displays two distinct regions: a rapid initial uptake referred to as the first stage and the other a greatly reduced uptake, referred to as the second stage. The rate of the first stage is reported as 942 mmol/h/g<sub>cat</sub> and the second stage as 8 mmol/h/g<sub>cat</sub>. This compares to the rate quoted in the literature of 1200 mmol/h/g<sub>cat</sub> as the maximum rate [1]. The enantiomeric excess at 90 % conversion was 40.2 %, which compares to the values in the literature of 42 % [1].

Table 3.2 Comparison of the values of maximum rate and enantiomeric excess between the reference and the best received Pt/SiO<sub>2</sub> catalysts

Entry	Catalyst	Maximum Rate (mmol/h/g <sub>cat</sub> )	ee at 90 % conversion (%)
1	EUROPT-1	942	40.2
2	M01060	186	11.1
3	M01271	204	12.4

[0.2 g catalyst; 27 ml dichloromethane; 34.5 mmol 2,3-butanedione; 5.66 mM cinchonidine; 10 bar H<sub>2</sub> pressure; 25°C; T = 25 ± 1°C; 1000 rpm]

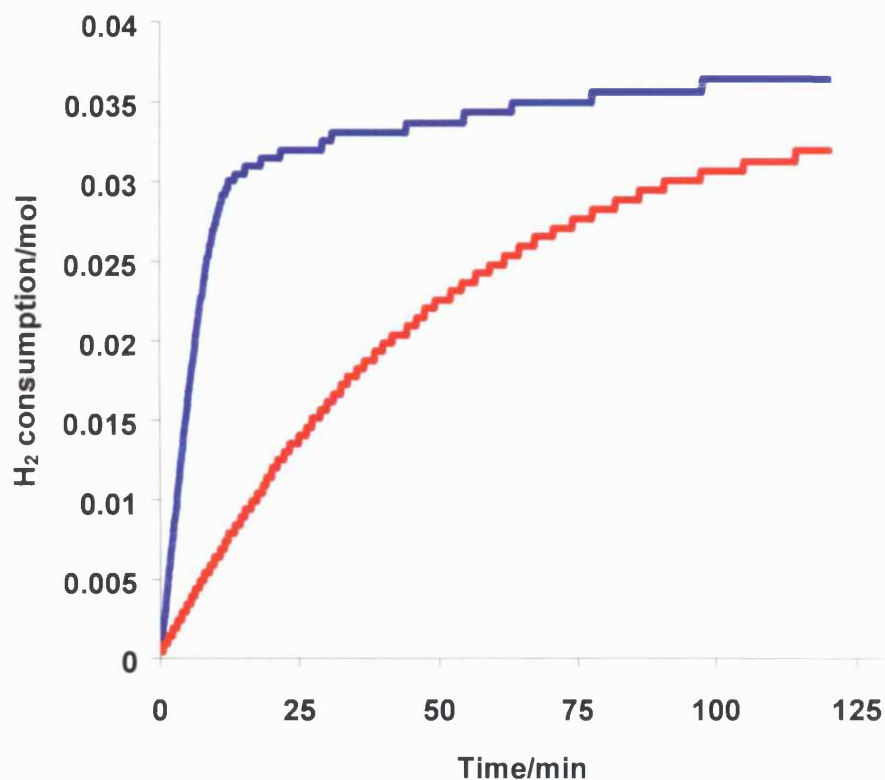


Fig 3.2. Hydrogen uptake curves for the standard 2,3-butanedione hydrogenation over EUROPT-1 (—) and M01271 (—)

[0.2 g catalyst; 27 ml dichloromethane; 34.5 mmol 2,3-butanedione; 5.66 mM cinchonidine; 10 bar H<sub>2</sub> pressure; 25°C; T = 25 ± 1°C; 1000 rpm]

### 3.2.2 Modification Protocol

The modification protocol for the enantioselective hydrogenation of 2,3-butanedione was investigated. Orito *et al.* originally showed that after 24 h pre-modification of the catalyst with alkaloid resulted in enantioselection [2]. However, recently this protracted

preparation has been deemed unnecessary and that the reaction could begin with no catalyst pre-modification [3].

Modification of the catalyst in the reactor vessel was carried out before addition of the reactant or during. These methods can be identified as pre-modification and *in situ* modification respectively. For pre-modification a slurry of catalyst and cinchonidine were stirred in the reactor vessel under atmospheric conditions. *In situ* modification of the catalyst, involved the commencement of the reaction with all components present.

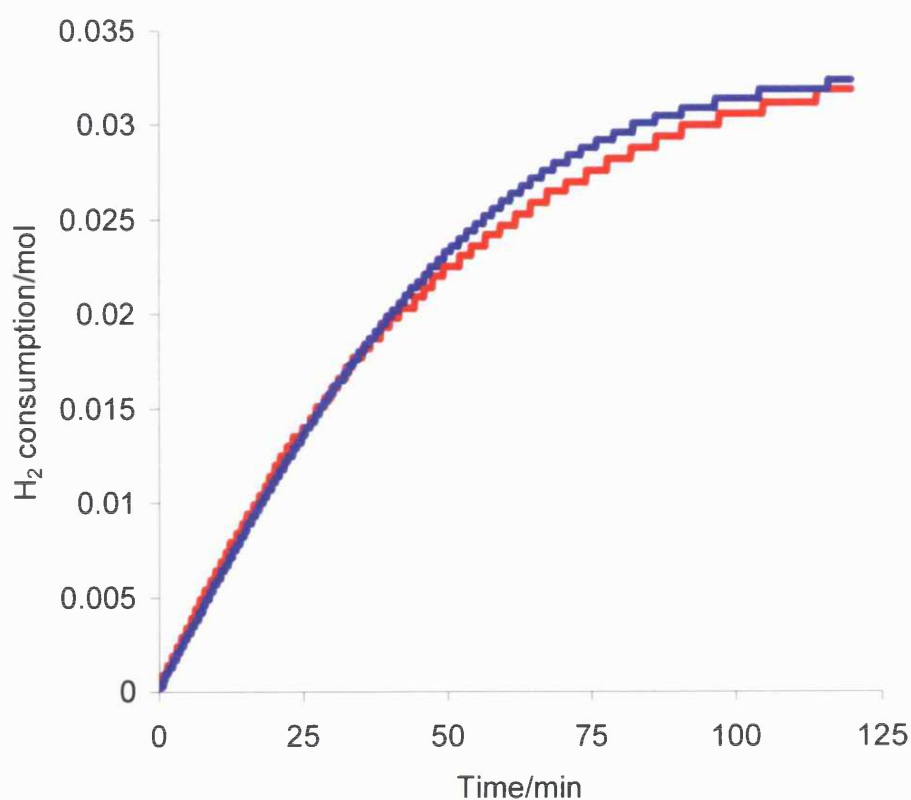


Fig 3.3. Hydrogen uptake curves for the standard 2,3-butanedione hydrogenation over M01271; pre-modified (—) and *in situ* modification (—)

[0.2 g catalyst; 27 ml dichloromethane; 34.5 mmol 2,3-butanedione; 5.66 mM cinchonidine; 10 bar H<sub>2</sub> pressure; 25°C; T = 25 ± 1°C; 1000 rpm]



The maximum rate of dione hydrogenation over a pre-modified or *in situ* modified catalyst was very similar; 196 and 204 mmol/h/g<sub>cat</sub> respectively (Fig. 3.3).

### 3.3 Optimisation of the standard reaction

#### 3.3.1 Influence of alkaloid concentration

The adsorption of cinchonidine on dispersed platinum can be said to poison the surface. This can be seen with cyclohexene hydrogenation over modified platinum catalysts (Table 3.8). However, with certain pro-chiral carbonyl containing substances, addition of cinchona alkaloid yields enantioselection and rate enhancement. Therefore, it was deemed crucial to investigate the effect of varying the modifier concentration. It has been reported that for these types of hydrogenation reactions both the ee and the rate pass through a maxima with increasing alkaloid concentration [4]. The standard conditions employ 5.66 mM of cinchonidine, this amount was halved; 2.83 mM and doubled; 11.32 mM and experiments were carried out over M01271. The effect of increasing the modifier concentration on the rate increased as follows: 11.32 < 5.66 < 2.83 mM (Table 3.3). The enantiomeric excess at 90 % conversion for concentrations 11.32, 5.66 and 2.83 mM were 10.4 %, 11.1 % and 15.4 % respectively. The maximum rate for the reaction carried out with 2.83 mM modifier concentration is comparable to the unmodified reaction.

Table 3.3 Influence of modifier concentration on values of rate and enantiomeric excess of 2,3-butanedione hydrogenation over M01271

Entry	Concentration (mM)	Maximum Rate (mmol/h/g <sub>cat</sub> )	ee at 90 % conversion (%)
1	2.83	498	15.4
2	5.66	204	11.1
3	11.32	114	10.4

[0.2 g catalyst; 27 ml dichloromethane; 34.5 mmol 2,3-butanedione; 10 bar H<sub>2</sub> pressure;

25°C; T = 25 ± 1°C; 1000 rpm]

### 3.3.2 Influence of Solvent

The choice of solvent has a marked effect on the rate of enantiomeric hydrogenations of carbonyl containing compounds [5]. The solvents investigated were compared to DCM under standard conditions, these included acetic acid, toluene and ethanol. Additionally acetic acid was used as a co-solvent, where 0.1 M (0.18g ) was added to another solvent. The uptake profiles of 2,3-butanedione hydrogenation for solvents and mixtures used are reported in Figure 3.4.

The reaction carried out in acetic acid yields a maximum rate for the first stage of 1254 mmol/h/g<sub>cat</sub> and for the second stage of 7 mmol/h/g<sub>cat</sub> (Table 3.4). In contrast the standard reaction in DCM does not enter the second stage over the experiment time. Ethanol as the solvent yielded a first stage rate of 480 mmol/h/g<sub>cat</sub> and a second stage rate of 10 mmol/h/g<sub>cat</sub>. The addition of 0.1 M AcOH to DCM resulted an increase in the maximum rate, however, this appears to be suppressed when compared to the single solvent.

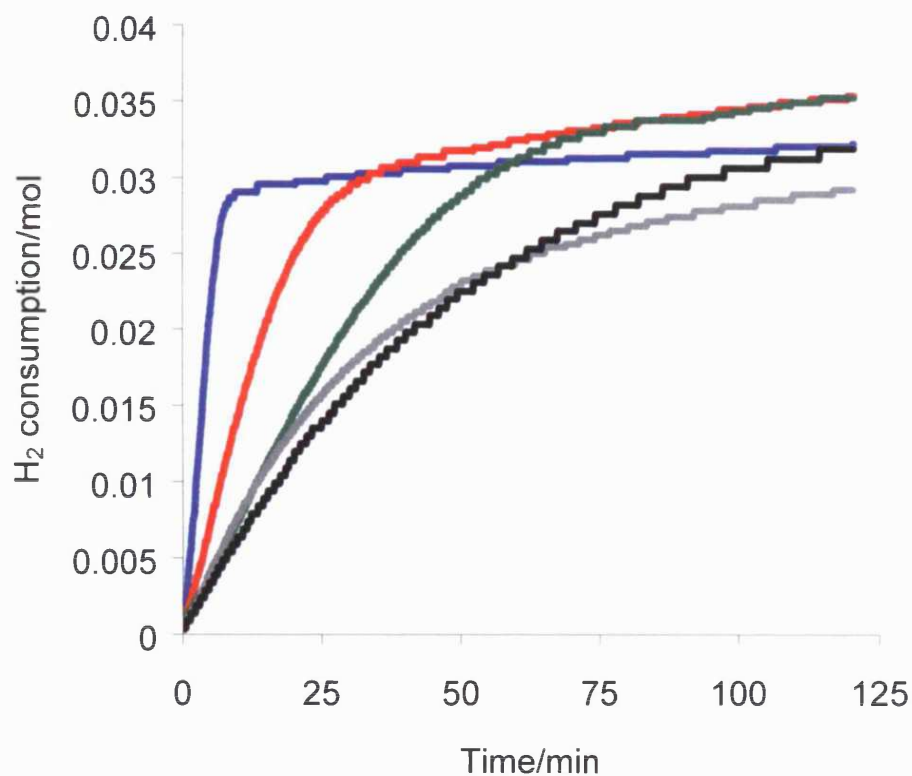


Fig 3.4. Hydrogen uptake curves for the standard 2,3-butanedione hydrogenation over M01271 in different solvents; AcOH (—), toluene/0.1 M AcOH (—), toluene (—), DCM/0.1 M AcOH (—), DCM (—)

[0.2 g catalyst; 27 ml solvent; 34.5 mmol 2,3-butanedione; 5.66 mM cinchonidine; 10 bar H<sub>2</sub> pressure; 25°C; T = 25 ± 1°C; 1000 rpm]

Where toluene was used in the standard reaction a modest improvement was gained over DCM, with a maximum rate of 240 mmol/h/g<sub>cat</sub>. Upon addition of acetic acid as a co-solvent the rate was improved further to 438 mmol/h/g<sub>cat</sub>. For reactions carried out in toluene and toluene with AcOH as co-solvent the second stage was entered and the rates were 14 and 15 mmol/h/g<sub>cat</sub> respectively.

Table 3.4 Influence of solvent on the maximum rate for the standard reaction

Entry	Solvent	Maximum Rate {First Stage} (mmol/h/g <sub>cat</sub> )	Maximum Rate {Second Stage} (mmol/h/g <sub>cat</sub> )
1	acetic acid	1254	7
2	dichloromethane	204	-
3	dichloromethane <sup>1</sup>	246	-
4	ethanol	480	10
5	toluene	240	14
6	toluene <sup>1</sup>	438	15

<sup>1</sup> = 0.1 M AcOH additive

[0.2 g catalyst; 27 ml solvent; 34.5 mmol 2,3-butanedione; 5.66 mM cinchonidine; 10 bar H<sub>2</sub> pressure; 25°C; T = 25 ± 1°C; 1000 rpm]

### 3.3.3 Influence of Pressure

Hydrogen pressure was investigated as part of optimising the reaction. The effect of increasing the pressure of 2,3-butanedione hydrogenation is illustrated in Figure 3.5. Cinchonidine modifier concentration was reduced to 2.83 mM from standard reaction conditions. The maximum rate of the hydrogenation over M01271 increases with increasing the reaction pressure as follows 10 < 20 < 30 bar. The corresponding rates are displayed in Table 3.5.

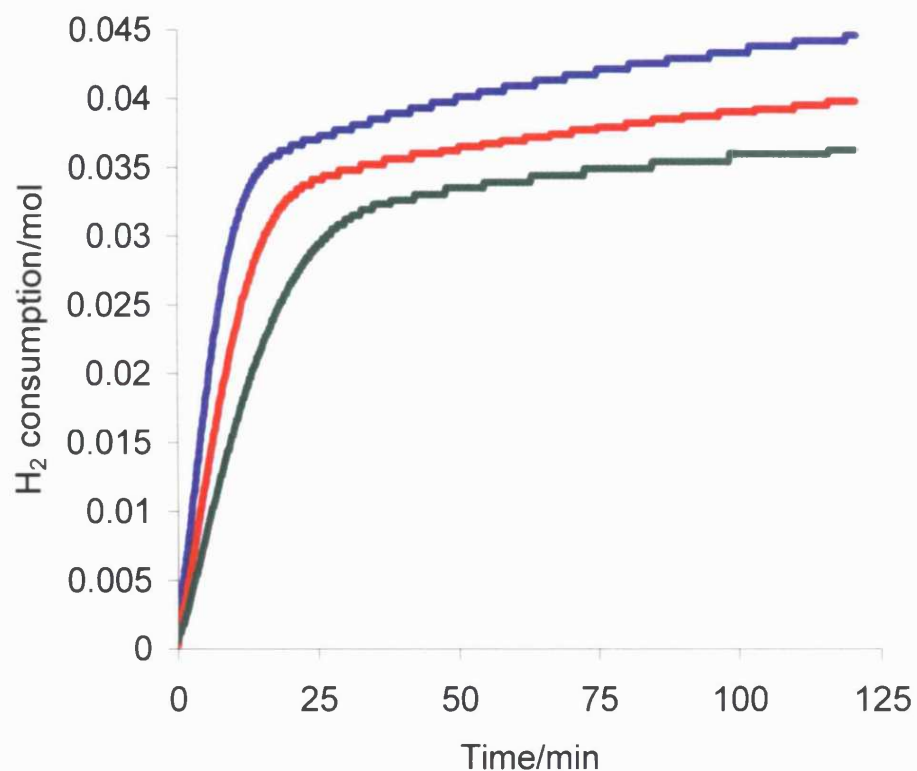


Fig 3.5. Hydrogen uptake curves for 2,3-butanedione hydrogenation over M01271 at different pressures; 10 bar (—), 20 bar (—) and 30 bar hydrogen pressure (—)

[0.2 g catalyst; 27 ml dichloromethane; 34.5 mmol 2,3-butanedione; 2.83 mM cinchonidine;  
25°C;  $T = 25 \pm 1^\circ\text{C}$ ; 1000 rpm]

Enantiomeric excess was measured at 90 % dione conversion for each of the reaction pressures used. An increase of ca. 9 % ee of (*R*)-hydroxybutanone was achieved where the reaction pressure was set at 30 bar. For 20 bar hydrogen pressure an increase of ca. 7 % was achieved.

Table 3.5 Influence of pressure on the values of rate for first and second stages of 2,3-butanedione over M01271 modified with 2.83 mM cinchonidine

Entry	Pressure (bar)	Maximum Rate {First Stage} (mmol/h/g <sub>cat</sub> )	Maximum Rate {Second Stage} (mmol/h/g <sub>cat</sub> )	ee at 90 % conversion (%)
1	10	498	9	12.4
2	20	732	11	19.8
3	30	1104	17	21.3

[0.2 g catalyst; 27 ml dichloromethane; 34.5 mmol 2,3-butanedione; 2.83 mM cinchonidine; 25°C; T = 25 ± 1°C; 1000 rpm]

### 3.3.4 Influence of Stirrer Speed

The transport of reactants to the active site on the metal surface must cross the phase boundary inherent in heterogeneous catalysis. Agitation of the reactants and catalyst with the use of stirring is used to overcome this. Thus variation of the speed of stirring can effect the degree of boundary crossing and hence the rate of reaction. This phenomenon was investigated by varying the stirring speed of the standard reaction. A range of 600 to 1300 rpm was used, with the respective rates of reaction displayed in Table 3.6. As the speed of stirring is increased, the rate of reaction increases as follows; 600 < 800 < 1200 < 1300 < 1000 rpm.



Table 3.6 Influence of reaction stirrer speed on the maximum rate

Entry	Stirrer speed (rpm)	Maximum Rate (mmol/h/g <sub>cat</sub> )
1	600	134
2	800	144
3	1000	204
4	1200	186
5	1300	192

[0.2 g catalyst; 27 ml dichloromethane; 34.5 mmol 2,3-butanedione; 5.66 mM cinchonidine; 10 bar H<sub>2</sub> pressure; 25°C; T = 25 ± 1°C; 1000 rpm]

### 3.4 Cyclohexene Hydrogenation

The purpose of hydrogenating cyclohexene over the received platinum catalysts was to further investigate the activity with the use of a well known reactant. Secondly the effect of alkaloid addition on this activity could be determined. The results obtained could then be carried over to the trickle-bed reactor study.

#### 3.4.1 Results of Cyclohexene Hydrogenation

Cyclohexene was hydrogenated over the received 2.5 % Pt/SiO<sub>2</sub> catalysts M01037, M01271 and M02023. Furthermore EUROPT-1 was used as a comparison, the rates of hydrogenation are displayed in Table 3.7. Both powdered catalysts 1037 and 1271 gave very similar maximum rates of 795 and 765 mmol/h/g<sub>cat</sub> respectively. This compares to a rate of 300 mmol/h/g<sub>cat</sub> for EUROPT-1 and 225 mmol/h/g<sub>cat</sub> for M02023. Due to the granular nature of the silica gel support for M02023 reducing the particle size was investigated.

Consequently where the catalyst was crushed to a maximum size of 250  $\mu\text{m}$  and minimum of 200  $\mu\text{m}$  the rate increased to 555  $\text{mmol/h/g}_{\text{cat}}$ . The rate of cyclohexene hydrogenation was further improved to 735  $\text{mmol/h/g}_{\text{cat}}$  upon crushing to a size of between 150 and 100  $\mu\text{m}$ .

Table 3.7 Values of the maximum rate for cyclohexene hydrogenation over various Pt/SiO<sub>2</sub> catalysts

Entry	Catalyst	Maximum Rate ( $\text{mmol/h/g}_{\text{cat}}$ )
1	EUROPT-1	300
2	M01271	795
3	M01271 <sup>1</sup>	195
4	M01037	765
5	M02023	225
6	M02023 <sup>2</sup>	735
7	M02023 <sup>3</sup>	555

<sup>1</sup> = Cinchonidine (5.66 mM); <sup>2</sup> = Crushed to 150  $\mu\text{m}$  particle size; <sup>3</sup> = Crushed to 250  $\mu\text{m}$  particle size

[0.2 g catalyst; 27 ml dichloromethane; 14 mmol cyclohexene; 10 bar H<sub>2</sub> pressure; 25°C; T = 25  $\pm$  1°C; 1000 rpm]

### 3.4.2 Addition of cinchonidine

The addition of the alkaloid cinchonidine to cyclohexene hydrogenation was investigated. Under standard conditions catalyst M01271 was modified during the reaction with cinchonidine at a concentration of 5.66 mM. The resulting rate of hydrogenation is reduced by a factor of approximately 75 % to 195  $\text{mmol/h/g}_{\text{cat}}$  (Table 3.7 entry 3). Further



modifier concentrations were investigated and the results observed appear logical. That is the less cinchonidine added the faster the rate of hydrogenation.

### 3.5 Discussion

#### 3.5.1 Standard reaction

The purpose of adopting a standard reaction from Slipszenko *et al.* [1] was two fold; firstly to compare the received platinum catalysts to the established conditions. Secondly to ascertain the most favourable catalyst characteristics for the enantioselective hydrogenation of 2,3-butanedione. The second aspect of this study would then be transferred to the production of an extrudate catalyst for use in the trickle-bed reactor. Therefore, while the best performing catalyst could be used to determine viable optimisation protocols the worst performing catalysts provide valuable information. The powdered catalysts M01037, M0134, M01270 and M01069 illustrate this principle. These catalysts exhibit poor rates and conversion of 2,3-butanedione at 2 h of experiment time. Two main factors can be ascribed to the poor performance; platinum surface area and pore characteristics. Table 3.8 illustrates the dual requirement for this particular reaction for both an optimal metal surface area and pore characteristics.

An established requirement for enantioselective hydrogenation over platinum catalysts is an optimum metal particle size. Supported platinum particles capable of optimum performance have a minimum and maximum size of 2 and 4 nm respectively [6]. The platinum must be firstly capable of supporting a modifier molecule in its lowest energy state and the reactants. Therefore, if the metal particle is too small then the likely outcome is

racemic product and in the case of pyruvate hydrogenation; no rate enhancement. Where the metal particle is too large product turn over becomes undesirable.

Table 3.8 Values of nitrobenzene activity and rate of 2,3-butanedione hydrogenation over various catalysts with their corresponding support and metal information

Entry	Catalyst	PSD (d50)	Pore Volume (ml/g)	Pore Diameter (Å)	Metal SA (m <sup>2</sup> /g)	NBA <sup>1</sup>	Maximum Rate (mmol/h/g <sub>cat</sub> )
1	M01271	10.2	0.86	61	1.9	35	204
2	M01037	49.9	1.06	132	0.6	31	48
3	M01034	96.3	1.06	132	0.6	22	54
4	M01069	8.9	1.78	179	0.2	30	24
5	M01270	10.7	0.45	23	1.7	27	78

<sup>1</sup> = nitrobenzene activity, Johnson Matthey standard catalyst test

[0.2 g catalyst; 27 ml dichloromethane; 34.5 mmol 2,3-butanedione; 5.66 mM cinchonidine; 10 bar H<sub>2</sub> pressure; 25°C; T = 25 ± 1°C; 1000 rpm]

The influence of the pore characteristics on enantioselective hydrogenation has received little attention. The requirement that both modifier and reactant are able to penetrate the inner areas of the catalyst for optimum activity is obvious. However, for larger applications, in particular for fixed bed reactors with large extruded catalysts, a balance between crush strength, for example and pore size exists. Catalyst attrition must be minimised in large reactors where the quantity of catalyst used can be on the tonne scale. Where large pore diameters and volumes are used the incidences of structural failure of the

catalyst increases. Therefore, the optimal pore characteristics for a small quantity of catalyst may not be applicable in certain scale up operations.

The metal surface area of the catalysts M01271 (entry 1) and M01270 (entry 5) are comparable; however, the maximum rate achieved is disparate. The pore character has the greatest influence therefore on catalyst M01270. Which implies that the minimum pore diameter and volume allowable for the enantioselective hydrogenation of 2,3-butanedione has been reached. Catalyst M01069 (entry 4) has a low metal surface area but a high pore diameter and volume, as a result is unable to support the studied reaction but is effective for nitrobenzene activity. The influence of the support particle size can be illustrated when catalysts M01034 (entry 3) and M01037 (entry 2) are compared. Catalyst M01037 has twice the support particle size of M01034 but both have identical surface areas and pore sizes and additionally identical metal surface areas. Both exhibit comparably poor activity towards enantioselective hydrogenation, but yield different values of nitrobenzene activity; 22 for M01034 vs. 31 for M01037. Interestingly the reference catalyst EUROPT-1 has a higher support particle size of 240 nm and performs well with the standard reaction. Parallels can be drawn about the support size influence on nitrobenzene activity and cyclohexene hydrogenation which will be discussed later. Thus the standard reaction is not purely influenced by the size of the support particle.

Values of rate achieved by the 2.5 % Pt/SiO<sub>2</sub> granular catalysts are modest, where the support size is much greater than the powdered catalysts (Table 3.9). Catalyst M02023 has a large pore diameter and volume along with a high metal surface area, which yielded the highest rate. When M01271 and M02027 are compared, with similar pore characteristics the influence of the metal surface area is great. Catalyst M02029 exhibits poor activity in the autoclave which is attributed to the restrictive pore dimensions. The metal surface area is sufficient to support the standard reaction on the catalyst surface as with 'egg shell'

catalysts. When the conversion at 2 h reaction time is compared to that of M01069 (Table 3.1) there is a modest increase of 10 %.

Table 3.9 Comparison of M01271 (powder) catalyst and the granular catalysts with respect to 2,3-butanedione hydrogenation

Entry	Catalyst	PSD (d50) ( $\mu\text{m}$ )	Pore Volume (ml/g)	Pore Diameter ( $\text{\AA}$ )	Metal SA ( $\text{m}^2/\text{g}$ )	Maximum Rate ( $\text{mmol/h/g}_{\text{cat}}$ )	Conversion after 2 h (%)
1	M01271	10.2	0.86	61	1.9	204	92
2	M01069	8.9	1.78	179	0.2	24	5
3	M02023	0.5-1 <sup>1</sup>	1.20	150	1.7	114	81
4	M02027	0.5-1 <sup>1</sup>	0.90	67	0.6	54	43
5	M02029	0.5-1 <sup>1</sup>	0.30	16	0.9	27	15

<sup>1</sup> = support size in mm

[0.2 g catalyst; 27 ml dichloromethane; 34.5 mmol 2,3-butanedione; 5.66 mM cinchonidine; 10 bar H<sub>2</sub> pressure; 25°C; T = 25 ± 1°C; 1000 rpm]

The interest in the kinetics of the 2.5 % Pt/SiO<sub>2</sub> catalysts was to develop an ideal extruded catalyst support for use in the trickle-bed reactor. The broad range of support and metal characteristics studied have provided an ideal set of dimensions as follows; PV > 0.40 ml/g, PD > 50 Å and a SA ≥ 300 m<sup>2</sup>/g (< 600 m<sup>2</sup>/g).

### 3.5.2 Optimisation

The reaction conditions provided by Slipsenko *et al.* [1] were applied to the 2.5 % Pt/SiO<sub>2</sub> catalysts and adopted as the standard reaction. However, the results obtained were modest when compared to the reported results with the use of 6.3 % Pt/SiO<sub>2</sub> catalyst EUROPT-1. Asymmetric hydrogenation of C=O containing pro-chiral compounds over platinum catalysts have benefited through altering a number of reaction parameters. These include adjusting the modifier concentration [4], variation of the reaction solvent [5] and increasing the reaction pressure [7]. From the results obtained in this study each will now be discussed.

Adsorption of a chiral modifier on to the platinum surface has been shown to influence the preference of an enantiomer from pro-chiral C=O containing compounds. The concentration of the modifier on the metal surface has a great impact on the outcome of such reactions. At high concentrations the surface can become blocked to reactant by a monolayer of modifier. Cinchonidine has been reported as adsorbing via the N atom of the quinoline moiety, at an angle of ca. 60° at high loading [8]. This phenomenon has been observed at elevated reaction temperatures which results in suppression of rate and enantiomeric excess [9]. At low alkaloid coverage the metal surface facilitates a higher proportion of racemic reactions and increases the susceptibility of cinchonidine hydrogenation. In the case of pyruvate hydrogenation results in loss of rate and a low ee [10]. Therefore, the optimum modifier concentration for enantioselective hydrogenation over platinum catalysts observes a volcano plot.

The immediate effect of doubling the alkaloid concentration of the standard reaction is a loss in maximum rate, however, the ee remains comparable (Table 3.3). Therefore, available racemic sites on the platinum surface can be said to be hindered by the increase in

surface coverage. This suggests that enantiomeric sites are available for asymmetric hydrogenation of 2,3-butanedione. Therefore, total poisoning of the metal surface was not achieved at this concentration.

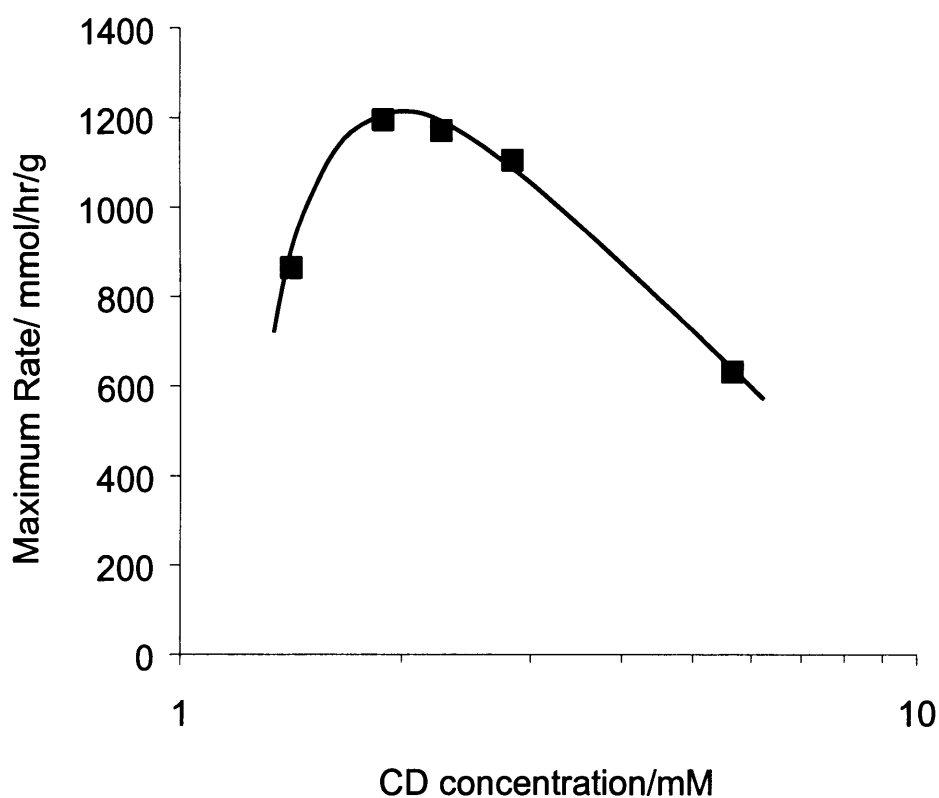


Fig. 3.6 Influence of modifier concentration on the maximum rate of 2,3-butanedione hydrogenation over M01271

[0.2 g catalyst; 27 ml dichloromethane; 34.5 mmol 2,3-butanedione; 30 bar H<sub>2</sub> pressure;  
25°C; T = 25 ± 1°C; 1000 rpm]

Decreasing the alkaloid concentration to half of the standard reaction yielded improved rate and ee (Table 3.3). The hydrogen uptake profile for this experiment is presented in Figure 3.5 (blue line). The reaction proceeds in a manner similar to that of the

reference catalyst EUROPT-1 (Fig 3.2). That is the first stage of the reaction; 2,3-butanedione to hydroxybutanone is distinct from the second stage and proceeds rapidly. Firstly this implies that there is a rate enhancement over the racemic reaction and secondly the standard reaction is hindered by excessive alkaloid.

The influence of varying the reaction pressure was initially studied over M01271 with a modifier concentration of 2.83 mM, however, this was extended to include concentrations down to 1.415 mM. A volcano plot of modifier concentration versus maximum rate could then be generated (Fig. 3.6). Increasing the pressure of the reaction by 10 bar yielded an improvement of the maximum rate by a factor of ca. 1.5.

When the reaction is carried out at 30 bar with an alkaloid concentration of 2.83 mM the maximum rate achieved (1104 mmol/h/g<sub>cat</sub>) is comparable to that achieved by EUROPT-1 at 10 bar and 5.66 mM CD concentration (942 mmol/h/g<sub>cat</sub>). The maximum pressure of the reactor was 30 bar, therefore, the reaction was only investigated to that level. Typically reactions of this type are studied at higher pressures, however, the effect of pressure has been reported as negligible [11]. The increase in rate observed with increasing pressure can be ascribed to greater access to the metal surface. Both butanedione and cinchonidine exhibit strong competition for the metal surface, an increase of hydrogen concentration at the surface facilitates enhanced product formation. In the case of pyruvate ester hydrogenation competition with CD for the surface is reduced [4], thus the influence of increased hydrogen concentration at the metal surface on activity is minor.

Further influence of increasing the reaction pressure results in an increase in the value of hydrogen uptake that the reaction proceeds in to the second stage (Fig. 3.6). With a reaction pressure of 10 bar the value of H<sub>2</sub> uptake is 31.5 mmol, compared to 35.8 mmol at 30 bar. These values correspond to a conversion of 91 % and 104 % for 10 and 30 bar respectively. The time period for the transition from first to second stage reactions has

become reduced at higher pressure. A similar short transition period is observed for the reaction over EUROPT-1 (Fig. 3.2). This suggests that the morphology of the supported metal of M01271 and EUROPT-1 differs. EUROPT-1 is described as having a relatively flat metal surface [12], which is able to overcome the competition for active sites of the reactants and modifier at 10 bar H<sub>2</sub> pressure. Whereas, for the M01271 the reaction pressure must be increased, along with a reduction of modifier concentration to achieve a similar short transition period. This infers that the platinum crystal of M01271 has greater 3D character.

Further reductions of the cinchonidine concentration were used to determine the optimum concentration for 2,3-butanedione hydrogenation at 30 bar hydrogen pressure (Fig 3.6). An alkaloid concentration of 1.88 mM gave the highest maximum rate of 1194 mmol/h/g<sub>cat</sub>. The optimal concentration was investigated by Li *et al.* over a 5 % Pt/Al<sub>2</sub>O<sub>3</sub> catalyst and the maximum rate of dione conversion corresponded to 1.0 mM [4].

The influence of solvent was investigated as part of the optimisation of the hydrogenation of 2,3-butanedione. Solvent effects have been well documented in the literature for heterogeneous enantioselective hydrogenation reactions [5, 13, 14]. The interaction of the solvent and modifier has been identified as a vital component of these reactions. Results can be related to the dielectric constant of the reaction solvent, however, acetic acid is an exception. Burgi *et al.* calculated the value of dipole moments for the conformations of cinchonidine to be *closed 2* > *closed 1* > *open 4* > *open 3* [15]. Therefore in solvents with a large dipolar moment the closed conformer is stabilised. Whereas, in solvents with lower polarity, that is, with a small dipolar moment the reverse is true. Hence, the trend of decreasing enantiomeric excess with increasing solvent polarity has been reported [4]. The proportion of the *open 3* conformation of the modifier for such reactions impacts greatly on the activity of the catalyst. In acetic acid the proportion of modifier exists predominately in *open 3*. This conformer is found in the 1:1 complex between the alkaloid



and pyruvate, via hydrogen bonding of the C9 OH and the protonated N of the quinuclidine ring. This yields enhanced rates of reaction and improved enantiomeric excess for pyruvate ester hydrogenation [16]. Where the solvent used has a higher dielectric constant, the *closed* conformers are stabilised [15]. This has been attributed to the lower enantioselectivity obtained with such solvents. The influence of solvent on the studied reaction is in agreement with the literature [4]. Hydrogenation of 2,3-butanedione in acetic acid results in a large rate enhancement, however, the ee is impaired (Table 3.10). Similarly when using ethanol as the reaction solvent the rate is enhanced but the ee is slightly depressed. Toluene was found to be the best solvent and the activity was enhanced with the addition of acetic acid (Table 3.10).

The depression of enantiomeric excess when using acetic acid has been ascribed to possible accelerated dimerisation of the dione. The strength of adsorption of the acid and the dione may also play a role in the removal of enantioselective sites through competitive adsorption with cinchonidine. However, there is evidence of the formation of cyclic complexes of cinchonidine and acetic acid [17]. The interaction of pyruvate and dione may differ in the presence of such complexes.

The addition of small amounts of acid to toluene resulted in enhanced rate, which has been reported in the literature for pyruvate hydrogenation [4, 18]. The beneficial use of small amounts of acid in the case of dione hydrogenation may increase the proportion of *open* 3. However, dimerisation of dione or complexes of modifier and acid may not prevail and depress the ee. Additionally the strong adsorption of toluene in the alkaloid free or racemic sites may further enhance the enantioselective hydrogenation of 2,3-butanedione [19]. The lowered ee from the use of ethanol as the reaction solvent is likely to be due to the stabilisation of the *closed* conformers adsorbing on the metal surface. The observed rate

increase, however, may be interpreted through increased dimer formation of reaction intermediates.

Table 3.10 Influence of solvent dielectric constant of the rate of 2,3-butanedione hydrogenation

Entry	Solvent	Dielectric constant	Maximum Rate (mmol/h/g <sub>cat</sub> )	ee at 90 % conversion (%)
1	toluene	2.4	240	15
3	DCM	8.9	204	12.4
4	ethanol	25.3	498	9.1
5	acetic acid	6.2	1254	6.0

[0.2 g catalyst; 27 ml solvent; 34.5 mmol 2,3-butanedione; 5.66 mM cinchonidine; 10 bar H<sub>2</sub> pressure; 25°C; T = 25 ± 1°C; 1000 rpm]

### 3.4.3 Cyclohexene hydrogenation

The use of cyclohexene hydrogenation to further understand some of the more basic factors which influence the dione reaction proved fruitful (Table 3.7). The results obtained showed that the received powder catalysts out performed EUROPT-1 and the granule M02023. Comparing M01037 and M01271 which achieved disparate performance when used in the standard reaction, gave similar rates of cyclohexene hydrogenation. This is supported by the results from the nitrobenzene hydrogenation carried out by Johnson Matthey, which is their standard test of catalyst activity. It is reasonable to postulate therefore, that the large support of EUROPT-1 and M02023 inhibit the rapid conversion of

cyclohexene compared to the powdered catalysts. This is substantiated by the crushing of M02023 to specific size ranges, where 100 to 150  $\mu\text{m}$  yields comparable rate of reaction to the powder catalysts.

However, the rate of conversion obtained over EUROPT-1 may be a combination of larger support size and a platinum morphology which comprises of fewer active sites. When M02023 was crushed to 200 to 250  $\mu\text{m}$  the rate improved and out performed EUROPT-1 which the majority of the support falls in that size range. As mentioned above the influence of increasing pressure on the reaction over M01271 reduced the transition from first to second stage hydrogenations. This replicated the short transition observed over EUROPT-1 at lower pressure and this suggested that the flat metal crystals of EUROPT-1 were responsible. Therefore, enhanced rate of cyclohexane formation over the received catalysts are afforded by the greater 3D character of the platinum crystals which contain more active sites. However, the reverse is true of the standard reaction where EUROPT-1 out performs the 2.5 % Pt/SiO<sub>2</sub> catalysts. The influence of cinchonidine on the hydrogenation of cyclohexene acts as a poison, as expected.

### 3.5 Conclusions

Hydrogenation of 2,3-butanedione was conducted in a stirred autoclave reactor over a number of 2.5 % Pt/SiO<sub>2</sub> catalysts modified with cinchonidine.

- (1) Screening of the 2.5 % Pt/SiO<sub>2</sub> powder and granular catalysts with the standard reaction provided ideal support characteristics for manufacture of catalysts with an extruded support; PV > 0.40 ml/g, PD > 50 Å and a SA  $\geq$  300 m<sup>2</sup>/g (< 600 m<sup>2</sup>/g)

- (2) The optimum alkaloid concentration was determined as 1.89 mM in DCM at 30 bar with M01271. The rate of 2,3-butanedione hydrogenation with these conditions was comparable to the rate over EUROPT-1 under standard reaction conditions.
- (3) Metal surface area was shown to be crucial for successful hydrogenation of 2,3-butanedione. Higher rates were achieved with catalysts having a metal surface area of greater than 1.7 m<sup>2</sup>/g. However, restrictive pore characteristics were shown to prevail over the size of the metal area.
- (4) Hydrogenation of cyclohexene indicated that the 2.5 % Pt/SiO<sub>2</sub> catalysts were very active compared to EUROPT-1. Indicating that the platinum particle was different and may be more 3D in character with more index planes present.

### 3.6 References

1. J. Slipszenko, S. Griffiths, P. Johnston, K. Simmons, W.A.H Vermeer and P.B. Wells, *J. Catal.*, **179** (1998) 267.
2. (a) Y. Orito, S. Imai, S. Niwa, *J. Chem. Soc. Jpn.*, (1979) 1257.; (b) Y. Orito, S. Imai, S. Niwa, *J. Chem. Soc. Jpn.*, (1980) 670.; (c) Y. Orito, S. Imai, S. Niwa, *J. Chem. Soc. Jpn.*, (1982) 137.
3. H.-U. Blaser, M. Garland, M. Muller and M. Studer, *J. Catal.*, **144** (1993) 569.
4. X. Li, N.F. Dummer, R.L. Jenkins, R.P.K. Wells, P.B. Wells, D.J. Willock, S.H. Taylor, P. Johnston and G.J. Hutchings, *Catal. Lett.*, **96** (2004) 147.
5. H.-U. Blaser, H.P. Jalett and J. Wiehl, *J. Mol. Catal.*, **68** (1991) 215.
6. A. Baiker, *J. Mol. Catal. A: Chemical.*, **115** (1997) 473.

- 
7. (a) Y. Sun, J. Wang, C. LeBlond, R.N. Landau and D.G. Blackmond, *J. Catal.*, **161** (1996) 759.; (b) Y. Sun, J. Wang, C. LeBlond, R.N. Landau and D.G. Blackmond, *J. Am. Chem. Soc.*, **118** (1996) 1348.; (c) Y. Sun, J. Wang, C. LeBlond, R.N. Landau and D.G. Blackmond, *J. Catal.*, **161** (1996) 752.
  8. T. Evans, A.P. Woodhead, A. Gutierrez-Sosa, G. Thornton, T.J. Hall, A.A. Davis, N.A. Young, P.B. Wells, R.J. Oldman, O. Plashkevych, O. Vahtras, H. Agren, V. Carravetta, *Surf. Sci.*, **436** (1999) 691.
  9. M. von Arx, N.F. Dummer, D.J. Willock, S.H. Taylor, R.P.K. Wells, P.B. Wells and G.J. Hutchings, *J. Chem. Soc. Chem. Commun.*, (2003) 1926.
  10. H.-U. Blaser, H.P. Jalett, D.M. Monti, A. Baiker and J.T. Wehrli, *Stud. Surf. Sci. Catal.*, **67** (1991) 147.
  11. M. Studer, V. Okafor and H.-U. Blaser, *J. Chem. Soc. Chem. Commun.*, (1998) 1053.
  12. S.D Jackson, M.B.T. Keegan, G.D. McLellan, P.A. Meheux, R.B. Moyes, G. Webb, P.B. Wells, R. Whyman and J. Willis, Preparation of Catalysts V (G. Ponchelot, P.A. Jacobs, P. Grange and B. Delmon, Eds. Elsevier, Amsterdam, 1991), p.211.
  13. B. Minder, T. Mallet, P. Scrabble and A. Baiker, *Catal. Lett.*, **29** (1995) 115.
  14. B. Minder, T. Mallet, K.H. Pickel, K. Steiner and A. Baiker, *Catal. Lett.*, **34** (1995) 1.
  15. T. Bürgi and A. Baiker, *J. Am. Chem. Soc.*, **120** (1998) 12920.
  16. I.M. Sutherland, A. Ibbotson, R.B. Moyes and P.B. Wells, *J. Catal.*, **125** (1990) 77.
  17. D. Ferri, T. Bürgi and A. Baiker, *J. Chem. Soc., Perkin Trans.*, **2** (1999) 1305.
  18. X. Li, X. You, P. Ying, J. Xiao and C. Li, *Topics in Catal.*, **25** (2003) 63
  19. X. Li and C. Li, *Catal. Lett.*, **77** (2001) 251.

*Chapter*  
*Four*

---

**Chapter 4: Trickle-bed Reactor****4.1 Introduction**

The aim of the experiments is to contrast the use of autoclave and trickle-bed reactor for the same reaction. Consequently certain information obtained from experiments with the autoclave reactor were transferred to the trickle-bed reactor for the enantioselective hydrogenation of 2,3-butanedione. In this chapter the application of these trends, investigations towards optimisation and reactions of other compounds for comparison are reported.

**4.2 Results of modification protocol**

Modification of catalysts in a stirred-tank reactor allows for an equilibrium of adsorption and desorption of the alkaloid to occur across the phase boundary. Due to the constant flow of material inherent in the TBR this equilibrium is disrupted. Therefore, it was necessary to investigate the optimum modification protocol. Analysis of the effluent from the catalyst bed with UV/Vis spectroscopy under atmospheres of He or He then H<sub>2</sub> were carried out. Both the catalyst M02023 and its bare silica gel support; M02473 were studied.

A solution of 0.17 mM cinchonidine dissolved in DCM was passed over a bed of M02023 and silicon carbide fines following the procedure in 2.3.2.5 under helium (Fig. 4.1). The effluent from the bed was analysed with UV/Vis spectroscopy at 315 nm, which corresponds to a transition of the quinoline ring system. There is a rapid uptake of alkaloid by the bed in the first 5 minutes of time-on-line. For the next 15 minutes no cinchonidine was detected in the effluent. From 30 minutes to 240 minutes time-on-line the concentration

of cinchonidine detected was stable at ca. 0.012 mM. This increased modestly to 0.02 mM at the sampling time of 300 minutes. During the experiment the spectra of the cinchonidine was unchanged, indicating no change to the molecule.

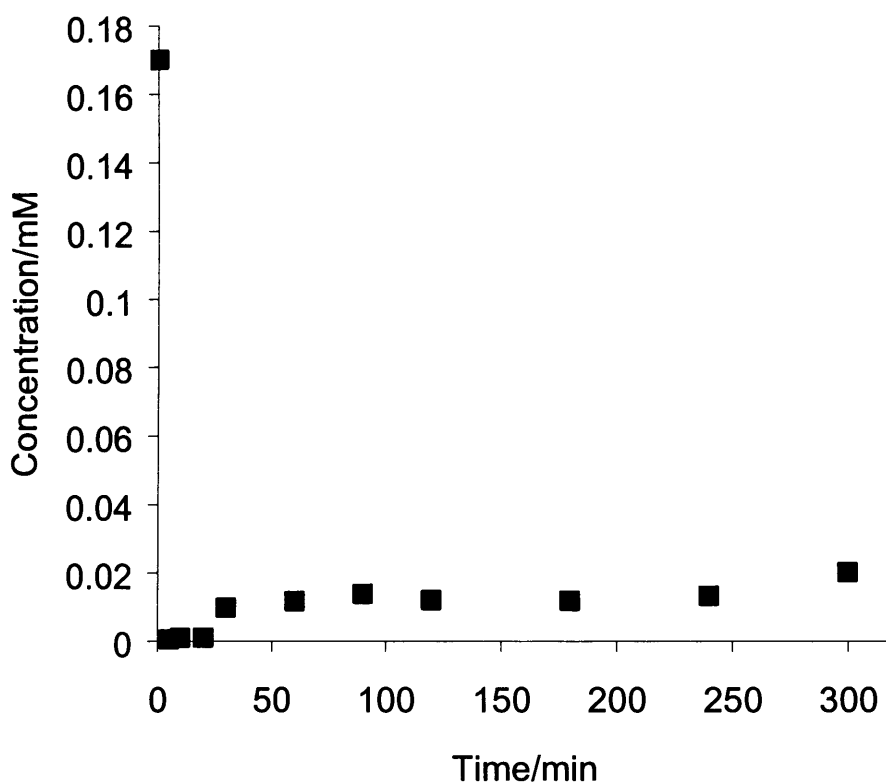


Fig. 4.1 Concentration of cinchonidine in effluent over M02023 under helium

[2 g catalyst; 0.17 mM cinchonidine in DCM at 1 ml/min; 0.5 barg He pressure, GHSV 4800 /h; 25°C; T = 25 ± 1°C]

This experiment was repeated with a fresh loading of catalyst; however, the gas feed was changed to hydrogen after the sampling point of 90 minutes time-on-line (Fig. 4.2). For the period of cinchonidine addition under helium the concentration mimicked the experiment



in Figure 4.1. Thereafter, under hydrogen the spectra of the modifier changed suggesting that the molecule had hydrogenated at the quinoline ring system. The concentration of alkaloid increased to 0.04 mM at 180 minutes, indicating that the molecule had decreased adsorption strength. The concentration then returned to ca. 0.018 mM by 330 minutes time-on-line.

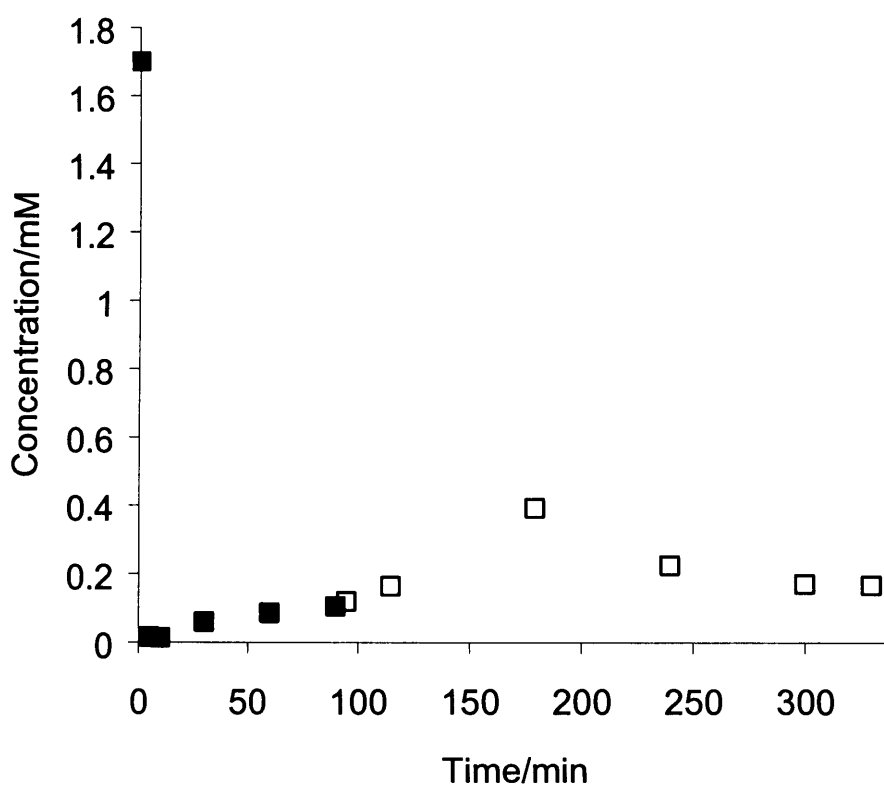


Fig. 4.2 Concentration of cinchonidine in effluent over M02023 under helium (■) and hydrogen (□)

[2 g catalyst; 0.17 mM cinchonidine in DCM at 1 ml/min; 0.5 barg He/H<sub>2</sub> pressure, GHSV 4800 /h; 25°C; T = 25 ± 1°C]

The experiment was repeated with the bare silica gel support (M02473) and accompanied by a change of gas feed to hydrogen (Fig. 4.3). The spectra of the cinchonidine in the effluent remained unchanged for the 300 minutes time-on-line. There was a steady increase of concentration in the effluent to ca. 0.035 mM at the sampling point at 300 minutes.

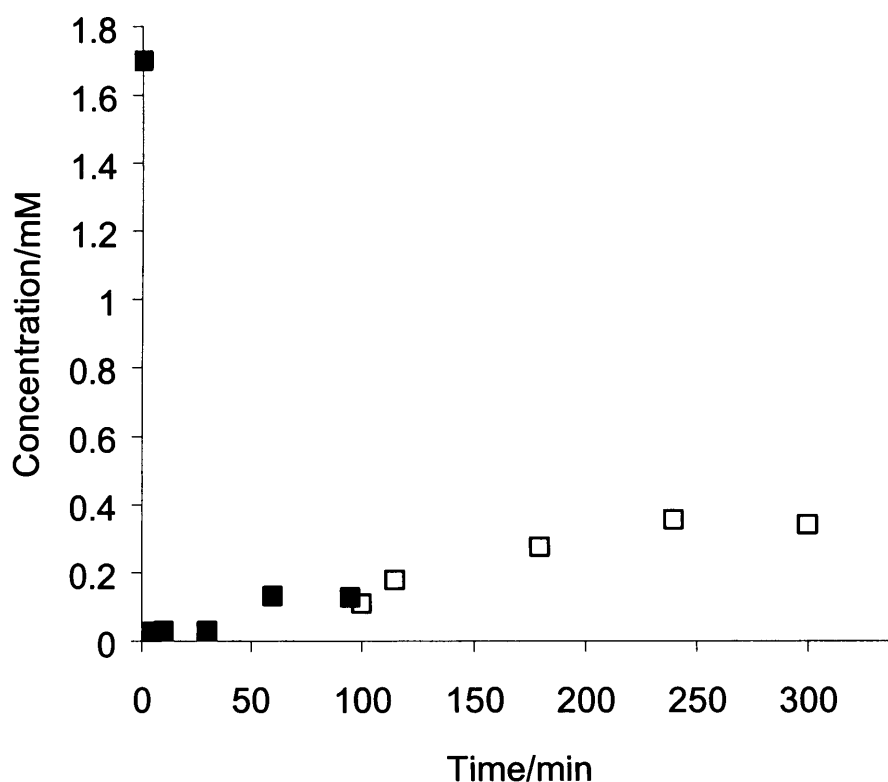


Fig. 4.3 Concentration of cinchonidine in effluent over M02473 under helium (■) and hydrogen (□)

[2 g catalyst; 0.17 mM cinchonidine in DCM at 1 ml/min; 0.5 barg He/H<sub>2</sub> pressure, GHSV 4800 /h; 25°C; T = 25 ± 1°C]

An attempt was made to measure the concentration of CD in the solvent effluent from an *ex situ* modified bed under helium. The dried modified catalyst was loaded in to the reactor and DCM was allowed to flow over the bed and samples were taken for UV/Vis analysis at regular intervals. Two modification concentrations were chosen (8.49 mM and 16.98 mM) and results are illustrated in Figure 4.4. Solvent passed over the bed for 60 minutes and the samples were analysed undiluted.

The concentration of cinchonidine exiting the bed follows an exponential type decay curve. The rate of cinchonidine removed from the bed modified with 8.49 mM reaches a pseudo steady state at 30 minutes of 0.156 mg<sub>CD</sub>/min.

#### 4.3 Results of cyclohexene hydrogenation

Hydrogenation of cyclohexene over granular 2.5 % Pt/SiO<sub>2</sub> was attempted in the trickle-bed reactor to compliment experiments in the autoclave. Catalyst M02023 (2g) was placed in the reactor and 0.1 M cyclohexene in DCM introduced at 1 ml/min. the reaction was carried out under 0.5 barg hydrogen with a GHSV of 4800 /h (Fig. 4.5). Conversion to cyclohexane was rapid and maintained near 100 % conversion for the duration of the experiment. Adsorption of cinchonidine on the catalyst in this reaction was investigated. The catalyst bed was pre-treated *in situ* with a solution of 0.849 mM cinchonidine in DCM under helium. The solution was then switched to the reaction mixture; 0.1 M cyclohexene and 8.49 mM CD in DCM and the gas changed to hydrogen (Fig. 4.6). Conversion to cyclohexane was rapid however, initially only achieved ca. 80 % conversion. This conversion decreased steadily to ca. 65 % at 300 minutes time-on-line.

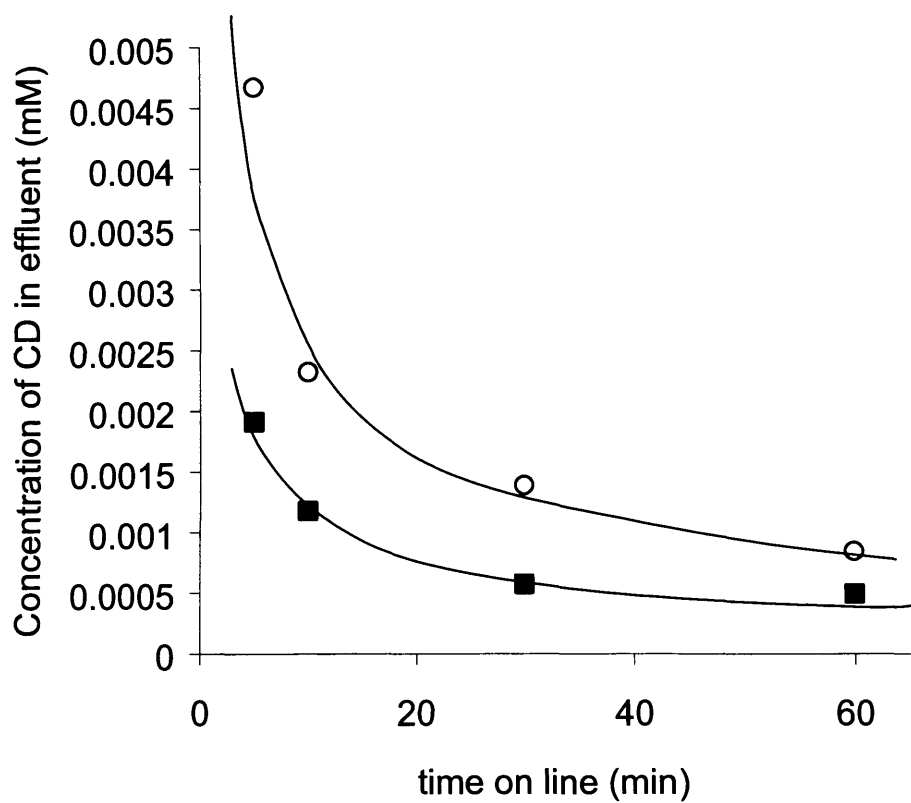


Fig. 4.4 Concentration of cinchonidine in DCM effluent over *ex situ* modified M02023

under helium. Concentration of *ex situ* modification solution;

8.49 mM (■) and 16.98 mM (○)

[2 g catalyst; DCM at 1 ml/min; 0.5 barg He pressure, GHSV 4800 /h; 25°C; T = 25 ± 1°C;

UV/Vis at 315 nm]

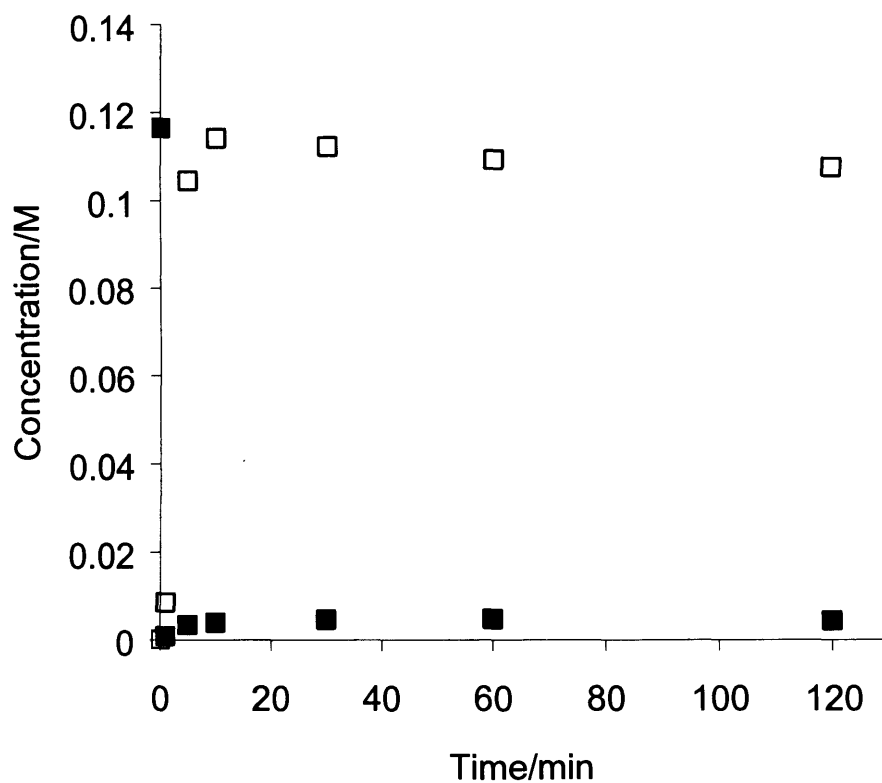


Fig. 4.5 Hydrogenation of cyclohexene (■) over M02023 to cyclohexane (□) following 5 min of DCM flow under He

[2 g catalyst; 0.1 M cyclohexene in DCM at 1 ml/min; 0.5 barg H<sub>2</sub> pressure, GHSV 4800 /h;  
25°C; T = 25 ± 1°C]

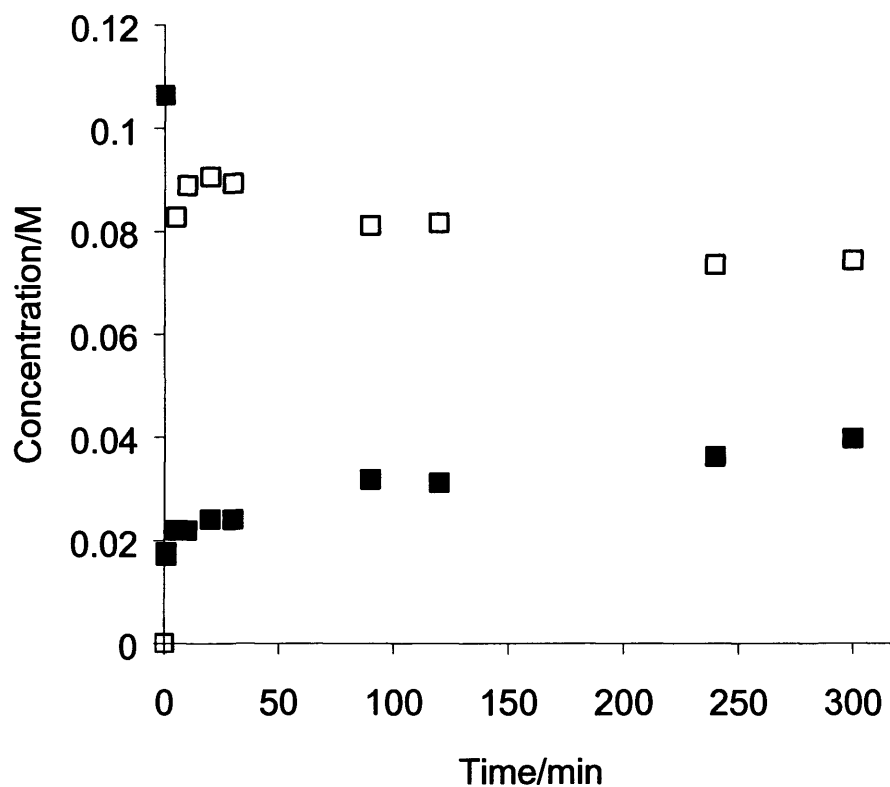


Fig. 4.6 Hydrogenation of cyclohexene (■) to cyclohexane (□) over *in situ* modified (0.0849 mM CD in DCM) M02023. Feedstock contained cinchonidine

[2 g catalyst; 0.1 M cyclohexene and 0.0849 mM CD in DCM at 1 ml/min; 0.5 barg H<sub>2</sub> pressure, GHSV 4800 /h; 25°C; T = 25 ± 1°C]

#### 4.4 Results of 2,3-Butanedione hydrogenation over M0202X series catalysts

The granular catalyst series (M0202X) were used for the hydrogenation of 2,3-butanedione in the trickle-bed reactor. Pertinent results from the autoclave investigation were applied to the experiments carried out in the trickle-bed reactor.

## 4.4.1 Hydrogenation of 2,3-butanedione in absence of alkaloid

Hydrogenation of 2,3-B was carried out over M02023 (2 g) in the absence of cinchonidine and Samples of reaction solution were analysed at intervals (Fig. 4.7). The catalyst bed was prepared according to the method in section 2.3.3; DCM was passed over the catalyst for 60 minutes under helium (GHSV 4800 /h). The reaction solution of 0.1 M 2,3-B in DCM was introduced in to the reactor under 0.5 barg hydrogen (GHSV 4800 /h).

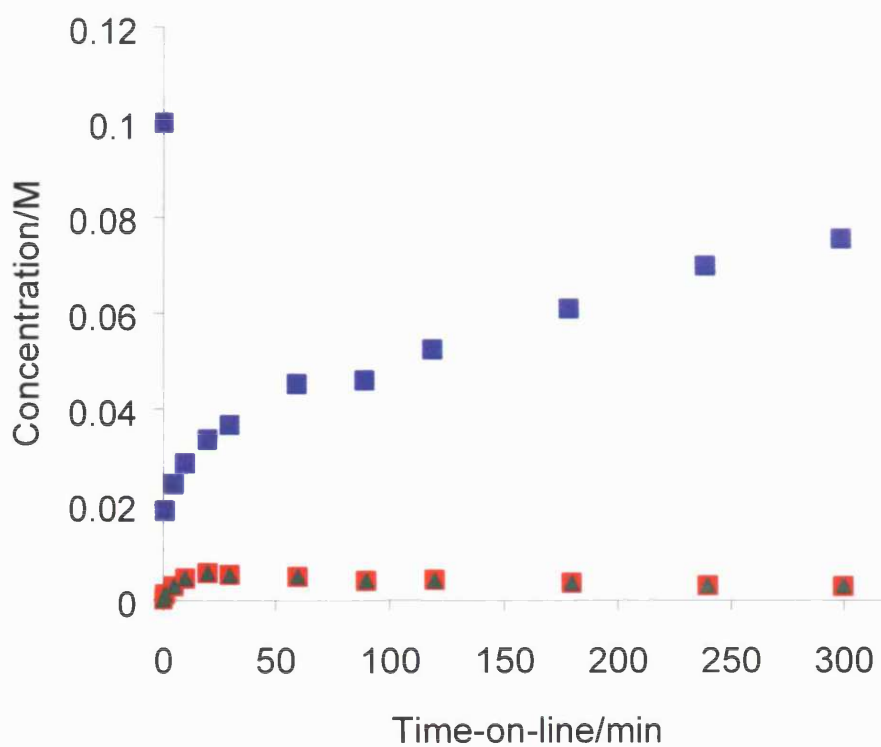


Fig. 4.7 Hydrogenation of 2,3-butanedione (■) over M02023 in absence of CD following 5 min of DCM flow under He. (R)-hydroxybutanone (■); (S)-hydroxybutanone (▲)

[2 g catalyst; 0.1 M 2,3-B in DCM at 1 ml/min; 0.5 barg H<sub>2</sub> pressure, GHSV 4800 /h; 25°C;

T = 25 ± 1°C]

The concentration of dione decreases rapidly to a minimum in the effluent. This then increases steadily over the course of the experiment. The concentration of the products; (*R*) and (*S*)-hydroxyketone were found to be in equal quantities i.e. racemic. Product formation increases to a maxima at 30 minutes time on line with a concentration of 0.0051 M. At 300 minutes the concentration of HK had reduced to 0.0028 M in the effluent stream.

#### 4.4.2 Influence of *in situ* modification of the catalyst bed on 2,3-butanedione hydrogenation

Experiments were carried out over the granular M0202X series of catalysts (Table 4.1). The catalyst bed was pre-modified *in situ* with a solution of 0.0849 mM CD which was allowed to flow over the bed at 1 ml/min under helium. A reaction feedstock containing 0.1 M 2,3-butanedione and 0.0849 mM CD in DCM was then passed over the bed under hydrogen at 0.5 barg. The concentration plots of starting material and products against time-on-line for the M0202X series are displayed in Appendix 7.4–7.7. Each displays a characteristic rapid decrease in dione concentration following introduction. With the exception of catalyst M02029 the other catalysts of the series achieved approximately 10 % conversion at 30 minutes. The enantiomeric excess of (*R*)-hydroxyketone was highest within the first 10 minutes of the reaction, decreasing as the reaction proceeded. Catalyst M02029, however, gave no enantioselection throughout the course of the reaction. Over a catalyst bed comprising of M02025 the (*R*)-enantiomer first stage product concentration was highest at 30 minutes with 0.013 M.



Table 4.1 Hydrogen of 2,3-butanedione over granule type catalysts in TBR after *in situ* modification.

Entry	Catalyst	Maximum concentration of ( <i>R</i> )-hydroxybutanone (M)	Maximum ee (%)
1	M02023	0.010	9
2	M02025	0.013	10
3	M02027	0.011	6
4	M02029	0.002	-

[2 g catalyst; 0.1 M 2,3-butanedione (8.49 mM CD) in DCM; 0.5 barg H<sub>2</sub> pressure; GHSV 4800 /h; 25°C; T = 25 ± 1°C]

#### 4.4.3 Influence of *ex situ* modification of catalyst bed on 2,3-butanedione hydrogenation

Modifying the catalyst bed *in situ* was deemed to be detrimental to the even distribution of alkaloid down the length of the bed. Therefore, employing an *ex situ* modification technique would allow for a more even distribution and better control of the resulting modified catalyst. Stirring the required amount of catalyst in a solution containing alkaloid followed by filtering and vacuum drying was attempted. This then allowed the initial modifier coverage on the catalyst to be altered reliably.

Two pre-modification concentrations were investigated which related to work with the autoclave. Concentrations of 8.49 mM and 16.98 mM were used to pre-modify catalyst M02023 (2 g) *ex situ* in DCM. After 10 minutes of stirring with the catalyst the 16.98 mM solution was analysed with UV spectroscopy. This showed that the uptake of cinchonidine was approximately 98 % of the original solution. This compares to the same experiment

carried out with the corresponding bare support (M02473) where the uptake was measured at 95 %. This infers that a large quantity of alkaloid was adsorbed on the silica gel support. Analysis of the wash solution from the *ex situ* modified bed under helium is displayed in Figure 4.5. The results indicate that a significant proportion of the modifier remains on the catalyst surface after washing for 60 minutes (Appendix 7.8/9).

The reaction mixture consisting of 0.01 M 2,3-B with no modifier was introduced at 1 ml/min to the reactor under 0.5 barg hydrogen. The enantiomeric excess to (*R*)-HK in the effluent from both catalysts increases to a maximum; then decreases over the course of the experiment. For the catalyst pre-modified with a solution containing 8.49 mM of CD this maximum occurs at 5 minutes, with an ee of 6 % and decreases to 2 % at 240 minutes time-on-line (Appendix 7.8). Whereas, for the catalyst pre-modified with 16.98 mM the ee reaches 12 % at 120 minutes and falls to 8 % at 240 minutes (Appendix 7.9). The characteristic adsorption of 2,3-B is present, however, is more pronounced where 16.98 mM was used. Conversion to (*R*)-HK is approx 8 % with the 16.98 mM CD solution, with the 8.49 mM CD solution it is 6 %. The concentration of *meso*-diol for both modified catalyst samples is relatively higher than for the *in situ* modified catalyst bed. This infers that the *ex situ* bed is more active; as the first stage product is then able to hydrogenate at another point in the bed. The decreased amount of modifier present on the surface may be responsible for this 'increase' in activity distribution.

#### 4.5 Results of methyl pyruvate hydrogenation

The enantioselective hydrogenation of methyl pyruvate in an autoclave is well documented [1,2]. Only recently have such reactions been studied over fixed bed reactors

such as the trickle-bed reactor [3-5]. For comparison to the experiments involving 2,3-butanedione, the hydrogenation of methyl pyruvate in the TBR was investigated.

#### 4.5.1 Hydrogenation over *ex situ* modified M02023 in DCM

Methyl pyruvate was hydrogenated over an *ex situ* modified catalyst bed with a feedstock containing CD. A catalyst sample of M02023 was added to a solution containing 16.98 mM and stirred for 10 minutes under atmospheric conditions, then filtered and vacuum dried. The catalyst bed was washed with DCM for 60 minutes under helium prior to the reaction.

The reaction solution of 0.1 M methyl pyruvate and 8.49 mM CD was then introduced to the bed under 0.5 barg of hydrogen pressure and the reaction begun (Fig. 4.8). The conversion of pyruvate is 80 % at 5 minutes and decreases to 60 % by 300 minutes time-on-line. The enantiomeric excess increases slowly over the reaction to a value of ca. 52 % at 300 minutes.

#### 4.5.2 Hydrogenation over *ex situ* modified M02023 in ethanol

The experiment carried out in 4.5.1 was repeated with ethanol as the solvent for the wash and feedstock solution (Fig. 4.9). The effect of changing the solvent is chiefly evident in the enantiomeric excess of (*R*)-methyl lactate. There is no transient period of increasing ee, which is ca. 40 % by 10 minutes time-on-line and is sustained for the reaction. Additionally conversion of methyl pyruvate remains stable at ca. 82 % for the duration of the experiment.

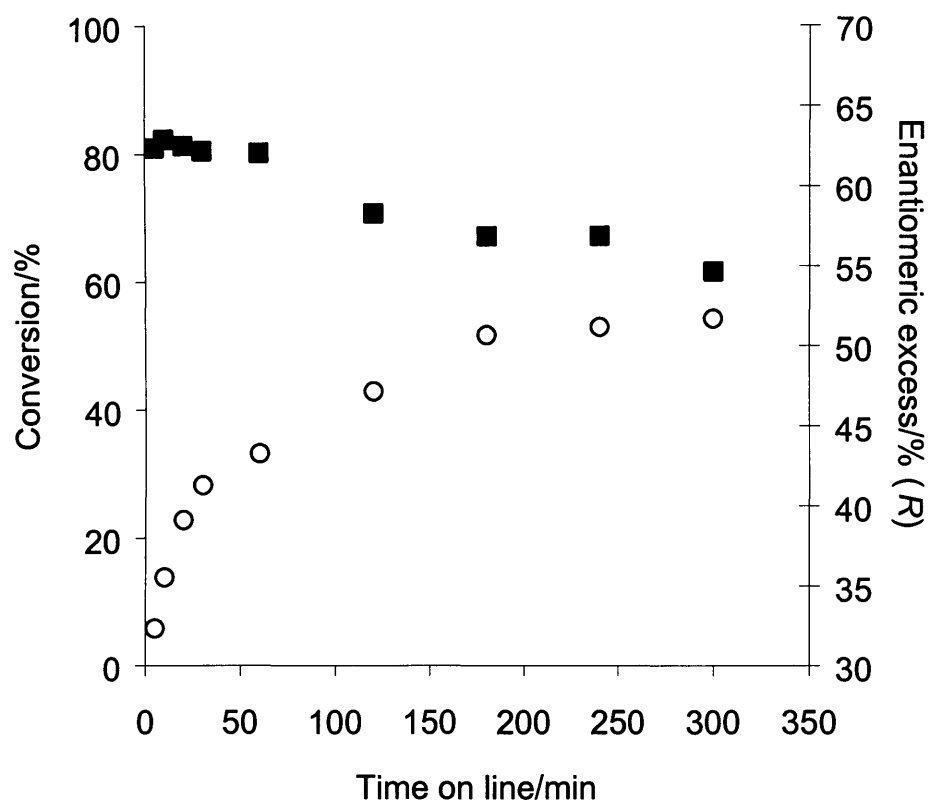


Fig. 4.8 Conversion of methyl pyruvate (■) over M02023 with the enantiomeric excess of (R)-methyl lactate (○)

[2 g catalyst; 0.1 M methyl pyruvate (8.49 mM CD) in DCM; 0.5 barg H<sub>2</sub> pressure; GHSV 4800 /h; 25°C; T = 25 ± 1°C]

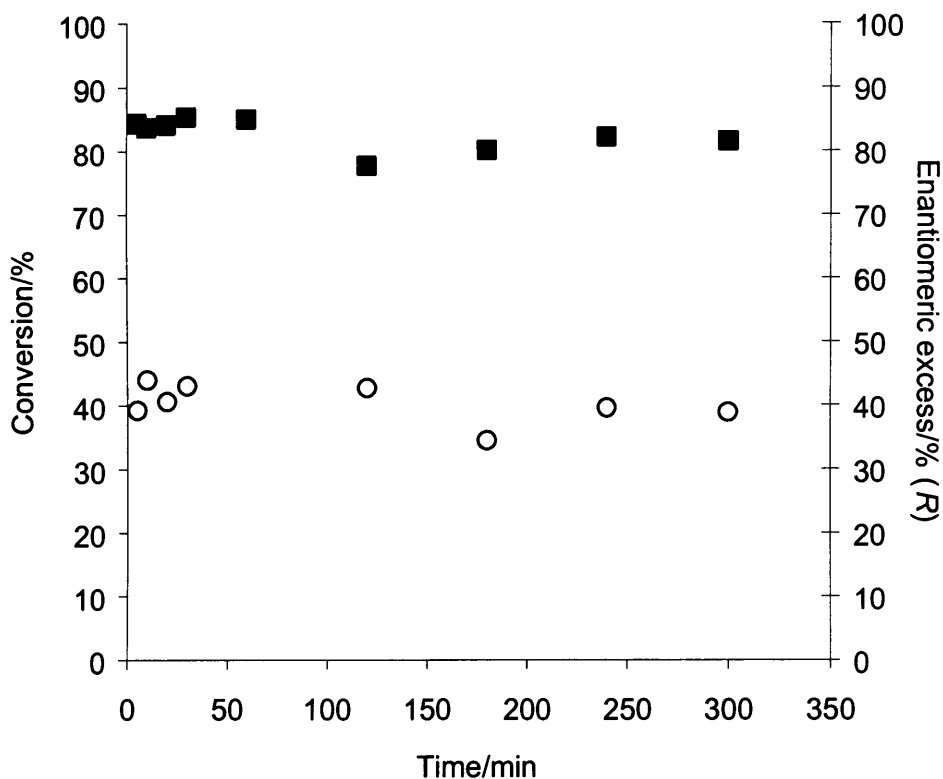


Fig. 4.9 Conversion of methyl pyruvate (■) over M02023 with the enantiomeric excess of (R)-methyl lactate (○)

[2 g catalyst; 0.1 M methyl pyruvate (8.49 mM CD) in EtOH; 0.5 barg H<sub>2</sub> pressure; GHSV 4800 /h; 25°C; T = 25 ± 1°C]

#### 4.6 Enantioselective hydrogenation over extruded catalysts in the trickle-bed reactor

Extruded catalysts are traditionally used in large fixed-bed reactors such as the trickle-bed reactor mainly for bulk chemical applications [6]. They have yet to be employed in enantioselective hydrogenation reactions where powdered catalysts are preferred for their

higher activity; due to their lower diffusion limitations [4]. The extruded supports were prepared by the Materials Centre in Birmingham and the metal impregnated by Johnson Matthey. The characteristics of the catalysts M03216 and M03217 are described in Table 2.4. Hydrogenation of cyclohexene, 2,3-butanedione and methyl pyruvate are described in the following sections.

#### 4.6.1 Hydrogenation of cyclohexene over extruded catalyst M03217

Cyclohexene was hydrogenated over M03217 in two different states; from dry and after an hour DCM wash. Reactant penetrating the inner areas of extruded catalysts is acknowledged as an important variable for successful fixed-bed reactions [7]. The degree of catalyst pre-wetting can determine the time taken for the reaction to reach steady state. The granule catalysts achieved high conversion of cyclohexene; ca. 96% within 5 minutes time-on-line.

Table 4.2 Influence of bed conditions on the hydrogenation of cyclohexene over M03217

Entry	Conditions	Conversion (%)
1	'dry'	59
2	'wet'	58

[2 g catalyst; 0.1 M cyclohexene in DCM; 0.5 barg H<sub>2</sub> pressure; GHSV 4800 /h; 25°C; T = 25 ± 1°C]

Table 4.2 displays the conversion of cyclohexene to cyclohexane over a 'dry' and a 'wet' M03217 catalyst. The conversion for the reaction begun with no prior treatment was

ca. 59 % and for the reaction carried out with pre-treatment the conversion was ca. 58 %. Both conditions yield conversions above 50 % at the 5 minute sample point and sustained this level for 120 minutes time-on-line.

#### 4.6.2 Hydrogenation of 2,3-butanedione over extruded catalysts

2,3-butanedione was hydrogenated over catalyst M03217 under different modification regimes. Firstly a pre-modification step was omitted and the reaction was carried out with modifier in the feed. Secondly the catalyst was pre-modified *ex situ* for 30 minutes with cinchonidine and the reaction proceeded with modifier in the feed.

Figure 4.10 illustrates the concentration of starting material and products exiting the bed at the sample points. Interestingly the product was determined to be racemic from GC analysis; however, the conversion is low (Table 4.3). At no stage during the experiment were any *stage 2* products detected in the analysis.

Table 4.3 Influence of pre-modification on the hydrogen of 2,3-butanedione over extruded type catalysts

Entry	Pre-modification concentration (mM)	Maximum concentration of ( <i>R</i> )-hydroxybutanone (M)	Maximum ee (%)
1	-	0.004	-
2	16.98	0.003	11.6

[2 g catalyst; 0.1 M 2,3-butanedione (8.49 mM CD) in DCM; 0.5 barg H<sub>2</sub> pressure; GHSV 4800 /h; 25°C; T = 25 ± 1°C]

The reaction over the pre-modified catalyst bed was enantioselective, yet the conversion of dione was lower than for the catalyst bed which was not pre-modified (Fig. 4.10 and Table 4.4). Enantioselectivity to (*R*)-hydroxybutanone reached a maximum value of ca. 12 % at 60 minutes time-on-line.

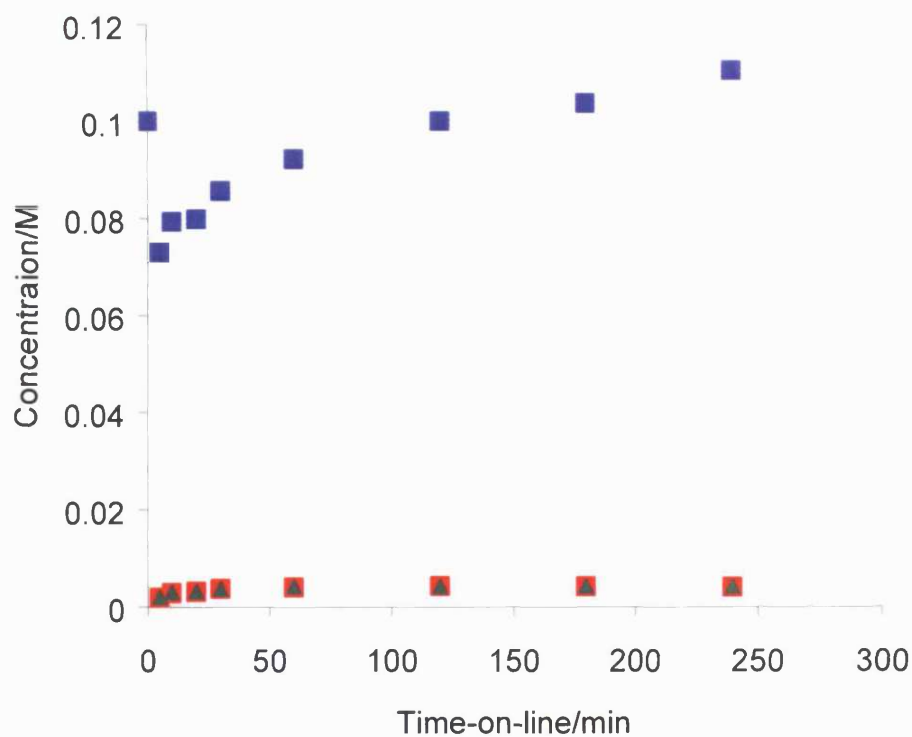


Fig.4.10 Concentration of 2,3-butanedione (■) and (*R*)/(*S*)-hydroxybutanone (■/▲) from reaction over M03217 with CD in feedstock

[2 g catalyst; 0.1 M 2,3-butanedione (8.49 mM CD) in DCM; 0.5 barg H<sub>2</sub> pressure; GHSV 4800 /h; 25°C; T = 25 ± 1°C]



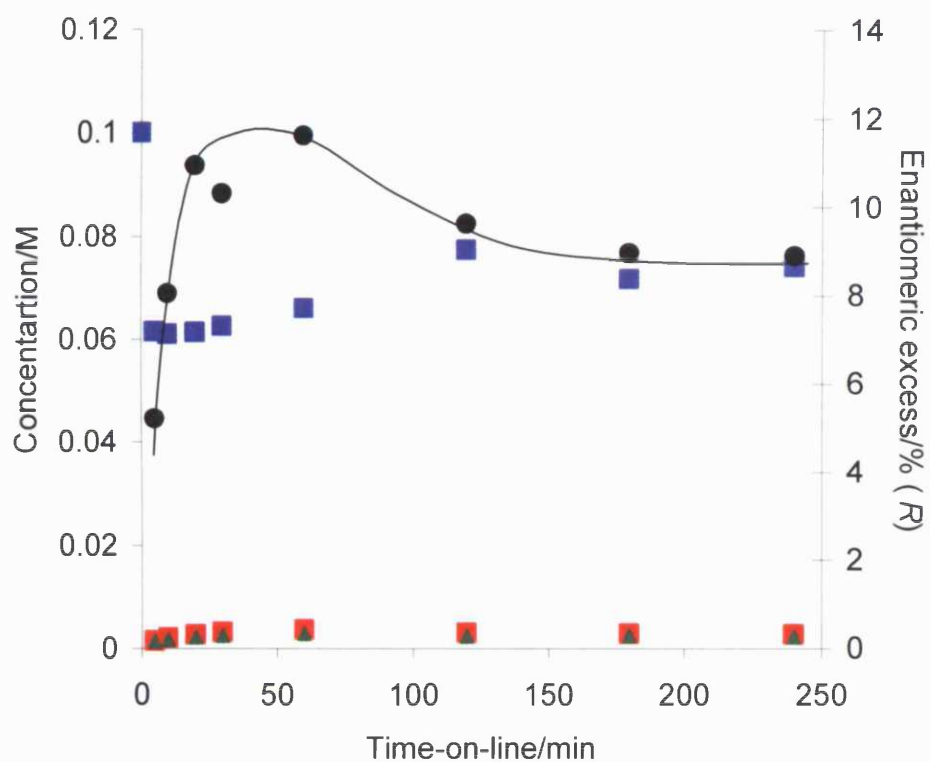


Fig.4.11 Concentration of 2,3-butanedione (■) and (R)/(S)-hydroxybutanone (■/▲) and ee (●) from reaction over pre-modified M03217 (16.98 mM CD) with CD in feedstock

[2 g catalyst; 0.1 M 2,3-butanedione (8.49 mM CD) in DCM; 0.5 barg H<sub>2</sub> pressure; GHSV 4800 /h; 25°C; T = 25 ± 1°C]

#### 4.6.3 Hydrogenation of methyl pyruvate over extruded catalysts

Hydrogenation of methyl pyruvate was carried out over the extrudate catalysts M03216 and M03217. The reaction protocol was identical for both experiments for comparison of the two catalysts. Catalyst samples were pre-modified *ex situ* and dried before loading in to the reactor and then washed with flowing DCM for 1 h under helium. The

reaction feedstock containing cinchonidine was then introduced in to the reactor under hydrogen.

For the reaction of 0.1 M methyl pyruvate over the catalyst bed comprising of M03216 yields a maximum ee of 37 % at 240 minutes after a large transient (Fig. 4.12). The conversion of pyruvate to lactate was determined to be ca. 20 % after an induction period of 60 minutes to reach steady state operation.

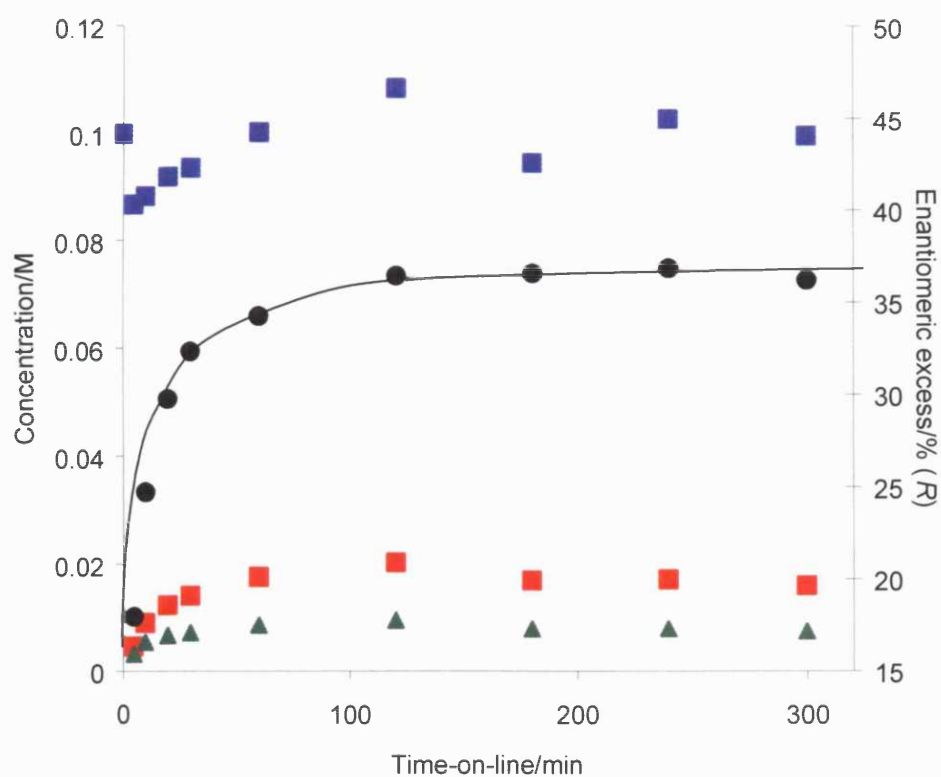


Fig.4.12 Concentration of methyl pyruvate (■) and (R)/(S)-methyl lactate (■/▲) and ee (●) from reaction over pre-modified M03216 (16.98 mM CD) with CD in feedstock

[2 g catalyst; 0.1 M 2,3-butanedione (8.49 mM CD) in DCM; 0.5 barg H<sub>2</sub> pressure; GHSV 4800 /h; 25°C; T = 25 ± 1°C]

Hydrogenation of methyl pyruvate over M03217 gave similar results to that over M03216. An enantiomeric excess to (*R*)-methyl lactate was observed with a value of ca. 36 % at the maxima and falls to 33 % at 300 minutes time-on-line (Fig. 4.13). The conversion of pyruvate was modestly higher over M03217 at ca. 28 % which falls to 24 % at 300 minutes.

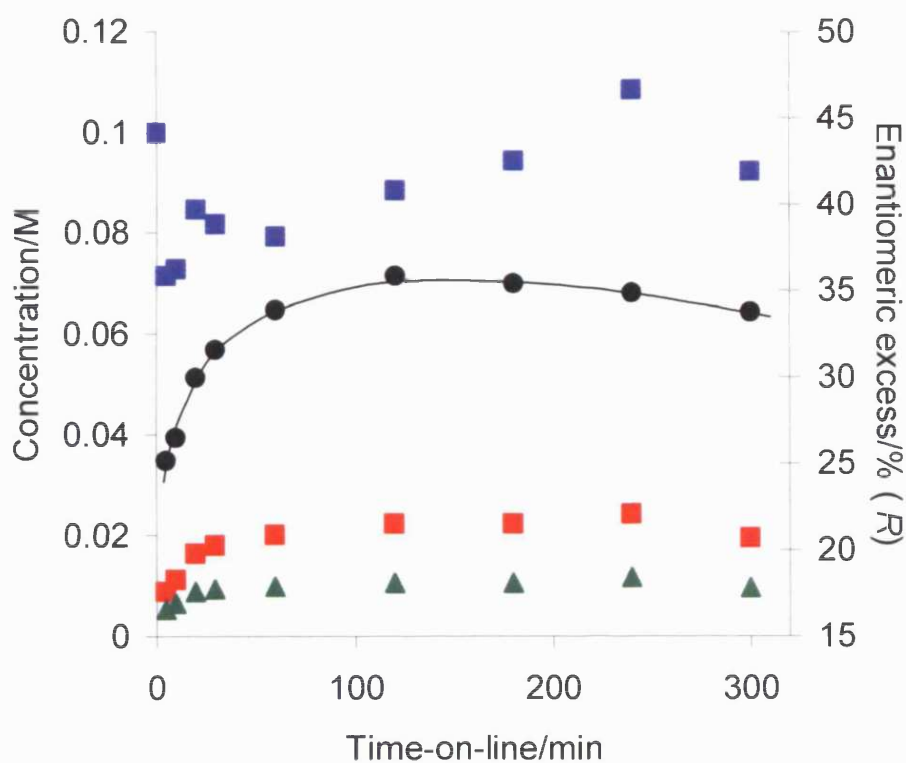


Fig.4.13 Concentration of methyl pyruvate (■) and (*R*)/(*S*)-methyl lactate (■/▲) and ee (●) from reaction over pre-modified M03217 (16.98 mM CD) with CD in feedstock

[2 g catalyst; 0.1 M 2,3-butanedione (8.49 mM CD) in DCM; 0.5 barg H<sub>2</sub> pressure; GHSV 4800 /h; 25°C; T = 25 ± 1°C]

---

## 4.7 Discussion

### 4.7.1 Modification Protocol

The use of a chiral modifier in trickle-bed reactors poses a number of problems associated with the design of said reactors and the action of modification. The influence of the reaction gas and the effect of flowing solvent through a modified fixed catalyst bed are of primary concern. In the literature a small number of reports have dealt with the outcome of bed modification on hydrogenation of a handful of carbonyl containing compounds [4,8]. However, there exists little information on the behaviour of alkaloid modifiers under reaction conditions in fixed-bed reactors. Reported in 4.2 are initial attempts to monitor with the use of UV/Vis spectroscopy this behaviour.

Enantioselective hydrogenation of a carbonyl containing compound in an autoclave is commonly achieved through the use of alkaloid modifier; typically in excess. As the system is sealed and usually operated at high pressures, replacement of denatured alkaloid takes place. Use of fixed-bed reactors for such reactions require a continual replacement of modifier to maintain high conversion and enantioselectivity [4]. This is achieved by dissolving the desired amount of modifier in the feedstock solution. Hydrogenation of alkaloid modifiers has been documented in the literature concerning autoclave experiments. The vinyl group of cinchonidine can be easily hydrogenated and results in no loss of enantioselection [9]. Hydrogenation of the quinoline ring system has been shown to diminish enantioselectivity, however, this was found with more aggressive conditions when in the presence of reactant [10].

Monitoring the effluent from the trickle-bed reactor under helium demonstrated that a steady state of modifier adsorption and desorption existed within 60 minutes time-on-line

and remained for a further 180 minutes (Fig. 4.1). Yet when the gas feed was changed to hydrogen; as illustrated in Figure 4.2, this equilibrium was disrupted. This has been attributed to hydrogenation of the quinoline ring system of the cinchonidine modifier. Therefore, under reaction conditions it is essential to replenish the modifier at the platinum surface. The result of a change of gas stream where no platinum is present on the catalyst yields no modifier hydrogenation (Fig. 4.3). However, the adsorption/desorption of alkaloid is disrupted which indicates that the modifier is in competition with hydrogen on the support. This suggests that under reaction conditions modifier molecules may desorb from the support material to re-adsorb further along the bed. This along with the fresh modifier entering the bed may over-crowd the metal surface at the lower end of the bed and result in a decrease of enantioselectivity.

Analysis of the wash solutions from an *ex situ* modified catalyst bed displays an exponential type of decay, with a high rate of modifier removal at the start of the experiment (Fig. 4.4). This is expected as there may be layers of modifier on the surface of the support which are weakly bound, thus easier to remove by the solvent. Where the catalyst has been modified with 8.49 mM of cinchonidine the effluent concentration at 30 and 60 minutes are similar. An approximate rate of modifier removal for this period was calculated to be 0.156 mg<sub>CD</sub>/min with a value of 0.104 g<sub>CD</sub> present on the catalyst at  $t = 0$ . Suggesting that the remaining modifier is more strongly adsorbed on the metal surface. Therefore, the commencement of the reaction at 60 minutes is better suited to achieve higher ee and conversion.

#### 4.7.2 Cyclohexene hydrogenation

Hydrogenation of a well known and relatively simple molecule such as cyclohexene in the autoclave generated valuable results reported in section 3.4. Hydrogenation of cyclohexene was used to ascertain information concerning the activity of the fixed-bed and the influence of cinchonidine addition. Cyclohexene was hydrogenated over a catalyst bed comprising of M02023 and silicon carbide fines. Two experiments were carried out; firstly in the absence of alkaloid (Fig. 4.5) and secondly with cinchonidine in the feedstock solution (Fig. 4.6). The reaction in the absence of modifier yielded ca. 96 % conversion for 120 minutes, whereas; with 8.49 mM cinchonidine in the feed the conversion fell from ca. 80 % to 65 %. The results over M02023 in the autoclave studies suggested that the catalysts were mass transfer limited compared to the powdered catalysts (Table 3.8). This was not the case in the trickle-bed reactor as the analysis confirmed that the bed was at near total activity within 5 to 10 minutes.

Addition of 8.49 mM cinchonidine to the feedstock depressed the activity of the catalyst bed by a factor of ca. 30 %. The plot of concentration against time-on-line (Fig. 4.6) shows that as the experiment advances the activity decreases. This can be attributed to the build up of modifier at the surface of the catalyst poisoning active platinum sites. The implications of continuous feeding of modifier present certain advantages and disadvantages. Continuous modification of the catalyst bed is essential to maintain a high enantiomeric excess. Conversely addition of excess modifier in the feed solution has potential to block active sites on the catalyst resulting in a drop in activity.

The pore character of M03217 was deemed to be un-restrictive compared to catalyst M02029. Hydrogenation can, therefore, occur at both surface and sub-surface sites of the catalyst. The catalysts supported modest activity for cyclohexene hydrogenation in both

'wet' and 'dry' conditions (58 % and 59 % respectively). These results were useful in the determination of a pre-treatment protocol for the enantioselective hydrogenation reactions over the extrudate catalysts.

#### 4.7.3 2,3-butanedione Hydrogenation

Hydrogenation of 2,3-butanedione in the trickle-bed reactor in the absence of alkaloid yielded a conversion of ca. 10 %. When compared to the results obtained from cyclohexene hydrogenation, under the same conditions, the activity to 2,3-butanedione was surprising. Following the results displayed in Figure 4.8 there appears to be a discrepancy between the concentration of dione in the effluent compared to the products. Therefore, conversion as calculated in the equation 2.6 could not be achieved and maximum concentrations of (*R*)-hydroxyketone have been reported as an alternative. The results suggests that the dione is strongly adsorbed on to the platinum surface, however, there may exist a delay before it desorbs or reacts. This phenomenon gives the false impression of high conversion in the first portion of the experiment.

This phenomenon is observed with the *in situ* addition of modifier to the catalyst bed prior to reaction. The discrepancy between dione and hydroxybutanone concentrations exist, as illustrated in Appendix 7.4-6. This trend is broken to a certain extent by the reaction over M02029; due to the restrictive pore character (Table 4.1).

2,3-butanedione (0.1 M) was hydrogenated over M02023 (2 g) in the autoclave for the calculated contact time of reactant in the TBR (5.25 min) at a hydrogen pressure of 1 barg. This experiment was attempted to obtain greater understanding of the results from the TBR. The concentration of (*R*)-hydroxyketone achieved in the autoclave with alkaloid and without was 0.006 M and 0.004 M respectively (Table 4.4). The trickle-bed reactor appears

to be a better reactor for such reactions at such mild conditions. The strong adsorption of dione at the metal surface may not be overcome by the reduced concentration of hydrogen from the liquid phase in the autoclave system. The enantiomeric excess achieved in the autoclave is approximately double that in the trickle-bed reactor. High catalyst loading in the autoclave has been shown to improve the enantioselection of 2,3-butanedione hydrogenation [11].

Table 4.4 Influence of reactor type on the hydrogen of 2,3-butanedione over M02023 catalyst

Entry	Reactor	Modification concentration (mM)	Maximum concentration of ( <i>R</i> )-hydroxybutanone (M)	Maximum ee (%)
1	TBR	-	0.005	-
2	TBR	8.49 <sup>1</sup>	0.010	9
3	AC <sup>2</sup>	-	0.004	-
4	AC <sup>2</sup>	11.3	0.006	20

TBR = trickle-bed reactor; AC = autoclave; <sup>1</sup> = feedstock solution; <sup>2</sup> = reaction time 5.25 minutes

[2 g catalyst; 0.1 M 2,3-butanedione DCM; 0.5 barg H<sub>2</sub> pressure (TBR); 1 barg H<sub>2</sub> pressure (AC); GHSV 4800 /h; 25°C; T = 25 ± 1°C]

*Ex situ* modification of the catalyst M02023 was carried out with two different modification solutions; 8.49 mM and 16.98 mM. Analysis of the subsequent hydrogenation reaction resulted in different enantiomeric excess behaviour respectively (Appendix 7.8/9). The lower modification solution gave an ee of ca. 6 %, whereas, for the greater solution the



resultant ee was 12 %. Interestingly the ee from the catalyst bed modified in 16.98 mM observes a large induction period before peaking at 12 % and dropping to 8 %. For the 8.49 mM catalyst bed the ee is at the maximum of 6 % rapidly, before falling to 4 % and recovering to 5 %. However, by the end of the experiment the ee has fallen to ca. 2%. Clearly the pre-modification solution has a great influence on the behaviour of the active site, even after 60 minutes of solvent wash. It must be noted however, that the maximum ee of 12 % is achieved at the maximum concentration of *meso*-diol analysed. Therefore, it can be assumed that a degree of kinetic resolution to enhance the ee, similar to that found in the autoclave work of Slipsenko *et al.* is occurring in both experiments [11]. Where no *meso*-diol was detected the ee had reached 6 %, which is the same for the lower pre-modification solution catalyst. Interestingly for both catalyst samples there is a decrease of ee in the effluent sample when *meso* butandiol is first detected, before recovering.

Hydrogenation of 2,3-butanedione over the extrudate catalyst M03217 was performed with and with out an *ex situ* pre-modification step. Catalyst pre-treatment with cinchonidine yielded a maximum ee to (*R*)-hydroxyketone of ca. 12 % (Fig. 4.10). Conversely the absence of a pre-treatment step afforded no enantiomeric excess, even with the inclusion of modifier in the feedstock solution (Fig. 4.11). The conversion of dione in both cases was poor, the concentration of hydroxyketone was found to be modestly higher in the experiment with out pre-modification.

The low conversion over the extruded catalysts suggests that the reactant may not fully penetrate the inner areas of the catalyst as with cyclohexene. This is compounded by the behaviour of 2,3-butanedione at the metal surface, which is strongly adsorbed. The benefit of this behaviour over the chosen amount of extruded catalyst is the absence of further reactions; that is hydroxyketone to diol. From the results the addition of modifier in the feedstock provides no enantioselectivity over the non pre-treated catalyst. Strong

competition between dione and cinchonidine and the insufficiency of metal sites available, due to diffusion limitation may be the cause. However, this phenomenon is not observed over the pre-modified catalyst, where a high ee of 12 % falls to ca. 9 % for the final 2 h time-on-line. The constant addition of modifier to the bed may be beneficial in this case. However, recent work has shown that stirring the catalyst in a slurry of cinchonidine dissolved in solvent had restructured the platinum particles to smaller more disperse particles [12]. This phenomenon was attributed to the improvements in enantioselection measured. However, the effect was observed in a slurry of toluene under an atmosphere of nitrogen.

#### 4.7.4 Methyl pyruvate hydrogenation

Hydrogenation of pyruvate esters over cinchonidine modified platinum catalysts has been shown to be very successful in fixed-bed reactors [3,8,13]. High conversion and enantiomeric excess have been reported, typically at high pressure and over powdered catalysts. The use of powdered catalysts in fixed-bed operations reduce mass transfer limitations associated with larger catalyst particles, such as beads and extrudates. Low pressure pyruvate hydrogenation reactions over the granule and extrudate platinum catalysts were attempted. The resulting activity and enantioselectivity will be compared in this section to the dione hydrogenations reported in 4.3.

The influence of solvent was studied with methyl pyruvate hydrogenation over an *ex situ* modified M02023 catalyst bed with cinchonidine in the feed solution. Solvents used were dichloromethane and ethanol, both gave high conversion of pyruvate and modest ee to (*R*)-lactate (Fig. 4.8 and Fig. 4.9 respectively). Interestingly the enantioselectivity of the reaction carried out in DCM improved over time, whereas, the ee of (*R*)-methyl lactate with

EtOH remained stable. In dichloromethane the conversion decreases modestly with time such that the maximum ee corresponds to a conversion of ca. 60 %.

The improved activity of the M02023 bed towards pyruvate hydrogenation can be principally ascribed to the weaker strength of adsorption of the pyruvate compared to the dione. The conversion of methyl pyruvate is greatly improved on the activity of the EUROPT-1 bed (0.4 g) of ca. 7 % conversion reported in [3]. The influence of ethanol on the enantioselection is markedly different when DCM is used. Solvent effects have been well reported in stirred tank systems and the activity and enantioselection have been related to the dielectric constant of the solvent used [14]. Ethanol is postulated to stabilise the *closed* conformers of cinchonidine in solution lowering the enantioselectivity of pyruvate hydrogenation. This benefits the ee of (*R*)-methyl pyruvate in the trickle-bed reactor in terms of stability compared to the results obtained in DCM. However, the ee in DCM after stabilising is ca. 12 % higher than in ethanol.

Hydrogenation of methyl pyruvate was investigated over the extruded catalysts identified as M03216 and M03217 (Fig. 4.12/Fig.4.13). The reaction protocol was identical to allow for comparison of the catalysts. A transient period of increasing enantiomeric excess of (*R*)-methyl lactate is observed for both M03216 and M03217 similar to Figure 4.9, yielding a maximum of ca. 37 % and 36 % respectively. Conversion of pyruvate is comparable for both extruded catalysts, reaching ca. 20 %. Compared to the hydrogenation of 2,3-butanedione over these catalysts and the granular M02023, pyruvate hydrogenation over extrudate has suffered. This can be ascribed to the lower adsorption strength of the pyruvate compared to the dione. This infers that the pyruvate may pass through the bed without reacting in the pores or at a sub-surface level. The surface area available with the granular M02023 can accommodate more pyruvate, compared to the extrudate catalyst.

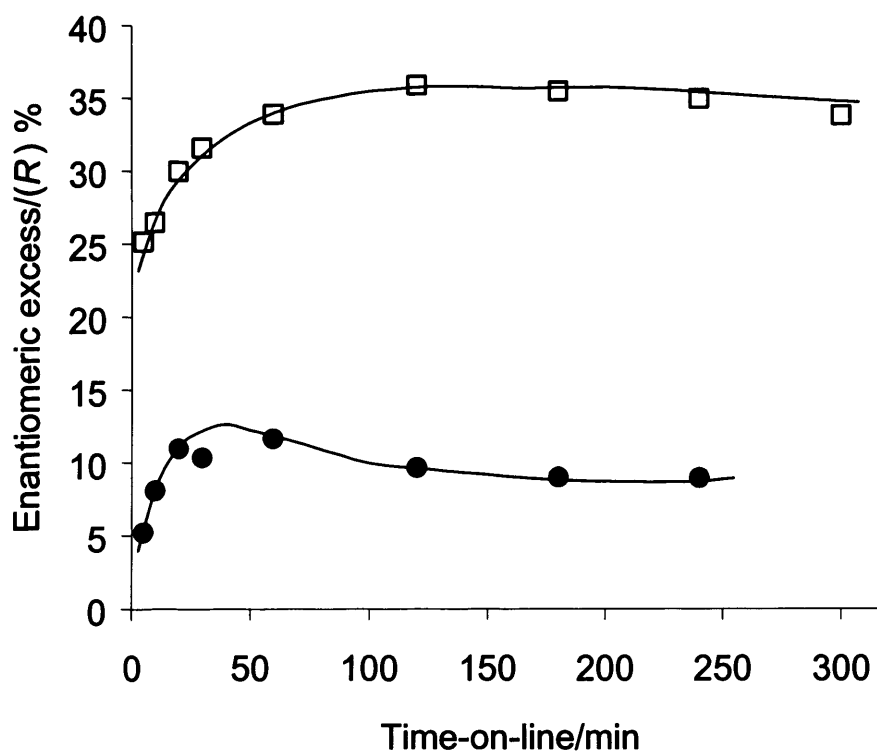


Fig.4.15 Enantiomeric excess of (*R*)-methyl lactate (□) and (*R*)-hydroxyketone (●) over pre-modified M03217 (16.98 mM CD) with CD in feedstock

[2 g catalyst; 0.1 M substrate (8.49 mM CD) in DCM; 0.5 barg H<sub>2</sub> pressure; GHSV 4800 /h;  
25°C; T = 25 ± 1°C]

Comparison of the enantiomeric excess of (*R*)-hydroxybutanone and (*R*)-methyl lactate as a function of time over pre-modified M03217 yields a number of points. Firstly; that the increase to the maximum ee for both products differs greatly (Fig. 4.15). For the dione reaction this occurs rapidly and then decreases modestly. For the pyruvate reaction the

ee increases slowly reaching the maximum considerably later in the experiment. Recent work by Li *et al.* illustrated that the optimum cinchonidine concentration for ethyl pyruvate compared to 2,3-butanedione was less by a factor of 10 [14]. The reactions carried out in the trickle-bed reactor exemplify this phenomenon; the modifier concentration used was determined to be the optimum for 2,3-butanedione hydrogenation in the autoclave.

Secondly, the experiment of 2,3-butanedione hydrogenation over un-treated M03217 it was clear that the effect of modifier addition in the feed was unnoticeable. However, the stability of the ee over the course of the reaction with pyruvate infers that, as with the dione reaction, constant addition of modifier is advantageous (Fig. 4.15). The stability of the ee may arise from the weaker competition of pyruvate and modifier for metal sites, compared to the case for the dione. Therefore, it is expected that for pyruvate hydrogenation over an *ex situ* un-treated M03217 bed would yield an ee, albeit lower.

#### 4.8 Conclusions

Enantioselective hydrogenation of 2,3-butandione was conducted in a small scale trickle-bed reactor. Additionally methyl pyruvate and cyclohexene were hydrogenated for comparison to the fixed-bed literature and results obtained in Chapter 3. Furthermore modification of the catalyst bed was investigated with UV/Vis spectroscopy.

- (5) From the UV/Vis analysis of the effluent solution from the trickle-bed reactor during *in situ* pre-modification, the quinoline ring system of cinchonidine was hydrogenated in the absence of reactant.

- (6) Hydrogenation of 2,3-butanedione was achieved over un-modified catalyst bed which exhibited poor activity compared to cyclohexene hydrogenation. The high strength of adsorption of the dione was thought to hinder the reaction in the mild conditions of the trickle-bed reactor.
- (7) Enantioselective hydrogenation of 2,3-butanedione was achieved at low conversion with an enantiomeric excess of ca. 12 %. This is similar to reactions conducted in the stirred tank reactor over the contact time in the trickle-bed reactor. *In situ* and *ex situ* alkaloid pre-modification techniques were attempted resulting in different values of ee as a function of time-on-line. The ee achieved with an *in situ* technique at its highest initially, compared to the slow increase of ee with an *ex situ* technique.
- (8) Addition of alkaloid in the feedstock was deemed necessary for maintaining the ee for methyl pyruvate hydrogenation, as reported in the literature. However, the increased competitive adsorption of the dione compared to the modifier from the feedstock to the surface was detrimental to the formation of an enantioselective site. Pre-modification of the catalyst enabled the formation of the enantioselective site prior to the introduction of dione, which was beneficial.

#### 4.9 References

1. M. Garland and H.-U. Blaser, *J. Am. Chem. Soc.*, **112** (1990) 7048.
2. G. Bond, P.A. Meheux, A. Ibbotson and P.B. Wells, *Catalysis Today*, **10** (1991) 371.
3. P. Meheux, A. Ibbotson and P.B. Wells, *J. Catal.*, **128** (1991) 441.
4. N. Künzle, R. Hess, T. Mallat and A. Baiker, *J. Catal.*, **186** (1999) 239.

5. E. Toukoniitty, P. Mäki-Arvela, A.K. Neyestanaki, T. Salmi, R. Sjöholm, R. Leino, E. Laine, P.J. Kooyman, T. Ollonqvist and J. Väyrynen, *App. Catal. A: Gen.*, **216** (2001) 73.
6. E.H Stitt, *Chem Eng. J.*, **90** (2002) 47.
7. K.D.P. Nigam, I. Iliuta and F. Larachi, *Chem. Eng. Process.*, **41** (2002) 365.
8. E. Toukniitty and D.Yu. Murzin, *Catal. Lett.*, **93** (2004) 171.
9. H.-U. Blaser, H.P. Jalett, D.M. Monti, A. Baiker and J.T. Wehrli, in '*Symposium on Structure-Activity Relationships in Heterogeneous Catalysis*', American Chemical Society, Boston (1990) p.79.b
10. H.-U. Blaser, H.P. Jalett, D.M. Monti, A. Baiker and J.T. Wehrli, *Stud. Surf. Sci. Catal.*, **67** (1991) 147.
11. J. Slipszenko, S. Griffiths, P. Johnston, K. Simmons, W.A.H Vermeer and P.B. Wells, *J. Catal.*, **179** (1998) 267.
12. R. Hess, F. Krumeich, T. Mallat and A. Biaker, *Catal. Lett.*, **92** (2004) 141.
13. N. Künzle, J.-W. Soler and A. Baiker, *Catal. Today.*, 79-80 (2003) 503.
14. X. Li, N.F. Dummer, R.L. Jenkins, R.P.K. Wells, P.B. Wells, D.J. Willock, S.H. Taylor, P. Johnston and G.J. Hutchings, *Catal. Lett.*, **96** (2004) 147.

*Chapter*  
*Five*



## Chapter 5: Gas Phase Reactor

### 5.1 Introduction

Enantioselective hydrogenations were attempted at the gas/solid interface over pre-modified supported platinum catalysts. Experiments involving the hydrogenation of carbonyl containing compounds were conducted in a fixed-bed plug reactor, in the absence of solvent. The conditions reported here were developed from initial investigations carried out by Von Arx *et al.* which involved 1,3-butadiene, crotonaldehyde, butyraldehyde and subsequently pyruvate ester hydrogenation over 5 % Pt/alumina [1,2].

### 5.2 Hydrogenation of substrates at gas/solid interface

Pro-chiral carbonyl containing compounds 2,3-butanedione and two pyruvate esters were hydrogenated in the gas phase over platinum catalysts; 2.5 % Pt/Silica (M01271), EUROPT-1, 5 % Pt/Alumina and a prepared 1 % Pt/ $\alpha$ -Alumina. The reaction protocol for these experiments are described in Chapter 2.5, changes to those conditions are reported in the relevant sections.

#### 5.2.1 Hydrogenation of 2,3-butanedione over pre-modified catalysts

The 2,3-butanedione conversion was hard to accurately determine at any reaction temperature. Additionally it was crucial to keep the saturator containing the dione at 0°C as at temperatures above this no reaction occurred. When this protocol was adhered to there existed a discrepancy between the amount of dione and product analysed, similar to the

results from the trickle-bed reactor (Section 4.4). However, from the analysis of a blank experiment with no modifier present yielded a maximum conversion of approximately 64 % was calculated. The amount of dione in the exit stream increased steadily, reaching a maximum after 140 minutes time-on-line. Over the pre-modified catalyst sample an ee of 15 %  $\pm$  5 % was determined, which persisted until no further product was detected. There were no products from the second stage reaction detected at any point in the dione experiments.

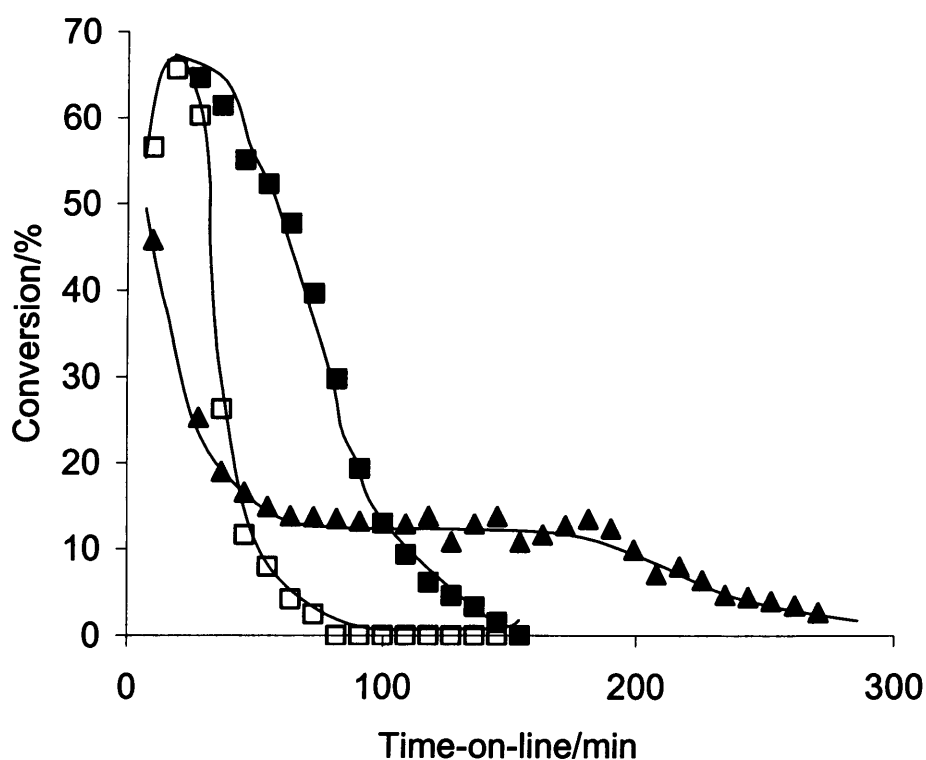


Fig. 5.1 Variation of conversion with time-on-line of 2,3-butanedione over pre-modified M01271 (■), un-modified M01271 (□) and EUROPT-1 (▲)

[0.025 g *ex situ* pre-modified (3.4 mM CD); 2,3-butanedione 0.025 g/h (0°C); T = 35°C;  
GHSV 96000 /h]

The reaction was repeated over EUROPT-1 at 35°C and product was detected for the duration of the 3.5 h experiment. The enantiomeric excess of (*R*)-hydroxybutanone was found to be 15 % ± 5 %, yet, the amount of product exiting the bed decreased slowly. The amount of dione exiting the bed was closer to a realistic picture of the activity of the catalyst bed, however, no reliable value of conversion can be quoted. From the experiment runs where no catalyst is present it was possible to tentatively determine an approximate conversion of 13 % with a maximum of 45 % (Fig. 5.1).

### 5.2.2 Hydrogenation of 2,3-butanedione over un-modified catalyst

2,3-butanedione was hydrogenated over M01271 in the absence of alkaloid at 35°C. The hydroxyketone product was racemic and after 60 minutes time-on-line was not detected in the exit stream. Additionally the amount of dione in the exit stream achieved a maximum after 60 minutes time-on-line. A maximum conversion was calculated from the blank reaction of 64 % (Fig. 5.1).

### 5.2.3 Standard reaction experiments carried out with pyruvate esters

Pyruvate esters were chosen for further investigation as they did not exhibit the strength of adsorption observed with 2,3-butanedione in the TBR. Secondly the results obtained could be compared to the previous work by Von Arx *et al.* which used an alumina supported platinum catalyst.

## 5.2.3.1 Hydrogenation of methyl pyruvate over alkaloid pre-modified catalyst samples

Methyl pyruvate was hydrogenated in the gas phase over the same 5 % Pt/Alumina catalyst as Von Arx [2]. The conversion of pyruvate is initially 100 %, however, decreased rapidly to ca. 10 % for the remainder of the experiment (Fig. 5.2). The enantiomeric excess of (*R*)-lactate increases initially to 30 %, then decreases to ca. 25 % during the decrease in conversion of the pyruvate. The ee is then maintained for the remainder of the experiment at this value.

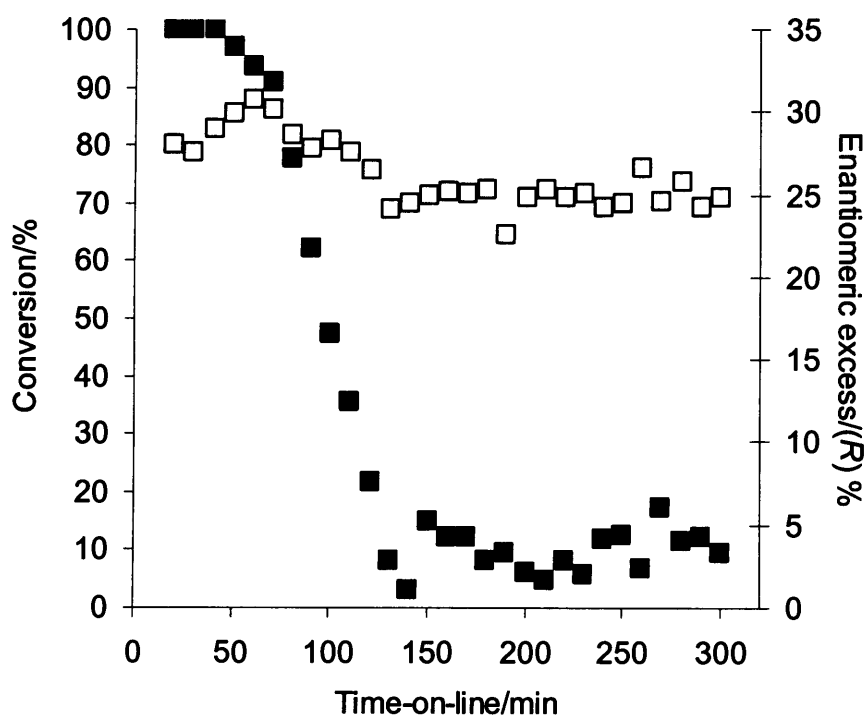


Fig. 5.2 Variation of conversion of methyl pyruvate (■) and ee of (*R*)-methyl lactate (□) over pre-modified 5 % Pt/Alumina with time-on-line

[0.025 g *ex situ* pre-modified (3.4 mM CD) catalyst; methyl pyruvate 0.066 g/h (20°C); T = 40°C; GHSV 96000 /h]

Catalyst M01271 was pre-modified with 3.4 mM cinchonidine in DCM. Flowing methyl pyruvate (20°C) over the catalyst resulted in an enantiomeric excess in favour of (*R*)-methyl lactate at 40 °C (Fig. 5.3). The conversion of pyruvate is sustained over the reaction period of 5 hours at 100 %. The ee initially rises at 60 minutes to ca. 36 % from 30 % and is maintained over the remaining reaction period. *The experimental protocol used and the subsequent results achieved will be now described as the standard reaction.*

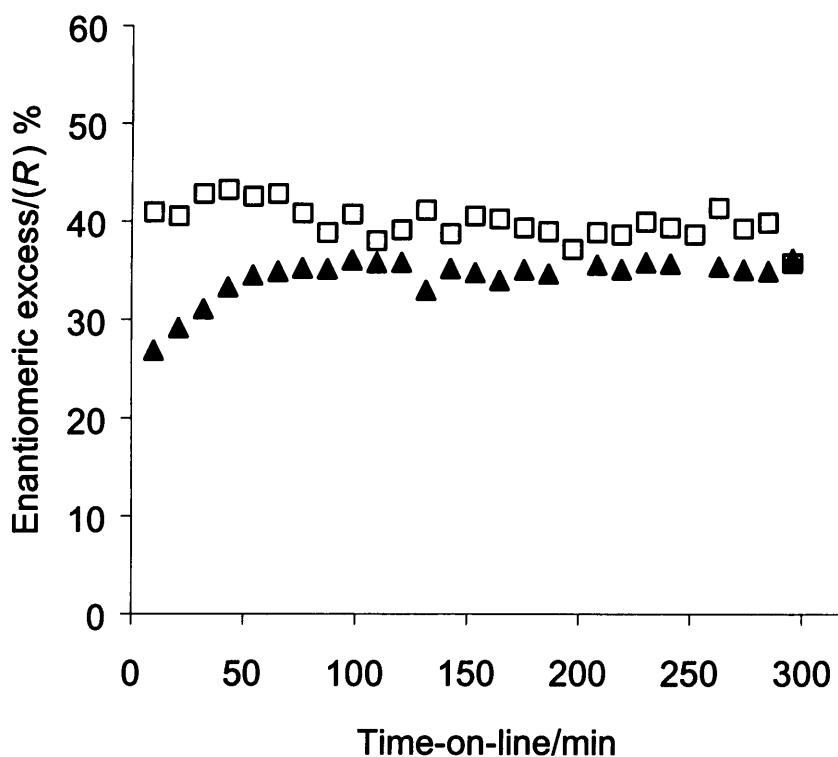


Fig. 5.3 Variation of enantiomeric excess of (*R*)-methyl lactate with time-on-line over pre-modified M01271 (▲) and EUROPT-1 (□) at 100 % conversion

[0.025 g *ex situ* pre-modified (3.4 mM CD) catalyst; methyl pyruvate 0.066 g/h (20°C); T = 40°C; GHSV 96000 /h]

Methyl pyruvate was enantioselectively hydrogenated over the reference catalyst EUROPT-1 (Fig. 5.3). The catalyst was pre-modified with 3.4 mM cinchonidine in DCM. Conversion of pyruvate was 100 % for the duration of the experiment. The enantiomeric excess of (*R*)-methyl lactate was ca. 40 %.

The 1% Pt/ $\alpha$ -Alumina catalyst was pre-modified with 0.34 mM cinchonidine in DCM. The enantiomeric excess of (*R*)-lactate achieved upon hydrogenation of methyl pyruvate was ca. 25 % (Fig. 5.4) and maintained for 5 h. The conversion decreased from 76 % to 10 % by 120 minutes and remained stable at that value.

#### 5.2.3.2 Hydrogenation of methyl pyruvate over un-modified catalyst samples

Methyl pyruvate was hydrogenated over unmodified 2.5 % Pt/Silica (25 mg) catalyst M01271. This experiment was repeated with the prepared 1% Pt/ $\alpha$ -Alumina catalyst (50 mg). For the silica gel supported catalyst 100 % conversion of the pyruvate to the racemic lactate was achieved and maintained for 5 h. The conversion for the unmodified 1% Pt/ $\alpha$ -Alumina decreased from 98 % to 57 % over 60 minutes (Fig. 5.4). The product analysis on-line consisted of equal amounts of (*R*)- and (*S*)-methyl lactate; i.e. racemic.

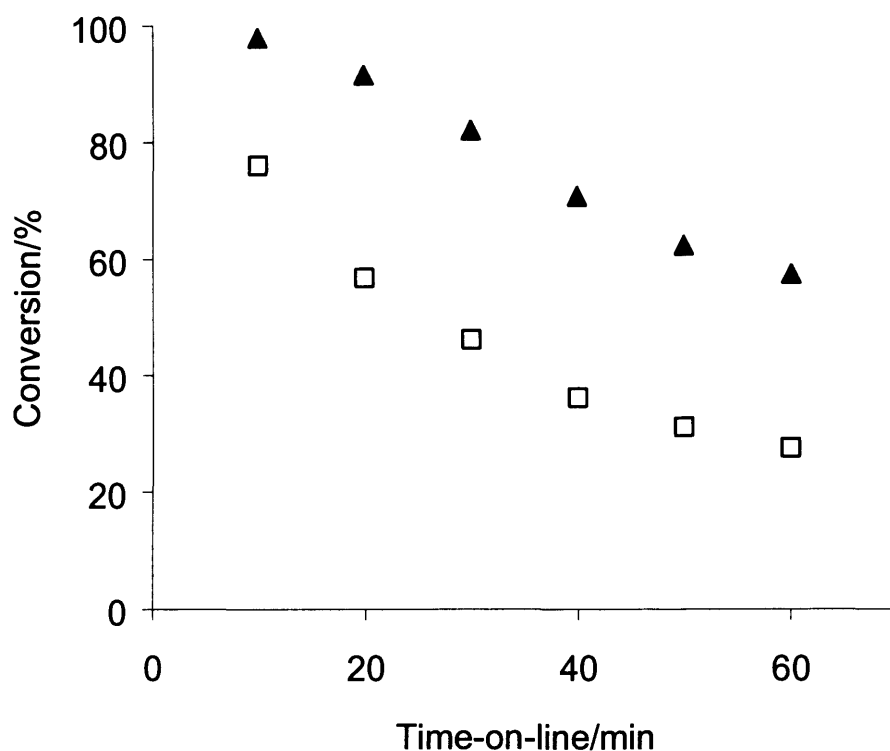


Fig. 5.4 Variation of conversion with time-on-line of methyl pyruvate over un-modified 1% Pt/α-Alumina (▲) and pre-modified 1% Pt/α-Alumina (□)

[0.050 g catalyst; 0.050 g *ex situ* pre-modified (0.34 mM CD) catalyst; methyl pyruvate 0.066 g/h (20°C); T = 40°C; GHSV 96000 /h]

### 5.2.3.3 Hydrogenation of ethyl pyruvate over catalyst M01271

Ethyl pyruvate was hydrogenated according to the standard reaction over a catalyst (M01271) pre-modified in 3.4 mM cinchonidine DCM solution. The enantiomeric excess achieved (ca. 35 %) was similar to methyl lactate.

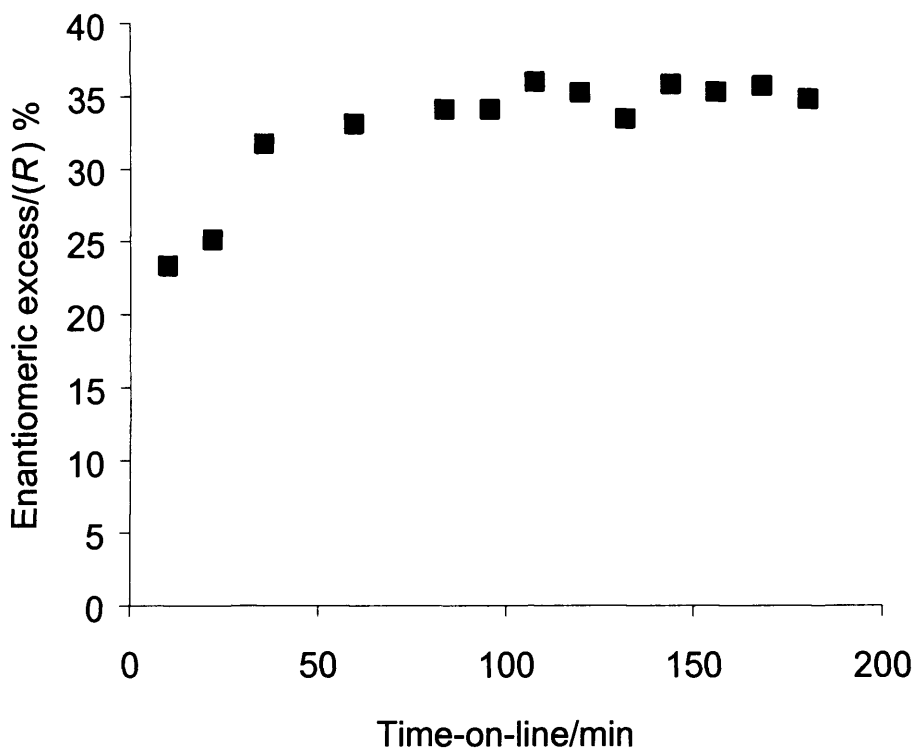


Fig. 5.5 Variation of ee with time-on-line of ethyl pyruvate over pre-modified M01271 (■)

[0.025 g *ex situ* pre-modified (0.34 mM CD) catalyst; ethyl pyruvate 0.066 g/h (20°C); T = 40°C; GHSV 96000 /h]

### 5.3 Investigation of the enantioselective site with methyl and ethyl pyruvate

A series of experiments were conducted to further understand the enantioselective hydrogenation of carbonyl containing pro-chiral compounds at the gas/solid interface. Reactions involved removal of the reactant vapour from the feed gas and reacting methyl pyruvate followed by ethyl pyruvate and *visa versa*. Additionally, ethyl pyruvate was added to the reaction of methyl pyruvate and *visa versa*, concurrent pyruvate hydrogenation and



pre-treating the modified catalyst bed with lactate enantiomers prior to pyruvate hydrogenation.

### 5.3.1 The effect of removing the reactant from the gas stream on the standard reaction

Removal of methyl pyruvate from the gas stream and then the subsequent re-introduction were investigated for periods of time. Reactant was passed over pre-modified M01271 catalyst for 100 minutes and then bypassed for 20, 40 and 60 minutes. The gas stream was then diverted back through the saturator containing the pyruvate.

The effect of 20 minutes without pyruvate on the ee of (*R*)-methyl lactate is reported in Figure 5.6. The conversion of pyruvate remains at 100 % for both periods of pyruvate hydrogenation. In the first period of reaction the transient rise of ee is present before the enantiomeric excess stabilising at ca. 35 %. During the break this rises to 45 %, however, the amount of product is negligible and has been omitted from the Figure. After the break of pyruvate the ee exhibits a modest transient period before stabilising at ca. 38 %.

The result of a break of 40 minutes in the absence of reactant is illustrated in Fig. 5.6. As with the experiment involving a 20 minute break, 100 % conversion is maintained for both periods of reaction. The initial transient rise in enantiomeric excess of (*R*)-lactate was observed, stabilising at ca. 37 %. After the re-introduction of pyruvate after 40 minutes the ee exhibits a shorter rise and stabilises at 37 % for the remainder of the experiment.

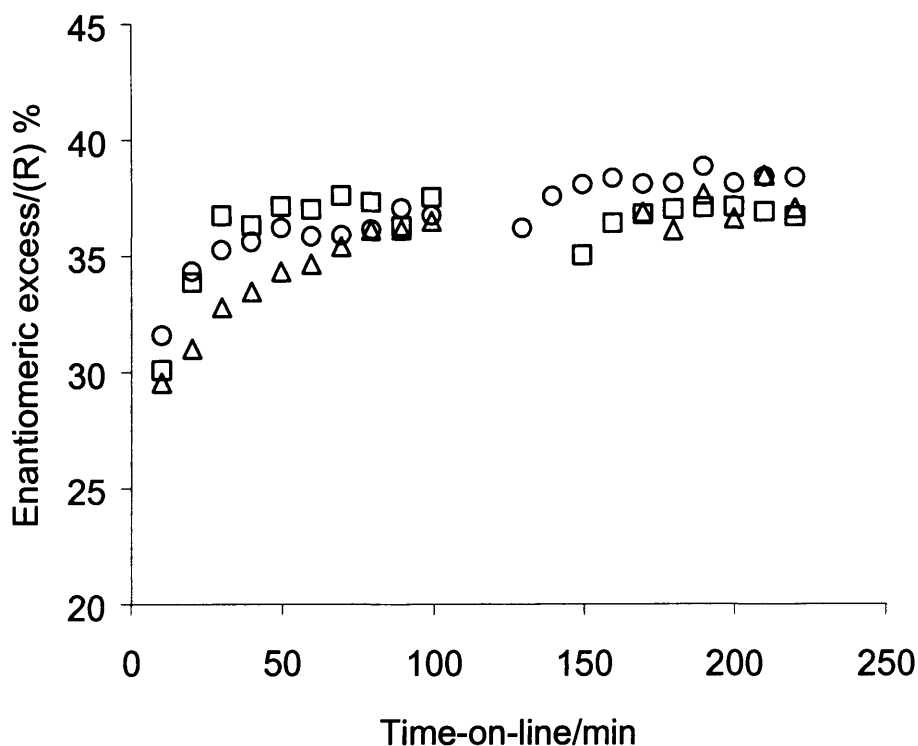


Fig. 5.6 Effect of diverting the pyruvate feed on the enantiomeric excess of (*R*)-methyl lactate with time-on-line: 20 min (○); 40 min (□); 60 min (Δ)

[0.025 g *ex situ* pre-modified M01271 (3.4 mM CD); methyl pyruvate (20°C); T = 40°C;  
GHSV 96000 /h]

Additionally displayed in Fig. 5.6 is the influence of applying a 60 min diversion of the pyruvate flow on the ee of (*R*)-lactate. The characteristic transient in ee is present over the first 60 minutes, reaching ca. 36 % by 100 min. Upon returning the reactant to the gas stream the resulting ee remains unchanged, however moderately unstable at ca. 36 %±4 %. The conversion is 100 % for the duration of both periods of reaction.

### 5.3.2 Sequential experiments

Methyl pyruvate was hydrogenated according to the standard reaction for 100 minutes time-on-line. Then the H<sub>2</sub>/He was diverted to another saturator containing ethyl pyruvate (Fig. 5.6). The ee for the methyl lactate increases to ca. 35 % during the 100 minutes. The ee for the ethyl lactate increased at a much slower rate after the switch when compared to a standard ethyl pyruvate reaction (Fig. 5.5). The opposite reaction was attempted with ethyl pyruvate reacting for 100 min, switching then to methyl pyruvate (Fig. 5.7). A transient period of increasing ee was observed for the ethyl lactate before stabilising ca. 35 %. Interestingly, an increase in the ee of (*R*)-methyl lactate was observed after the switch, however, this was slow, achieving ca. 33 % by the end of the experiment. Comparison of the enantiomeric excess after the switch to the values before the switch, shows suppression for both methyl and ethyl lactate. However, this phenomenon is more pronounced with the case of ethyl lactate. Conversion of pyruvate in all cases was 100 % and maintained for the duration of the experiment.

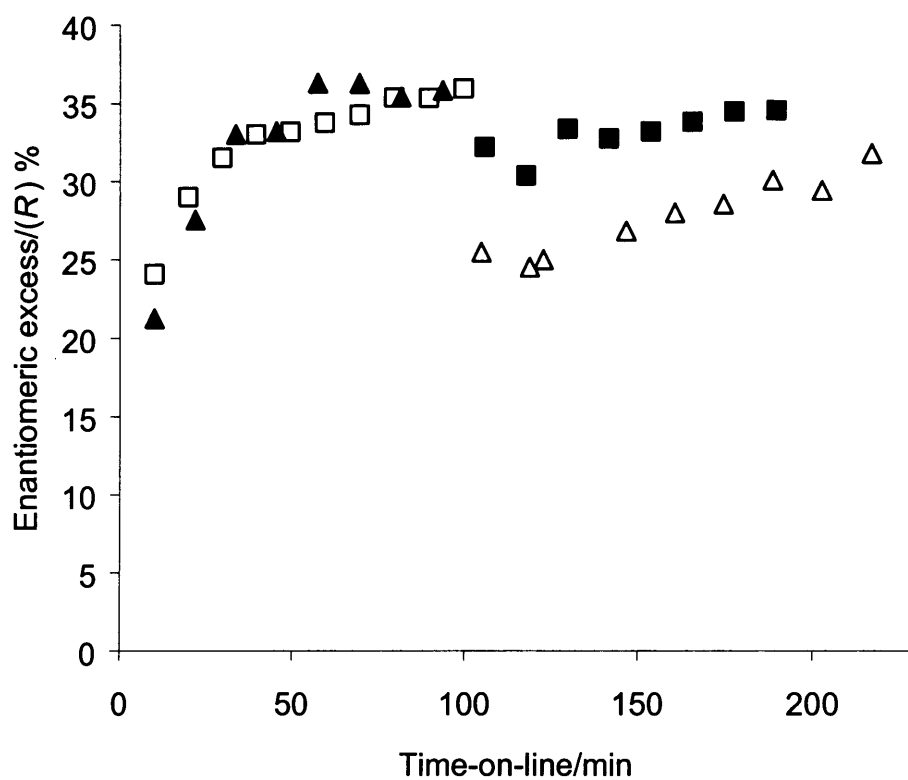


Fig. 5.7 Influence on the enantiomeric excess of (*R*)-lactate of diverting the gas feed from methyl pyruvate (□) to ethyl pyruvate (Δ) and ethyl pyruvate (▲) to methyl pyruvate (■) with time-on-line

[0.025 g *ex situ* pre-modified M01271 (3.4 mM CD); pyruvate (20°C); T = 40°C; GHSV 96000 /h]

### 5.3.3 Introduction experiments

Experiments were carried out with either methyl or ethyl pyruvate for 100 minutes time-on-line, then the gas feed was diverted to allow the other pyruvate to react concurrently. The results for the methyl pyruvate introduction to ethyl pyruvate

hydrogenation are shown in Fig. 5.8. Enantiomeric excess for the (*R*)-ethyl lactate increases to ca. 35 % at 100 min. Introduction of methyl pyruvate caused a modest drop in the ee of ethyl lactate, before increasing to the same value yielded before the introduction. The ee for (*R*)-methyl lactate from introduction increased from 26 % ca. 33 % over the remaining 2 h time-on-line.

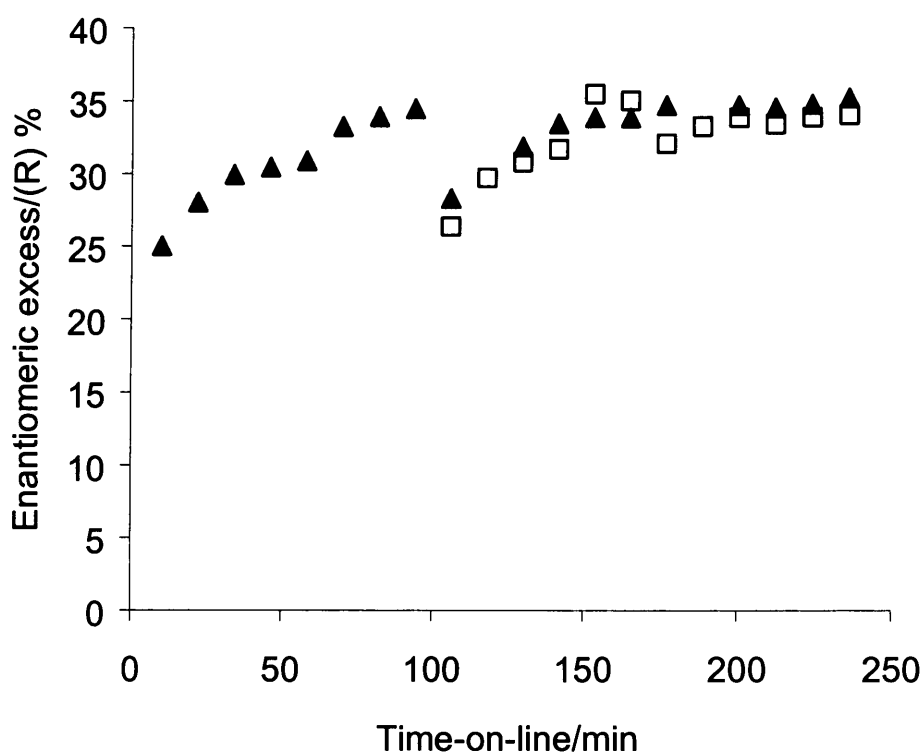


Fig. 5.8 Influence on the enantiomeric excess of (*R*)-ethyl lactate (▲) with the introduction methyl pyruvate with time on line; methyl lactate (□)

[0.025 g *ex situ* pre-modified M01271 (3.4 mM CD); pyruvate (20°C); T = 40°C; GHSV  
96000 /h]

When ethyl pyruvate is introduced at 100 min a drop in the ee of (*R*)-methyl lactate is observed, comparable to the opposite experiment (Fig. 5.9). The ee of the methyl lactate displays the initial transient rise to ca. 36 % at 100 min. Following the introduction of ethyl pyruvate to the reaction stream a slow increase of ee occurs, stabilising at ca. 35 %.

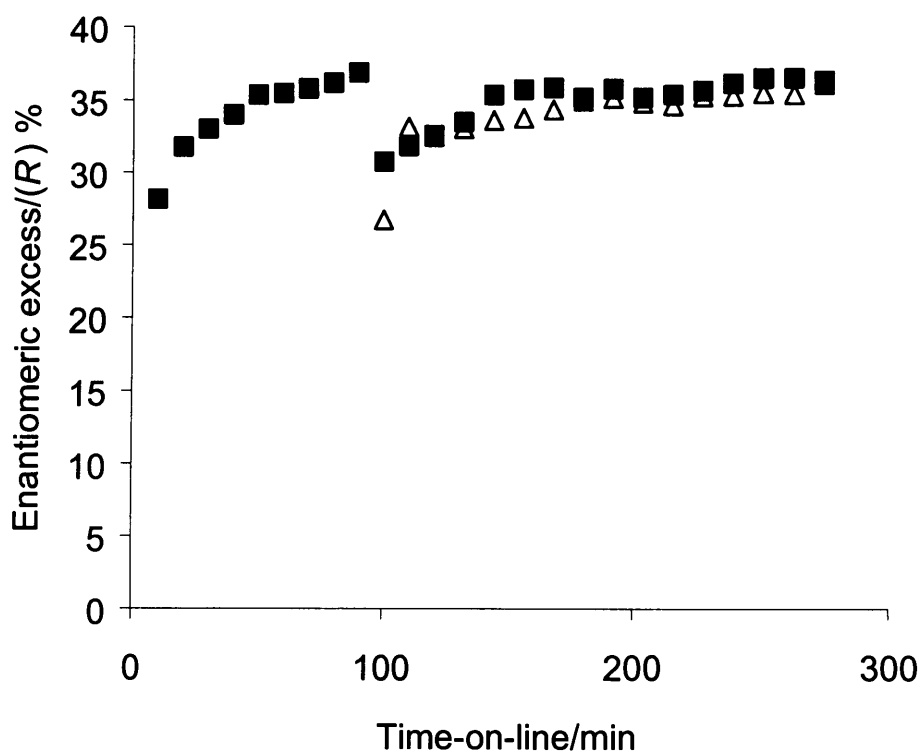


Fig. 5.9 Influence on the enantiomeric excess of (*R*)-methyl lactate (■) with the introduction ethyl pyruvate with time on line; ethyl lactate (Δ)

[0.025 g *ex situ* pre-modified M01271 (3.4 mM CD); pyruvate (20°C); T = 40°C; GHSV  
96000 /h]

## 5.3.4 Reaction of both methyl and ethyl pyruvate over pre-modified catalyst

An experiment was carried out with both methyl and ethyl pyruvate hydrogenated concurrently over pre-modified M01271 according to the standard reaction conditions (Fig. 5.10).

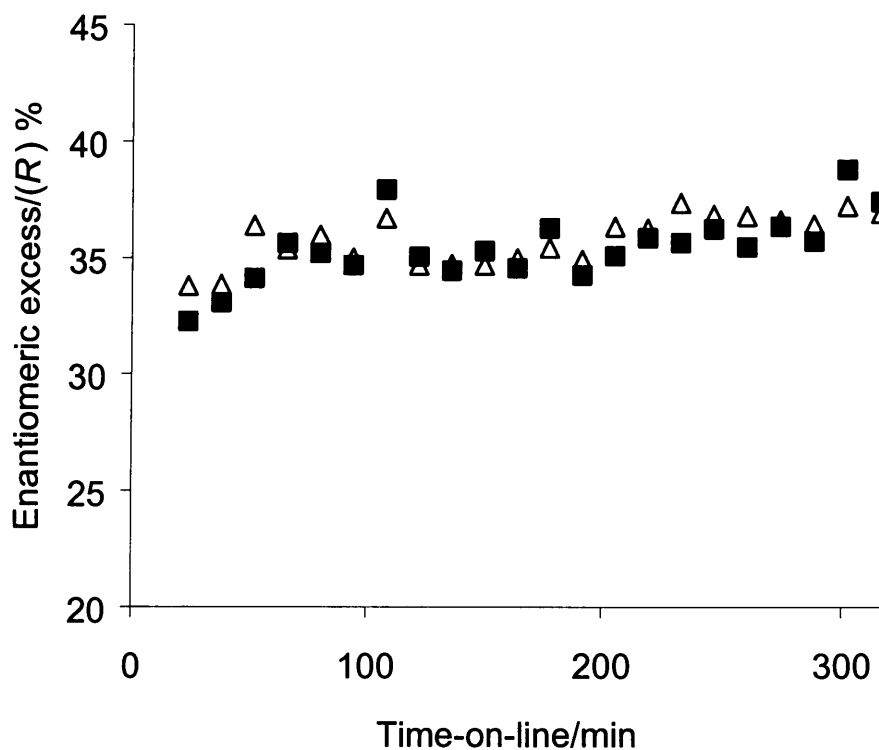


Fig. 5.10 Influence on the enantiomeric excess of (*R*)-methyl lactate (■) and (*R*)-ethyl lactate (Δ) of concurrent hydrogenation of methyl pyruvate and ethyl pyruvate over pre-modified M01271 with time on line

[0.025 g *ex situ* pre-modified M01271 (3.4 mM CD); methyl/ethyl pyruvate (20°C); T = 40°C; GHSV 96000 /h]

The substrates were contained in separate saturators, through which the gas flow was diverted to start the reaction. A modest transient rise of 33 to 36 % ee was observed for both substrates, however, the values are less stable than with separate reactions. There is no significant further rise in ee over the reaction period, both achieved ca. 36 % ee.

### 5.3.5 Influence of lactate pre-treatment on the standard reaction

Experiments were carried out where initially ethyl lactate was passed over the catalyst for 100 minutes, at which time the lactate was switched off. The gas feed was then diverted through a saturator containing ethyl pyruvate and the reactions were begun. Pre-treatment of the pre-modified catalysts were achieved using (*S*), (*R*), a racemic mixture and a mixture of 20 % (*R*)-ethyl lactate in (*S*)-ethyl lactate. The conversion of pyruvate for all experiments was 100 % for the duration of the hydrogenation experiment.

Pre-treatment with (*S*)-lactate for 100 min before the gas flow was diverted through the pyruvate observably suppressed the ee of (*R*)-lactate achieved. After a short transient rise the enantiomeric excess stabilised ca. 34 % after 30 min time-on-line (Fig. 5.11).

Using a racemic mixture of ethyl lactate to pre-treat the catalyst resulted in a long period of increasing enantiomeric excess (Fig. 5.11). The rise of ee covered a range from 28 % ee to ca. 42 % ee at 200 min and thereafter.

An ee of 44 % (*R*)-ethyl lactate was achieved after the pre-treatment of the catalyst bed with (*R*)-lactate (Fig. 5.11). The first injection has been omitted from the Figure as the value included material from the pre-treatment step. The experiment was repeated with an identical result. The increase of ee was longer than the transient rise associated with the standard reaction of ethyl pyruvate.



Pre-treatment of the catalyst with a mixture of 20 % (*R*)/(*S*)-ethyl lactate is displayed in Figure 5.11. The resulting ee post pre-treatment follows a similar trend to the pre-treatment with a racemic mixture. After a similarly long rise the enantiomeric excess achieved ca. 42 %.

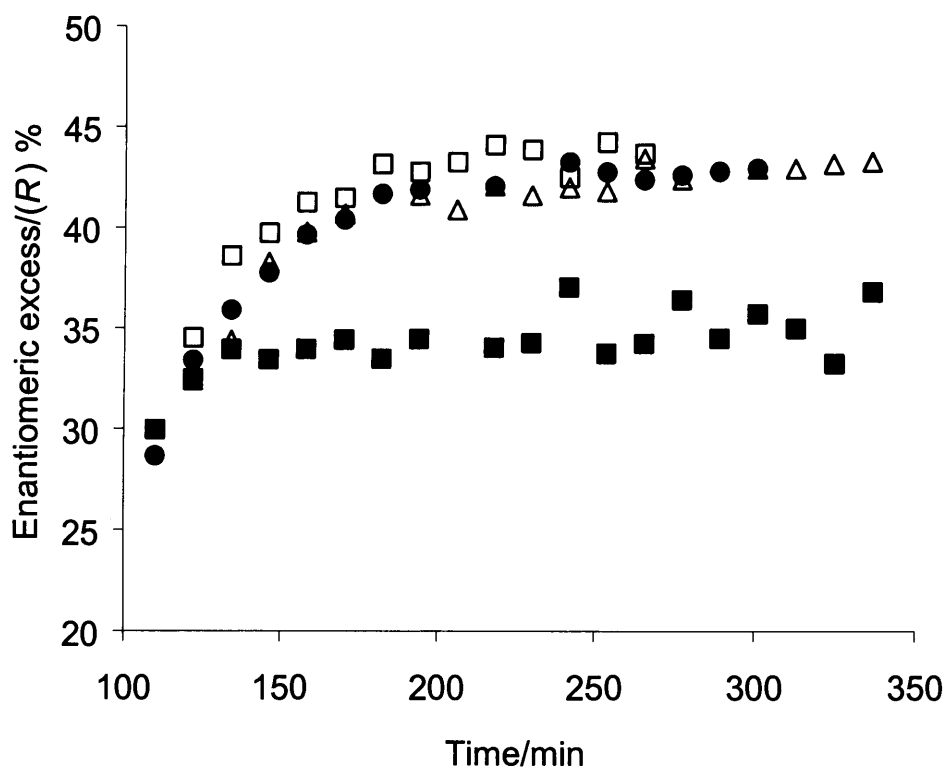


Fig. 5.11 Influence of bed pre-treatment with (*R*)-ethyl lactate (□), (*S*)-ethyl lactate (■), 20 % (*R*) in (*S*)-ethyl lactate (Δ) and racemic lactate (●) on the subsequent enantiomeric excess of (*R*)-ethyl lactate

[0.025 g *ex situ* pre-modified M01271 (3.4 mM CD); ethyl lactate/pyruvate (20°C); T = 40°C; GHSV 96000 /h]

#### 5.4 Influence of the reaction conditions on the standard reaction

Variables of the experimental protocol from the standard reaction were changed in order to further understand the hydrogenation of methyl pyruvate in the gas phase. The influence of cinchonine, furnace temperature, saturator temperature, addition of DCM to the saturator, catalyst mass and pre-modification solvent were investigated.

##### 5.4.1 Influence of alkaloid on the standard reaction

An excess of (*S*)-methyl lactate was obtained over a cinchonine (3.4 mM) pre-modified M01271 catalyst (Fig. 5.12). The ee remains steady for the duration of the reaction at ca. 19 %. The conversion remained at 100 % for the period of the 3 h time-on-line. A mixture of 1.7 mM CD and 1.7 mM CN in DCM was used to pre-modify M01271. Methyl pyruvate was hydrogenated over this modified catalyst (Fig. 5.12). Conversion was 100 % for the duration of the experiment and the enantiomeric excess was ca. 12 % (*R*)-methyl lactate.

##### 5.4.2 Influence of Furnace Temperature on the Standard Reaction

The standard reaction was carried out under different reaction temperatures. The reaction was investigated at 25 °C, 30 °C, 40 °C and 50 °C. The conversion of methyl pyruvate was 100 % for the reaction duration for the temperatures studied. A transient period of increasing enantiomeric excess was observed as illustrated in Figure 5.13. The ideal temperature of those studied was 40 °C with a maximum ee of 37 %. The maximum

observed ee at 25 °C and 30 °C was 31 % and 34 % respectively. At 50 °C the maximum ee decreases to 33 %.

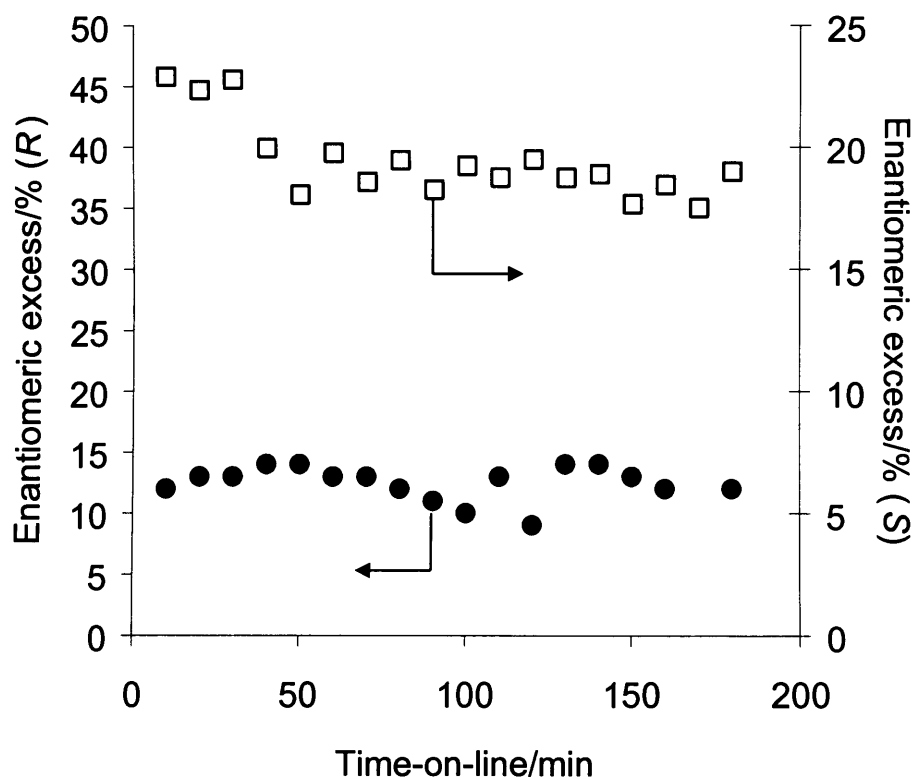


Fig. 5.12 Influence of alkaloid on the ee of methyl lactate with time-on-line: M01271 modified with cinchonine (□); 1:1 mixture of cinchonidine and cinchonine (●)

[0.025 g catalyst; pre-modified (3.4 mM) catalyst; methyl pyruvate 0.066 g/h (20°C); T = 40°C; GHSV 96000 /h]

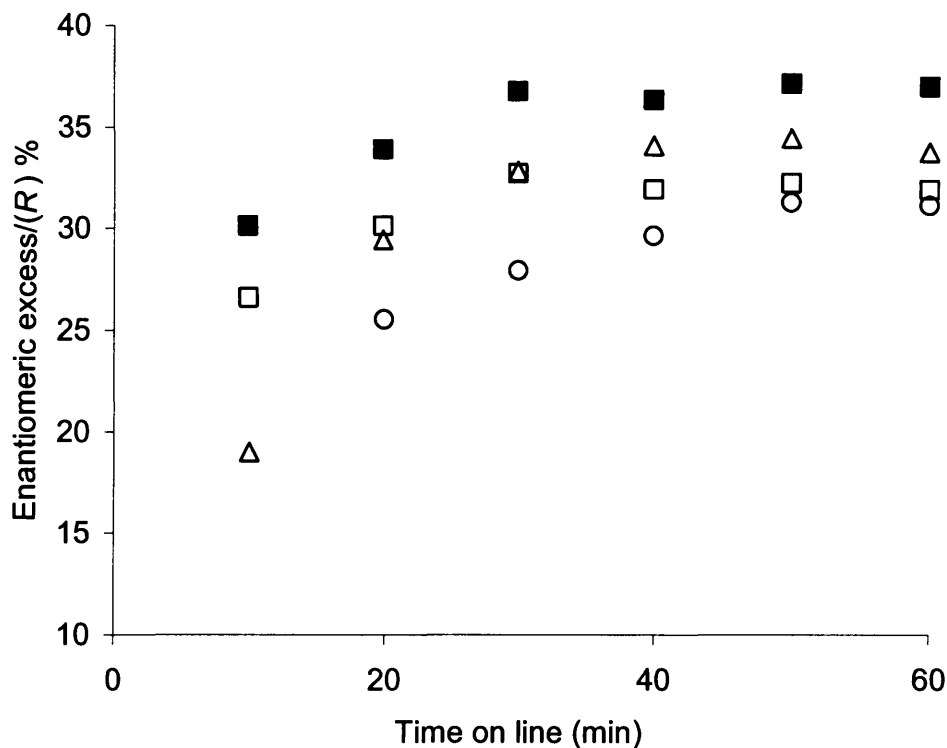


Fig. 5.13 Influence of the reaction temperature on the ee of (*R*)-methyl lactate with time-on-line. T = 25 °C (o); T = 33 °C (Δ); T = 40 °C (■); T = 50 °C (□)

[0.025 g *ex situ* pre-modified M01271 (3.4 mM CD); methyl pyruvate 0.066 g/h (20°C); T = 40 °C; GHSV 96000 /h]

#### 5.4.3 Influence of Saturator Temperature

Altering the temperature of the saturator containing the reactant varies the vapour pressure and therefore the amount of material entering the reactor (Table 5.1). A range of temperatures were investigated from 0°C to 50°C. The effect on the conversion of pyruvate (Table 5.1) and ee of (*R*)-lactate are directly related to the amount of substrate present in the feed. At low pyruvate concentrations, when the saturator is at 0°C or 20°C the conversion is

maintained for up to 3 h time-on-line. When the temperature was increased to 40°C and 50°C the conversion of pyruvate began to decrease from 30 min and 10 min time-on-line respectively.

Table 5.1 Influence of saturator temperature on rate of methyl pyruvate entering the reactor and ee of (*R*)-methyl lactate

Entry	Saturator Temp (°C)	Rate of MePy (g/h)	Maximum ee (%)
1	0	0.011	43
2	20	0.066	36
3	40	0.1375	33
4	50	0.2348	30

[0.025 g *ex situ* pre-modified M01271 (3.4 mM CD); T = 40 °C; GHSV 96000 /h]

The effect on the ee of (*R*)-methyl lactate is modest at all temperatures studied compared to the standard reaction (Table 5.1). With a saturator at 0°C an increase is observed of ca. 7 % over the reaction duration; this compared with a decrease of ca. 5 % at 50°C. In all cases a transient of increasing ee was observed, however, for temperatures higher than 20°C the ee after this period was found to be depressed.

#### 5.4.4 Addition of dichloromethane to methyl pyruvate

The action of solvent was investigated under standard reaction conditions for the enantioselective hydrogenation of methyl pyruvate. Dichloromethane was added to the

saturator containing the pyruvate and the reaction started as detailed in section 2.5. The effect on the enantiomeric excess of (*R*)-methyl lactate and conversion of pyruvate is illustrated in Fig. 5.14. The addition of DCM to the saturator appears to depress the transient period of increasing ee observed in the standard reaction. The enantiomeric excess remains stable at ca. 36 % for the duration of the experiment. Secondly the conversion of pyruvate decreases modestly over the course of the reaction to ca. 91 %.

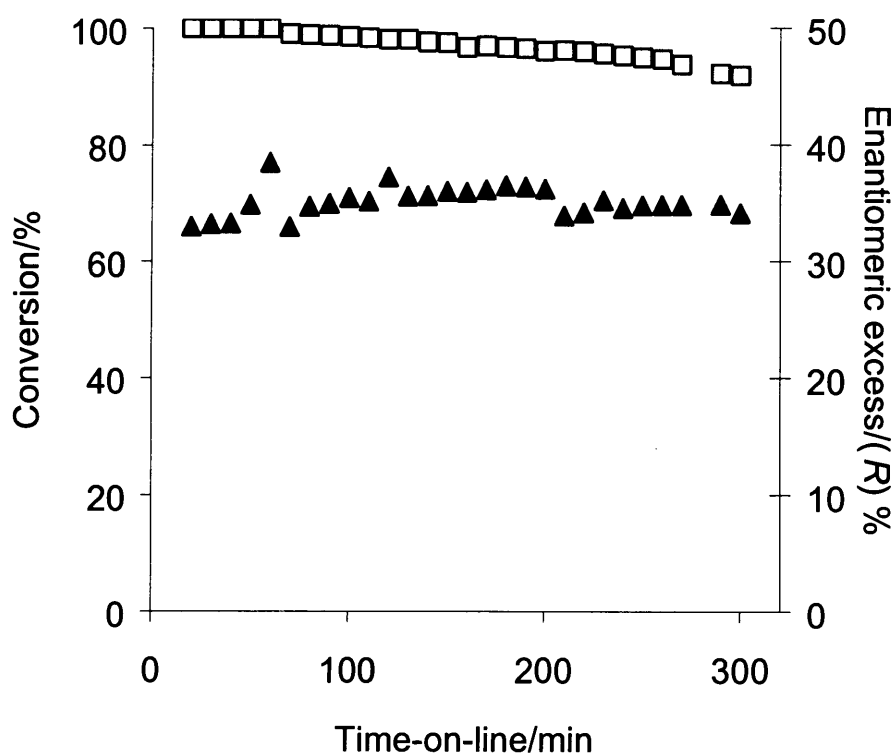


Fig. 5.14 Influence of addition of DCM to the saturator on the conversion of methyl pyruvate and ee of (*R*)-methyl lactate with time-on-line

[0.025 g *ex situ* pre-modified M01271 (3.4 mM CD); methyl pyruvate and DCM (20°C); T = 40°C; GHSV 96000 /h]

## 5.4.5 Effect of catalyst mass on the standard reaction

The effect of catalyst mass was investigated on the asymmetric hydrogenation of methyl pyruvate. Samples of pre-modified catalyst of mass 6.25 mg, 12.5 mg, 20 mg, and 25 mg were used. The samples were mixed thoroughly with a bare silica gel powder to ensure the space velocity was the same as the standard reaction. The effect on the conversion of methyl pyruvate to methyl lactate is illustrated in Figure 5.15.

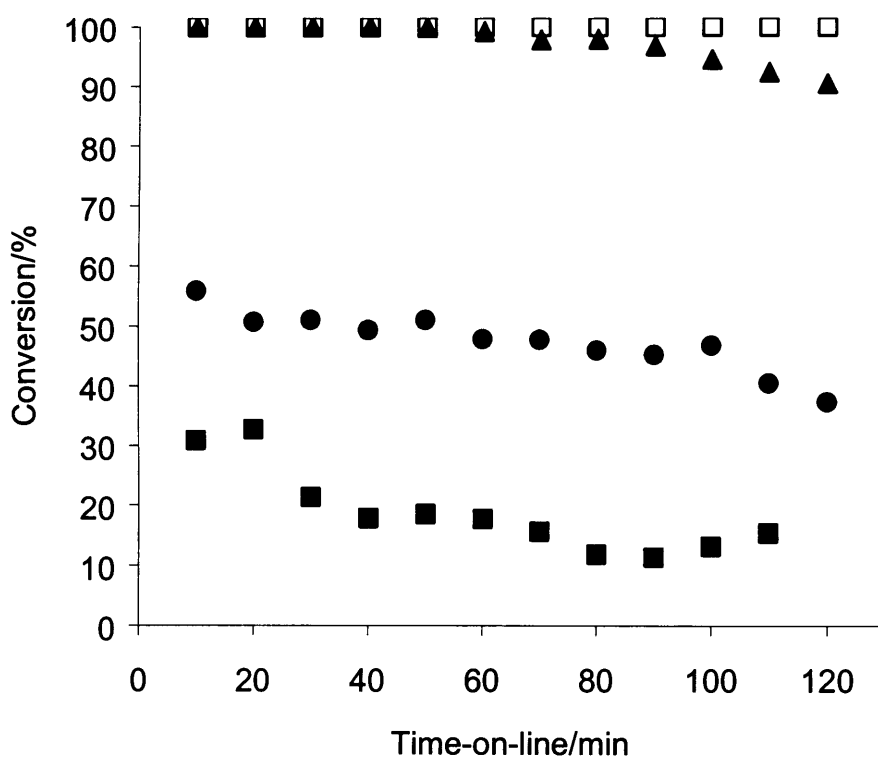


Fig. 5.15 Influence of catalyst mass in the bed on the conversion of methyl pyruvate: 25 mg (□); 20 mg (▲); 12.5 mg (●); 6.25 mg (■)

[0.025 g *ex situ* pre-modified M01271 (3.4 mM CD); methyl pyruvate 0.066 g/h (20°C); T = 40°C; GHSV 96000 /h]

Decreasing the mass from 25 mg to 20 mg causes the conversion to decrease steadily at 60 minutes from 100 %. Further decreases in catalyst mass exhibit step wise drops in conversion. With 12.5 mg of catalyst the conversion is approx 45 % and shows a modest decrease over the reaction period. The conversion with 6.25 mg of catalyst is approx 20 % over the reaction period, however, is less stable.

#### 5.4.6 Influence of pre-modification solvent on the standard reaction

The solvent used in the pre-modification of the catalyst with cinchonidine for the gas phase hydrogenation of methyl pyruvate was investigated. The solvents chosen were: DCM, toluene, ethanol and acetic acid. Hydrogenation over the pre-modified catalysts gave 100 % methyl pyruvate conversion over the 3 h reaction; however, there were significant differences in the behaviour of the ee of (*R*)-lactate (Fig. 5.16).

With dichloromethane or toluene as pre-modification solvents, the ee was relatively stable after the first hour at *ca.* 35 %. Conversely using ethanol or acetic acid as pre-modification solvents resulted in an initially higher ee of *ca.* 40 %. However, the ee became unstable after the first hour of the reaction and decreased. Where ethanol was used in the pre-modification solution this instability occurs earlier at *ca.* 40 minutes. All however, exhibited an initial transient period of increasing enantiomeric excess.



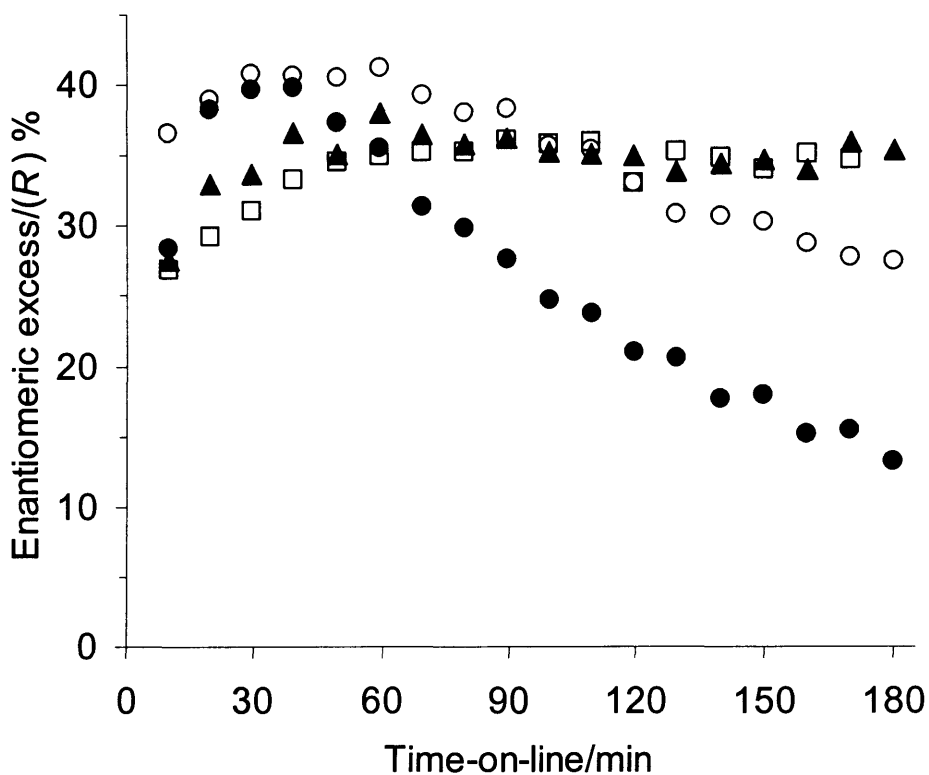


Fig. 5.16 Influence of the pre-modification solvent on the enantiomeric excess of (*R*)-methyl lactate: DCM (□); toluene (▲); EtOH (●); AcOH (○)

[0.025 g *ex situ* pre-modified M01271 (3.4 mM CD); methyl pyruvate 0.066 g/h (20°C); T = 40°C; GHSV 96000 /h]

## 5.5 Discussion

### 5.5.1 Justification of hydrogenation at the gas/solid interface

Enantioselective hydrogenation at the gas/solid interface has been rarely reported [3,4]. Investigations prior to the work reported here have involved micro-porous zeolites

under conditions where capillary condensation of the reactants may have occurred. To ensure that this phenomenon was not present for the hydrogenation of pyruvate esters over the supplied porous catalysts two steps were taken: Firstly, using the Kelvin equation (equation 2.3) to determine whether the experimental conditions would facilitate such condensation [2 *Supplementary Data*]; secondly, to prepare a catalyst without an intra-particle pore structure and repeat the standard reaction.

The Kelvin equation relates the vapour pressure in a pore in which the meniscus radius is to the surface tension and molar volume of the liquid. This equation is used in the B.E.T calculation of surface area of a solid. The Meniscus radius is taken as the pore radius as no measurement of the contact angle of methyl pyruvate could be obtained. Using the density of methyl pyruvate at 25°C (1.13 g/mol) the molar density of the liquid is therefore, given as 90.3 ml/mol. The surface tension of methyl pyruvate was assumed to be 35 mN/m from measurements of pent-3-one (25 mN/m) and ethyl diol (45 mN/m). A plot of partial pressure at 40°C (standard reaction temperature) vs. pore radius could then be completed (Appendix 7.10). Such that with a pore radius of ca. 40 Å the vapour pressure will be halved. The vapour pressure of methyl pyruvate was measured at 0, 10, 20, 30 and 40°C with a device described in section 2.7. Thus the partial pressure at the reaction temperature of 40°C was estimated to be 130 Torr or 0.17 atm (Appendix 7.11). Under reaction conditions  $p/p^{\circ} = 0.019$ , i.e. the experimental partial pressure of pyruvate is a factor of ca. 50 below the normal vapour pressure and would require a pore radius of less than 5 Å to condense (Appendix 7.10). The catalyst M01271 has a pore radius of 30.5 Å (Table 2.2) with negligible pores  $\leq 5$  Å. Hence this data confirm the reaction occurs at the gas/solid interface.

The preparation of the  $\alpha$ -Alumina support and subsequently the 1 % Pt/ $\alpha$ -Alumina catalyst is detailed in section 2.1.1.4. The absence of any intra-particle pore structure confirmed that the enantioselective hydrogenation of methyl pyruvate was occurring at the

gas/solid interface (Fig. 5.4). The enantiomeric excess of (*R*)-methyl lactate achieved ca. 25 % which persisted for 5 h time-on-line.

### 5.5.2 2,3-butanedione hydrogenation

The enantioselective gas-phase hydrogenation of 2,3-butanedione was not very successful in terms of reaction longevity or high conversion. However, the results obtained have provided information which may be useful to interpret aspects of reaction where solvent is present and general catalyst morphology.

In all reactions involving the dione over un-modified and alkaloid modified platinum the amount of product decreases with time-on-line (Fig. 5.1). This phenomenon is more pronounced over the unmodified M01271 catalyst compared to modified EUROPT-1. The reaction is unable to proceed further than 60 minutes time-on-line in the case of the unmodified catalyst. This can be ascribed to saturation of the active metal surface with dione and other higher mass species. The strength of adsorption of dione is compounded by the absence of solvent and does not desorb readily. However, where alkaloid is present the reaction proceeds for a further 80 minutes time-on-line in the case of the pre-modified catalyst. Indicating that a form of rate enhancement of the first stage reaction is afforded by alkaloid modification, as the adsorption strength of the hydroxyketone is less than the dione. This may be exacerbated by the morphology of the platinum particles on M01271. From the results of the autoclave studies this catalyst was deemed to have a greater 3D character, with higher index planes (Table 3.8) when compared to EUROPT-1. The results over EUROPT-1 suggest that the Pt particles have a flat morphology. This benefits the removal of un-reacted dione and hydroxyketone from more reactive sites, thus extending the life of the catalyst (Fig. 5.1). The high rate of dione hydrogenation observed in solvent over EUROPT-1

compared to M01271 under the same conditions (Fig. 3.2) infers that the ability to transport un-reacted material away from the active surface is clearly advantageous. EUROPT-1 facilitates this transport under competition of reacting species and solvent or other reactants.

The enantiomeric excess achieved by both pre-modified M01271 and EUROPT-1 of ca. 15 %, but was unstable, however persisted at this approximate value until no product was detected. Therefore, the connection between conversion and ee, typically observed in autoclave investigations is lost [5]. In the absence of solvent the enantioselective site is maintained, while the surrounding non-selective i.e. racemic sites are poisoned by reactant or higher mass products. This phenomenon will be discussed further with reference to the results of pyruvate hydrogenation.

### 5.5.2 Pyruvate ester hydrogenation

The unsuccessful hydrogenation of 2,3-butanedione prompted a more thorough investigation of the gas-phase hydrogenation of the pyruvate esters; methyl and ethyl pyruvate. Methyl pyruvate was used as the reactant for the standard reaction over M01271 pre-modified *ex situ* with 3.4 mM solution of cinchonidine in DCM. The results of this reaction yielded 100 % conversion and an ee of ca. 36 % at 40°C with a saturator temperature of 20°C (Table 5.1). Over an un-modified catalyst the conversion of pyruvate was 100% to a racemic mixture of (*R*)/(*S*)-lactate. The significance of this result is put in to context when compared to the results obtained over the prepared 1 % Pt/ $\alpha$ -Alumina. The unmodified catalyst yields a higher conversion of pyruvate than that of the modified catalyst. This infers that the presence of alkaloid in this reaction provides no rate enhancement and serves to inhibit the overall reaction. However, the increased dispersion and metal surface area of the 2.5 % Pt/Silica achieves complete conversion of pyruvate with or without

modifier. When compared to the hydrogenation of dione where the presence of alkaloid is beneficial for enantioselective hydrogenation.

Table 5.2 Values of conversion and enantiomeric excess of the standard reaction

Entry	Catalyst	Pre-modification solution (Alkaloid) {concentration/mM}	Substrate	Conversion (%)	Maximum ee (%)
1	M01271	(CD) {3.4}	2,3-B	64	20
2	M01271	(CD) {3.4}	MePy	100	37
3	M01271	(CN) {3.4}	MePy	100	19 <sup>c</sup>
4	M01271	(CD) {3.4}	EtPy	100	35
5	1 % Pt/ $\alpha$ - Alumina <sup>a</sup>	(CD) {0.34}	MePy	78 <sup>b</sup>	26
6	5 % Pt/Alumina	(CD) {3.4}	MePy	100 <sup>b</sup>	30
7	EUROPT-1	(CD) {3.4}	MePy	100	43

<sup>b</sup> = conversion decreased with time-on-line; <sup>c</sup> = (*S*)-methyl lactate

[0.025 g catalyst (<sup>a</sup> = 0.050 g); pre-modified in DCM; substrate 20°C; GHSV 96000 /h; T = 40°C]

The opposite is observed with pyruvate, where hydrogenation can be said to be poisoned by cinchonidine. However, the reaction of both pyruvate and dione on the platinum are similar. In both cases there exists enantio- and non-selective sites which, in the absence of solvent are effectively equal. Where solvent is present the hydrogenation of pyruvate occurs primarily at the enantioselective site. Hence the large rate enhancement associated with cinchonidine modified platinum compared to un-modified platinum. The rate

enhancement afforded by alkaloid addition in dione hydrogenation is typically much smaller. Indicating racemic sites are closer in energy to the enantioselective sites in the presence of dione. Thus a model may be put forward to interpret the results obtained (Fig. 5.17).

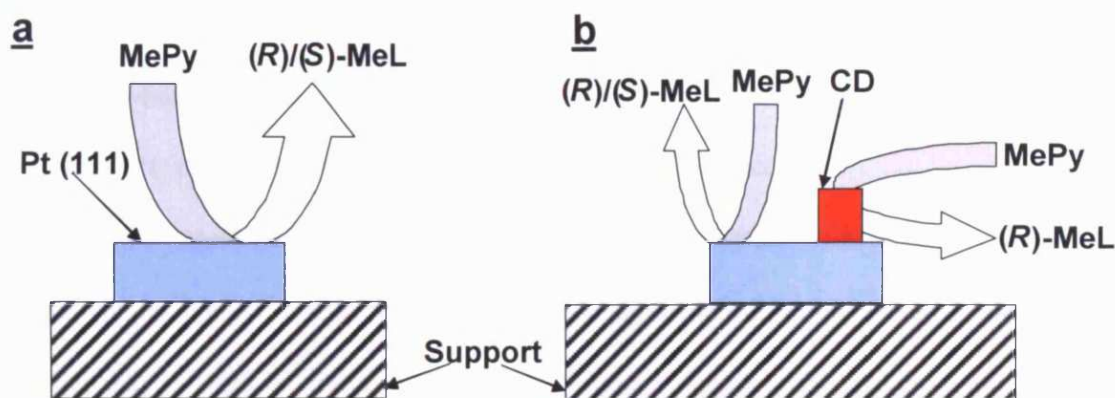


Fig. 5.17 Schematic representation of the proposed model of gas-phase hydrogenation of pro-chiral carbonyl containing compounds; MePy : methyl pyruvate; MeL : methyl lactate;

CD : cinchonidine

The model for the un-modified catalyst (Fig. 5.17a) indicates that the platinum crystal supports 100 % hydrogenation of the pyruvate molecules that adsorb to racemic lactate. The addition of a modifier molecule; cinchonidine, does not inhibit the total conversion of pyruvate, however, imposes enantioselection upon the product at that site. Thus the enantiomeric excess can be said to be close to 100 % to (*R*)-lactate in this case similar to the liquid phase reactions [6]. With the near enantiomer cinchonine a similar level of selection should be achieved in favour of the (*S*)-lactate. Therefore, the combination of the products from the modified and un-modified sites return a lower value; in this case ca. 36 % or just over 2 to 1, (*R*) to (*S*).

Hydrogenation of 2,3-butanedione over the model system would return values of enantiomeric excess only seen during kinetic resolution in the liquid phase and 100 %

conversion. However, this is not the case as the maximum ee was ca. 20 % and the conversion decreases with time-on-line from ca. 75 %. Here the assumption that model system are built from are exposed as the conversion of 2,3-butanedione does not occur rapidly. Due to the strength of adsorption exhibited by the dione on the surface of the platinum, which becomes easily saturated. Hence the experimental caveat that the saturator be kept at 0°C to limit the amount of material entering the reactor.

The model system has a proposed platinum crystal with a flat, planar (111) morphology. Upon this plane there is space for only two modifiers to adsorb. This is clearly not the case with a real world system, where kinks and step sites are abundant, leading to many index planes. Comparison of EUROPT-1 and M01271 have yielded strong evidence that the morphology of the platinum crystals are very different. The reference catalyst EUROPT-1 is known to have a relatively flat crystal existing in predominately (111) configuration [7]. This is closer to the model system than the M01271 catalyst which has been suggested to have a particle of 3D character with higher index planes. This is supported by the high activity towards cyclohexene hydrogenation (Table 3.8) and the low rate of 2,3-butanedione hydrogenation (Table 3.5).

The enantiomeric excess achieved over the model system should be stable and consistent from the start of the reaction. This is observed with the hydrogenation of methyl pyruvate over EUROPT-1, yet not over M01271. The existence of an initial transient of rising ee over M01271 has been commonly observed in the liquid phase [8-12]. Explanations to the origin of this phenomenon have been suggested, however, there is no definite edict. Of these postulations two are relevant; these include removal of surface impurities at the enantioselective site [10] and conformation change of the modifier [11]. The former theory has credence in the gas phase system as the absence of solvent requires the reactant to remove surface impurities. This process, however, can be reasoned to occur rapidly due to

the total conversion of pyruvate from the start of the reaction. The relatively slow increase of ee infers that for this theory to hold true the impurities would have to be, therefore, local to the enantioselective site. The later theory involving a conformational change of the alkaloid on the surface could account for the transient rise of ee. Adsorption of cinchonidine occurs during the pre-modification stage in a solvent. Modifier dissolved in the solvent would exist predominately in one of the four conformations described in Chapter 1. The model system assumes that this conformation is 100 % *open 3* and that adsorption is via the quinoline ring system. However, in the real system this is unlikely to be the case, rather the conformation changes *in situ* to resemble the model system. Hence why the enantiomeric excess reaches a level and no further increase is observed. The time scale of this change, however, would be ca. 50 minutes, which appears counter intuitive with respect to molecular dynamics.

Additionally the model system assumes that rotation about the C8 C9 bond and therefore, the quinuclidine moiety is restricted; *a static system*. The absence of solvent which is accepted as holding cinchonidine in a conformation, should allow the adsorbed modifier to rotate freely. This infers that the modifier can exist in the two conformations corresponding to the way the ring system is adsorbed, at any time (i.e. *closed 1* and *open 3* or *closed 2* and *open 4*). It has been reported that no enantioselective reaction can occur in which the conformation is *closed 1* or *closed 2*, as the quinuclidine moiety is unavailable to interact with the pyruvate. Therefore, to achieve efficient enantioselection the modifier must be forced in to an *open 3* conformation or similar. Under reaction conditions the interaction of an *open 3* modifier and pyruvate at the platinum surface may be thermodynamically favourable. Such that the modifier would adopt this conformation, as opposed to rotating about the C8 and C9 bond. Thus the adsorption of reactant in the enantioselective site would encounter all adsorbed cinchonidine molecules in the *open 3* conformation corresponding to the end of the transient rise of ee.



To investigate this phenomenon a number of experiments were conducted involving by-passing the saturator containing the reactant and reacting methyl pyruvate followed by ethyl pyruvate and *visa versa*. The effect of diverting the gas feed from the saturator is illustrated in Figure 5.6; breaks of 20, 40 and 60 minutes were employed. Following the breaks of 20 and 40 minutes a transient rise of the ee of (*R*)-methyl lactate was observed. This suggests that the modifier has reverted to a state similar to that at the start of the reaction. The re-introduction of reactant and the subsequent interaction with the modifier instigate the conformational restriction observed just before the diversion. In the case of the 20 minute by-pass this proves beneficial as after the transient rise, the value of the ee increases ca. 3 %. After the interval from pyruvate of 60 minutes the ee showed no rise and was unstable. The action of hydrogen on the modifier; partial hydrogenation for example may be the cause.

Reactions of methyl pyruvate following ethyl pyruvate were carried out to obtain further information on the enantioselective site (Fig. 5.7). Hydrogenating the smaller methyl pyruvate after ethyl pyruvate and *visa versa* would highlight if the enantioselective site is specific to one reactant. When methyl pyruvate is substituted by ethyl pyruvate the resulting ee of the (*R*)-ethyl lactate with time-on-line is very different compared to the standard reaction with ethyl pyruvate. The enantiomeric excess increases slowly, however, does not achieve a similar value as with the standard reaction. To a similar extent the hydrogenation of methyl pyruvate is influenced by the prior ethyl pyruvate hydrogenation. However, in this case the ee is higher from the introduction of the smaller substrate. The suppositions of these experiments are that the enantioselective site is specific and is not transformed to the optimum arrangement rapidly.

Investigations in the liquid phase performed in an autoclave which involved an injection of ethyl or methyl pyruvate to a reaction of methyl or ethyl pyruvate has been

reported [11]. The ee of methyl lactate enhanced when ethyl pyruvate had been completely hydrogenated. The opposite experiment gave no ee enhancement for ethyl lactate reacting after methyl pyruvate. These sets of experiments were repeated in the gas phase under standard reaction conditions. In both cases the effect on the ee of the primary reaction after introduction of the other reactant was a rapid drop to a value similar to the start of the reaction. Additionally in both cases recovery to the value prior to introduction was similar to the time scale of the original transient rise. This behaviour suggests that the enantioselective site becomes disorganized in the presence of the introduced species. In effect the modifier may be forced to switch between two conformations to accommodate both the new and previously reacting species. The effect of this switching is seen in the slow increase of the ee for both species. The implication of this phenomenon is that the enantioselective site is highly specific in the gas phase, as with the liquid phase.

The results from the experiment involving both methyl and ethyl pyruvate, hydrogenating concurrently give credence to this theory (Fig. 5.10). Compared to the corresponding exclusive reactions the enantiomeric excess achieved was unstable. This indicates that the enantioselective site is able to change conformation, however, at the expense of the ee. There is a case for an enantioselective site with a 'memory'; that is the incoming reactants are affected by the previous reactant effect on the modifier. Such that methyl pyruvate following ethyl pyruvate would require a change for the modifier and visa versa, the ee may be impaired as a result of the time spent for this correction. As the racemic reaction would proceed un-hindered, thus resulting in the modest instability of the ee.

Pre-treatment with lactates of the modified catalyst bed was conducted with the aim of further understanding the enantioselective site. Similar experiments were carried out in the liquid phase by Li *et al.* [11]. These involved the addition of (*R*), (*S*), and a racemic mixture of methyl lactate to the pre-modification solution in a 1:1 molar ratio with

cinchonidine. Additionally methyl lactates were added to the reaction solution of ethyl pyruvate. The influence of the addition of these lactates in the pre-modification step was negligible on either rate or ee. Addition of lactates in the reaction solution afforded little effect upon the ee of ethyl lactate, regardless of the chirality of the additive. However, the initial rate was influenced by the chirality of the methyl lactate additive. Addition of (*S*)-lactate afforded a slight enhancement, conversely the addition of (*R*)-lactate caused a slight decrease. The initial rate was greatly reduced by addition of the racemic lactate. The results were attributed to competitive adsorption at the enantioselective site, in the case of addition of (*R*)-lactate. However, further explanation for the results of (*S*)-lactate and the racemic mixture were not forthcoming due to the increased complexity of the system.

For the gas-phase reactions the pre-treatment period was for 100 minutes and the lactates used were: (*R*), (*S*), a mixture of 20 % (*R*) in (*S*) and a racemic mixture. The influence of this procedure on the ee of the hydrogenation of ethyl pyruvate is illustrated in Figure 5.11. Compared to the ee achieved over un-treated M01271, pre-treatment with (*R*)-ethyl lactate or a mixture containing (*R*)-ethyl lactate was beneficial, with an improvement of ca. 5-8 %. The transient of increasing ee that is present was twice the time period compared to the standard reaction. The time scale of the rise in the ee with time-on-line. Pre-treatment with (*S*)-ethyl lactate resulted in a modest drop in the ee of the hydrogenated species of ca. 2 %. These results add another dimension to the gas-phase hydrogenation of pyruvate; there exists a strong, lasting influence by the product on the enantioselective site. The product must interact with the modifier and/or platinum surface such that the incoming reactant would preferentially adsorb in the enantioselective site. The overall ee can be said to be enhanced modestly due to this increased preference to react at an altered enantioselective site, over a racemic site. Blocking sites by the adsorption of the product can be dismissed, as the on-line GC analysis of the pre-treatment period indicated otherwise.

#### 5.5.4 The Influence of pre-modification conditions on the standard reaction

##### 5.5.4.1 Pre-modification modifier concentration

The concentration of cinchonidine alkaloid in the pre-modification step was investigated with the standard reaction (Fig. 5.12). The pre-modification solution contained 0.34 mM of cinchonidine in DCM. Interestingly the ee was initially higher at ca. 37 %, which decreased with time-on-line to 0 % and no rise was observed with the standard reaction. The lower amount of modifier at the surface would be expected to function similar to that of the higher amount in the gas phase. At lower overall values of enantiomeric excess according to the proposed model. At this low cinchonidine coverage, which is initially equal to that of the standard reaction in terms of ee, the enantioselective site is clearly damaged thereafter. Interpretation of the results suggests that cinchonidine may be hydrogenated at the quinoline ring, consequently the decrease of ee is observed.

Hydrogenation of the quinoline ring system of the cinchonidine molecule has been shown to inhibit enantioselective hydrogenation. The accepted model in the liquid phase requires cinchonidine to adsorb flat via this ring system for high ee. At high temperatures the angle of the ring system to the platinum surface is increased, which is accompanied by a reduction in ee [13]. Partial hydrogenation of the quinoline ring system has a similar effect by increasing the angle of adsorption to the surface [14]. However, in stirred tank reactors this can be over come through replacement of fresh modifier from the liquid phase. The results in the gas phase infer that the without replacement of fresh alkaloid the ee is unable to remain at a stable level as enjoyed by the standard reaction. Indeed the origin of the transient rise in ee may occur due to removal of damaged modifier from the surface of the platinum to the support. Replacement may be due to migrating cinchonidine species from the

support. An exchange equilibrium may therefore, be in effect where surface modifier concentration persists as with the liquid phase reaction.

#### 5.5.4.2 Influence of the pre-modification solvent

The influence of solvent on the Orito reaction has been extensively investigated in the liquid phase in stirred tank reactors [15]. The influence of solvent on the enantiomeric excess and rate in the liquid phase is significant and can be linked to the dielectric constant of the solvent. Generally the lower the dielectric constant of the solvent the higher the ee; with the exception of acetic acid. Solvent choice has been investigated over M01271 (Fig. 3.9) in the autoclave and over M02023 (Fig. 4.9) with the hydrogenation of methyl pyruvate in the trickle-bed reactor. The solvents investigated with the standard reaction in the gas phase were as follows; DCM (standard reaction), toluene, ethanol and acetic acid. Investigations in the literature with liquid phase reactions have focused on the pre-modification solvent vs. the reaction solvent [16]. The effect was clear; that the pre-modification solvent did not influence the outcome of the reaction. It was concluded that any effect would be lost when the catalyst came into contact with the reaction solvent.

During the pre-modification step the cinchonidine modifier was dissolved in these solvents and added to the catalyst and then stirred. The influence on the ee of (*R*)-methyl lactate is illustrated in Figure 5.16.

Where toluene was used in the pre-modification step the influence on the ee was similar to when DCM had been used. A transient of increasing ee is observed which lasts for the same period of time as with the DCM reaction which then reaches a similar value; ca. 36%. The dielectric constant of toluene is given as 2.4, a low constant has been linked to the higher abundance of the *open 3* conformation of cinchonidine in solution [17].

Dichloromethane has a dielectric constant of 8.9, a similar low value which may be used to rationalise the similar results after the transient period of increasing ee. During this transient period the higher values of ee observed where toluene was used suggests that an increased abundance of *open 3* CD existed at the surface. However, the modifier reverts back to the most favourable reaction conformation thereafter, as seen in the case of the reaction with DCM as pre-modification solvent.

Using ethanol as the pre-modification solvent resulted in a striking loss of the ee of (*R*)-methyl lactate at 40 minutes time-on-line. Additionally, prior to 40 minutes time-on-line the enantiomeric excess increased rapidly from 28 % ca. 40 %. However, the conversion remained 100 % for the duration of the experiment. Experiments carried out in the liquid phase have shown that while the rate has been high, the ee achieved was low [12]. This phenomenon was rationalized by linking the dielectric constant of ethanol; 25.3 to the proportion of *open 3* cinchonidine present in solution. Solvents with high dielectric constants tend to stabilise the closed conformers. However, the observed results suggest a different reaction dynamic may be occurring.

The use of dielectric constants of solvents used in liquid phase reactions to justify the observed results can not be applied to gas-phase reactions as profitably. It may be more beneficial in this case to elucidate from the results of both the use of ethanol and acetic acid in the pre-modification step a different postulation.

When acetic acid was used as the solvent in the pre-modification step the influence on the ee of (*R*)-methyl lactate with time-on-line is similar to using ethanol. There exists a rapid increase of the ee, which then is stable for a short period at ca. 42 % before decreasing thereafter to ca. 25 % at 3 h time-on-line. As with the results from the use of ethanol as pre-modification solvent, the conversion is 100 % for the reaction duration. The initially high ee achieved infer that during the pre-modification stirring the basic cinchonidine has reacted

with the strongly acidic acetic acid and the weakly acidic ethanol. This results in the protonation of the quinuclidine moiety, associated with the adsorbed *open 3* conformation. The remaining species may not be removed from the metal surface during the filtering and vacuum drying step. Thus during the reaction these species may interact with the reactant and/or the enantioselective site. Such that initially the protonation of the quinuclidine ring is advantageous for the modest improvement in the ee observed. However, the by-products from this incidence appear to be detrimental to the long-term stability of the enantiomeric excess.

#### 5.5.4.3 Influence of alkaloid

Changing the alkaloid modifier of the standard reaction to cinchonine resulted in the expected sense of enantiomeric excess of (*S*)-methyl lactate. However, the ee was lower than over the cinchonidine modified catalyst at ca. 20 % (Fig. 5.12). This result was confirmed by the hydrogenation of methyl pyruvate over M01271 modified with a solution of equal parts cinchonidine and cinchonine. The enantiomeric excess achieved was modest at ca. 12 %, however, to (*R*)-methyl lactate.

Reactions conducted in the liquid phase with cinchonine have shown comparable results to results over cinchonidine modified Pt/Silica catalyst in ethanol [18]. Where a mixture has been applied to the catalyst the ee achieved has been close to 0 % or very low to (*R*)-lactate. Therefore, the value achieved in the gas phase for CN and the CD:CN mixture are interesting. The result implies that the cinchonidine enantioselective site is favoured by the incoming pyruvate molecule in the gas-phase reactions. Thus the enantiofacial adsorption of the pyruvate ester which reacts to form the (*R*)-lactate is energetically preferred.

#### 5.5.4.4 Influence of the reaction temperature and saturator temperature

The temperature of the reactor and the saturator are of particular importance in reactions involving a reactant vapour and porous catalyst. For a reaction of a particular substrate to occur at the gas/solid interface successfully, both reactor and saturator temperatures have to be balanced. However, the Orito reaction is limited to a maximum temperature in the liquid phase of 50-60°C. For temperature increases above ca. 35°C there is a step-wise decrease in the ee of (*R*)-lactate achieved. The effect of temperature on the adsorption mode of cinchonidine on platinum is well known [13]. The angle of adsorption of the quinoline ring system increases at elevated temperatures, such that enantioselection is impaired. The enantioselective hydrogenation of methyl pyruvate in the gas phase has been reported to occur up to 60°C over 5 % Pt/Alumina, with an ee of 40 % compared to 35 % in the liquid phase [2]. Reported in section 5.5.2 is an ee of 32 % of (*R*)-methyl lactate over 2.5 % Pt/Silica at 50°C. At lower reaction temperatures the ee is impaired to a greater extent; ca. 27 % at 25°C. However, both reactions were conducted with a saturator temperature of 20°C. The influence of the saturator temperature of the ee of (*R*)-methyl lactate is illustrated in Table 5.1. With a low saturator temperature the amount of material entering the reactor is reduced. Interestingly there is an enhancement of the ee with a saturator temperature of 0°C which can be tentatively linked to the preferential hydrogenation at the enantioselective site. The reduced amount of material at the surface of the platinum may permit greater reactant migration, to locate the enantioselective site. Therefore, at lower reaction temperatures it would be beneficial to lower the saturator temperature to ensure a successful reaction at the gas/solid interface. Indeed if conditions permit it would be advantageous to conduct the reaction at lower temperatures; 0-10°C. In the liquid phase lower reaction temperatures have



enhanced the enantiomeric excess achieved [19]. Thus if the saturator temperature could be lowered accordingly, a similar enhancement may be afforded in the gas phase.

#### 5.5.4.5 Effect of catalyst mass on the standard reaction

A series of experiments were conducted to determine whether the standard reaction was dominated by diffusion limitations. The catalyst mass was increased from 6.25 mg to 25 mg with the remaining bed mass provided by bare silica gel for consistent space velocity. The conversion of pyruvate increased with increasing catalyst mass. A value of moles of pyruvate converted per hour per gram of catalyst could then be calculated. This yielded a value of ca. 0.025 mol/h/g<sub>cat</sub> for the different masses used. Therefore, the reaction can be said to be operating without diffusion control.

#### 5.5.4.6 Influence of solvent addition to the saturator on the standard reaction

The addition of dichloromethane to the saturator containing methyl pyruvate was shown to influence both the conversion and ee of the standard reaction (Fig. 5.14). The conversion of pyruvate decreased modestly over the course of the reaction. The enantiomeric excess increased slowly from the start of the reaction to values comparable to those from the standard reaction. The results suggest that the DCM is competing for adsorption sites with the pyruvate. Competitive adsorption at the enantioselective site, can be said to disrupt the time required to improve the ee, compared to the standard reaction. The ee does increase, however, which indicates that the origin of the transient rise is not due to removal of surface impurities. The solvent has a much higher vapour pressure than pyruvate at 20°C, such that the amount of material analysed at the start of the reaction is greater by a factor of over 10

compared to the end. The increase in enantiomeric excess can be shown to increase with time-on-line during the decrease of DCM in the feed.

## 5.6 Conclusions

In this investigation pro-chiral C=O containing compounds were enantioselectively hydrogenated at the gas/solid interface. Several experimental variables were studied along with an examination of the enantioselective site of the cinchona modifier adsorbed on the platinum surface.

(9) Confirmed that the hydrogenation of pyruvate esters occurs at the gas/solid interface with the use of the Kelvin equation to estimate the effective partial pressure for condensation as a function of pore radius. Reactions over a prepared 1 % Pt/ $\alpha$ -alumina catalyst which has no intra-particle pores structure substantiate this claim.

(10) Cinchonidine is a poison in the gas-phase enantioselective hydrogenation of pyruvate esters, however, appears beneficial with dione reactions. Higher conversion of pyruvate was achieved over un-modified 1 % Pt/ $\alpha$ -alumina when compared to the pre-modified equivalent.

(11) Using methyl and ethyl pyruvate and lactates to investigate the enantioselective site present on the metal surface in the gas phase elucidated the following; (a) the enantioselective site is specific to the reactant's size/morphology, (b) adsorption of the lactate product as a catalyst pre-treatment can influence the

enantioselective site, (c) the enantioselective site is not static and requires time to regain the maximum enantioselectivity following a break of reactant flow.

(12) The outcome of the gas-phase reaction of pyruvate esters and 2,3-butanedione is very dependent on the reaction conditions. Principally the reaction temperature and temperature of the saturator containing the reactant. Additionally the pre-modification solvent and the alkaloid modifier used are important variables.

(13) Similar to liquid phase reactions of pyruvate over modified platinum catalysts, a transient of increasing enantiomeric excess was observed. However, this phenomenon is linked to the increasing conversion with time in the liquid phase. In the gas-phase the increasing ee with conversion is decoupled.

(14) Results from the experiments involving 2,3-butanedione over M01271 and EUROPT-1 further developed the theory that the platinum particle on M01271 has greater 3D character.

## 5.6 References

1. M. von Arx and G.J. Hutchings, *New J. Chem.*, **27** (2003) 1367.
2. M. von Arx, N.F. Dummer, D.J. Willock, S.H. Taylor, R.P.K. Wells, P.B. Wells and G.J. Hutchings, *J. Chem. Soc. Chem. Commun.*, (2003) 1926.
3. S. Feast, D. Bethell, P.C.B. Page, F. King, C.H. Rochester, M.R.H. Siddiqui, D.J. Willock and G.J. Hutchings, *J. Chem. Soc. Chem. Commun.*, (1995) 2409.
4. A. López-Martínez and M.A. Keane, *J. Mol. Catal. A: Chem.*, **153** (2000) 257.

5. M. Garland and H.-U. Blaser, *J. Am. Chem. Soc.*, **112** (1990) 7048.
6. B. Török, K. Balázsik, M. Török, Gy. Szöllösi and M. Bartók, *Ultrasonics Sonochem.*, **7** (2000) 151.
7. S.D Jackson, M.B.T. Keegan, G.D. McLellan, P.A. Meheux, R.B. Moyes, G. Webb, P.B. Wells, R. Whyman and J. Willis, Preparation of Catalysts V (G. Ponchelot, P.A. Jacobs, P. Grange and B. Delmon, Eds. Elsevier, Amsterdam, 1991), p.211.
8. (a) I.M. Sutherland, A. Ibbotson, R.B. Moyes and P.B. Wells, *J. Catal.*, **125** (1990) 77.;  
(b) P. Meheux, A. Ibboston and P.B. Wells, *J. Catal.*, **128** (1991) 441.
9. (a) Y. Sun, J. Wang, C. LeBlond, R.N. Landau and D.G. Blackmond, *J. Catal.*, **161** (1996) 752.; (b) U.K. Singh, R.N. Landau, Y. Sun, C. LeBlond, D.G. Blackmond, S.K. Tanielyan and R.L. Augustine, *J. Catal.*, **154** (1995) 91.
10. T. Mallet, Z. Bodnar, B. Minder, K. Borszky and A. Baiker, *J. Catal.*, **168** (1997) 183.
11. X. Li, R.P.K. Wells, P.B. Wells and G.J. Hutchings, *J. Catal.*, **221** (2004) 653.
12. X. Li, N.F. Dummer, R.L. Jenkins, R.P.K. Wells, P.B. Wells, D.J. Willock, S.H. Taylor, P. Johnston and G.J. Hutchings, *Catal. Lett.*, **96** (2004) 147.
13. A.F. Carley, M.K. Rajumon, M.W. Roberts and P.B. Wells, *J. Chem. Soc. Faraday Trans.*, **91** (1995) 2167.
14. B. Minder, T. Mallat, A. Baiker, G. Wang, T. Heinz and A. Pfaltz, *J. Catal.*, **154** (1995) 371.
15. A. Baiker, *J. Mol. Catal. A; Chem.*, **115** (1997) 473.
16. X. Li, Ph.D Thesis, Cardiff University, (2000).
17. T. Bürgi and A. Baiker, *J. Am. Chem. Soc.*, **120** (1990) 12920.
18. P.J. Collier, T.J. Hall, J.A. Iggo, P. Johnston, J.A. Slipszenko, P.B. Wells and R. Whyman, *J. Chem. Soc. Chem. Commun.*, (1998) 1451.
19. M. Bartók, B. Török, K. Balázsik and T. Bartók, *Catal. Lett.*, **73** (2001) 127.

*Chapter*  
*Six*

---

**Chapter Six: Final Comments and Future Work****6.1 Final comments**

Comparisons have been drawn of the enantioselective hydrogenation of 2,3-butanedione over cinchonidine modified platinum catalysts in the liquid and gas-phase. Experiments were conducted with a stirred autoclave and fixed-bed reactor in the liquid phase and micro-flow reactor in the gas-phase. Experimental conditions in each case were shown to greatly influence the outcome of the hydrogenation of 2,3-butanedione.

Utilising the rate of 2,3-butanedione hydrogenation in the autoclave over the IMI-2 2.5 % Pt/Silica catalysts, an ideal set of support characteristics was provided. These studies were complimented by using a series of granular catalysts (0.5-1.0 mm) in the trickle-bed reactor with the same reaction. The results were used to guide continuous catalyst manufacture at the Birmingham materials centre for the production of silica gel extrudates.

The dione hydrogenation reaction was optimised in the autoclave through the use of different solvent, increased pressure and decreased modifier concentration. Consequently the IMI-2 catalyst used gave comparable results to the best catalyst in the literature (EUROPT-1).

Cyclohexene hydrogenation was evaluated as a probe reaction to determine catalyst activity in the trickle-bed reactor. Furthermore, the affect of cinchonidine modifier was investigated. The results from these experiments facilitated the reaction optimisation in the trickle-bed reactor and comparison with the autoclave data.

Under present experimental protocol it has been demonstrated that the trickle-bed reactor is a suitable instrument for fine chemical synthesis. The enantioselective

hydrogenation of methyl pyruvate gave high initial conversion (80 %) and a modest enantiomeric excess (52 %).

The hydrogenation of methyl pyruvate at the gas/solid interface was confirmed with the use of the Kelvin equation to estimate the effective partial pressure for condensation as a function of pore radius. Reactions over a prepared 1 % Pt/ $\alpha$ -alumina catalyst which has no intra-particle pores structure verified this claim.

Experiments conducted in the gas phase over alkaloid pre-modified platinum catalysts are beneficial for 2,3-butanedione hydrogenation. However, the adsorbed alkaloid can be considered a poison for pyruvate ester hydrogenation as the un-modified reaction was shown to be more active. Such that the rate enhancement afforded in the liquid phase for the equivalent reaction is lost.

The modification of the platinum surface with cinchonidine results in an enantioselective site which is substrate specific in the gas phase. This is similar to the results reported in the literature with liquid phase reactions. These results have developed a new model which indicates that the interaction of reactant at the enantioselective site is dependent on the substrate.

## 6.2 Future work

### (1) Diversification of cinchona alkaloids

At present many different cinchona alkaloids have been shown to induce enantioselectivity when adsorbed on platinum. Some have exhibited intriguing results, such as inversion of the enantiomeric excess from expected outcome, based on the main structural elements. Additionally, alkaloid molecules have been prepared in which the conformation is

rigid. The use of a fixed-bed reactor with such modifiers may prove very advantageous for further investigations of the enantioselective site. The use of a rigid modifier in the hydrogenation of pyruvate esters at the gas/solid interface would be particularly useful.

(2) Further investigations into the origin of the transient period

The initial transient of increasing enantiomeric excess is still a matter for debate. Exploiting the techniques and results obtained in the gas phase over modified platinum catalyst with the hydrogenation of methyl and ethyl pyruvate, further substrates could be prepared. The different interactions of the pyruvate ester substrates were shown to influence the outcome modestly. Increases in the size of the substrate may yield a greater affect on the subsequent enantiomeric excess. This would facilitate the proposal of an origin to the transient period in the liquid phase.

(3) Commission a high pressure trickle-bed reactor with temperature control

The reaction conditions utilised in the trickle-bed reactor are mild compared to those found in the literature. The activity of the IMI-2 2.5 % Pt/Silica catalysts were found to be high with respect to cyclohexene and methyl pyruvate hydrogenation. However, further enhancements in conversion and enantiomeric excess could not be achieved through optimisation of conditions. Commissioning a high pressure fixed-bed reactor with temperature control would prove beneficial in improving the reactions carried out over the well characterised platinum catalysts.



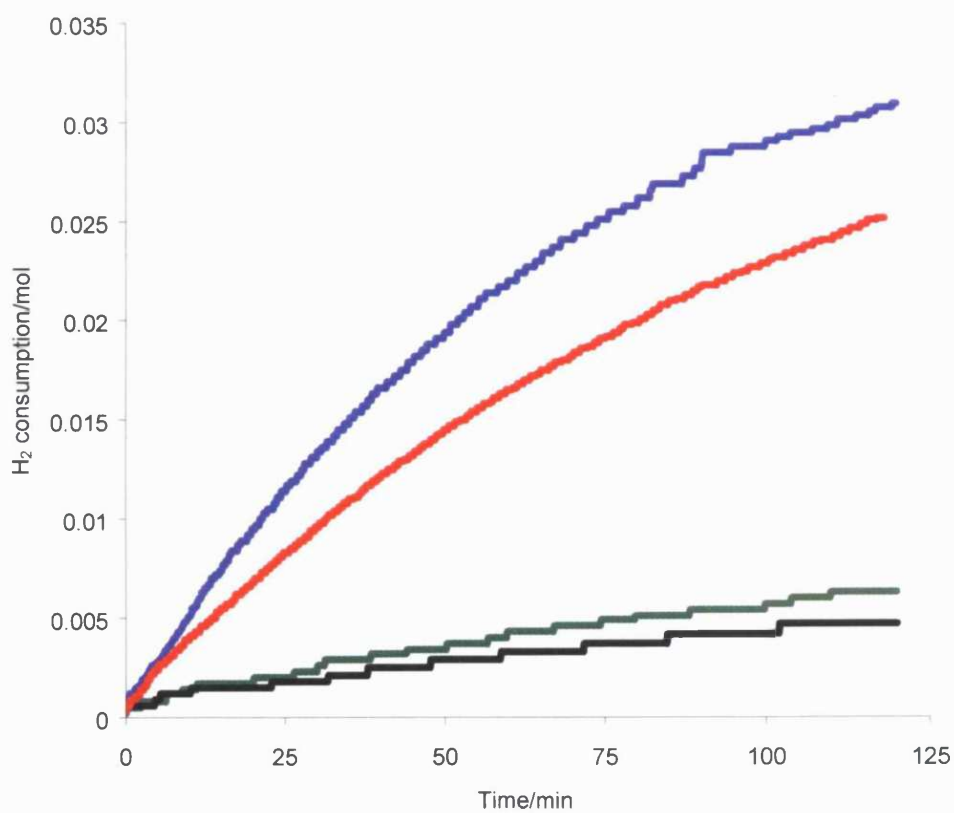
(4) Broadening the use of fixed-bed reactors

Utilising the trickle-bed and gas phase reactors for enantioselective hydrogenations of pro-chiral C=C and C=N containing species. The effectiveness of the Pt-cinchona-pyruvate system has been the focus of attention with continuous operation. Using a variety of supported metal catalysts, novel substrates may be hydrogenated over a fixed catalyst bed. The lower activity and modest ee exhibited in stirred tank reactions with a Pd-cinchona-substituted alkene system may benefit from a fixed-bed reactor with a recycle system.

*Chapter*  
*Seven*

## Chapter Seven: Appendix

7.1 Hydrogen uptake as a function of time for 2,3-butanedione hydrogenation over catalysts with the same support characteristics under standard reaction conditions.

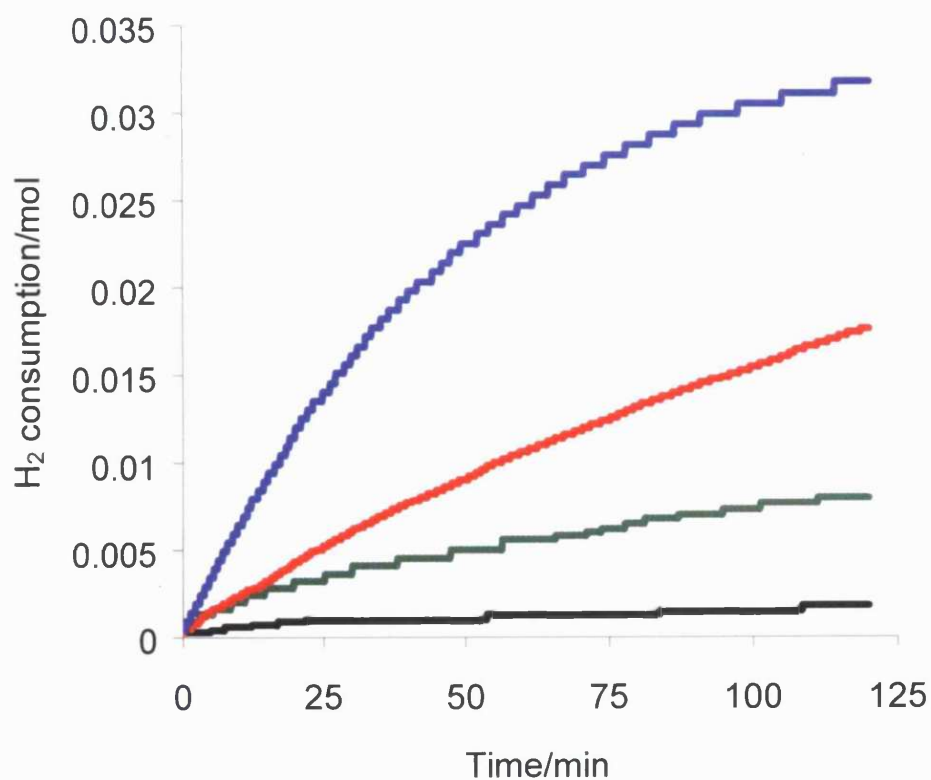


Catalyst; M01060 (—), M01061 (—), M01037 (—), M01034 (—)

[0.2 g catalyst; 27 ml dichloromethane; 34.5 mmol 2,3-butanedione; 5.66 mM cinchonidine;

10 bar H<sub>2</sub> pressure; 25°C; T = 25 ± 1°C; 1000 rpm]

7.2 Hydrogen uptake as a function of time for 2,3-butanedione hydrogenation over catalysts with the same support particle size but different support characteristics under standard reaction conditions.

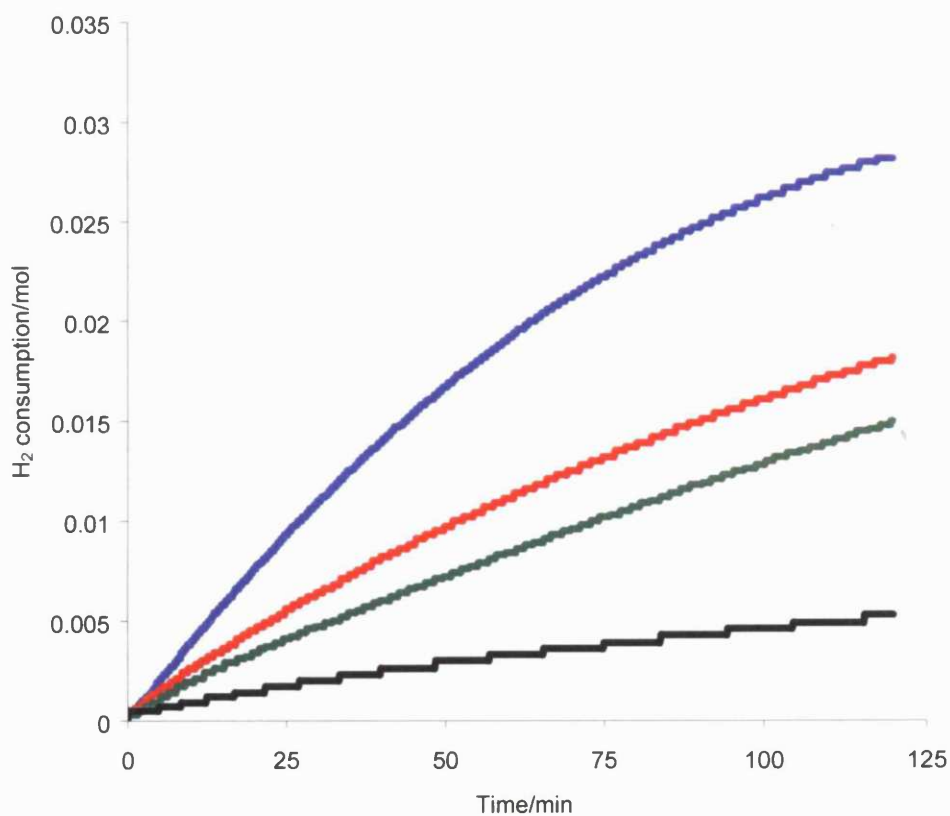


Catalyst; M01271 (—), M01071 (—), M01270 (—), M01069 (—)

[0.2 g catalyst; 27 ml dichloromethane; 34.5 mmol 2,3-butanedione; 5.66 mM cinchonidine;

10 bar H<sub>2</sub> pressure; 25°C; T = 25 ± 1°C; 1000 rpm]

7.3 Hydrogen uptake as a function of time for 2,3-butanedione hydrogenation over granular catalysts under standard reaction conditions.

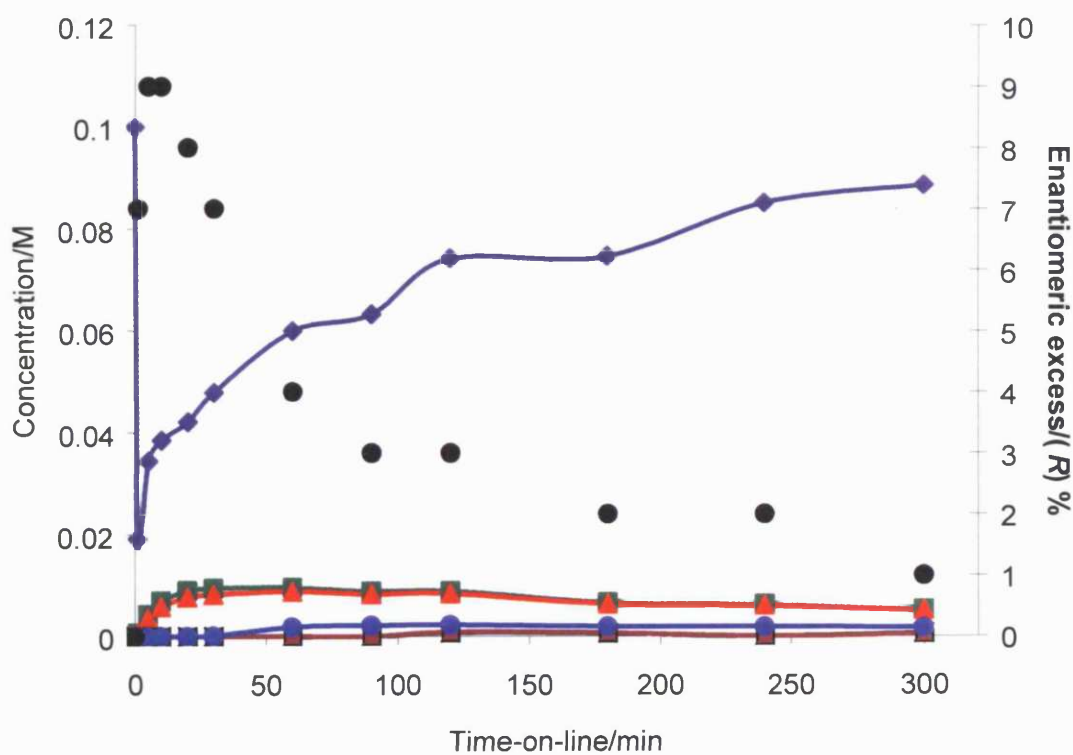


Catalyst; M02023 (—), M02025 (—), M02027 (—), M02029 (—)

[0.2 g catalyst; 27 ml dichloromethane; 34.5 mmol 2,3-butanedione; 5.66 mM cinchonidine;

10 bar H<sub>2</sub> pressure; 25°C; T = 25 ± 1°C; 1000 rpm]

7.4 Concentration and enantiomeric excess as a function of time for 0.1 M 2,3-butanedione hydrogenation over *in situ* pre-modified M02023 with cinchonidine in the feedstock.



Substrate; 2,3-butanedione (—), (*R*)-hydroxybutanone (—), (*S*)-hydroxybutanone (—),

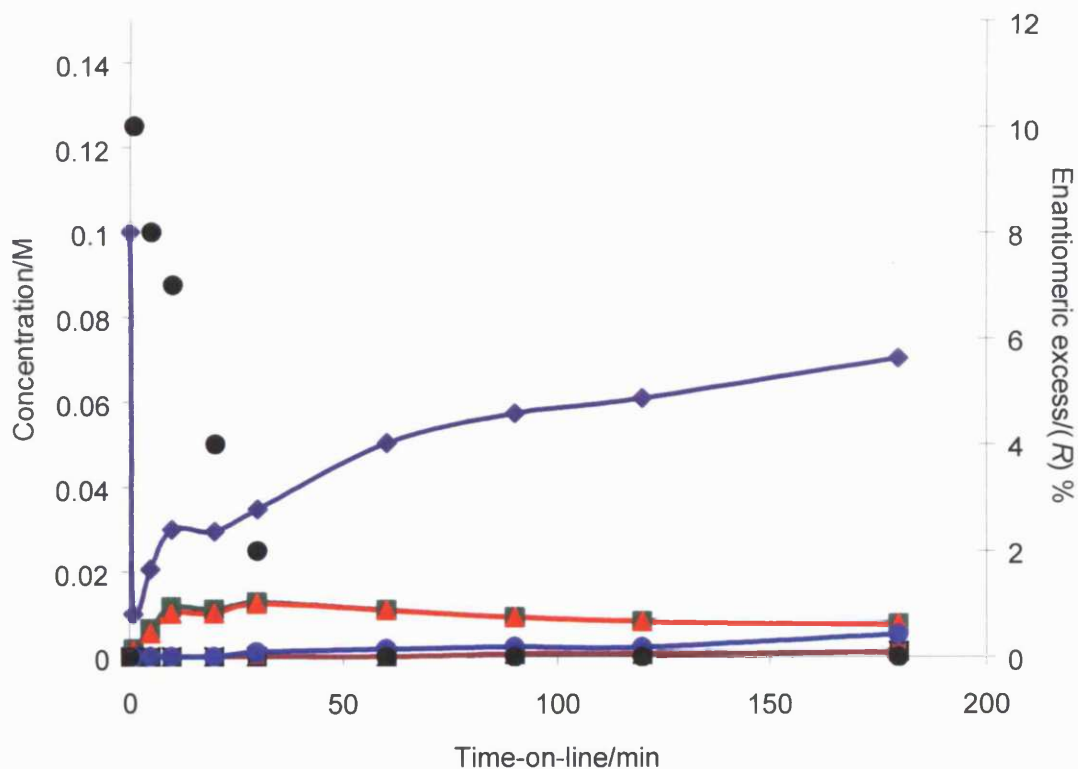
(*R,R*)-butanediol (—), (*S,S*)-butanediol (—), meso butanediol (—)

Enantiomeric excess; (●)

[2 g catalyst; 0.1 M 2,3-butanedione (8.49 mM CD) in DCM; 0.5 barg H<sub>2</sub> pressure; GHSV

4800 /h; 25°C; T = 25 ± 1°C]

7.5 Concentration and enantiomeric excess as a function of time for 0.1 M 2,3-butanedione hydrogenation over *in situ* pre-modified M02025 with cinchonidine in the feedstock.



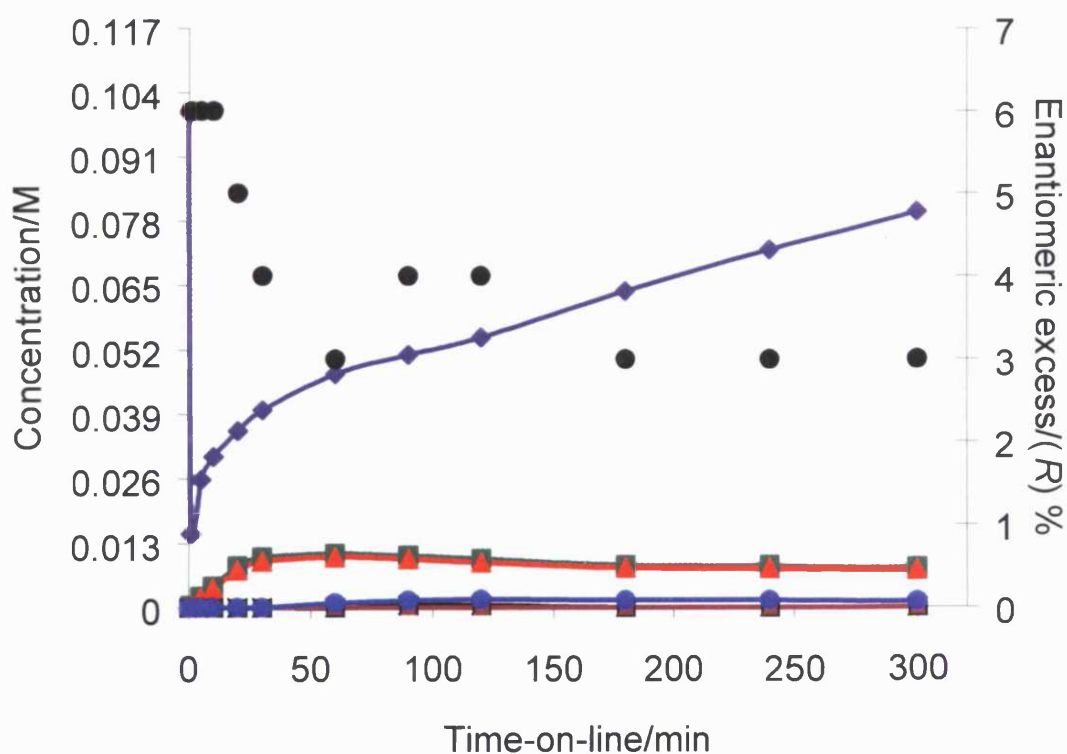
Substrate; 2,3-butanedione (—), (*R*)-hydroxybutanone (—), (*S*)-hydroxybutanone (—),

(*R,R*)-butanediol (—), (*S,S*)-butanediol (—), meso butanediol (—)

Enantiomeric excess; (●)

[2 g catalyst; 0.1 M 2,3-butanedione (8.49 mM CD) in DCM; 0.5 barg H<sub>2</sub> pressure; GHSV  
4800 /h; 25°C; T = 25 ± 1°C]

7.6 Concentration and enantiomeric excess as a function of time for 0.1 M 2,3-butanedione hydrogenation over *in situ* pre-modified M02027 with cinchonidine in the feedstock.

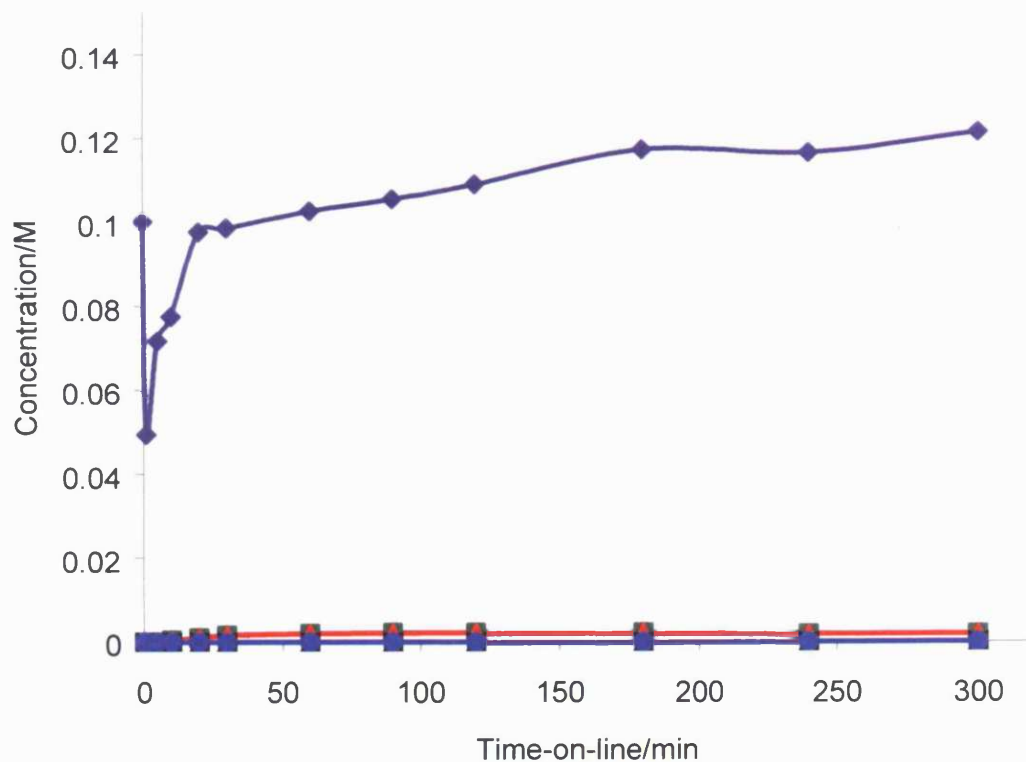


Substrate; 2,3-butanedione (●), (*R*)-hydroxybutanone (▲), (*S*)-hydroxybutanone (△),  
 (*R,R*)-butanediol (■), (*S,S*)-butanediol (□), meso butanediol (◆)  
 Enantiomeric excess; (●)

[2 g catalyst; 0.1 M 2,3-butanedione (8.49 mM CD) in DCM; 0.5 barg H<sub>2</sub> pressure; GHSV  
 4800 /h; 25°C; T = 25 ± 1°C]



7.7 Concentration and enantiomeric excess as a function of time for 0.1 M 2,3-butanedione hydrogenation over *in situ* pre-modified M02029 with cinchonidine in the feedstock.

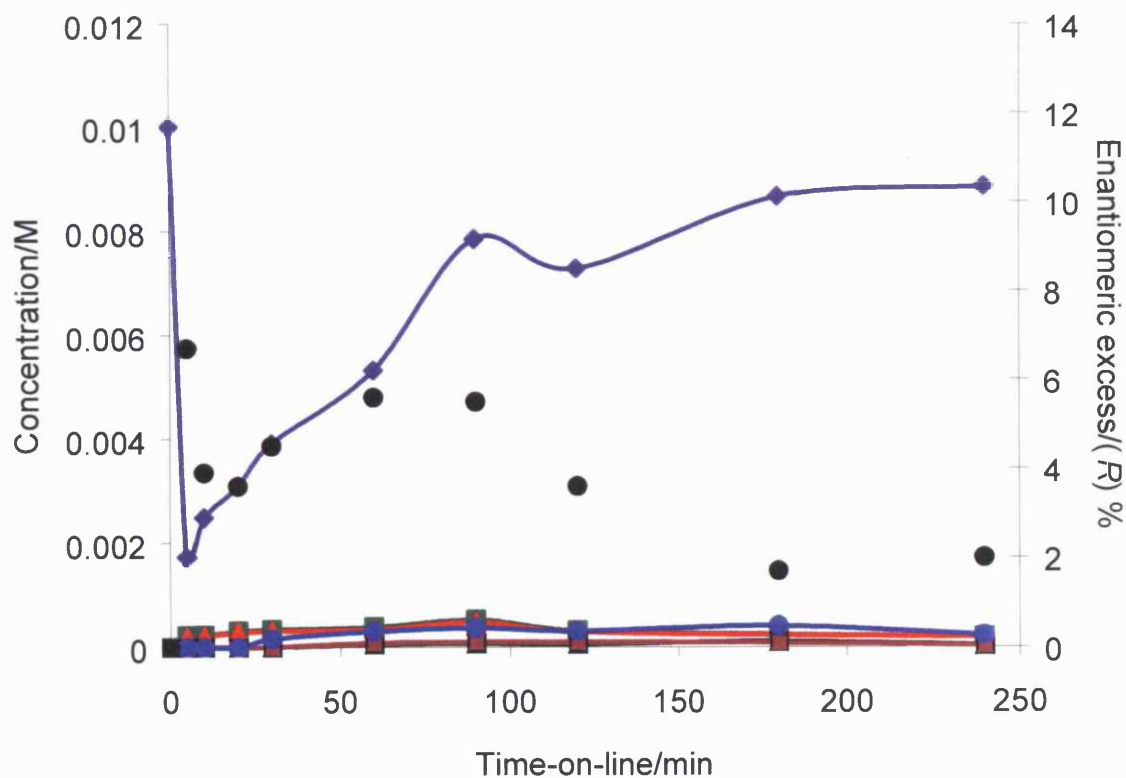


Substrate; 2,3-butanedione (—●—), (*R*)-hydroxybutanone (—■—), (*S*)-hydroxybutanone (—■—),  
(*R,R*)-butanediol (—■—), (*S,S*)-butanediol (—■—), meso butanediol (—■—)

Enantiomeric excess; (●)

[2 g catalyst; 0.1 M 2,3-butanedione (8.49 mM CD) in DCM; 0.5 barg H<sub>2</sub> pressure; GHSV  
4800 /h; 25°C; T = 25 ± 1°C]

7.8 Concentration and enantiomeric excess as a function of time for 0.01 M 2,3-butanedione hydrogenation over *ex situ* pre-modified (8.49 mM CD) M02023 with cinchonidine in the feedstock.



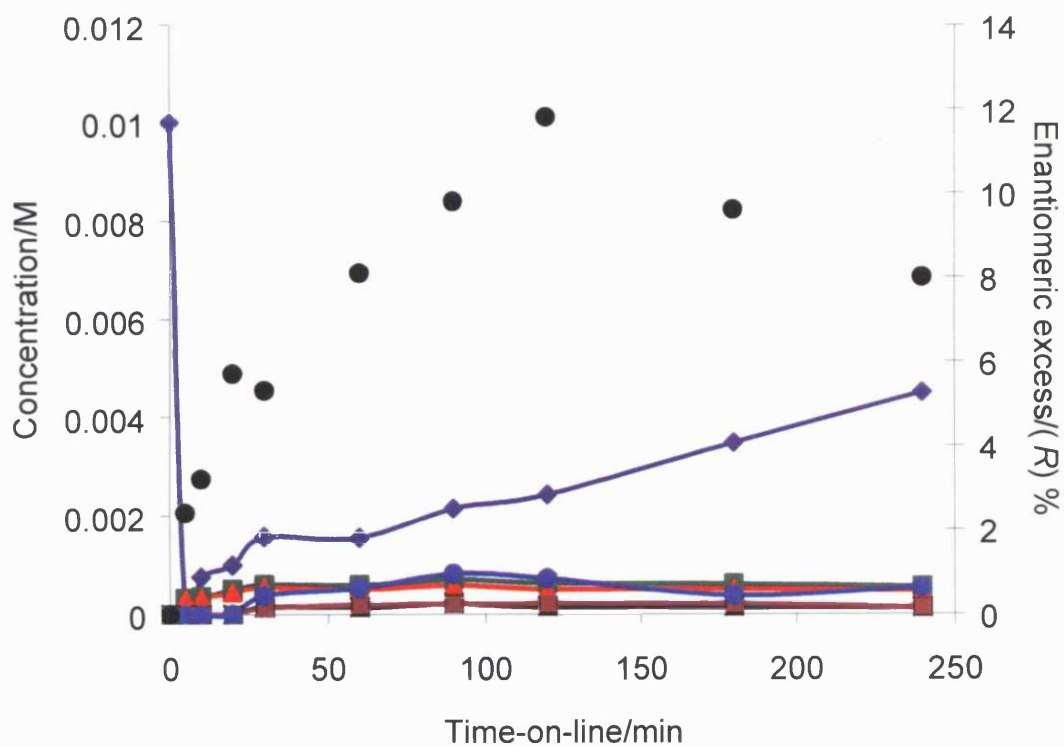
Substrate; 2,3-butanedione (—◆—), (*R*)-hydroxybutanone (—■—), (*S*)-hydroxybutanone (—■—),

(*R,R*)-butanediol (—■—), (*S,S*)-butanediol (—■—), meso butanediol (—■—)

Enantiomeric excess; (●)

[2 g catalyst (8.49 mM CD); 0.1 M 2,3-butanedione (8.49 mM CD) in DCM; 0.5 barg H<sub>2</sub> pressure; GHSV 4800 /h; 25°C; T = 25 ± 1°C]

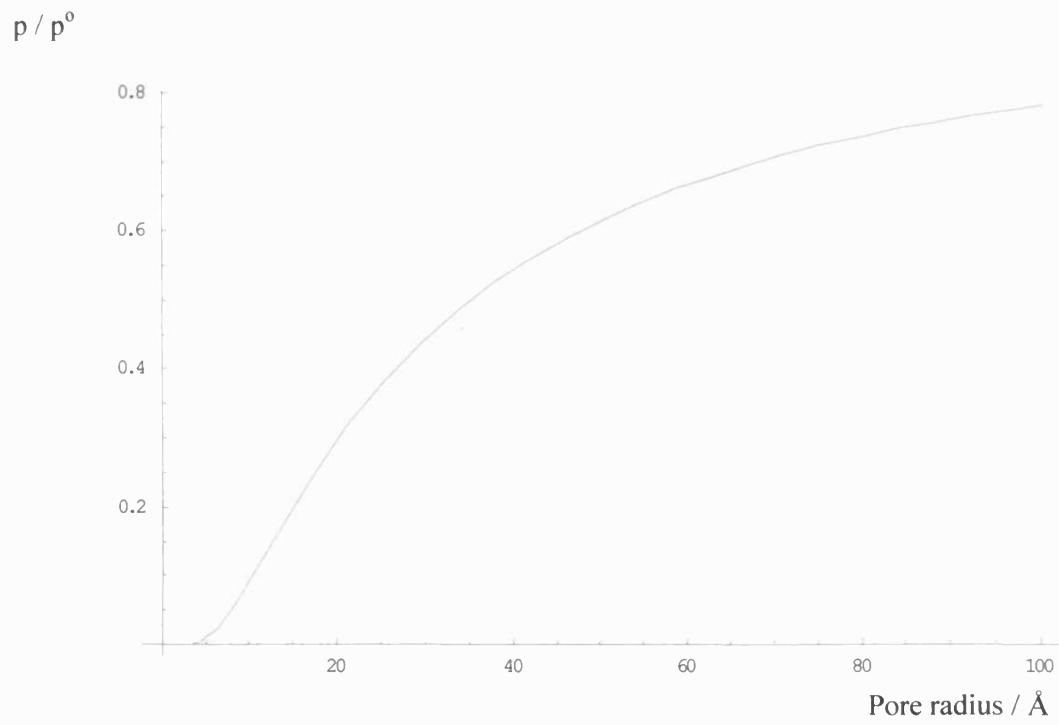
7.9 Concentration and enantiomeric excess as a function of time for 0.01 M 2,3-butanedione hydrogenation over *ex situ* pre-modified (16.98 mM CD) M02023 with cinchonidine in the feedstock.



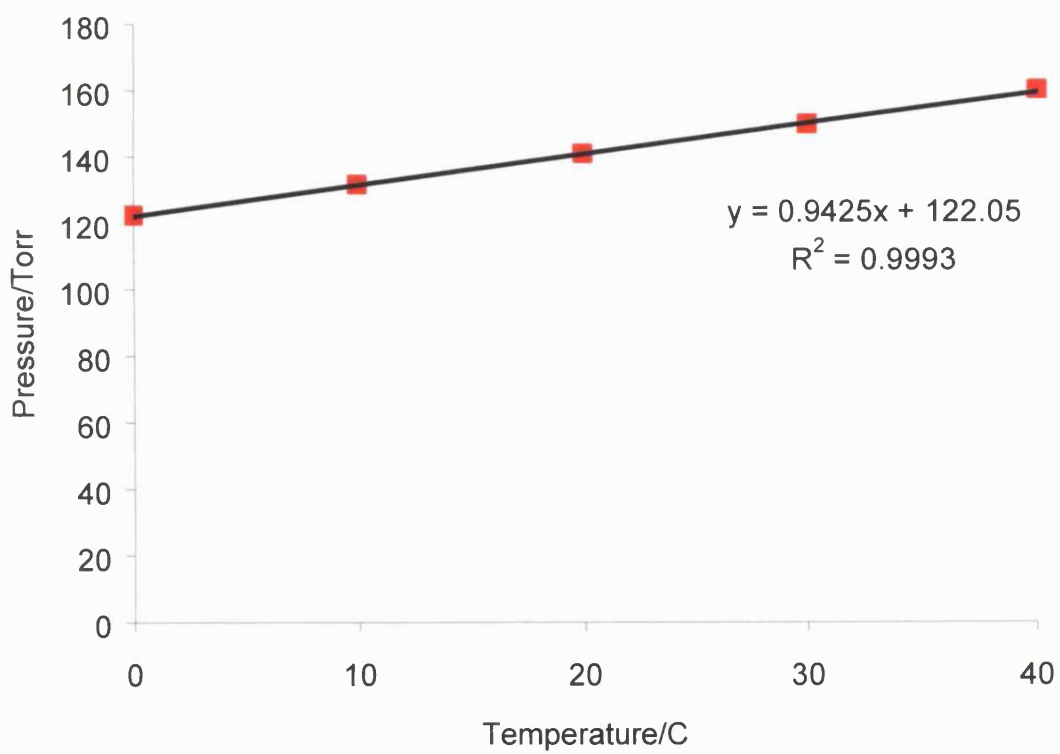
Substrate; 2,3-butanedione (—◆—), (*R*)-hydroxybutanone (—■—), (*S*)-hydroxybutanone (—■—),  
 (*R,R*)-butenediol (—■—), (*S,S*)-butenediol (—■—), meso butenediol (—■—)  
 Enantiomeric excess; (●)

[2 g catalyst (16.98 mM CD); 0.1 M 2,3-butanedione (8.49 mM CD) in DCM; 0.5 barg H<sub>2</sub> pressure; GHSV 4800 /h; 25°C; T = 25 ± 1°C]

7.10 Kelvin equation plot



## 7.11 Vapour pressure of methyl pyruvate (Section 2.8)



‘There is nothing, Sir, too little for so little a creature as man.

It is by studying little things that we attain the great art of  
having as little misery and as much happiness as possible.’

— Samuel Johnson

